Hybrid Satellite-Terrestrial Cooperative Systems : Performance Analysis and System Dimensioning

Sokchenda Sreng

Université de Toulouse

THÈSE

En vue de l'obtention du

DOCTORAT DE L'UNIVERSITÉ DE TOULOUSE

Délivré par :
Institut National Polytechnique de Toulouse (INP Toulouse)

Discipline ou spécialité :

Réseaux, Télécoms, Systèmes et Architectures

Présentée et soutenue par :
Sokchenda SRENG

le : mardi 11 décembre 2012

Titre :

HYBRID SATELLITE-TERRESTRIAL COOPERATIVE SYSTEMS:
PERFORMANCE ANALYSIS AND SYSTEM DIMENSIONING

Ecole doctorale :
Mathématiques Informatique Télécommunications (MITT)

Unité de recherche :
Institut de Recherche en Informatique de Toulouse (IRIT)-UMR 5505

Directeur(s) de Thèse :
Mme. Marie-Laure BOUCHERET, Directrice de thèse
M. Benoît ESCRIG, Co-directeur de thèse

Rapporteurs :

Mme. Maryline HELARD, Professeur à INSA Rennes
M. Daniel ROVIRAS, Professeur à CNAM Paris

Membre(s) du jury :
Mme. Maryline HELARD, Professeur à INSA Rennes, Rapporteur/Président
M. Daniel ROVIRAS, Professeur à CNAM Paris, Rapporteur
Mme. Caroline BES, Docteur Ingénieur à CNES, Examinatrice
Mme. Marie-Laure BOUCHERET, Professeur à INPT-ENSEEIHT, Membre
M. Benoît ESCRIG, Maître de Conférences à ENSEIRB-MATMECA, Membre

ANNÉE 2012

THÈSE

présentée

pour obtenir le titre de

Docteur de l'Institut National Polytechnique de Toulouse

Ecole Doctorale Mathématiques Informatique Télécommunications de Toulouse

Spécialité : Réseaux, Télécoms, Systèmes et Architectures

par

Sokchenda Sreng

Hybrid satellite-terrestrial cooperative systems: performance analysis and system dimensioning

Soutenue le 11 décembre 2012 devant le jury composé de :

Mme. Maryline Helard	Professeur à INSA Rennes	Rapporteur
M. Daniel Roviras	Professeur à CNAM Paris	Rapporteur
Mme. Caroline Bes	Docteur Ingénieur à CNES	Examinatrice
Mme. Marie-Laure Boucheret	Professeur à INPT-ENSEEIHT	Directrice de thèse
M. Benoît Escrig	Maître de Conférences à ENSEIRB-MATMECA	Co-directeur de thèse

préparée à l'Institut de Recherche en Informatique de Toulouse

IRIT/INP-ENSEEIHT – 2, rue Charles Camichel – BP7122 – 31071 Toulouse Cedex 7

Remerciements

Je remercie avant tout ma directrice de thèse, Mme. Marie-Laure Boucheret et mon co-directeur de thèse, M. Benoit Escrig pour tout leur dynamisme, leur tolérance, leur disponibilité, leurs compétences scientifiques et leurs idées que j'ai pu apprécier tout au long de ma thèse. Ce travail n'aurait jamais pu aboutir sans eux, qui ont toujours su me consacrer des moments de leur temps, me guider et me conseiller et me témoigner leur soutien et leur confiance. Je souhaite leur transmettre l'expression de ma plus profonde et sincère gratitude. J'ai beaucoup appris en travaillant avec eux et je les remercie de tout mon coeur.

Je tiens à exprimer mes remerciements les plus sincères aux membres du jury de thèse qui ont accepté de juger ce travail. Je suis profondément reconnaissant à mes deux rapporteurs, Mme. Maryline Helard, Prof. à INSA de Rennes et M. Daniel Roviras, Prof. à CNAM Paris, d'avoir accepté de lire et évaluer ma thèse. Je remercie également Mme. Caroline Bes, Docteur Ingénieur à CNES Toulouse, qui a accepté d'être examinatrice de ma thèse.

Ma gratitude s'adresse aussi à tous mes collègues de l'IRIT, enseignants, chercheurs, doctorants, techniciens, secrétaires, pour leur sympathie et convivialité au sein du laboratoire. Merci pour les aides permanentes reçues du personnel du laboratoire. Je remercie en particulier Sylvie Eichen, Sylvie Armengaud et Frédéric Peyré qui ont été disponibles à chaque fois que j'ai eu besoin d'une aide.

Je remercie en particulier Bouchra Bennama, Romain Tajan, Olivier Chabiron, Cecile Bazot, Adder Rahim Halimi et Yoann Altmann qui m'ont aidé à répondre à un certain nombre de questions pratiques, techniques, ou scientifiques. Je voudrais adresser aussi un grand merci à tous les doctorants de l'équipe IRT à l'ENSEEIHT pour ses soutiens.

J'aimerais remercier également Mme. Corinne Mailhes, directrice administrative du Laboratoire TESA, qui m'a accepté de travailler là bas pendent 3 semaines du mois d'août. Je remercie aussi Dévid Bonaci, Panha Pech, Raoul Prévost, Victor Bissoli Nicolau, Florian Cazes et Chao Lin, qui m'a accueilli pendent ce temps.

J'adresse mes chaleureux remerciements à Monsieur et Madame Mom Lor, pour leur accueille depuis mon premier arrivé à Toulouse. Je remercie également à tous les étudiants cambodgiens à Toulouse.

Je dédie ce doctorat à ma mère et à mon père, dont les bénédictions m'ont suivi tout au long, et sans lesquelles je n'en serais pas là. Je leur remercie pour leurs encouragements de continuer mes études en France et je leur exprime toute mon admiration, mon affection et ma gratitude.

Enfin, je tiens à remercier la France, en particulier le gouvernement français qui m'a financé et accueilli sur son territoire et de m'avoir donné l'opportunité de continuer les études supérieures. Ce pays représente ma porte vers le monde extérieur et il occupera toujours une grande place dans mon coeur.

Merci infiniment encore à tous.

Résumé

Les systèmes de communications par satellite sont utilisés dans le contexte de la radiodiffusion, de la navigation, du sauvetage et du secours aux sinistrés, car ils permettent de fournir des services sur une large zone de couverture. Cependant, cette zone de couverture est limitée par l'effet de masquage provoqué par des obstacles qui bloquent la liaison directe entre le satellite et un utilisateur terrestre. L'effet de masquage devient plus sévère en cas de satellites à faibles angles d'élévation ou lorsque l'utilisateur est à l'intérieur. Pour résoudre ce problème, les Systèmes Coopératifs Hybride Satellite-Terrestre (HSTCS) ont été proposés.

Dans un système HSTCS, l'utilisateur mobile peut profiter de la diversité spatiale en recevant des signaux à la fois du satellite et des relais terrestres. Les gap-fillers fixes ou mobiles sont utilisés pour relayer le signal satellite. La plupart des systèmes de diffusion par satellite utilisent les gap-fillers fixes alors que les gap-fillers mobiles sont nécessaires en cas de communications d'urgence lorsque l'infrastructure fixe n'est pas disponible. Dans les scénarios d'urgence (incendie, tremblement de terre, inondations, explosion) l'infrastructure terrestre existante est endommagée, donc les HSTCSs sont appropriés pour mettre à jour des informations qui permettent aux sauveteurs d'intervenir efficacement et en toute sécurité. En particulier, une mise en oeuvre rapide et souple est nécessaire, ce qui pourrait être fourni par le déploiement de gap-fillers mobiles (véhicule ou portable). Plusieurs scénarios coopératifs et techniques de transmission ont déjà été proposés et étudiés. Cependant, la plupart des méthodes proposées ne fournissent qu'une analyse de performance fondée sur la simulation alors que les expressions analytiques de la probabilité de coupure et de la Probabilité d'Erreur Symbole (SEP) n'ont pas encore été établies.

Cette thèse se focalise sur l'analyse de performances des systèmes HSTCS. La probabilité de coupure et SEP du système utilisant le schéma de transmission Selective Decode-and-Forward (SDF), avec ou sans sélection de relais, est évaluée dans le cas des modulations MPSK et MQAM. Cette expression analytique permet de concevoir le système HSTCS. Ces résultats sont applicables aux cas des relais fixes ou mobiles. La seconde partie de cette thèse est consacrée à des problèmes de synchronisation (décalage en temps et en fréquence ainsi que l'étalement Doppler). La mobilité des utilisateurs crée l'étalement Doppler qui détruit l'orthogonalité des sous-porteuses dans les signaux de type Orthogonal Frequency Division Multiplexing (OFDM). Cette perte d'orthogonalité engendre de l'interférence entre sous-porteuses (ICI) et donc une dégradation des performances du système en termes de SEP. Dans ce cas, on présente les conditions dans lesquelles cette dégradation peut être compensée par une augmentation du Rapport Signal sur Bruit (SNR) du côté de l'émetteur. Le résultat dépend du schéma de modulation et aussi de la vitesse des utilisateurs.

Abstract

Satellite communication systems are used in the context of broadcasting, navigation, rescue, and disaster relief since they allow the provision of services over a wide coverage area. However, this coverage area is limited by the masking effect caused by obstacles that block the Line-Of-Sight (LOS) link between the satellite and a terrestrial user. The masking effect becomes more severe in case of low satellite elevation angles or when the user is indoor. To address this issue, Hybrid Satellite-Terrestrial Cooperative Systems (HSTCSs) have been proposed.

In an HSTCS, the mobile user can exploit the diversity advantages by receiving signals from both satellite and terrestrial components. Fixed or mobile gap-fillers are used to relay the satellite signal. Most of satellites broadcasting systems have been implemented using fixed gap-fillers while mobile gap-fillers are needed in emergency cases when the fixed infrastructure is not available. In emergency scenarios (e.g., fire, earthquake, flood and explosion), the existing terrestrial infrastructure has been destroyed. So, an HSTCS is appropriate for transmitting the information between the rescuers and the central office. This allows the rescuers to operate efficiently. In particular, a fast and flexible implementation is needed and this could be provided by deploying mobile gap fillers (vehicle or mobile handheld). Recently, the topic of HSTCSs has gain interest in the research community. Several cooperative scenarios and transmission techniques have been proposed and studied. However, most of existing approaches only provide a performance analysis based on simulation results and the analytical expression of the exact Symbol Error Probability (SEP) is generally not provided.

This dissertation focuses on the performance analysis of HSTCSs. The exact closed-form outage

probability and SEP of Selective Decode-and-Forward (SDF) transmission scheme with and without relay selection are derived for both M-ary phase shift keying (MPSK) and M-ary quadrature amplitude modulation (MQAM) schemes. This analytical SEP helps in designing and dimensioning HSTCSs. Our results are applicable to both fixed and mobile relaying techniques. Another part of the dissertation is dedicated to synchronization issues (time, frequency shifting/spreading). The mobility of users induces a Doppler spread in the Orthogonal Frequency Division Multiplexing (OFDM) signal that destroys the orthogonality of subcarriers. The loss of orthogonality produces Inter-subCarrier Interference (ICI) and hence a degradation of the system performance in terms of SEP. In this case, we present the conditions in which this degradation can be compensated for by an increase in the Signal to Noise Ratio (SNR) at the transmitter side. The result depends on both the modulation scheme and the speed of the mobile users.

Acronymes

AF	Amplify-and-Forward
AS	Average Shadowing
AWGN	Additive White Gaussian Noise
CDF	Cumulative Distribution Function
CGC	Complementary Ground Component
CSI	Channel State Information
CRC	Cyclic Redundancy Check
DF	Decode-and-Forward
DVB-SH	Digital Video Broadcasting-Service to Handheld
DVB-T	Digital Video Broadcasting-Terrestrial
EGC	Equal Gain Combining
FDMA	Frequency Division Multiple Access
FHS	Frequent Heavy Shadowing
GEO	Geostationary Earth Orbit
GI	Guard Interval
GMT	Ground Mobile Terminal
GPS	Global Positioning System
HISTCS	Hybrid/Integrated Satellite-Terrestrial Cooperative System
HSTCS	Hybrid Satellite-Terrestrial Cooperative System
ICI	Inter-subCarrier Interference

ILS	Infrequent Light Shadowing
ISI	Inter-Symbol Interference
ISTS	Integrated Satellite-Terrestrial System
LOE	Low Earth Orbit
LMS	Land Mobile Satellite
LOS	Line-Of-Sight
MGF	Moment Generating Function
MIP	Megaframe Initialization Packet
MPSK	M-ary Phase Shift Keying
MQAM	M-ary Quadrature Amplitude Modulation
MRC	Maximum Ratio Combining
NLOS	Non Line-Of-Sight
OFDM	Orthogonal Frequency Division Multiplexing
PDF	Probability Density Function
P/S	Parallel to Serial
QPSK	Quadrature Phase Shift Keying
SC	Selection Combining
SDF	Selective Decode-and-Forward
SEP	Symbol Error Probability
SFN	Single Frequency Network
SHIP	SH frame Information Packet
SNR	Signal-to-Noise Ratio
S/P	Serial to Parallel
TDMA	Time Division Multiple Access

Contents

List of Figures

List of Tables

Introduction

Motivation

Satellite systems are used in the context of broadcasting, navigation, rescue, and disaster relief since they allow the provision of services over a wide coverage area. However, this coverage area is limited by the masking effect caused by obstacles that block the Line-Of-Sight (LOS) link between the satellite and a terrestrial user. It is the main limitation of Mobile Satellite Systems (MSSs). To improve the system availability, which is characterized by the percentage of time that the LOS between the terrestrial user and the satellite exists, the multi-satellite diversity technique has been proposed [Vog97, AV97]. In multi-satellite diversity techniques, two or more satellites transmit simultaneously the information to a terrestrial user. In order to obtain the maximum system availability, each satellite should be situated in an appropriate position which can provide the LOS link to the terrestrial user when other satellite-destination links are in non-LOS conditions (i.e., the LOS links between satellites and destination terminals should not be correlated). It has been shown in [VCS02] that in order to have at least one LOS link among two satellite-destination links, the azimuth separation of the two satellites must be higher than $\pi/4$. Although the multi-satellite diversity can improve the system availability, there are still some limitations for example when the user terminal is indoor. The cost of using several satellites is another issue when implementing multi-satellite diversity techniques. To address this issue, Hybrid/Integrated Satellite-Terrestrial Cooperative Systems (HISTCSs) have been proposed [CGK09, KK10].

In an HISTCS, the terrestrial segment is used to relay the satellite signal to the destination node. The main difference between hybrid and integrated systems is on whether both space and terrestrial

segments use a common network and spectrum. In an integrated system, a terrestrial cellular network can be used as an alternative system to connect the terrestrial user with respect to the satellite one [EWL+05]. Both satellite and ground segments also use the same frequency band. In a hybrid system, the terrestrial gap fillers (repeaters) can be employed to forward the satellite signal in non LOS conditions [CCL+08]. Both satellite and terrestrial relays use the different frequency band.

In a Hybrid Satellite-Terrestrial Cooperative System (HSTCS), the mobile user can exploit the spatial diversity by receiving signals from both satellite and terrestrial components. Fixed or mobile gap-fillers are used to relay the satellite signal by implementing Amplify-and-Forward (AF), Fixed Decode-and-Forward (FDF) or Selective Decode-and-Forward (SDF) transmission schemes [LTW04, LW03]. In the AF transmission scheme, all relays amplify both the source message and the channel noise which leads to some performance degradations. In the FDF transmission scheme, all relays decode the source messages (demodulate) first and then re-encode (re-modulate) the signal before forwarding to the destination node while in the SDF transmission scheme, only the relays that can decode the source messages correctly are allowed to retransmit the signals. This SDF transmission scheme prevents the retransmission of erroneous messages to the destination node. Most of satellite broadcasting systems have been implemented using fixed gap-fillers. However, mobile gap-fillers are needed in emergency cases when the fixed infrastructure is not available. In emergency scenarios (e.g., fire, earthquake, flood and explosion), the existing terrestrial infrastructure has been destroyed. So, an HSTCS is appropriate for transmitting the information between the rescuers and the central office. This allows the rescuers to operate efficiently [IBdRH+08, DRMJS09]. In particular, a fast and flexible implementation is needed and this could be provided by deploying mobile gap fillers (vehicle or mobile handheld).

Several cooperative scenarios for HSTCSs have been proposed for different kind of applications. In [MJDR10], the delay diversity technique for a hybrid satellite-terrestrial DVB-SH system has been studied. In this scenario, user stations receive different versions of the same signal with different delays: one signal from the satellite and other signals from terrestrial relays. No combiner is implemented. In [AKKP10], space-time codes and rate compatible turbo codes have been implemented to achieve diversity gains and additional coding gains. Recently, hybrid satellite-terrestrial systems employing

mobile gap fillers have been presented in [CIdRH10, PED+11]. In [CIdRH10], a hybrid solution based on a cooperative ad-hoc networking approach has been proposed for terrestrial links while the DVB-SH and the Next Generation Universal Mobile Satellite Telecommunications Systems (S-UMTS) standards are considered for forward (satellite broadcasting) and return (user terminal to satellite) links respectively. In [PED+11], a two time-slot scenario has been presented. The satellite broadcasts the information to terrestrial users in a first time slot and in a second time slot, non-masked terminals are used to relay the information toward masked terminals. Note that the Symbol Error Probability (SEP) performance has not been studied yet in [CIdRH10, PED+11].

Although the cooperative diversity techniques can increase the system availability by receiving the signal directly from the source and also from the relays, the additional bandwidth is needed for the relay transmissions. To minimize the bandwidth consumption while keeping the maximum diversity order, Bletsas et al.[BKRL06] have proposed an opportunistic cooperative protocol in which only one relay is used for forwarding the message to the destination. Two criteria for selecting the best relay have been studied. The first criterion is to choose the relay which maximizes the minimum of the source-relay and the relay-destination channel gain, while the second criterion is based on the maximization of the harmonic mean of both channel gains. It has been illustrated in [CwSZL10] that the outage performance of both selection techniques are the same in the high-SNR regime. The bandwidth consumption can be further decreased by implementing on-demand cooperation together with the best relay selection [Esc10].

The outage probability and the average SEP are two criteria for evaluating and designing communication systems. These two parameters can be obtained via simulation or via computation. However, most of the previous papers on HSTCSs have provided only the SEP performance based on simulations. The exact closed-form outage probability and SEP of HSTCSs have not been derived yet.

Objective of the dissertation

This dissertation aims at providing the analytical outage probability and SEP of HSTCSs. In order to derive the outage probability or the SEP of an HSTCS, an appropriate Land Mobile Satellite (LMS) channel model is needed. The most popular LMS channel models are the Loo's model [Loo85,

Loo90, Loo91, LB98], the Lutz's model [LCD+91], and the Fontan's model [PFHS+08, PFVCB+98, FVCC+01]. In the Loo's model, the amplitude of the LOS component is assumed to be lognormally distributed while the multipath interference has a Rayleigh distribution. The Lutz's model differs from the Loo's model. The latter model is a single state model whereas the Lutz's model is described by two states, the good state (Rice model) and the bad state (Suzuki model). The Fontan's model consists of three states: LOS, moderate shadowing and deep shadowing. Moreover, each state of the Fontan's model is described by the Loo's model. Recently, a new shadowed Rice model for the LMS channel has been proposed in [ALAK03]. In this model, the amplitude of the LOS is characterized by the Nakagami distribution and the amplitude of the multipath components is characterized by the Rayleigh distribution. It has been shown in [ALAK03] that this new model provides a similar fit to the experimental data as the Loo's model but with significantly less computational burden. In the following sections, we will use this new LMS channel model to derive the outage probability and the average SEP of HSTCSs.

In this dissertation, we investigate the performance in terms of outage probability and SEP of an HSTCS using fixed or mobile relays[1] over independent but not necessarily identically distributed fading channels. In the first phase, the satellite broadcasts its signal to all relay nodes and the destination node. In the second phase, the relay nodes forward the satellite signal to the destination node using the SDF transmission scheme. The exact closed-form outage probability and SEP expressions of an SDF transmission scheme with and without relay selection have been derived for general M-ary Phase Shift Keying (MPSK) and M-ary Quadrature Amplitude Modulation (MQAM) over the independent identically distributed (i.i.d) and independent non identically distributed (i.n.i.d) fading channels. Such closed-form solutions are highly desirable because they allow for rapid and efficient evaluation of the system performance. The analytical results are then confirmed using Monte Carlo simulations. Moreover, the SEP performance of the OFDM-HSTCS is also investigated and the performance degradation due to Doppler spread is studied.

The rest of this dissertation is organized as follows.

[1] The mobile relay nodes can be vehicles or mobile handhelds.

- Chapter 1 describes the HSTCS and cooperative transmission schemes. Both LMS and terrestrial channel models are also discussed. Some special functions used in this dissertation are also presented.

- Chapter 2 focuses on the performance evaluation of the HSTCS. The SDF transmission scheme is implemented and the exact closed-form outage probability and SEP are derived for general MPSK and MQAM modulation schemes over independent but not necessarily identically distributed fading channels.

- In chapter 3, the SDF transmission scheme with the best relay selection is performed and the exact closed-form outage probability and SEP are derived for general MPSK and MQAM modulation schemes over independent but not necessarily identically distributed fading channels.

- Chapter 4 dedicates to the performance analysis of the OFDM-HSTCS. The Doppler spread issue and the system performance degradation are examined.

Chapter 1

Hybrid satellite-terrestrial cooperative systems

Contents

This first chapter describes the HSTCS model, the forwarding schemes, the cooperative mode, the relay selection schemes and the combining techniques. Moreover, the LMS channel and the terrestrial channel models are also presented since it is very important for system performance evaluation. In the last section, some special functions that are used in this dissertation are provided.

1.1 System overview

The architecture of an HSTCS is presented in Fig. 1.1. The transmission scheme is divided into two phases. In the first phase, the satellite broadcasts the satellite signal to the relays and the destination.

In the second phase, the relays forward the satellite signal to the destination.

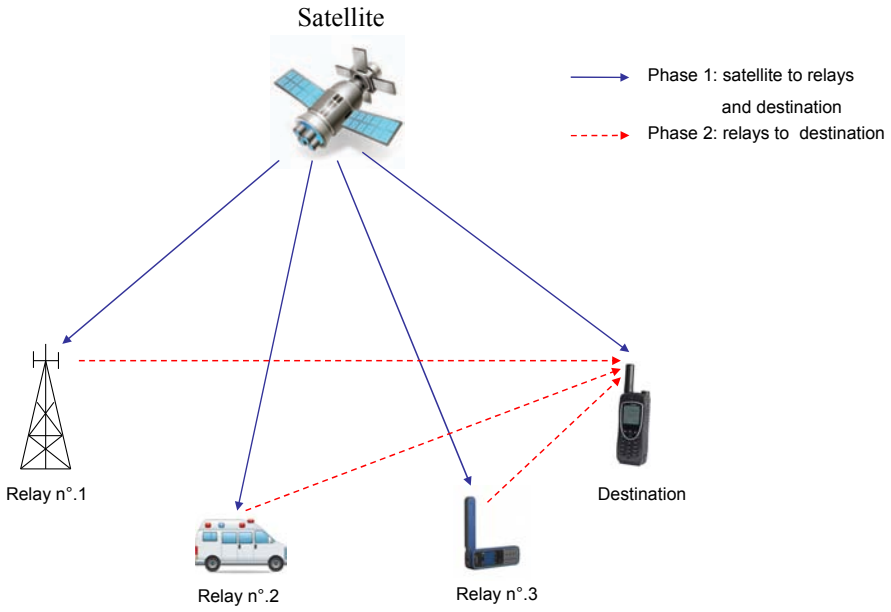

Figure 1.1: HSTCS with 3 relays and one destination.

The destination node can receive the satellite signal from both satellite and the relay nodes. Then, the destination can exploit the spatial diversity by combining the direct and indirect link signals. The relays can be fixed or mobile depending on the scenario. When the LOS link between the satellite and the destination node is not available, the destination node can still receive the satellite signal from the relay links. So, the communication is still possible.

1.1.1 Forwarding schemes

A cooperative scenario with one relay and one destination is presented in Fig 1.2. A typical cooperative scenario can be modeled with two orthogonal phases, Time Division Multiple Access (TDMA) or Frequency Division Multiple Access (FDMA), in order to avoid interference between the two phases.

In a cooperative scenario, the relay can forward the source information to the destination by using the Amplify-and-Forward (AF), Fixed Decode-and-Forward (FDF), or Selective Decode-and-Forward (SDF) transmission schemes [LTW04].

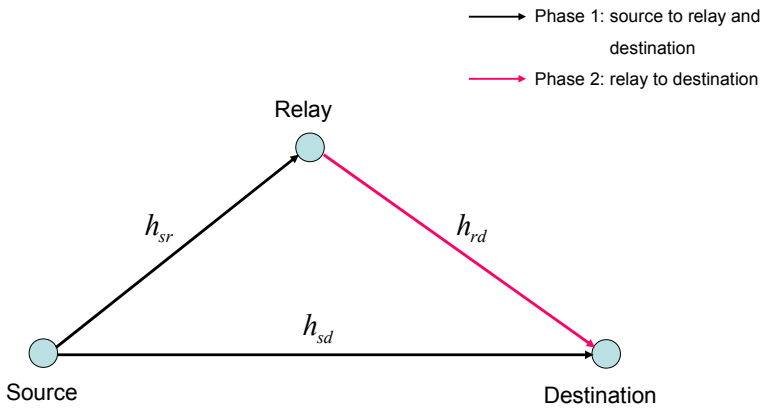

Figure 1.2: Cooperative scenario with one relay and one destination.

In the first phase, the source transmits the information to the relay and the destination node. The base band received signal at the destination, y_{sd}, and at the relay, y_{sr}, can be modeled as follows

$$\begin{aligned} y_{sd} &= \sqrt{P_s} h_{sd} x + n_{sd} \\ y_{sr} &= \sqrt{P_s} h_{sr} x + n_{sr} \end{aligned} \tag{1.1}$$

where P_s is the transmitted power at the source, x is the transmitted symbol, h_{sd} and h_{sr} are the channel coefficients of the source-destination and the source-relay links respectively, and n_{sd} and n_{sr} are the Additive White Gaussian Noise (AWGN) with zero mean and variance N_0.

In the second phase, the relay forwards the source information to the destination node. The

received signal at the destination can be modeled as below

$$y_{rd} = f\left(y_{sr}\right) h_{rd} + n_{rd} \tag{1.2}$$

where the function $f(.)$ depends on the forwarding schemes.

Amplify-and-Forward

In an AF transmission scheme, the relay just only amplifies the received signal from the source and then forwards it to the destination. However, the noise is also amplified. In this case, the function $f\left(y_{sr}\right)$ is a factor and is given by

$$f\left(y_{sr}\right) = \beta_r y_{sr}, \text{ where } \beta_r \leq \frac{\sqrt{P_r}}{\sqrt{P_s|h_{sr}|^2 + N_0}} \tag{1.3}$$

If $P_s = P_r = P$ and β_r takes the maximum value, hence,

$$\beta_r = \frac{\sqrt{P}}{\sqrt{P|h_{sr}|^2 + N_0}}. \tag{1.4}$$

Therefore, the input-output signal model of AF scheme can be modeled as follows

- Phase 1,

$$\begin{aligned} y_{sd} &= \sqrt{P} h_{sd} x + n_{sd} \\ y_{sr} &= \sqrt{P} h_{sr} x + n_{sr} \end{aligned} \tag{1.5}$$

- Phase 2,

$$y_{rd} = \frac{\sqrt{P}}{\sqrt{P|h_{sr}|^2 + N_0}} \sqrt{P} h_{rd} h_{sr} x + n'_{rd} \tag{1.6}$$

where

$$n'_{rd} = \frac{\sqrt{P}}{\sqrt{P|h_{sr}|^2 + N_0}} h_{rd} n_{sr} + n_{rd} \tag{1.7}$$

we assume that n_{sr} and n_{rd} are independent, hence, n'_{rd} is an AWGN with zero mean and variance

$$N'_0 = \left(\frac{P|h_{rd}|^2}{P|h_{sr}|^2 + N_0} + 1\right) N_0. \tag{1.8}$$

Fixed Decode-and-Forward

In an FDF transmission scheme, the relays decode the source message and re-encode before forwarding to the destination. In this scheme, the function $f(y_{sr})$ can be written as

$$f(y_{sr}) = \hat{x} \tag{1.9}$$

where $\hat{x}$ is the decoded symbol.

When the source-relay links are strongly faded, the relays cannot decode the source message correctly. So, the destination will receive an erroneous source message from the relay and this results in a performance degradation.

The input-output signal model of FDF scheme can be modeled as follows

- Phase 1,

$$\begin{aligned} y_{sd} &= \sqrt{P_s} h_{sd} x + n_{sd} \\ y_{sr} &= \sqrt{P_s} h_{sr} x + n_{sr} \end{aligned} \tag{1.10}$$

- Phase 2,

$$y_{rd} = h_{rd} \hat{x} + n_{rd} \tag{1.11}$$

Selective Decode-and-Forward

In an SDF transmission scheme, the process is the same as in the FDF scheme but only the relays that can decode the source message correctly are allowed to forward the signal to the destination node. This prevents the retransmission of erroneous messages to the destination node. The function $f(y_{sr})$ can be written as

$$f(y_{sr}) = \begin{cases} \hat{x}, \text{ if the relay can decode the source message correctly} \\ 0, \text{ otherwise.} \end{cases} \tag{1.12}$$

Therefore, the input-output signal model of SDF scheme can be modeled as follows

- Phase 1,

$$\begin{aligned} y_{sd} &= \sqrt{P_s} h_{sd} x + n_{sd} \\ y_{sr} &= \sqrt{P_s} h_{sr} x + n_{sr} \end{aligned} \tag{1.13}$$

- Phase 2,

$$y_{rd} = \begin{cases} h_{rd}\hat{x} + n_{rd}, & \text{if the relay can decode the source message correctly} \\ 0, & \text{otherwise.} \end{cases} \tag{1.14}$$

Comparison of the AF and SDF diversity gains

The performance comparison of AF, FDF and SDF schemes over Rayleigh fading channels has been studied in [RLSSK09]. The comparison has been done at the high-SNR regime. It has been shown that for a 1-relay system, the AF and SDF schemes provide the same outage probability and the diversity order is equal to 2 while the diversity order of FDF is equal to one.

On the other hand, the SEP performance comparison of AF and SDF schemes can be described as follows.

- When the channel link quality of the source-relay link is much lower than the one of the relay-destination link, the diversity gain of the SDF scheme is higher than the one of the AF scheme.
- When the channel link quality of the source-relay link is much higher than the one of the relay-destination link, the SDF and the AF schemes provide the same performance in terms of diversity gain.
- When the channel link quality of the source-relay link is the same as the one of the relay-destination link, the SDF scheme provides better performance in term of diversity gain than the AF scheme for modulation schemes with high number of constellation point. For modulation schemes with a small number of constellation points, the performance advantage of an SDF scheme is negligible compared with the one of an AF scheme.

We can see that the SEP performance of an SDF scheme is always not lower than the one of an AF scheme.

1.1.2 Relay selection schemes

In a typical cooperative system, the orthogonal channels must be allocated to the direct and the relayed links in order to avoid the interference between each transmission link. So, when the number

of relays increases, the number of the channels is also increasing. This requires more bandwidth consumption. To reduce the bandwidth consumption, relay selection schemes have been proposed in [QB04, BKRL06]. With a relay selection scheme, one or several relays are selected for forwarding the source signal. Since not all the relays are involved in the forwarding scheme, some bandwidth can be saved. Several relay selection schemes have been proposed [BKRL06, SMY10a, QB04, SMY10b]. In this dissertation, we will focus on timer based selection schemes. In the timer based selection schemes of [BKRL06, SMY10a], only one relay is selected. This relay, the best relay, will retransmit the source signal when its timer expires[2]. The main issue consists in designing a selection scheme that avoids the collision of two relays having their timer expiring in the same contention window. However, the timer based selection scheme is attractive because of its simplicity.

In the selection scheme of the best relay [BKRL06], only the relay which provides the highest received SNR at the receiver is allowed to forward the source message to the destination node. So, this scheme requires less bandwidth comparing to the scheme without relay selection. Two criteria for selecting the best relay have been studied in [BKRL06]. The first criterion is to choose the relay which maximizes the minimum of the source-relay and the relay-destination channel gain, while the second criterion is based on the maximization of the harmonic mean of both channel gains. It has been illustrated in [CwSZL10] that the outage performance of both selection techniques are the same in the high-SNR regime.

1.1.3 Combining techniques

Consider a combining system with M received signal branches as represented in Fig. 1.3. Let the received signal from each branch defined by

$$y_i = h_i s + n_i, \text{ for } i = 1, \ldots, M \tag{1.15}$$

where s is the transmitted symbol with the average transmitted power P_s, h_k and n_k represent the complex channel coefficient and the AWGN of the k^{th} branch respectively. The AWGN is assumed to have the variance N_0. So, the average received SNR of the k^{th} branch is given as $\gamma_k = |h_k|^2 \frac{P_s}{N_0}$.

[2]The timer is inversely proportional to the channel gain

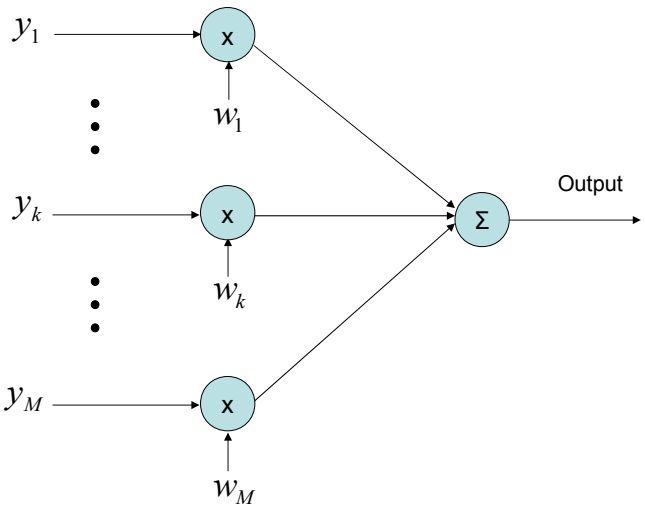

Figure 1.3: Combining system with M branches.

The weighting gain w_k $(k = 1, \ldots, M)$ in Fig. 1.3 depends on the combining technique. The classical combining techniques are Selection Combining (SC), Maximum Ratio Combining (MRC) and Equal Gain Combining (MRC).

Selection combining

In the SC technique, the branch that provides the highest SNR is chosen for further processing. Therefore,

$$w_k = \begin{cases} 1, \text{ if } \gamma_k = \max_{i \in M}(\gamma_i) \\ 0, \text{ otherwise,} \end{cases} \tag{1.16}$$

where γ_i is the SNR of the i^{th} branch.

So, the output SNR of the selection combining is $\gamma_{out} = \max_{i \in M}(\gamma_i)$. Moreover, this selection

scheme requires only the measurement of the signal power while the phase shifter or variable gains are not required.

Maximum ratio combining

In the MRC technique, the weighting coefficient w_k is chosen to maximize the total output SNR. It has been shown in [SA05] that the output SNR is maximized when $w_k = conj(h_k)$.

And the total output SNR is given by

$$\gamma_{out} = \sum_{i=1}^{M} \gamma_i. \tag{1.17}$$

Equal gain combining

In the EGC technique, the coefficient w_k is chosen as

$$w_k = \exp\left(-j\angle h_k\right). \tag{1.18}$$

where $\angle h_k$ is the argument of the complex channel coefficient h_k.

In this case, the total output SNR is given by

$$\gamma_{out} = \frac{\left(\sum_{i=1}^{M} |h_i|\right)^2}{M} \frac{P_s}{N_0}. \tag{1.19}$$

In terms of the complexity, the SC is the easiest technique because it requires only a measurement of the received SNR at each branch. The phase and the amplitude are not needed. On the other hand, both MRC and EGC require the phase information. Furthermore, the measurement of the channel gain is needed too for the MRC technique. However, the MRC is the optimum combining technique and provides better performance than SC and EGC.

1.2 Channel propagation models

The characteristic of the channel propagation can be described by the variation of the received signal over time and frequency. This variation can be divided into two categories, large-scale fading and

small-scale fading. The large-scale fading consists of a long term path loss and the shadowing due to the obstacles such as buildings, trees. The long term path loss depends on the distance and the frequency of the transmitted signal. On the other hand, the small-scale fading is due to constructive and destructive interference of the multipath signal components. This small-scale fading occurs at the spatial scale of the order of the carrier wavelength. The large-scale fading is more relevant to issues such as cell-site planning while the small-scale multipath fading is more relevant to the design of reliable and efficient communication systems.

The received power at the destination side can be modeled by the expression below

$$P_R = P_T G_T G_R k \frac{\lambda^2}{d^\beta} \alpha_{shad} \alpha_{fading} \tag{1.20}$$

where d is the distance from the transmitter to the receiver, P_T is the transmit power, G_T (G_R respectively) is the transmit antenna gain (receive antenna gain respectively). The free-space path loss is characterized by the term $k\lambda^2/d^\beta$, where λ is the wavelength, k is a constant value and β is the path loss exponent ranging from 2 to 6 and depends on the propagation environment. The parameters α_{shad} and α_{fading} are the positive random variables representing the variation of the received power due to shadowing and multipath fading respectively.

1.2.1 Characteristics of fading channels

The characteristics of fading channels can be mainly described by two properties, one based on the multipath time delay spread parameter, and another one based on the Doppler spread parameter.

Slow versus fast fading

This characteristic is very important for the system performance evaluation and is related to the coherence time T_{coh} of the channel, which measures the period of time over which the fading process is correlated in the time domain. The coherence time is inversely proportional to the Doppler spread F_d.

$$T_{coh} \propto \frac{1}{F_d} \tag{1.21}$$

The fading is said to be slow if the symbol time period is much lower than the coherence time, i.e., $T_s < T_{coh}$; otherwise it is considered fast.

Frequency-flat versus frequency-selective fading

This characteristic is also important for the system performance evaluation. The frequency selectivity is related to the coherence bandwidth B_{coh} which is inversely proportional to the maximum delay spread τ_{max}

$$B_{coh} \propto \frac{1}{\tau_{max}} \tag{1.22}$$

The coherence bandwidth measures the frequency range over which the fading process is correlated in the frequency domain. The fading is considered to be frequency-flat when all the signal bandwidth B_s is affected in a similar manner, i.e., $B_s < B_{coh}$; otherwise the channel is considered as frequency-selective.

1.2.2 Terrestrial channel model

Rayleigh

The Rayleigh distribution is used to characterize the multipath fading channel with no LOS link. The probability density function (PDF) of the channel fading amplitude α is given by [SA05]

$$f_\alpha(x) = \frac{x}{b} \exp\left(-\frac{x^2}{2b}\right), \; x \geq 0 \tag{1.23}$$

and the PDF of the channel fading power α^2 is distributed according to an exponential distribution and given by

$$f_{\alpha^2}(y) = \frac{1}{2b} \exp\left(-\frac{y}{2b}\right), \; y \geq 0 \tag{1.24}$$

where $2b$ is the average channel power.

Rice

The Rician distribution is frequently used to model the multipath fading channel consisting of one strong direct LOS link and other indirect links. The PDF of the channel fading amplitude α is given

by [SA05]

$$f_\alpha(x) = \frac{2(1+K)x}{\Omega} \exp\left(-\frac{(1+K)\,x^2}{\Omega} - K\right) I_0\left(2x\sqrt{\frac{K(K+1)}{\Omega}}\right),\ x \geq 0 \tag{1.25}$$

and the PDF of the channel fading power α^2 is distributed according to a noncentral chi-square distribution given by

$$f_{\alpha^2}(y) = \frac{(1+K)}{\Omega} \exp\left(-\frac{(1+K)\,y}{\Omega} - K\right) I_0\left(2\sqrt{\frac{K(K+1)y}{\Omega}}\right),\ y \geq 0 \tag{1.26}$$

where $0 \leq K \leq +\infty$ is the Rice parameter and I_0 is the first order modified Bessel function. When $K = 0$, the Rician channel becomes the Rayleigh channel and it becomes no fading channel when $K \to +\infty$.

Nakagami-m

The Nakagami-m model has been proposed in [Nak60]. The PDF of the channel fading amplitude α is given by

$$f_\alpha(x) = \frac{2m^m x^{2m-1}}{\Omega^m \Gamma(m)} \exp\left(-\frac{mx^2}{\Omega}\right),\ x \geq 0 \tag{1.27}$$

and the PDF of the channel fading power α^2 is distributed according to a Gamma distribution and given by

$$f_{\alpha^2}(y) = \frac{m^m y^{m-1}}{\Omega^m \Gamma(m)} \exp\left(-\frac{my}{\Omega}\right),\ y \geq 0 \tag{1.28}$$

where $\Gamma(.)$ is the Gamma function, Ω is the average power of the multipath component, and m is the fading parameter of the distribution which ranges from the one sided Gaussian distribution ($m = 1/2$) to non-fading AWGN channel ($+\infty$) by passing the Rayleigh distribution ($m = 1$). For $m \geq 1$, we obtain one-to-one mapping between the m parameter and the Rician K factor, allowing the Nakagami-m distribution to closely approximate the Rice distribution, and this mapping is given by

$$K = \frac{\sqrt{m^2 - m}}{m - \sqrt{m^2 - m}} \tag{1.29}$$

$$m = \frac{(K+1)^2}{(2K+1)} \tag{1.30}$$

It has been shown that the Nakagami-m model characterizes well the outdoor radio mobile channel and the multipath indoor channel model as well.

1.2.3 LMS channel models

The land mobile satellite (LMS) channel model is very important for the performance evaluation of the MSSs. On the other hand, the conventional channel models used in the terrestrial propagation cannot be used to characterize the LMS channel because of the differences observed in LOS and shadowing links. The most popular LMS models are Loo's model [Loo85, Loo90, Loo91, LB98], Lutz's model [LCD+91] and Fontan's model [PFVCB+98, FVCC+01, PFHS+08].

Loo's model

In the Loo's model, the amplitude of the LOS component is assumed to be a lognormally distributed while the multipath interference has a Rayleigh distribution. The received complex envelope signal is given in [Loo85] as

$$r\exp(j\theta) = z\exp(j\phi_0) + w\exp(j\phi), \text{ for } z, w > 0 \tag{1.31}$$

where the phases ϕ_0 and ϕ are uniformly distributed between 0 and 2π, z is lognormally distributed and w is Rayleigh distribution.

If z is temporarily kept constant, then the conditional PDF of r is a PDF of Rician distribution

$$f(r|z) = \frac{r}{b_0}\exp\left[-\frac{(r^2+z^2)}{2b_0}\right] I_0\left(\frac{rz}{b_0}\right) \tag{1.32}$$

where $2b_0$ represents the average scattered power due to the multipath components, $I_0(.)$ is the modified Bessel function of the zeroth order.

So, the total PDF of the amplitude r is given as below

$$\begin{aligned} f(r) &= \int_0^{+\infty} f(r|z)f(z)dz \\ &= \frac{r}{(b_0\sqrt{2\pi d_0})}\int_0^{+\infty}\frac{1}{z}\exp\left[-\frac{(\ln z-\mu)^2}{2d_0}\right]\exp\left[-\frac{(r^2+z^2)}{2b_0}\right] I_0\left(\frac{rz}{b_0}\right)dz,\ r\geq 0 \end{aligned} \tag{1.33}$$

where μ and $\sqrt{d_0}$ are the mean and standard deviation of the lognormal distribution respectively.

Lutz's model

The Lutz's model is described by two states, good channel state (Rice model) and bad channel state (Suzuki model).

In a good channel state, the PDF of the received power is given by

$$f_{good}(s) = c \exp\left[-c(s+1)\right] I_0\left(2c\sqrt{s}\right) \tag{1.34}$$

where c is the Rice factor.

In a bad channel state, the PDF of the received power is written as

$$f_{bad}(s) = \int_0^{+\infty} \frac{10}{\sqrt{2\pi}\sigma \ln 10} \frac{1}{s_0^2} \exp\left[-\frac{\left(10\log_{10} s_0 - \mu\right)^2}{2\sigma^2}\right] \exp\left(-\frac{s}{s_0}\right) ds_0. \tag{1.35}$$

And the total PDF which takes into account both two channel states can be written as below

$$f_{total}(s) = (1-A) f_{good}(s) + A f_{bad}(s) \tag{1.36}$$

where A is the time share of bad state channel and $1-A$ is the time share of good state channel.

Fontan's model

The Fontan's model consists of three states, LOS, moderate shadowing and deep shadowing [PFVCB+98, FVCC+01]. Recently, this three-state model has been reviewed and modeled as the two states model [FLCA07, FR08, PCPFB+10]. This two-state are termed, "Good" and "Bad" states, representing a range of LOS-to-moderate shadowing and moderate-to-deed shadowing, respectively.

The original three-state model is described as follows.

- The signal variations within each state are modeled by a Loo's distribution. The three parameters of the each state distribution are α, the direct signal attenuation in dB, ψ, the direct signal standard deviation in dB, and MP, the average multipath power, also in dB.

  The relation between these three parameters and those of Loo's model are

$$\begin{aligned} \alpha(\text{dB relative to LOS}) &= 20\log_{10}\left(e^{\mu}\right) \\ \psi(\text{dB}) &= 20\log_{10}\left(e^{\sqrt{d_0}}\right) \\ MP(\text{dB relative to LOS}) &= 20\log_{10}\left(2b_0\right). \end{aligned} \tag{1.37}$$

- The transitions between states are modeled by a first-order, discret-time Markov chain characterized by two matrices, $\mathbf{W}$, the state probability matrix, and $\mathbf{P}$, the state transition probability matrix.

The parameters of each state distribution, the state probability matrix and the state transition probability matrix can be found in [PFVCB+98, CFV+99].

Shadowed rician model

Recently, a new shadowed Rice model for LMS channels has been proposed [ALAK03]. In this model, the amplitude of the LOS is characterized by the Nakagami distribution and the amplitude of the multipath components is characterized by the Rayleigh distribution. It has been shown that this new model provides a similar fit to the experimental data as the Loo's model but with significantly less computational burden. The PDF of the channel fading amplitude is defined as

$$f(r) = \left(\frac{2b_0 m}{2b_0 m + \Omega}\right)^m \frac{r}{b_0} \exp\left(-\frac{r^2}{2b_0}\right) {}_1F_1\left(m; 1; \frac{\Omega r^2}{2b_0\left(2b_0 m + \Omega\right)}\right), \text{ for } r \geq 0 \tag{1.38}$$

where $2b_0$ is the average power of the scatter component, m is the Nakagami parameter which ranges from 0 to $+\infty$ and Ω is the average power of the LOS component. When $m = 0$, this PDF becomes a Rayleigh PDF and when $m = \infty$, it becomes a Rice PDF.

And the PDF of the channel fading power is given by

$$f(s) = \left(\frac{2b_0 m}{2b_0 m + \Omega}\right)^m \frac{1}{2b_0} \exp\left(-\frac{s}{2b_0}\right) {}_1F_1\left(m; 1; \frac{\Omega s}{2b_0\left(2b_0 m + \Omega\right)}\right), \text{ for } s \geq 0 \tag{1.39}$$

The relation between the parameters of this model (b_0, m, Ω) and Loo's model (b_0, μ, d_0) has been provided in [ALAK03] by

$$\begin{aligned} \mu &= \frac{1}{2}\left[\ln\left(\frac{\Omega}{m}\right) + \Psi\left(m\right)\right] \\ d_0 &= \frac{\Psi'\left(m\right)}{4}. \end{aligned} \tag{1.40}$$

where $\Psi(.)$ and $\Psi'(.)$ are the psi function and its first derivative respectively [MOS66]. Some parameters of the shadowed rician model which corresponding to the Loo's model parameters are given in Table. 1.1 and 1.2.

Table 1.1: Loo's parameters [Loo85, Loo90] and corresponding parameters of shadowed rician model [ALAK03].

	Loo's model			Shadowed Rice model	
	μ	$\sqrt{d_0}$	b_0	m	Ω
Infrequent Light Shadowing (ILS)	0.115	0.115	0.158	19.4	1.29
Frequent Heavy Shadowing (FHS)	-3.914	0.806	0.063	0.739	8.97×10^{-4}
Overall Results (OR)	-0.690	0.230	0.251	5.21	0.278
Average Shadowing (AS)	-0.115	0.161	0.126	10.1	0.835

Table 1.2: Loo's parameters [BS92, KKM97] and corresponding parameters of shadowed rician model [ALAK03].

		Loo's model			Shadowed Rice model	
	Data set no.	μ	$\sqrt{d_0}$	b_0	m	Ω
Data sets of Barts and Stutzman [BS92]	1	-0.341	0.099	0.005	26	0.515
	2	-0.528	0.187	0.0129	7.64	0.372
	3	-0.935	0.128	3.97×10^{-3}	15.8	0.159
	4	-1.092	0.15	0.0126	11.6	0.118
Data set of Karasawa et al. [KKM97]	5	-1.15	0.345	0.0158	2.56	0.123

1.3 Special functions

1.3.1 Gamma function

The Gamma function is defined in [GR07] for all complex numbers except the non-positive integers.

$$\Gamma(z) = \int_0^{+\infty} t^{z-1} e^{-t} dt \tag{1.41}$$

where $z \in C$ and $\mathrm{Re}(z) > 0$. If n is a positive integer,

$$\Gamma(n) = (n-1)!. \tag{1.42}$$

1.3.2 Beta function

This function is defined in [GR07] by

$$B(x,y) = \int_0^1 t^{x-1}(1-t)^{y-1}dt \tag{1.43}$$

where $(x,y) \in C$ and $\mathrm{Re}(x) > 0, \mathrm{Re}(y) > 0$. Another representation of Beta function is represented by

$$B(x,y) = \frac{\Gamma(x)\Gamma(y)}{\Gamma(x+y)} = B(y,x). \tag{1.44}$$

1.3.3 General hypergeometric function

The general hypergeometric function is defined in [GR07] as below

$${}_pF_q(a_1,...,a_p;b_1,...,b_q;z) = \sum_{n=0}^{\infty} \frac{(a_1)_n \ldots (a_p)_n}{(b_1)_n \ldots (b_q)_n \, n!} z^n \tag{1.45}$$

where $(x)_n = \Gamma(x+n)/\Gamma(x)$ is a Pochhammer symbol. This series is convergent when $|z| < 1$.

When $p = q = 1$, ${}_pF_q(.)$ becomes a confluent hypergeometric function ${}_1F_1(.)$ defined by

$${}_1F_1(a;b;z) = \sum_{n=0}^{\infty} \frac{(a)_n}{(b)_n} \frac{z^n}{n!}$$

And when $p = 2$ and $q = 1$, ${}_pF_q(.)$ becomes a gauss hypergeometric function ${}_2F_1(.)$ defined by

$${}_2F_1(a,b;c;z) = \sum_{n=0}^{\infty} \frac{(a)_n \, (b)_n}{(c)_n \, n!} z^n \tag{1.46}$$

1.3.4 Lauricella function

The Lauricella function [Ext76] is defined as

$$\begin{aligned} F_D^{(n)}(a, b_1, \ldots, b_n; c; x_1, \ldots, x_n) &\triangleq \sum_{i_1,\ldots,i_n=0}^{+\infty} \frac{(a)_{i_1+\ldots+i_n}}{(c)_{i_1+\ldots+i_n}} \prod_{j=1}^{n} (b_j)_{i_j} \frac{x_j^{i_j}}{i_j!}, \ \max\{|x_i|\}_{i=1}^{n} < 1 \\ &= \frac{1}{B(a, c-a)} \int_0^1 t^{a-1}(1-t)^{c-a-1} \prod_{i=1}^{n} (1-x_i t)^{-b_i} dt, \\ &\quad \mathrm{Re}(c) > \mathrm{Re}(a) > 0, \end{aligned} \tag{1.47}$$

where $(a)_i \triangleq \Gamma(a+i)/\Gamma(a)$ is the Pochammer symbol for $i \geq 0$, $B(a,b) \triangleq \Gamma(a)\Gamma(b)/\Gamma(a+b)$ denotes the Beta function, and Re(.) denotes the real part. When the number of variables n is equal to one, $F_D^{(1)}$ reduces to a gaussian hypergeometric function ${}_2F_1(a, b_1; c; x_1)$ and when n is equal to two, $F_D^{(2)}$ reduces to an Appell hypergeometric function $F_1(a, b_1, b_2; c; x_1, x_2)$ defined by

$$\begin{aligned} F_1(a, b_1, b_2; c; x_1, x_2) &= \frac{1}{B(a, c-a)} \int_0^1 t^{a-1}(1-t)^{c-a-1}(1-x_1 t)^{-b_1}(1-x_2 t)^{-b_2} dt, \\ &\quad \mathrm{Re}(c) > \mathrm{Re}(a) > 0. \end{aligned} \tag{1.48}$$

Some properties of Lauricella function

$$F_D^{(N+1)}(a, b, e_1, \ldots, e_N; c; x, y, \ldots, y) = F_1(a, b, \sum_{i=1}^{N} e_i; c; x, y) \tag{1.49}$$

$$F_D^{(5)}(a, b_1, b_2, b_3, b_4, b_5; c; x, y, z, 0, 0) = F_D^{(3)}(a, b_1, b_2, b_3; c; x, y, z) \tag{1.50}$$

$$F_D^{(5)}(a, b_1, b_2, b_3, b_4, b_5; c; x, 0, y, z, 0) = F_D^{(3)}(a, b_1, b_3, b_4; c; x, y, z) \tag{1.51}$$

$$F_D^{(5)}(a, b_1, b_2, b_3, b_4, b_5; c; x, y, z, y, z) = F_D^{(3)}(a, b_1, b_2 + b_4, b_3 + b_5; c; x, y, z) \tag{1.52}$$

1.4 Conclusion

In this chapter, the architecture of an HSTCS has been presented. The cooperative transmission schemes have been discussed. The SDF scheme outperforms both the AF and FDF schemes in terms of outage probability and SEP. This SDF scheme is selected for evaluating the HSTCS performance in the next chapters of this dissertation. Furthermore, the terrestrial channel and the LMS channel models have been presented. The shadowed Rice model will be used for the outage probability and the SEP computation in this dissertation since it represents the generalization channel model which provides a similar fit to the experimental data as the Loo's model and with significantly less computational burden.

Chapter 2

Performance analysis of HSTCSs

Contents

In this chapter, we study the performance in terms of the outage probability and the SEP of an HSTCS. An SDF scheme is implemented between a source node (the satellite) and a destination node (a terrestrial station). In the first phase, the satellite broadcasts its signal to all relay nodes and the destination node. In the second phase, only relay nodes which can successfully decode the satellite message are allowed to retransmit the satellite signal. Then, the destination node exploits the diversity gain using the MRC technique.

Furthermore, the exact closed-form expressions of the outage probability and the average SEP of the arbitrary MPSK and MQAM signaling over independent but not necessarily identically distributed fading channels are derived by using the Moment Generating Function (MGF) analysis approach. The outage expressions are represented in terms of a sum of general hypergeometric functions ${}_pF_q(.)$ and the SEP expressions are represented in terms of a finite sum of Lauricella hypergeometric functions $F_{\mathbf{D}}^{(\mathbf{n})}(.)$, which can be numerically computed using their integral or converging series representation. The analytical expressions shows excellent agreement with the simulation results.

2.1 System and channel models

Consider an HSTCS where a satellite (s) transmits information to a destination node (d), with the assistance of L mobile relay nodes r_1, r_2, ..., r_L as shown in Fig. 2.1. The transmission is divided into two phases. In the first phase (broadcasting phase), the satellite broadcasts its signal to the set of L relay nodes and the destination node. The baseband received signal at the destination and the relay r_i can be modeled, respectively, as

$$\begin{aligned} y_{sd} &= \sqrt{E_s} h_{sd} x + n_{sd} \\ y_{sr_i} &= \sqrt{E_s} h_{sr_i} x + n_{sr_i} \end{aligned} \tag{2.1}$$

where E_s is the average transmitted energy per symbol of the satellite, h_{sd} is the channel coefficient between the satellite and the destination, h_{sr_i} is the channel coefficient between the satellite and the relay r_i, x is the transmitted symbol with unit power, n_{sd} and n_{sr_i} are the additive white Gaussian noise (AWGN) of the satellite-destination link and at the satellite-relay r_i link respectively.

We define the decoding set C (with cardinality $|C|$) as the set of relays that can decode the satellite message correctly. The relay node is said to belong to the decoding set provided that the received SNR on a channel between the source and the relay node is high enough to allow for successful decoding. We have $|C| \leq L$. In the second phase (relaying phase), only the relay nodes which belong to the set C are allowed to forward the re-modulated signals to the destination node using orthogonal channels[3]. In the following analysis, we assume that both satellite and terrestrial links use the same modulation scheme. The baseband received signal at the destination from the relay r_i can be modeled as

$$y_{r_i d} = \begin{cases} \sqrt{E_{r_i}} h_{r_i d} \widehat{x} + n_{r_i d}, & \text{when } r_i \in C \\ 0, & \text{otherwise} \end{cases} \tag{2.2}$$

where E_{r_i} is the average transmitted energy per symbol of the relay r_i, $h_{r_i d}$ is the channel coefficient between the relay r_i and the destination, $\widehat{x}$ is the decoded symbol at the relay r_i with unit power and $n_{r_i d}$ is the AWGN of the relay r_i-destination link. In SDF schemes, the decoded symbol $\widehat{x}$ is assumed

[3] These orthogonal channels can be allocated to the relays using Frequency Division Multiple Access (FDMA), Time Division Multiple Access (TDMA) or Space Time Coding (STC).

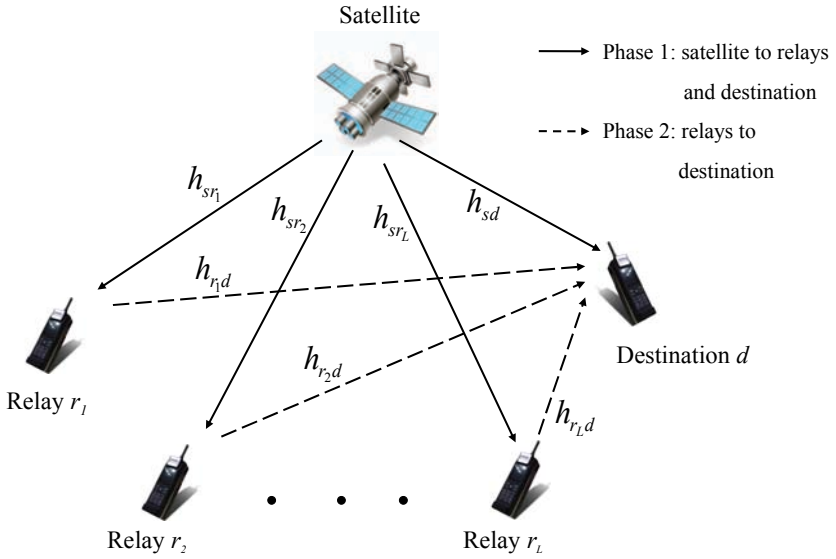

Figure 2.1: Hybrid satellite-terrestrial system with L relays and one destination.

to be error free, i.e., $\widehat{x} = x$. This can be achieved by allowing the decoding of the satellite message only when the received SNR allows for a successful decoding or by using a Cyclic Redundancy Check (CRC). Then the destination combines the direct and the relay links signals using the MRC technique.

We assume that the channels are frequency-flat, slow fading and independent but not necessarily identically distributed fading channels. We also assume that the Channel State Information (CSI) is perfectly known at the receiver and not known at the transmitter[4]. Furthermore, we assume that the AWGN terms of all links have zero mean and equal variance N_0. The statistics of the channel models are defined as follows.

- The satellite-destination and the satellite-relay links are modeled as LMS fading channels [ALAK03]. The probability density function (PDF), $f_{|h_{sx}|^2}(y)$ of the power channel gain, $|h_{sx}|^2$,

[4]Because of the slow fading, accurate channel estimation is possible at receivers.

is given in [ALAK03] as

$$f_{|h_{sx}|^2}(y) = \frac{1}{2b_{sx}} \left(\frac{2b_{sx}m_{sx}}{2b_{sx}m_{sx} + \Omega_{sx}} \right)^{m_{sx}} \exp\left(-\frac{y}{2b_{sx}} \right) \times {}_1F_1\left(m_{sx}; 1; \frac{\Omega_{sx} y}{2b_{sx}\left(2b_{sx}m_{sx} + \Omega_{sx}\right)} \right), \text{for } y > 0 \tag{2.3}$$

where the second subscript $x \equiv d$ and $x \equiv r_i$ when we deal with the satellite to the destination and the satellite to the relay r_i channels respectively. The parameter Ω_{sx} is the average power of the LOS component, $2b_{sx}$ is the average power of the multipath component, and m_{sx} is the Nakagami parameter ranging from 0 to ∞. When $m_{sx} = 0$, the PDF of $|h_{sx}|$ becomes a Rayleigh PDF and when $m_{sx} = \infty$, it becomes a Rice PDF. The function ${}_1F_1(a; b; z)$ is the confluent hypergeometric function defined in [GR07] by

$${}_1F_1(a; b; z) = \sum_{n=0}^{\infty} \frac{(a)_n}{(b)_n} \frac{z^n}{n!}$$

where $(x)_n = x(x+1)...(x+n-1)$.

- The i^{th} relay-destination link is modeled as a Nakagami-m fading channel. The PDF, $f_{|h_{r_i d}|^2}(y)$, of the power channel gain, $|h_{r_i d}|^2$, is defined in [SA05] as

$$f_{|h_{r_i d}|^2}(y) = \frac{(m_{r_i d})^{m_{r_i d}}}{\Gamma(m_{r_i d})(\Omega_{r_i d})^{m_{r_i d}}} y^{m_{r_i d}-1} \exp\left(-\frac{m_{r_i d}}{\Omega_{r_i d}} y \right), \quad \text{for } y > 0 \text{ and } m_{r_i d} \geq 1/2 \tag{2.4}$$

where $\Gamma(.)$ is the Gamma function, $\Omega_{r_i d}$ is the average power of the multipath component and $m_{r_i d}$ is the average power of the LOS component.

2.2 SEP analysis

In this section, we derive the exact closed-form SEP expressions of the HSTCS. First, we evaluate the SEP of the direct link.

2.2.1 Average SEP of the direct link

The instantaneous received SNR of the direct link at the receiver is given by

$$\gamma_{sd} = |h_{sd}|^2 \times \overline{\gamma}_{sd} \tag{2.5}$$

where $\overline{\gamma}_{sd} = E_s/N_0$, is the average transmit SNR per symbol of the satellite-destination link.

So, the PDF of γ_{sd} can be written as

$$\begin{aligned} f_{\gamma_{sd}}(y) &= \frac{1}{\overline{\gamma}_{sd}} \times f_{|h_{sd}|^2}\left(\frac{y}{\overline{\gamma}_{sd}}\right) \\ &= \frac{1}{2b_{sd}\overline{\gamma}_{sd}}\left(\frac{2b_{sd}m_{sd}}{2b_{sd}m_{sd}+\Omega_{sd}}\right)^{m_{sd}} \exp\left(-\frac{y}{2b_{sd}\overline{\gamma}_{sd}}\right) \\ &\times {}_1F_1\left(m_{sd};1;\frac{\Omega_{sd}y}{2b_{sd}\overline{\gamma}_{sd}(2b_{sd}m_{sd}+\Omega_{sd})}\right), \text{for } y>0. \end{aligned} \tag{2.6}$$

Hence, the MGF of γ_{sd} can be evaluated as follows

$$\phi_{\gamma_{sd}}(s) = \mathbb{E}\left[e^{-sy}\right] = \int_0^\infty e^{-sy} f_{\gamma_{sd}}(y)dy \tag{2.7}$$

where $\mathbb{E}$ [.] is the mathematical expectation operation. By using the table of integrals in [GR07], $\phi_{\gamma_{sd}}(s)$ can be expressed as below

$$\phi_{\gamma_{sd}}(s) = \frac{(2b_{sd}m_{sd})^{m_{sd}}\left(1+2b_{sd}\overline{\gamma}_{sd}s\right)^{m_{sd}-1}}{\left[\left(2b_{sd}m_{sd}+\Omega_{sd}\right)\left(1+2b_{sd}\overline{\gamma}_{sd}s\right)-\Omega_{sd}\right]^{m_{sd}}}. \tag{2.8}$$

Using the MGF-based analysis method [SA05], we will, in the following parts, derive the closed-form error rates for several modulation schemes in uncorrelated fading channels.

M-ary phase-shift keying (MPSK)

The average SEP of the direct link for coherent MPSK signals is given by [AT01]

$$\begin{aligned} P_{sd,MPSK}(E) &= \frac{1}{\pi}\int_0^{\pi-\frac{\pi}{M}} \phi_{\gamma_{sd}}\left(\frac{g_{MPSK}}{\sin^2\theta}\right) d\theta \\ &= \underbrace{\frac{1}{\pi}\int_0^{\frac{\pi}{2}} \phi_{\gamma_{sd}}\left(\frac{g_{MPSK}}{\sin^2\theta}\right) d\theta}_{I^{sd}_{1,MPSK}} + \underbrace{\frac{1}{\pi}\int_{\frac{\pi}{2}}^{\pi-\frac{\pi}{M}} \phi_{\gamma_{sd}}\left(\frac{g_{MPSK}}{\sin^2\theta}\right) d\theta}_{I^{sd}_{2,MPSK}} \end{aligned} \tag{2.9}$$

where

$$g_{MPSK} = \sin^2(\pi/M). \tag{2.10}$$

The first integral

$$I^{sd}_{1,MPSK} = \frac{1}{\pi}\int_0^{\frac{\pi}{2}} \phi_{\gamma_{sd}}\left(\frac{g_{MPSK}}{\sin^2\theta}\right) d\theta \tag{2.11}$$

can be calculated by replacing (2.8) into (2.9) and changing the variable $t = \cos^2(\theta)$ and using the equation 1.48 below

$$\begin{aligned} F_1(a,b_1,b_2;c;x_1,x_2) &= \frac{1}{B(a,c-a)}\int_0^1 t^{a-1}(1-t)^{c-a-1}(1-x_1t)^{-b_1}(1-x_2t)^{-b_2}dt, \\ &\quad \mathrm{Re}(c) > \mathrm{Re}(a) > 0, \end{aligned}$$

where $B(a,b) \triangleq \Gamma(a)\Gamma(b)/\Gamma(a+b)$ denotes the Beta function, and Re(.) denotes the real part.

Hence, $I^{sd}_{1,MPSK}$ can be obtained as

$$I^{sd}_{1,MPSK} = \frac{(2b_{sd}m_{sd})^{m_{sd}}\, G^{m_{sd}-1}_{1,MPSK}}{4G^{m_{sd}}_{2,MPSK}} F_1\left(\frac{1}{2}, 1-m_{sd}, m_{sd}; 2; \frac{1}{G_{1,MPSK}}, \frac{2b_{sd}m_{sd}}{G_{2,MPSK}}\right) \tag{2.12}$$

where

$$\begin{aligned} G_{1,MPSK} &= 1 + 2b_{sd}\overline{\gamma}_{sd}g_{MPSK}, \\ G_{2,MPSK} &= 2b_{sd}m_{sd} + 2b_{sd}\overline{\gamma}_{sd}g_{MPSK}(2b_{sd}m_{sd} + \Omega_{sd}). \end{aligned} \tag{2.13}$$

The second integral $I^{sd}_{2,MPSK}$ can be rewritten as

$$I^{sd}_{2,MPSK} = \frac{1}{\pi}\int_{\frac{\pi}{M}}^{\frac{\pi}{2}} \phi_{\gamma_{sd}}\left(\frac{g_{MPSK}}{\sin^2\theta}\right) d\theta. \tag{2.14}$$

Making the variable change $t = \cos^2(\theta) / \cos^2(\pi/M)$, we have the closed-form for $I^{sd}_{2,MPSK}$ as shown below

$$I^{sd}_{2,MPSK} = \frac{\sqrt{\omega}\,(2b_{sd}m_{sd})^{m_{sd}}\,G^{m_{sd}-1}_{1,MPSK}}{\pi G^{m_{sd}}_{2,MPSK}} F^{(3)}_D\left(\frac{1}{2}, -\frac{1}{2}, 1-m_{sd}, m_{sd}; \frac{3}{2}; \omega, \frac{\omega}{G_{1,MPSK}}, \frac{2b_{sd}m_{sd}\omega}{G_{2,MPSK}}\right) \tag{2.15}$$

where $\omega = 1 - g_{MPSK}$ and $F^{(3)}_D$ is the Lauricella function [Ext76] defined in equation 1.47 as.

$$\begin{aligned} F^{(n)}_D(a, b_1, \ldots, b_n; c; x_1, \ldots, x_n) &\triangleq \sum_{i_1,\ldots,i_n=0}^{+\infty} \frac{(a)_{i_1+\ldots+i_n}}{(c)_{i_1+\ldots+i_n}} \prod_{j=1}^{n} (b_j)_{i_j} \frac{x_j^{i_j}}{i_j!},\ \max\{|x_i|\}_{i=1}^{n} < 1 \\ &= \frac{1}{B(a, c-a)} \times \int_0^1 t^{a-1}(1-t)^{c-a-1} \prod_{i=1}^{n} (1-x_i t)^{-b_i} dt, \\ &\mathrm{Re}(c) > \mathrm{Re}(a) > 0, \end{aligned}$$

where $(a)_i \triangleq \Gamma(a+i)/\Gamma(a)$ is the Pochammer symbol for $i \geq 0$, $B(a,b) \triangleq \Gamma(a)\Gamma(b)/\Gamma(a+b)$ denotes the Beta function, and Re(.) denotes the real part.

So, the average SEP of the direct link, $P_{sd,MPSK}(E)$ is finally given as follows

$$\begin{aligned} P_{sd,MPSK}(E) = &\frac{(2b_{sd}m_{sd})^{m_{sd}}\,G^{m_{sd}-1}_{1,MPSK}}{4G^{m_{sd}}_{2,MPSK}} F_1\left(\frac{1}{2}, 1-m_{sd}, m_{sd}; 2; \frac{1}{G_{1,MPSK}}, \frac{2b_{sd}m_{sd}}{G_{2,MPSK}}\right) \\ &+ \frac{\sqrt{\omega}\,(2b_{sd}m_{sd})^{m_{sd}}\,G^{m_{sd}-1}_{1,MPSK}}{\pi G^{m_{sd}}_{2,MPSK}} F^{(3)}_D\left(\frac{1}{2}, -\frac{1}{2}, 1-m_{sd}, m_{sd}; \frac{3}{2}; \omega, \frac{\omega}{G_{1,MPSK}}, \frac{2b_{sd}m_{sd}\omega}{G_{2,MPSK}}\right). \end{aligned} \tag{2.16}$$

M-ary quadrature amplitude modulation (MQAM)

The average SEP of the direct link for coherent MQAM signals is given by [AT01]

$$P_{sd,MQAM}(E) = \underbrace{\frac{4q}{\pi}\int_0^{\frac{\pi}{2}} \phi_{\gamma_{sd}}\left(\frac{g_{MQAM}}{\sin^2\theta}\right) d\theta}_{I^{sd}_{1,MQAM}} - \underbrace{\frac{4q^2}{\pi}\int_0^{\frac{\pi}{4}} \phi_{\gamma_{sd}}\left(\frac{g_{MQAM}}{\sin^2\theta}\right) d\theta}_{I^{sd}_{2,MQAM}} \tag{2.17}$$

where $g_{MQAM} = 3/2(M-1)$ and $q = \left(1 - 1/\sqrt{M}\right)$. Using the same computation as in (2.11), the first integral

$$I_{1,MQAM}^{sd} = \frac{4q}{\pi} \int_0^{\frac{\pi}{2}} \phi_{\gamma_{sd}} \left(\frac{g_{MQAM}}{\sin^2 \theta} \right) d\theta \tag{2.18}$$

can be obtained as

$$I_{1,MQAM}^{sd} = \frac{q \left(2b_{sd} m_{sd}\right)^{m_{sd}} G_{1,MQAM}^{m_{sd}-1}}{G_{2,MQAM}^{m_{sd}}} F_1 \left(\frac{1}{2}, 1 - m_{sd}, m_{sd}; 2; \frac{1}{G_{1,MQAM}}, \frac{2b_{sd} m_{sd}}{G_{2,MQAM}} \right) \tag{2.19}$$

where

$$\begin{aligned} G_{1,MQAM} &= 1 + 2b_{sd} \overline{\gamma}_{sd} g_{MQAM}, \\ G_{2,MQAM} &= 2b_{sd} m_{sd} + 2b_{sd} \overline{\gamma}_{sd} g_{MQAM} \left(2b_{sd} m_{sd} + \Omega_{sd}\right). \end{aligned} \tag{2.20}$$

Making the change of variable $t = 1 - \tan^2 \theta$ in the second integral

$$I_{2,MQAM}^{sd} = \frac{4q^2}{\pi} \int_0^{\frac{\pi}{4}} \phi_{\gamma_{sd}} \left(\frac{g_{MQAM}}{\sin^2 \theta} \right) d\theta \tag{2.21}$$

we can find the closed-form as shown below

$$I_{2,MQAM}^{sd} = \frac{2q^2 \left(2b_{sd} m_{sd}\right)^{m_{sd}} L_{1,MQAM}^{m_{sd}-1}}{3\pi L_{2,MQAM}^{m_{sd}}} F_D^{(3)} \left(1, 1, 1 - m_{sd}, m_{sd}; \frac{5}{2}; \frac{1}{2}, \frac{G_{1,MQAM}}{L_{1,MQAM}}, \frac{G_{2,MQAM}}{L_{2,MQAM}} \right) \tag{2.22}$$

where

$$\begin{aligned} L_{1,MQAM} &= 1 + 4b_{sd} \overline{\gamma}_{sd} g_{MQAM}, \\ L_{2,MQAM} &= 2b_{sd} m_{sd} + 4b_{sd} \overline{\gamma}_{sd} g_{MQAM} (2b_{sd} m_{sd} + \Omega_{sd}). \end{aligned} \tag{2.23}$$

So, the average SEP of the direct link, $P_{sd,MQAM}(E)$, is finally given by

$$\begin{aligned} P_{sd,MQAM}(E) = &\frac{q \left(2b_{sd} m_{sd}\right)^{m_{sd}} G_{1,MQAM}^{m_{sd}-1}}{G_{2,MQAM}^{m_{sd}}} F_1 \left(\frac{1}{2}, 1 - m_{sd}, m_{sd}; 2; \frac{1}{G_{1,MQAM}}, \frac{2b_{sd} m_{sd}}{G_{2,MQAM}} \right) \\ &- \frac{2q^2 \left(2b_{sd} m_{sd}\right)^{m_{sd}} L_{1,MQAM}^{m_{sd}-1}}{3\pi L_{2,MQAM}^{m_{sd}}} F_D^{(3)} \left(1, 1, 1 - m_{sd}, m_{sd}; \frac{5}{2}; \frac{1}{2}, \frac{G_{1,MQAM}}{L_{1,MQAM}}, \frac{G_{2,MQAM}}{L_{2,MQAM}} \right). \end{aligned} \tag{2.24}$$

2.2.2 Average SEP of the HSTCS

In this subsection, we evaluate the closed-form SEP of the HSTCS. The MGF of the total instantaneous received SNR at the MRC output is first derived. Then, we use this MGF to evaluate the average SEP.

The instantaneous received SNR

The instantaneous received SNR at the output of the MRC is given as

$$\gamma_{MRC}^{SDF} = \gamma_{sd} + \sum_{i \in C} \gamma_{r_i d}. \tag{2.25}$$

Actually, it will be difficult to find the PDF of γ_{MRC}^{SDF} given in (2.25) because the decoding set C is unknown. To treat this problem we invoke the technique described in [BH06], where the system in Fig. 2.1 can be considered as a communication system consisting of $L+1$ effective paths between the satellite and the destination. Let path number 0 be the s to d direct link and path i be the $s \to r_i \to d$ relayed link where $i = 1, ..., L$. Let χ_i be the instantaneous received SNR of the relayed link i at the destination which takes into account both the s to r_i and the r_i to d link. Therefore, the PDF of χ_i can be obtained as

$$\begin{aligned} f_{\chi_i}(y) = {} & f_{\chi_i | r_i \text{ Decodes Incorrectly}}(y) \Pr\left[r_i \text{ Decodes Incorrectly}\right] \\ & + f_{\chi_i | r_i \text{ Decodes Correctly}}(y) \Pr\left[r_i \text{ Decodes Correctly}\right]. \end{aligned} \tag{2.26}$$

So, equation (2.25) can be rewritten as

$$\gamma_{MRC}^{SDF} = \gamma_{sd} + \sum_{i=1}^{L} \chi_i = \gamma_{sd} + \gamma_{DF} \tag{2.27}$$

where

$$\gamma_{DF} = \sum_{i=1}^{L} \chi_i. \tag{2.28}$$

The probability that the relay r_i decodes incorrectly is the average SEP, P_{sr_i}, of the satellite-relay r_i link. And the probability that the relay r_i decodes correctly is $(1 - P_{sr_i})$. This P_{sr_i} can be calculated by using the same approach as in (2.9) for the MPSK modulation scheme and as in (2.17)

for the MQAM modulation scheme. The expressions of P_{sr_i} are given by equations (2.29) and (2.30) for MPSK and MQAM modulation schemes respectively.

$$P_{sr_i,MPSK}(E) = \frac{(2b_{sr_i}m_{sr_i})^{m_{sr_i}}\, U_{1,MPSK}^{m_{sr_i}-1}}{4U_{2,MPSK}^{m_{sr_i}}} F_1\left(\frac{1}{2}, 1-m_{sr_i}, m_{sr_i}; 2; \frac{1}{U_{1,MPSK}}, \frac{2b_{sr_i}m_{sr_i}}{U_{2,MPSK}}\right) + \frac{\sqrt{\omega}\,(2b_{sr_i}m_{sr_i})^{m_{sr_i}}\, U_{1,MPSK}^{m_{sr_i}-1}}{\pi U_{2,MPSK}^{m_{sr_i}}} F_D^{(3)}\left(\frac{1}{2}, -\frac{1}{2}, 1-m_{sr_i}, m_{sr_i}; \frac{3}{2}; \omega, \frac{\omega}{U_{1,MPSK}}, \frac{2b_{sr_i}m_{sr_i}\omega}{U_{2,MPSK}}\right) \tag{2.29}$$

$$P_{sr_i,MQAM}(E) = \frac{q\,(2b_{sr_i}m_{sr_i})^{m_{sr_i}}\, U_{1,MQAM}^{m_{sr_i}-1}}{U_{2,MQAM}^{m_{sr_i}}} F_1\left(\frac{1}{2}, 1-m_{sr_i}, m_{sr_i}; 2; \frac{1}{U_{1,MQAM}}, \frac{2b_{sr_i}m_{sr_i}}{U_{2,MQAM}}\right) - \frac{2q^2\,(2b_{sr_i}m_{sr_i})^{m_{sr_i}}\, V_{1,MQAM}^{m_{sr_i}-1}}{3\pi V_{2,MQAM}^{m_{sr_i}}} F_D^{(3)}\left(1, 1, 1-m_{sr_i}, m_{sr_i}; \frac{5}{2}; \frac{1}{2}, \frac{U_{1,MQAM}}{V_{1,MQAM}}, \frac{U_{2,MQAM}}{V_{2,MQAM}}\right) \tag{2.30}$$

where

$$U_{1,MPSK} = 1 + 2b_{sr_i}\overline{\gamma}_{sr_i}g_{MPSK},\ U_{2,MPSK} = 2b_{sr_i}m_{sr_i} + 2b_{sr_i}\overline{\gamma}_{sr_i}g_{MPSK}(2b_{sr_i}m_{sr_i} + \Omega_{sr_i}),$$

$$U_{1,MQAM} = 1 + 2b_{sr_i}\overline{\gamma}_{sr_i}g_{MQAM},\ U_{2,MQAM} = 2b_{sr_i}m_{sr_i} + 2b_{sr_i}\overline{\gamma}_{sr_i}g_{MQAM}(2b_{sr_i}m_{sr_i} + \Omega_{sr_i}),$$

$$V_{1,MQAM} = 1 + 4b_{sr_i}\overline{\gamma}_{sr_i}g_{MQAM},\ V_{2,MQAM} = 2b_{sr_i}m_{sr_i} + 4b_{sr_i}\overline{\gamma}_{sr_i}g_{MQAM}(2b_{sr_i}m_{sr_i} + \Omega_{sr_i}).$$

The conditional PDF of $f_{\chi_i|r_i \text{ Decodes Incorrectly}}(y)$ is given by

$$f_{\chi_i|r_i \text{ Decodes Incorrectly}}(y) = \delta(y) \tag{2.31}$$

where $\delta(y)$ is the Dirac Delta function. And the conditional PDF of $f_{\chi_i|r_i \text{ Decodes Correctly}}(y)$ is given by

$$\begin{aligned} f_{\chi_i|r_i \text{ Decodes Correctly}}(y) &= \frac{1}{\overline{\gamma}_{r_id}} \times f_{|h^2_{r_id}|}\left(\frac{y}{\overline{\gamma}_{r_id}}\right) \\ &= \frac{(m_{r_id})^{m_{r_id}}}{\Gamma(m_{r_id})(\Omega_{r_id}\overline{\gamma}_{r_id})^{m_{r_id}}} \times y^{m_{r_id}-1} \exp\left(-\frac{m_{r_id}}{\Omega_{r_id}\overline{\gamma}_{r_id}}y\right) \end{aligned} \tag{2.32}$$

where $\overline{\gamma}_{r_id} = E_{r_i}/N_0$ is the average transmit SNR per symbol of the relay r_i.

Therefore, the equation (2.63) can be written as

$$f_{\chi_i}(y) = P_{sr_i}\delta(y) + (1-P_{sr_i})\frac{(m_{r_id})^{m_{r_id}}}{\Gamma(m_{r_id})(\Omega_{r_id}\overline{\gamma}_{r_id})^{m_{r_id}}} \times y^{m_{r_id}-1} \exp\left(-\frac{m_{r_id}}{\Omega_{r_id}\overline{\gamma}_{r_id}}y\right). \tag{2.33}$$

MGF of the total received SNR

The MGF of γ_{MRC}^{SDF} can be obtained as

$$\phi_{\gamma_{MRC}^{SDF}}(s) = \phi_{\gamma_{sd}}(s) \prod_{i=1}^{L} \phi_{\chi_i}(s) \tag{2.34}$$

where $\phi_{\chi_i}(s)$ is the MGF of χ_i and given by

$$\phi_{\chi_i}(s) = \int_0^\infty e^{-sy} f_{\chi_i}(y) dy = P_{sr_i} + (1 - P_{sr_i}) \left(\frac{m_{r_i d}}{m_{r_i d} + s\overline{\gamma}_{r_i d} \Omega_{r_i d}} \right)^{m_{r_i d}}. \tag{2.35}$$

By using the following property,

$$\prod_{k=1}^{L} (1 + A_k) = 1 + \sum_{k=1}^{L} \sum_{\lambda_1=1}^{L-k+1} \sum_{\lambda_2=\lambda_1+1}^{L-k+2} \cdots \sum_{\lambda_k=\lambda_{k-1}+1}^{L} \prod_{n=1}^{k} A_{\lambda_n}, \tag{2.36}$$

the MGF of γ_{MRC}^{SDF} is finally given by

$$\begin{aligned} \phi_{\gamma_{MRC}^{SDF}}(s) = {} & \phi_{\gamma_{sd}}(s) \left(\prod_{i=1}^{L} P_{sr_i} \right) + \phi_{\gamma_{sd}}(s) \left(\prod_{i=1}^{L} P_{sr_i} \right) \\ & \times \sum_{k=1}^{L} \sum_{\lambda_1=1}^{L-k+1} \sum_{\lambda_2=\lambda_1+1}^{L-k+2} \cdots \sum_{\lambda_k=\lambda_{k-1}+1}^{L} \prod_{n=1}^{k} \left(\frac{1 - P_{sr_{\lambda_n}}}{P_{sr_{\lambda_n}}} \right) \left(1 + s \frac{\overline{\gamma}_{r_{\lambda_n} d} \Omega_{r_{\lambda_n} d}}{m_{r_{\lambda_n} d}} \right)^{-m_{r_{\lambda_n} d}}. \end{aligned} \tag{2.37}$$

M-ary phase-shift keying (M-PSK)

The average SEP of the HSTCS for coherent MPSK signals is given by [AT01]

$$P_{s,MPSK}^{SDF}(E) = \frac{1}{\pi} \int_0^{\pi - \frac{\pi}{M}} \phi_{\gamma_{MRC}^{SDF}} \left(\frac{g_{MPSK}}{\sin^2 \theta} \right) d\theta \tag{2.38}$$

where $g_{MPSK} = \sin^2(\pi/M)$. By using the same computation as (2.9), we can get $P^{SDF}_{s,MPSK}(E)$ as shown below

$$
\begin{aligned}
P^{SDF}_{s,MPSK}(E) = {} & \frac{(2b_{sd}m_{sd})^{m_{sd}}\, G^{m_{sd}-1}_{1,MPSK}}{4G^{m_{sd}}_{2,MPSK}} \left(\prod_{i=1}^{L} P_{sr_i}\right) F_1\left(\frac{1}{2}, 1-m_{sd}, m_{sd}; 2; \frac{1}{G_{1,MPSK}}, \frac{2b_{sd}m_{sd}}{G_{2,MPSK}}\right) \\
& + \frac{\sqrt{\omega}\,(2b_{sd}m_{sd})^{m_{sd}}\, G^{m_{sd}-1}_{1,MPSK}}{\pi G^{m_{sd}}_{2,MPSK}} \left(\prod_{i=1}^{L} P_{sr_i}\right) \\
& \times F^{(3)}_D\left(\frac{1}{2}, -\frac{1}{2}, 1-m_{sd}, m_{sd}; \frac{3}{2}; \omega, \frac{\omega}{G_{1,MPSK}}, \frac{2b_{sd}m_{sd}\omega}{G_{2,MPSK}}\right) \\
& + \frac{(2b_{sd}m_{sd})^{m_{sd}}\, G^{m_{sd}-1}_{1,MPSK}}{2\pi G^{m_{sd}}_{2,MPSK}} \left(\prod_{i=1}^{L} P_{sr_i}\right) \sum_{k=1}^{L} \sum_{\lambda_1=1}^{L-k+1} \sum_{\lambda_2=\lambda_1+1}^{L-k+2} \cdots \sum_{\lambda_k=\lambda_{k-1}+1}^{L} \\
& \prod_{n=1}^{k} \left(\frac{1-P_{sr_{\lambda_n}}}{P_{sr_{\lambda_n}}}\right) \left(\frac{m_{r_{\lambda_n}d}}{H_{\lambda_n,MPSK}}\right)^{m_{r_{\lambda_n}d}} \frac{\Gamma\left(\frac{1}{2}\right)\Gamma\left(\frac{3}{2}+\sum_{n=1}^{k} m_{r_{\lambda_n}d}\right)}{\Gamma\left(2+\sum_{n=1}^{k} m_{r_{\lambda_n}d}\right)} F^{(k+2)}_D\left(\frac{1}{2}, 1-m_{sd},\right. \\
& \left. m_{sd}, m_{r_{\lambda_1}d}, \ldots, m_{r_{\lambda_k}d}; 2+\sum_{n=1}^{k} m_{r_{\lambda_n}d}; \frac{1}{G_{1,MPSK}}, \frac{2b_{sd}m_{sd}}{G_{2,MPSK}}, \frac{m_{r_{\lambda_1}d}}{H_{\lambda_1,MPSK}}, \ldots, \frac{m_{r_{\lambda_k}d}}{H_{\lambda_k,MPSK}}\right) \\
& + \frac{\sqrt{\omega}\,(2b_{sd}m_{sd})^{m_{sd}}\, G^{m_{sd}-1}_{1,MPSK}}{\pi G^{m_{sd}}_{2,MPSK}} \left(\prod_{i=1}^{L} P_{sr_i}\right) \sum_{k=1}^{L} \sum_{\lambda_1=1}^{L-k+1} \sum_{\lambda_2=\lambda_1+1}^{L-k+2} \cdots \sum_{\lambda_k=\lambda_{k-1}+1}^{L} \\
& \prod_{n=1}^{k} \left(\frac{1-P_{sr_{\lambda_n}}}{P_{sr_{\lambda_n}}}\right) \left(\frac{m_{r_{\lambda_n}d}}{H_{\lambda_n,MPSK}}\right)^{m_{r_{\lambda_n}d}} F^{(k+3)}_D\left(\frac{1}{2}, -\frac{1}{2}-\sum_{n=1}^{k} m_{r_{\lambda_n}d}, 1-m_{sd}, m_{sd},\right. \\
& \left. m_{r_{\lambda_1}d}, \ldots, m_{r_{\lambda_k}d}; \frac{3}{2}; \omega, \frac{\omega}{G_{1,MPSK}}, \frac{2b_{sd}m_{sd}\omega}{G_{2,MPSK}}, \frac{m_{r_{\lambda_1}d}\omega}{H_{\lambda_1,MPSK}}, \ldots, \frac{m_{r_{\lambda_k}d}\omega}{H_{\lambda_k,MPSK}}\right)
\end{aligned}
\tag{2.39}
$$

where

$$
H_{\lambda_n,MPSK} = m_{r_{\lambda_n}d} + g_{MPSK}\Omega_{r_{\lambda_n}d}\overline{\gamma}_{r_{\lambda_n}d}. \tag{2.40}
$$

In the case of independent and identically distributed (i.i.d) fading channels, all relays are experiencing the same fading environment, i.e., $m_{sr_i} = m_{sr}$, $b_{sr_i} = b_{sr}$, $\Omega_{sr_i} = \Omega_{sr}$ and $b_{r_id} = b_{rd}$ for all $i \in L$. Moreover, we assume that $\overline{\gamma}_{r_id} = \overline{\gamma}_{rd} = \overline{\gamma}$ for all $i \in L$. So, $H_{i,MPSK} = H_{MPSK}$ for all $i \in L$.

By using the properties of the Lauricella function as shown below

$$\begin{aligned} F_D^{(2L+N)}(a, b_1, \ldots, b_N, d, e, \ldots, d, e; c; x_1, \ldots, x_N, y, z, \ldots, y, z) \\ = F_D^{N+2}(a, b_1, \ldots, b_N, Ld, Le; c; x_1, \ldots, x_N, y, z), \\ \text{for } |y| < 1 \text{ and } |z| < 1, \end{aligned} \tag{2.41}$$

the average SEP, $P_{s,MPSK}^{SDF}(E)$ can be simplified as in equation (2.42).

$$\begin{aligned} P_{s,MPSK}^{SDF}(E) = & \frac{(2b_{sd}m_{sd})^{m_{sd}} G_{1,MPSK}^{m_{sd}-1}}{2\pi G_{2,MPSK}^{m_{sd}}} (P_{sr})^L \sum_{k=0}^{L} \binom{L}{k} \left(\frac{1-P_{sr}}{P_{sr}}\right)^k \left(\frac{m_{rd}}{H_{MPSK}}\right)^{km_{rd}} \frac{\Gamma\left(\frac{1}{2}\right)\Gamma\left(\frac{3}{2}+km_{rd}\right)}{\Gamma\left(2+km_{rd}\right)} \\ & \times F_D^{(3)}\left(\frac{1}{2}, 1-m_{sd}, m_{sd}, km_{rd}; 2+km_{rd}; \frac{1}{G_{1,MPSK}}, \frac{2b_{sd}m_{sd}}{G_{2,MPSK}}, \frac{m_{rd}}{H_{MPSK}}\right) \\ & + \frac{\sqrt{\omega}\,(2b_{sd}m_{sd})^{m_{sd}} G_{1,MPSK}^{m_{sd}-1}}{\pi G_{2,MPSK}^{m_{sd}}} (P_{sr})^L \sum_{k=0}^{L} \binom{L}{k} \left(\frac{1-P_{sr}}{P_{sr}}\right)^k \left(\frac{m_{rd}}{H_{MPSK}}\right)^{km_{rd}} \\ & \times F_D^{(4)}\left(\frac{1}{2}, -\frac{1}{2}-km_{rd}, 1-m_{sd}, m_{sd}, km_{rd}; \frac{3}{2}; \omega, \frac{\omega}{G_{1,MPSK}}, \frac{2b_{sd}m_{sd}\omega}{G_{2,MPSK}}, \frac{m_{rd}\omega}{H_{MPSK}}\right). \end{aligned} \tag{2.42}$$

In the special case where the Nakagami-m parameter $m_{r_id} = 1$***, all relay-destination links are Rayleigh fading channels. Equation (2.39) becomes as follows***

$$\begin{aligned} P_{s,MPSK}^{SDF}(E) = & \frac{(2b_{sd}m_{sd})^{m_{sd}} G_{1,MPSK}^{m_{sd}-1}}{4G_{2,MPSK}^{m_{sd}}} \prod_{i=1}^{L} \left(\frac{H_{i,MPSK}}{K_{i,MPSK}}\right) F_D^{(2L+2)}\left(\frac{1}{2}, 1-m_{sd}, m_{sd}, -1, 1, \ldots,\right. \\ & \left. -1, 1; 2; \frac{1}{G_{1,MPSK}}, \frac{2b_{sd}m_{sd}}{G_{2,MPSK}}, \frac{1}{H_{1,MPSK}}, \frac{1}{K_{1,MPSK}}, \ldots, \frac{1}{H_{L,MPSK}}, \frac{1}{K_{L,MPSK}}\right) \\ & + \frac{\sqrt{\omega}\,(2b_{sd}m_{sd})^{m_{sd}} G_{1,MPSK}^{m_{sd}-1}}{\pi G_{2,MPSK}^{m_{sd}}} \prod_{i=1}^{L} \left(\frac{H_{i,MPSK}}{K_{i,MPSK}}\right) F_D^{(2L+3)}\left(\frac{1}{2}, -\frac{1}{2}, 1-m_{sd}, m_{sd}, -1, 1, \ldots,\right. \\ & \left. -1, 1; \frac{3}{2}; \omega, \frac{\omega}{G_{1,MPSK}}, \frac{2b_{sd}m_{sd}\omega}{G_{2,MPSK}}, \frac{\omega}{H_{1,MPSK}}, \frac{\omega}{K_{1,MPSK}}, \ldots, \frac{\omega}{H_{L,MPSK}}, \frac{\omega}{K_{L,MPSK}}\right) \end{aligned} \tag{2.43}$$

where

$$\begin{aligned} H_{i,MPSK} &= 1 + P_{sr_i,MPSK}\Omega_{r_id}\overline{\gamma}_{r_id}g_{MPSK}, \\ K_{i,MPSK} &= 1 + \Omega_{r_id}\overline{\gamma}_{r_id}g_{MPSK}. \end{aligned} \tag{2.44}$$

And equation (2.42) changes to the expression below

$$
\begin{aligned}
P_{s,MPSK}^{SDF}(E) = & \frac{(2b_{sd}m_{sd})^{m_{sd}}\, G_{1,MPSK}^{m_{sd}-1}}{4G_{2,MPSK}^{m_{sd}}} \left(\frac{H_{MPSK}}{K_{MPSK}}\right)^{L} \\
& \times F_D^{(4)}\left(\frac{1}{2}, 1-m_{sd}, m_{sd}, -L, L; 2; \frac{1}{G_{1,MPSK}}, \frac{2b_{sd}m_{sd}}{G_{2,MPSK}}, \frac{1}{H_{MPSK}}, \frac{1}{K_{MPSK}}\right) \\
& + \frac{\sqrt{\omega}\,(2b_{sd}m_{sd})^{m_{sd}}\, G_{1,MPSK}^{m_{sd}-1}}{\pi G_{2,MPSK}^{m_{sd}}} \left(\frac{H_{MPSK}}{K_{MPSK}}\right)^{L} \\
& \times F_D^{(5)}\left(\frac{1}{2}, -\frac{1}{2}, 1-m_{sd}, m_{sd}, -L, L; \frac{3}{2}; \omega, \frac{\omega}{G_{1,MPSK}}, \frac{2b_{sd}m_{sd}\omega}{G_{2,MPSK}}, \frac{\omega}{H_{MPSK}}, \frac{\omega}{K_{MPSK}}\right)
\end{aligned}
\tag{2.45}
$$

which indicates that a full diversity order of $L+1$ is obtained when the number of participating relays is L (see appendix C).

M-ary quadrature amplitude modulation (MQAM)

The average SEP of the HSTCS for coherent MQAM signals is given by [AT01]

$$
P_{s,MQAM}^{SDF}(E) = \frac{4q}{\pi}\int_0^{\frac{\pi}{2}} \phi_{\gamma_{MRC}^{SDF}}\left(\frac{g_{MQAM}}{\sin^2\theta}\right) d\theta - \frac{4q^2}{\pi}\int_0^{\frac{\pi}{4}} \phi_{\gamma_{MRC}^{SDF}}\left(\frac{g_{MQAM}}{\sin^2\theta}\right) d\theta \tag{2.46}
$$

where $g_{MQAM} = 3/2(M-1)$ and $q = \left(1 - 1/\sqrt{M}\right)$. $P^{SDF}_{s,MQAM}$ can be calculated by using the same approach as in (2.17). Hence, $P^{SDF}_{s,MQAM}$ is given by

$$
\begin{aligned}
P^{SDF}_{s,MQAM}(E) = {} & \frac{q\left(2b_{sd}m_{sd}\right)^{m_{sd}} G^{m_{sd}-1}_{1,MQAM}}{G^{m_{sd}}_{2,MQAM}} \left(\prod_{i=1}^{L} P_{sr_i}\right) F_1\left(\frac{1}{2}, 1-m_{sd}, m_{sd}; 2; \frac{1}{G_{1,MQAM}}, \frac{2b_{sd}m_{sd}}{G_{2,MQAM}}\right) \\
& - \frac{2q^2\left(2b_{sd}m_{sd}\right)^{m_{sd}} L^{m_{sd}-1}_{1,MQAM}}{3\pi L^{m_{sd}}_{2,MQAM}} \left(\prod_{i=1}^{L} P_{sr_i}\right) \\
& \times F^{(3)}_D\left(1, 1, 1-m_{sd}, m_{sd}; \frac{5}{2}; \frac{1}{2}, \frac{G_{1,MQAM}}{L_{1,MQAM}}, \frac{G_{2,MQAM}}{L_{2,MQAM}}\right) \\
& + \frac{2q\left(2b_{sd}m_{sd}\right)^{m_{sd}} G^{m_{sd}-1}_{1,MQAM}}{\pi G^{m_{sd}}_{2,MQAM}} \left(\prod_{i=1}^{L} P_{sr_i}\right) \sum_{k=1}^{L} \sum_{\lambda_1=1}^{L-k+1} \sum_{\lambda_2=\lambda_1+1}^{L-k+2} \cdots \sum_{\lambda_k=\lambda_{k-1}+1}^{L} \\
& \prod_{n=1}^{k} \left(\frac{1-P_{sr_{\lambda_n}}}{P_{sr_{\lambda_n}}}\right) \left(\frac{m_{r_{\lambda_n}d}}{H_{\lambda_n,MQAM}}\right)^{m_{r_{\lambda_n}d}} \frac{\Gamma\left(\frac{1}{2}\right)\Gamma\left(\frac{3}{2} + \sum_{n=1}^{k} m_{r_{\lambda_n}d}\right)}{\Gamma\left(2 + \sum_{n=1}^{k} m_{r_{\lambda_n}d}\right)} F^{(k+2)}_D\left(\frac{1}{2}, 1-m_{sd}, m_{sd},\right. \\
& \left. m_{r_{\lambda_1}d}, \ldots, m_{r_{\lambda_k}d}; 2 + \sum_{n=1}^{k} m_{r_{\lambda_n}d}; \frac{1}{G_{1,MQAM}}, \frac{2b_{sd}m_{sd}}{G_{2,MQAM}}, \frac{m_{r_{\lambda_1}d}}{H_{\lambda_1,MQAM}}, \ldots, \frac{m_{r_{\lambda_k}d}}{H_{\lambda_k,MQAM}}\right) \\
& - \frac{q^2\left(2b_{sd}m_{sd}\right)^{m_{sd}} L^{m_{sd}-1}_{1,MQAM}}{\pi L^{m_{sd}}_{2,MQAM}} \left(\prod_{i=1}^{L} P_{sr_i}\right) \sum_{k=1}^{L} \sum_{\lambda_1=1}^{L-k+1} \sum_{\lambda_2=\lambda_1+1}^{L-k+2} \cdots \sum_{\lambda_k=\lambda_{k-1}+1}^{L} \\
& \prod_{n=1}^{k} \left(\frac{1-P_{sr_{\lambda_n}}}{P_{sr_{\lambda_n}}}\right) \left(\frac{m_{r_{\lambda_n}d}}{Q_{\lambda_n MQAM}}\right)^{m_{r_{\lambda_n}d}} \frac{1}{\left(\frac{3}{2} + \sum_{n=1}^{k} m_{r_{\lambda_n}d}\right)} F^{(k+3)}_D\left(1, 1, 1-m_{sd}, m_{sd},\right. \\
& \left. m_{r_{\lambda_1}d}, \ldots, m_{r_{\lambda_k}d}; \frac{5}{2} + \sum_{n=1}^{k} m_{r_{\lambda_n}d}; \frac{1}{2}, \frac{G_{1,MQAM}}{L_{1,MQAM}}, \frac{G_{2,MQAM}}{L_{2,MQAM}}, \frac{H_{\lambda_1,MQAM}}{Q_{\lambda_1,MQAM}}, \ldots, \frac{H_{\lambda_k,MQAM}}{Q_{\lambda_k,MQAM}}\right)
\end{aligned}
\tag{2.47}
$$

where

$$
\begin{aligned}
H_{i,MQAM} &= m_{r_id} + g_{MQAM}\Omega_{r_id}\overline{\gamma}_{r_id}, \\
Q_{i,MQAM} &= m_{r_id} + 2g_{MQAM}\Omega_{r_id}\overline{\gamma}_{r_id}.
\end{aligned}
\tag{2.48}
$$

In the case of i.i.d fading channels, all relays are experiencing the same fading environment, i.e., $m_{sr_i} = m_{sr}$, $b_{sr_i} = b_{sr}$, $\Omega_{sr_i} = \Omega_{sr}$ and $b_{r_id} = b_{rd}$ for all $i \in L$. And we assume that $\overline{\gamma}_{r_id} = \overline{\gamma}_{rd} = \overline{\gamma}$ for all $i \in L$. So, $H_{i,MQAM} = H_{MQAM}$ and $Q_{i,MQAM} = Q_{MQAM}$ for all $i \in L$. By using the properties of the Lauricella function as shown in (2.41), the average SEP, $P^{SDF}_{s,MQAM}(E)$ can be simplified as in

equation (2.49).

$$
\begin{aligned}
P_{s,MQAM}^{SDF}(E) = & \frac{2q\left(2b_{sd}m_{sd}\right)^{m_{sd}} G_{1,MQAM}^{m_{sd}-1}}{\pi G_{2,MQAM}^{m_{sd}}} \left(P_{sr}\right)^{L} \sum_{k=0}^{L} \binom{L}{k} \left(\frac{1-P_{sr}}{P_{sr}}\right)^{k} \frac{\Gamma\left(\frac{1}{2}\right)\Gamma\left(\frac{3}{2}+km_{rd}\right)}{\Gamma\left(2+km_{rd}\right)} \\
& \times \left(\frac{m_{rd}}{H_{MQAM}}\right)^{km_{rd}} F_{D}^{(3)}\left(\frac{1}{2}, 1-m_{sd}, m_{sd}, km_{rd}; 2+km_{rd}; \frac{1}{G_{1,MQAM}}, \frac{2b_{sd}m_{sd}}{G_{2,MQAM}}, \frac{m_{rd}}{H_{MQAM}}\right) \\
& - \frac{q^{2}\left(2b_{sd}m_{sd}\right)^{m_{sd}} L_{1,MQAM}^{m_{sd}-1}}{\pi L_{2,MQAM}^{m_{sd}}} \left(P_{sr}\right)^{L} \sum_{k=0}^{L} \binom{L}{k} \left(\frac{1-P_{sr}}{P_{sr}}\right)^{k} \left(\frac{m_{rd}}{Q_{MQAM}}\right)^{km_{rd}} \left(\frac{1}{\frac{3}{2}+km_{rd}}\right) \\
& \times F_{D}^{(4)}\left(1, 1, 1-m_{sd}, m_{sd}, km_{rd}; \frac{5}{2}+km_{rd}; \frac{1}{2}, \frac{G_{1,MQAM}}{L_{1,MQAM}}, \frac{G_{2,MQAM}}{L_{2,MQAM}}, \frac{H_{MQAM}}{Q_{MQAM}}\right).
\end{aligned}
\tag{2.49}
$$

In the special case where the Nakagami-m parameter $m_{r_id} = 1$***, all relay-destination links are Rayleigh fading channels. Equation (2.47) becomes as follows***

$$
\begin{aligned}
P_{s,MQAM}^{SDF}(E) = & \frac{q\left(2b_{sd}m_{sd}\right)^{m_{sd}} G_{1,MQAM}^{m_{sd}-1}}{G_{2,MQAM}^{m_{sd}}} \prod_{i=1}^{L} \left(\frac{H_{i,MQAM}}{K_{i,MQAM}}\right) F_{D}^{(2L+2)}\left(\frac{1}{2}, 1-m_{sd}, m_{sd}, -1, 1, \ldots,\right. \\
& \left. -1, 1; 2; \frac{1}{G_{1,MQAM}}, \frac{2b_{sd}m_{sd}}{G_{2,MQAM}}, \frac{1}{H_{1,MQAM}}, \frac{1}{K_{1,MQAM}}, \ldots, \frac{1}{H_{L,MQAM}}, \frac{1}{K_{L,MQAM}}\right) \\
& - \frac{2q^{2}(2b_{sd}m_{sd})^{m_{sd}} L_{1,MQAM}^{m_{sd}-1}}{3\pi L_{2,MQAM}^{m_{sd}}} \prod_{i=1}^{L} \left(\frac{W_{i,MQAM}}{Z_{i,MQAM}}\right) F_{D}^{(2L+3)}\left(1, 1, 1-m_{sd}, m_{sd}, -1, 1, \ldots,\right. \\
& \left. -1, 1; \frac{5}{2}; \frac{1}{2}, \frac{G_{1,MQAM}}{L_{1,MQAM}}, \frac{G_{2,MQAM}}{L_{2,MQAM}}, \frac{H_{1,MQAM}}{W_{1,MQAM}}, \frac{K_{1,MQAM}}{Z_{1,MQAM}}, \ldots, \frac{H_{L,MQAM}}{W_{L,MQAM}}, \frac{K_{L,MQAM}}{Z_{L,MQAM}}\right)
\end{aligned}
\tag{2.50}
$$

where

$$
\begin{aligned}
H_{i,MQAM} &= 1 + P_{sr_i,MQAM}\Omega_{r_id}\overline{\gamma}_{r_id}g_{MQAM}, \;\; K_{i,MQAM} = 1 + \Omega_{r_id}\overline{\gamma}_{r_id}g_{MQAM}, \\
W_{i,MQAM} &= 1 + 2P_{sr_i,MQAM}\Omega_{r_id}\overline{\gamma}_{r_id}g_{MQAM}, \;\; Z_{i,MQAM} = 1 + 2\Omega_{r_id}\overline{\gamma}_{r_id}g_{MQAM}.
\end{aligned}
\tag{2.51}
$$

And equation (2.49) changes to the expression below

$$\begin{aligned} P_{s,MQAM}^{SDF}(E) = & \frac{q\left(2b_{sd}m_{sd}\right)^{m_{sd}} G_{1,MQAM}^{m_{sd}-1}}{G_{2,MQAM}^{m_{sd}}} \left(\frac{H_{MQAM}}{K_{MQAM}}\right)^{L} \\ & \times F_D^{(4)}\left(\frac{1}{2}, 1-m_{sd}, m_{sd}, -L, L; 2; \frac{1}{G_{1,MQAM}}, \frac{2b_{sd}m_{sd}}{G_{2,MQAM}}, \frac{1}{H_{MQAM}}, \frac{1}{K_{MQAM}}\right) \\ & - \frac{2q^2\left(2b_{sd}m_{sd}\right)^{m_{sd}} L_{1,MQAM}^{m_{sd}-1}}{3\pi L_{2,MQAM}^{m_{sd}}} \left(\frac{W_{MQAM}}{Z_{MQAM}}\right)^{L} \\ & \times F_D^{(5)}\left(1, 1, 1-m_{sd}, m_{sd}, -L, L; \frac{5}{2}; \frac{1}{2}, \frac{G_{1,MQAM}}{L_{1,MQAM}}, \frac{G_{2,MQAM}}{L_{2,MQAM}}, \frac{H_{MQAM}}{W_{MQAM}}, \frac{K_{MQAM}}{Z_{MQAM}}\right) \end{aligned} \tag{2.52}$$

which again indicates that a full diversity order of $L+1$ is obtained when the number of participating relays is L (see appendix D).

2.3 Outage analysis

In this section, we analyze the outage probability of an HSTCS. First, we evaluate the outage probability of the direct link and then we evaluate the outage probability of the HSTCS. For the sake of simplicity, we derive the outage probability of the system when the terrestrial links are Rayleigh fading ($m_{r_id} = 1$).

2.3.1 Outage probability of the direct link

The instantaneous mutual information I_{sd} of the direct link is given by

$$I_{sd} = \frac{1}{L+1}\log_2\left(1+\gamma_{sd}\right) = \frac{1}{L+1}\log_2\left(1+\frac{E_s}{N_0}|h_{sd}|^2\right). \tag{2.53}$$

The fraction $1/(L+1)$ comes from the fact that there are $L+1$ channels allocated to the L relay links and to one direct link.

So, the outage probability P_{sd}^{out} of the direct link is defined as

$$\begin{aligned} P_{sd}^{out} &= \Pr\left[I_{sd} < R\right] = \Pr\left[\gamma_{sd} < 2^{(L+1)R} - 1\right] \\ &= \Pr\left[\gamma_{sd} < \gamma_{th}\right] = F_{\gamma_{sd}}(\gamma_{th}) \end{aligned} \tag{2.54}$$

where R denotes the target spectral efficiency (in bits/s/Hz), $\gamma_{th} = 2^{(L+1)R} - 1$ and $F_{\gamma_{sd}}(y)$ denotes the CDF of γ_{sd}. We have that

$$F_{\gamma_{sd}}(y) = \int_0^y f_{\gamma_{sd}}(\tau)d\tau. \tag{2.55}$$

By using the Maclaurin series expansions of $\exp(-x)$,

$$\exp(-x) = \sum_{j=0}^{+\infty}(-1)^j \frac{x^j}{j!} \tag{2.56}$$

and the table of integrals in [GR07], the CDF of γ_{sd} is obtained as below

$$F_{\gamma_{sd}}(y) = A_{sd} y {}_1F_1\left(m_{sd}; 2; B_{sd}y\right) + \sum_{j=1}^{+\infty}(-1)^j \frac{A_{sd} y^{(j+1)}}{(j+1)!(2b_{sd}\overline{\gamma}_{sd})^j} {}_2F_2\left(j+1, m_{sd}; j+2, 1; B_{sd}y\right) \tag{2.57}$$

where

$$A_{sd} = \frac{1}{2b_{sd}\overline{\gamma}_{sd}} \left(\frac{2b_{sd}m_{sd}}{2b_{sd}m_{sd} + \Omega_{sd}}\right)^{m_{sd}},$$
$$B_{sd} = \frac{\Omega_{sd}}{2b_{sd}\overline{\gamma}_{sd}(2b_{sd}m_{sd} + \Omega_{sd})},$$

and

$${}_pF_q(a_1, ..., a_p; b_1, ..., b_q; z) = \sum_{n=0}^{\infty} \frac{(a_1)_n \ldots (a_p)_n}{(b_1)_n \ldots (b_q)_n \, n!} z^n \tag{2.58}$$

is the general hypergeometric function defined in [GR07] and $(x)_n = x(x-1)(x-2)\cdots(x-n+1)$ is a Pochhammer symbol.

Hence, the outage probability of the direct link is given as follows

$$P_{sd}^{out} = A_{sd}\gamma_{th} {}_1F_1\left(m_{sd}; 2; B_{sd}\gamma_{th}\right) + \sum_{j=1}^{+\infty}(-1)^j \frac{A_{sd}(\gamma_{th})^{(j+1)}}{(j+1)!(2b_{sd}\overline{\gamma}_{sd})^j} {}_2F_2\left(j+1, m_{sd}; j+2, 1; B_{sd}\gamma_{th}\right). \tag{2.59}$$

2.3.2 Outage probability of the HSTCS

To derive the outage probability of the system we need to know the PDF or the CDF of the instantaneous received SNR at the output of the MRC.

The instantaneous mutual information I_{SDF} of the HSTCS is given as

$$I_{SDF} = \frac{1}{L+1}\log_2\left(1+\tilde{\gamma}_{MRC}^{SDF}\right) \tag{2.60}$$

where $\tilde{\gamma}_{MRC}^{SDF}$ is the instantaneous received SNR at the output of the MRC and is given as

$$\tilde{\gamma}_{MRC}^{SDF} = \gamma_{sd} + \sum_{i\in C}\gamma_{r_i d}. \tag{2.61}$$

So, the outage probability P_{SDF}^{out} of the the HSTCS is defined as

$$\begin{aligned} P_{SDF}^{out} &= \Pr\left[I_{SDF} < R\right] = \Pr\left[\tilde{\gamma}_{MRC}^{SDF} < 2^{(L+1)R}-1\right] \\ &= \Pr\left[\tilde{\gamma}_{MRC}^{SDF} < \gamma_{th}\right] = F_{\tilde{\gamma}_{MRC}^{SDF}}(\gamma_{th}) \end{aligned} \tag{2.62}$$

Actually, it will be difficult to find the PDF of $\tilde{\gamma}_{MRC}^{SDF}$ given in (2.61) because the decoding set C is unknown. To treat this problem we invoke the technique described in [BH06], where the system in Fig. 2.1 can be considered as a communication system consisting of $L+1$ effective paths between the satellite and the destination. Let path number 0 be the s to d direct link and path i be the $s \to r_i \to d$ relayed link where $i = 1, ..., L$. Let $\tilde{\chi}_i$ be the instantaneous received SNR of the relayed link i at the destination which takes into account both the s to r_i and the r_i to d link. Therefore, the PDF of $\tilde{\chi}_i$ can be obtained as

$$\begin{aligned} f_{\tilde{\chi}_i}(y) = {} & f_{\tilde{\chi}_i|r_i \text{ Decodes Incorrectly}}(y)\Pr\left[r_i \text{ Decodes Incorrectly}\right] \\ & + f_{\tilde{\chi}_i|r_i \text{ Decodes Correctly}}(y)\Pr\left[r_i \text{ Decodes Correctly}\right]. \end{aligned} \tag{2.63}$$

So, equation (2.61) can be rewritten as

$$\tilde{\gamma}_{MRC}^{SDF} = \gamma_{sd} + \sum_{i=1}^{L}\tilde{\chi}_i = \gamma_{sd} + \tilde{\gamma}_{DF} \tag{2.64}$$

where

$$\tilde{\gamma}_{DF} = \sum_{i=1}^{L}\tilde{\chi}_i. \tag{2.65}$$

The probability that the relay r_i decodes incorrectly is the outage probability, $P_{sr_i}^{out}$, of the satellite-relay r_i link and the probability that the relay r_i decodes correctly is $(1 - P_{sr_i}^{out})$. This $P_{sr_i}^{out}$ can be

calculated by using the same approach as in (2.54) and is given as below

$$P_{sr_i}^{out} = A_{sr_i}\gamma_{th}{}_1F_1\left(m_{sr_i};2;B_{sr_i}\gamma_{th}\right) + \sum_{j=1}^{+\infty}(-1)^j\frac{A_{sr_i}(\gamma_{th})^{(j+1)}}{(j+1)!(2b_{sr_i}\overline{\gamma}_{sr_i})^j}{}_2F_2\left(j+1,m_{sr_i};j+2,1;B_{sr_i}\gamma_{th}\right) \tag{2.66}$$

where

$$\begin{aligned} A_{sr_i} &= \frac{1}{2b_{sr_i}\overline{\gamma}_{sr_i}}\left(\frac{2b_{sr_i}m_{sr_i}}{2b_{sr_i}m_{sr_i}+\Omega_{sr_i}}\right)^{m_{sr_i}}, \\ B_{sr_i} &= \frac{\Omega_{sr_i}}{2b_{sr_i}\overline{\gamma}_{sr_i}(2b_{sr_i}m_{sr_i}+\Omega_{sr_i})}. \end{aligned} \tag{2.67}$$

The conditional PDF of $f_{\tilde{\chi}_i|r_i \text{ Decodes Incorrectly}}(y)$ is given by

$$f_{\tilde{\chi}_i|r_i \text{ Decodes Incorrectly}}(y) = \delta(y),\ y \geq 0 \tag{2.68}$$

where $\delta(y)$ is the Dirac Delta function. And the conditional PDF of $f_{\tilde{\chi}_i|r_i \text{ Decodes Correctly}}(y)$ is given by

$$f_{\tilde{\chi}_i|r_i \text{ Decodes Correctly}}(y) = f_{\gamma_{r_id}}(y) = \beta_i\exp(-\beta_i y) = \frac{1}{2b_{r_id}\overline{\gamma}_{r_id}}\exp(-\frac{y}{2b_{r_id}\overline{\gamma}_{r_id}}),\ y \geq 0 \tag{2.69}$$

where $\beta_i = \frac{1}{2b_{r_id}\overline{\gamma}_{r_id}}$ and $\overline{\gamma}_{r_id} = E_{r_i}/N_0$ is the average transmit SNR per symbol of the relay r_i.

Therefore, equation (2.63) can be written as, for $y \geq 0$,

$$f_{\tilde{\chi}_i}(y) = P_{sr_i}^{out}\delta(y) + (1-P_{sr_i}^{out})\beta_i\exp(-\beta_i y) \tag{2.70}$$

Hence, the PDF of $\tilde{\gamma}_{DF}$ is given by

$$f_{\tilde{\gamma}_{DF}}(y) = f_{\tilde{\chi}_1}(y) * f_{\tilde{\chi}_2}(y) * \ldots * f_{\tilde{\chi}_L}(y) \tag{2.71}$$

where the symbol $*$ denotes the convolution product. After some mathematical computations, the

PDF of $\tilde{\gamma}_{DF}$ can be written as below

$$\begin{aligned} f_{\tilde{\gamma}_{DF}}(y) &= \left(\prod_{i=1}^{L} P_{sr_i}^{out}\right)\left[\delta(y) + \sum_{k=1}^{L}\sum_{\lambda_1=1}^{L-k+1}\sum_{\lambda_2=\lambda_1+1}^{L-k+2}\cdots\sum_{\lambda_k=\lambda_{k-1}+1}^{L}\right. \\ &\left.\prod_{n=1}^{k}\left(\frac{1-P_{sr_{\lambda_n}}^{out}}{P_{sr_{\lambda_n}}^{out}}\right)\left(f_{\gamma_{r_{\lambda_1}d}}(y) * \ldots * f_{\gamma_{r_{\lambda_k}d}}(y)\right)\right] \\ &= \left(\prod_{i=1}^{L} P_{sr_i}^{out}\right)\left[\delta(y) + \sum_{k=1}^{L}\sum_{\lambda_1=1}^{L-k+1}\sum_{\lambda_2=\lambda_1+1}^{L-k+2}\cdots\sum_{\lambda_k=\lambda_{k-1}+1}^{L}\prod_{n=1}^{k}\left(\frac{1-P_{sr_{\lambda_n}}^{out}}{P_{sr_{\lambda_n}}^{out}}\right) f_{RD}(y)\right]. \end{aligned} \tag{2.72}$$

where

$$f_{RD}(y) = f_{\gamma_{r_{\lambda_1}d}}(y) * \ldots * f_{\gamma_{r_{\lambda_k}d}}(y). \tag{2.73}$$

In the following, we will evaluate the outage probability over independent but non identically distributed (i.n.i.d) and i.i.d fading channels.

Independent non identically distributed fading channels

By using the convolution product formula given in [Akk08], the expression $f_{RD}(y)$ is given as below

$$f_{RD}(y) = \sum_{n=1}^{k} \frac{\beta_{\lambda_1}\ldots\beta_{\lambda_k}}{\prod_{m=1,m\neq n}^{k}(\beta_{\lambda_m}-\beta_{\lambda_n})}\exp(-\beta_{\lambda_n}y). \tag{2.74}$$

Hence, the PDF of $\tilde{\gamma}_{DF}$ is given as follows

$$\begin{aligned} f_{\tilde{\gamma}_{DF}}(y) = \left(\prod_{i=1}^{L} P_{sr_i}^{out}\right)\left[\delta(y) + \sum_{k=1}^{L}\sum_{\lambda_1=1}^{L-k+1}\sum_{\lambda_2=\lambda_1+1}^{L-k+2}\cdots\sum_{\lambda_k=\lambda_{k-1}+1}^{L}\right. \\ \left.\prod_{n=1}^{k}\left(\frac{1-P_{sr_{\lambda_n}}^{out}}{P_{sr_{\lambda_n}}^{out}}\right)\sum_{n=1}^{k}\frac{\beta_{\lambda_1}\ldots\beta_{\lambda_k}}{\prod_{m=1,m\neq n}^{k}(\beta_{\lambda_m}-\beta_{\lambda_n})}\exp(-\beta_{\lambda_n}y)\right]. \end{aligned} \tag{2.75}$$

The CDF of $\tilde{\gamma}_{DF}$ can be computed easily and given as follows

$$\begin{aligned} F_{\tilde{\gamma}_{DF}}(y) &= \int_0^y f_{\tilde{\gamma}_{DF}}(\tau)d\tau \\ &= \left(\prod_{i=1}^{L} P_{sr_i}^{out}\right)\left[1 + \sum_{k=1}^{L}\sum_{\lambda_1=1}^{L-k+1}\sum_{\lambda_2=\lambda_1+1}^{L-k+2}\cdots\sum_{\lambda_k=\lambda_{k-1}+1}^{L}\right. \\ &\left.\prod_{n=1}^{k}\left(\frac{1-P_{sr_{\lambda_n}}^{out}}{P_{sr_{\lambda_n}}^{out}}\right)\sum_{n=1}^{k}\frac{\beta_{\lambda_1}\ldots\beta_{\lambda_k}}{\beta_{\lambda_n}\prod_{m=1,m\neq n}^{k}(\beta_{\lambda_m}-\beta_{\lambda_n})}\left(1-\exp\left(-\beta_{\lambda_n}y\right)\right)\right]. \end{aligned} \tag{2.76}$$

It is well known that the PDF of the sum of two independent random variables is the convolution product of these two variables. Therefore, the PDF of $\tilde{\gamma}_{MRC}^{SDF}$ is given as

$$f_{\tilde{\gamma}_{MRC}^{SDF}}(y) = \int_{-\infty}^{+\infty} f_{\tilde{\gamma}_{DF}}(y-\tau) f_{\gamma_{sd}}(\tau) d\tau. \tag{2.77}$$

After some mathematical calculations, the CDF of $\tilde{\gamma}_{MRC}^{SDF}$ can be expressed as

$$F_{\tilde{\gamma}_{MRC}^{SDF}}(y) = \int_{0}^{y} F_{\tilde{\gamma}_{DF}}(y-\tau) f_{\gamma_{sd}}(\tau) d\tau. \tag{2.78}$$

By using the Maclaurin series expansions of $\exp(-x)$ and the table of integrals in [GR07], the CDF of $\tilde{\gamma}_{MRC}^{SDF}$, $F_{\tilde{\gamma}_{MRC}^{SDF}}(y)$, can be obtained as below

$$\begin{aligned} F_{\tilde{\gamma}_{MRC}^{SDF}}(y) = \left(\prod_{i=1}^{L} P_{sr_i}^{out}\right) \Bigg[F_{\gamma_{sd}}(y) + \sum_{k=1}^{L} \sum_{\lambda_1=1}^{L-k+1} \sum_{\lambda_2=\lambda_1+1}^{L-k+2} \cdots \sum_{\lambda_k=\lambda_{k-1}+1}^{L} \prod_{n=1}^{k} \left(\frac{1-P_{sr_{\lambda_n}}^{out}}{P_{sr_{\lambda_n}}^{out}}\right) \\ \times \sum_{n=1}^{k} \frac{\beta_{\lambda_1} \ldots \beta_{\lambda_k}}{\beta_{\lambda_n} \prod_{m=1, m\neq n}^{k} (\beta_{\lambda_m} - \beta_{\lambda_n})} \Bigg(F_{\gamma_{sd}}(y) - A_{sd} \exp(-\beta_{\lambda_n} y) \Bigg[y_1 F_1(m_{sd}; 2; B_{sd} y) \\ + \sum_{j=1}^{+\infty} (-1)^j \left(\frac{1}{2b_{sd}\overline{\gamma}_{sd}} - \frac{1}{2b_{r_{\lambda_n}d}\overline{\gamma}_{r_{\lambda_n}d}}\right)^j \frac{y^{j+1}}{(j+1)!} {}_2F_2\left(j+1, m_{sd}; j+2, 1; B_{sd} y\right) \Bigg] \Bigg) \Bigg]. \end{aligned} \tag{2.79}$$

Hence, the outage probability of HSTCS over i.n.i.d fading channels is finally given by

$$\begin{aligned} P_{SDF}^{out} = \left(\prod_{i=1}^{L} P_{sr_i}^{out}\right) \Bigg[P_{sd}^{out} + \sum_{k=1}^{L} \sum_{\lambda_1=1}^{L-k+1} \sum_{\lambda_2=\lambda_1+1}^{L-k+2} \cdots \sum_{\lambda_k=\lambda_{k-1}+1}^{L} \prod_{n=1}^{k} \left(\frac{1-P_{sr_{\lambda_n}}^{out}}{P_{sr_{\lambda_n}}^{out}}\right) \\ \times \sum_{n=1}^{k} \frac{\beta_{\lambda_1} \ldots \beta_{\lambda_k}}{\beta_{\lambda_n} \prod_{m=1, m\neq n}^{k} (\beta_{\lambda_m} - \beta_{\lambda_n})} \Bigg(P_{sd}^{out} - A_{sd} \exp(-\beta_{\lambda_n} \gamma_{th}) \Bigg[\gamma_{th1} F_1(m_{sd}; 2; B_{sd} \gamma_{th}) \\ + \sum_{j=1}^{+\infty} (-1)^j \left(\frac{1}{2b_{sd}\overline{\gamma}_{sd}} - \frac{1}{2b_{r_{\lambda_n}d}\overline{\gamma}_{r_{\lambda_n}d}}\right)^j \frac{\gamma_{th}^{j+1}}{(j+1)!} {}_2F_2\left(j+1, m_{sd}; j+2, 1; B_{sd} \gamma_{th}\right) \Bigg] \Bigg) \Bigg]. \end{aligned} \tag{2.80}$$

Independent identically distributed fading channels

In the case of i.i.d fading channels, i.e. $\beta_i = \beta = \frac{1}{2b_{rd}\overline{\gamma}_{rd}}$ for all $i \in L$. And we assume that $\overline{\gamma}_{r_i d} = \overline{\gamma}_{rd} = \overline{\gamma}$ for all $i \in L$. By using the convolution product formula given in [Akk08], the expression $f_{RD}(y)$ is given as below

$$f_{RD}(y) = \frac{\beta^k y^{k-1}}{(k-1)!} \exp(-\beta y). \tag{2.81}$$

Hence, the PDF of $\tilde{\gamma}_{DF}$ can be expressed as follows

$$f_{\tilde{\gamma}_{DF}}(y) = (P_{sr}^{out})^L \left[\delta(y) + \sum_{k=1}^{L} \binom{L}{k} \left(\frac{1 - P_{sr}^{out}}{P_{sr}^{out}} \right)^k \frac{\beta^k y^{k-1}}{(k-1)!} \exp(-\beta y) \right]. \tag{2.82}$$

And the CDF of $\tilde{\gamma}_{DF}$ can be evaluated by using the table of integrals in [GR07],

$$F_{\tilde{\gamma}_{DF}}(y) = \int_0^y f_{\tilde{\gamma}_{DF}}(\tau) d\tau = (P_{sr}^{out})^L \left[1 + \sum_{k=1}^{L} \binom{L}{k} \left(\frac{1 - P_{sr}^{out}}{P_{sr}^{out}} \right)^k \left(1 - \exp(-\beta y) \sum_{m=0}^{k-1} \frac{\beta^m y^m}{m!} \right) \right]. \tag{2.83}$$

So, the CDF of $\tilde{\gamma}_{MRC}^{SDF}$ can be computed by using the same approach as in 2.78 and is finally given as follows,

$$\begin{aligned} F_{\tilde{\gamma}_{MRC}^{SDF}}(y) &= \int_0^y F_{\tilde{\gamma}_{DF}}(y-\tau) f_{\gamma_{sd}}(\tau) d\tau \\ &= (P_{sr}^{out})^L \left[F_{\gamma_{sd}}(y) + \sum_{k=1}^{L} \binom{L}{k} \left(\frac{1 - P_{sr}^{out}}{P_{sr}^{out}} \right)^k \left(F_{\gamma_{sd}}(y) - A_{sd} \exp(-\frac{y}{2b_{rd}\overline{\gamma}_{rd}}) \sum_{m=0}^{k-1} \left(\frac{1}{2b_{rd}\overline{\gamma}_{rd}} \right)^m \right. \right. \\ &\times \left[\frac{y^{m+1}}{(m+1)!} {}_1F_1(m_{sd}; m+2; B_{sd}y) + \sum_{j=1}^{+\infty} (-1)^j \left(\frac{1}{2b_{sd}\overline{\gamma}_{sd}} - \frac{1}{2b_{rd}\overline{\gamma}_{rd}} \right)^j \right. \\ &\left. \left. \left. \times \frac{y^{m+j+1}}{(m+j+1)!} {}_2F_2(j+1, m_{sd}; m+j+2, 1; B_{sd}y) \right] \right) \right]. \end{aligned} \tag{2.84}$$

Therefore, the outage probability of HSTCS over i.i.d fading channels is finally given as

$$\begin{aligned} P_{SDF}^{out} &= (P_{sr}^{out})^L \left[P_{sd}^{out} + \sum_{k=1}^{L} \binom{L}{k} \left(\frac{1 - P_{sr}^{out}}{P_{sr}^{out}} \right)^k \left(P_{sd}^{out} - A_{sd} \exp(-\frac{\gamma_{th}}{2b_{rd}\overline{\gamma}_{rd}}) \sum_{m=0}^{k-1} \left(\frac{1}{2b_{rd}\overline{\gamma}_{rd}} \right)^m \right. \right. \\ &\times \left[\frac{\gamma_{th}^{m+1}}{(m+1)!} {}_1F_1(m_{sd}; m+2; B_{sd}\gamma_{th}) + \sum_{j=1}^{+\infty} (-1)^j \left(\frac{1}{2b_{sd}\overline{\gamma}_{sd}} - \frac{1}{2b_{rd}\overline{\gamma}_{rd}} \right)^j \right. \\ &\left. \left. \left. \times \frac{\gamma_{th}^{m+j+1}}{(m+j+1)!} {}_2F_2(j+1, m_{sd}; m+j+2, 1; B_{sd}\gamma_{th}) \right] \right) \right]. \end{aligned} \tag{2.85}$$

Although the outage probability in (2.80) and (2.85) is expressed as an infinite sum of general hypergeometric functions, it is convergent when the number of terms j in the sum of (2.80) and (2.85) is high enough, i.e., $j \gg 1$.

Table 2.1: LMS channel parameters [ALAK03]

	Data set		
	b_{sx}	m_{sx}	Ω_{sx}
Frequent Heavy Shadowing (FHS)	0.063	0.739	8.97×10^{-4}
Average Shadowing (AS)	0.126	10.1	0.835
Infrequent Light Shadowing (ILS)	0.158	19.4	1.29

2.4 Simulation results

In this section, the outage probability and the average SEP of an HSTCS are obtained through simulation. These simulation results are compared to the analytical results presented in the previous sections. The outage and SEP curves are plotted versus the average transmit SNR per symbol, E_s/N_0, for different number of participating relays $L = 0, 1, 2, 3$ ($L = 0$, corresponds to the direct transmission only). The numerical values for the LMS channel are shown in Table 2.1. The target spectral efficiency R is assumed to be $1/(L+1)$ bits/s/Hz which corresponds to $\gamma_{th} = 0\ dB$. We assume that the average transmit SNR per symbol of the satellite-destination link is equal to the one of the relay-destination links ($E_s/N_0 = E_{r_i}/N_0$). The figures show that our analytical results show excellent agreement with the simulation results for both i.n.i.d fading channels and i.i.d fading channels. This confirms the accuracy of our performance analysis.

2.4.1 Outage curves

Fig. 2.2 shows the outage probability of an HSTCS over i.n.i.d fading channels when the direct link experiences the FHS. The first, the second and the third satellite-relay links experience the ILS, the FHS and the AS respectively while their terrestrial links experience the Rayleigh fading with the average power channel gain equal to 1, 0.5 and 0.25 respectively. We can observe in the figure that the 1-relay system provides a diversity gain of 11.5 dB at the outage rate of 10^{-1} over the direct link while the 3-relay system provides a diversity gain of 14 dB over the direct link at the same outage rate. We can also notice that the 2-relay system does not provide much diversity gain over the 1-relay

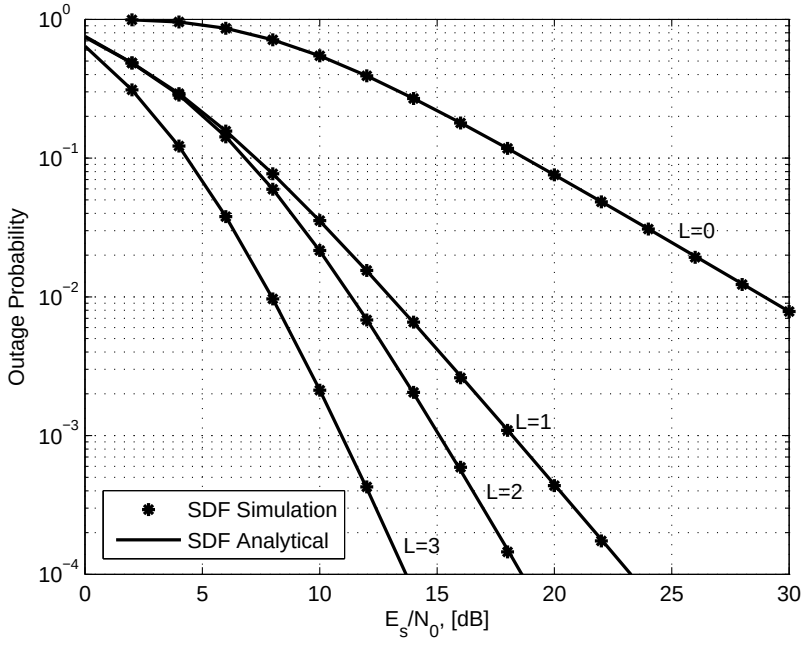

Figure 2.2: The outage probability of an HSTCS versus the average transmit SNR, E_s/N_0, when the direct link experiences the FHS. The first, the second and the third satellite-relay links experience the ILS, the FHS and the AS respectively while their terrestrial links experience the Rayleigh fading with the average power channel gain equal to 1, 0.25 and 0.5 respectively.

system in the low-SNR regime. This is because of the strong fading of the second relay link.

Fig. 2.3 plots the outage probability of an HSTCS over i.i.d fading channels when both direct and satellite-relay links experience the FHS and the terrestrial links are Rayleigh fading with the same average power channel gain equal to unity. In this case, we can achieve approximately 5.5 dB of diversity gain at the outage probability of 10^{-1} when only one relay is participating. In addition, this diversity gain does increase to approximately 8.5 dB when $L = 3$.

2.4.2 SEP curves

Figs. 2.4 and 2.5 show the average SEP of 8PSK and 16QAM HSTCS respectively over i.n.i.d fading channels. The channel parameters for each curve simulation are summarized in Table 2.2 and the

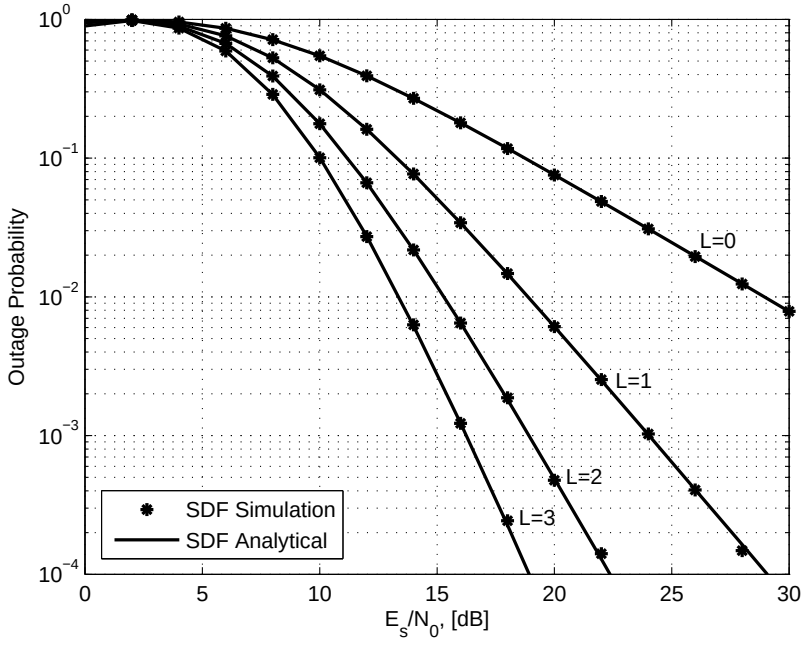

Figure 2.3: The outage probability of an HSTCS versus the average transmit SNR, E_s/N_0, when both direct and satellite-relay links experience the FHS and the terrestrial links are Rayleigh fading with the average power channel gain equal to unity.

diversity gains at the SEP of 10^{-1} are provided in Table 2.3. We can see from the Fig. 2.4 that the SEP curves of the 3-relay system and 2-relay system are nearly superimposed. This effect comes from the fact that the third relay link experiences the FHS.

Furthermore, Figs. 2.6 and 2.7 show the average SEP of QPSK and 16QAM HSTCS respectively over i.i.d fading channels. The channel parameters for each curve simulation are described in Table 2.4 and the diversity gains at the SEP of 10^{-1} are given in Table 2.5.

In order to see the diversity properties of HSTCSs, we compare SEP curves of a system in which the average transmit SNR per symbol of each relay, E_{r_i}/N_0, is equal to E_s/N_0 ($E_{r_i}/N_0 = E_s/N_0$) with a system in which the total average transmit SNR per symbol of all relays is equal to E_s/N_0 $\left(\sum_{i=1}^{L} E_{r_i}/N_0 = E_s/N_0\right)$, as shown in Figs. 2.8 and 2.9 for the case of QPSK and 16QAM respectively. We can observe from Figs. 2.8 and 2.9 that the diversity order is always $L+1$ for these two different

Table 2.2: Parameters of SEP simulation curves over i.n.i.d fading channels

	Modulation scheme	$s-r_i$ links	r_i-d links
Fig. 2.4	8PSK	$s-r_1$: ILS	r_1-d: $m_{r_1d}=3.5$
		$s-r_2$: AS	r_2-d: $m_{r_2d}=5.6$
		$s-r_3$: FHS	r_3-d: $m_{r_3d}=1.2$
Fig. 2.5	16QAM	$s-r_1$: AS	r_1-d: $m_{r_1d}=1$
		$s-r_2$: FHS	r_2-d: $m_{r_2d}=0.5$
		$s-r_3$: ILS	r_3-d: $m_{r_3d}=2.8$

Table 2.3: Diversity gain of the HSTCS at the SEP of 10^{-1} over i.n.i.d fading channels

	1-relay system	2-relay system	3-relay system
Fig. 2.4	12.5 dB	15 dB	15.5 dB
Fig. 2.5	10 dB	11 dB	15 dB

Table 2.4: Parameters of SEP simulation curves over i.i.d fading channels

	Modulation scheme	$s-r$ links	$r-d$ links
Fig. 2.6	QPSK	$s-r$: FHS	$r-d$: $m_{r_2d}=1$
Fig. 2.7	16QAM	$s-r$: AS	$r-d$: $m_{r_2d}=1$

Table 2.5: Diversity gain of the HSTCS at the SEP of 10^{-1} over i.i.d fading channels

	One-relay system	Two-relay system	Three-relay system
Fig. 2.6	7 dB	10 dB	12 dB
Fig. 2.7	10 dB	13 dB	15 dB

transmit SNR per symbol scenarios.

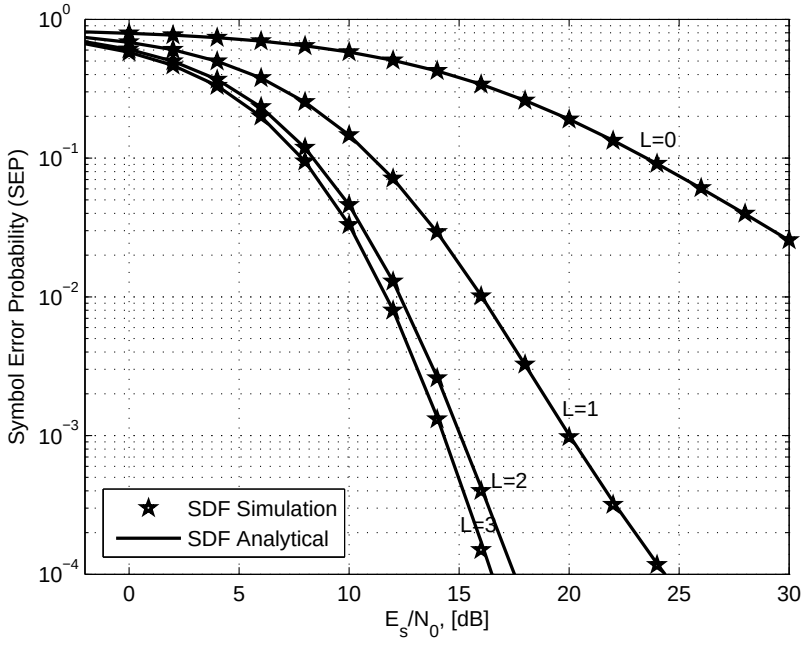

Figure 2.4: The average SEP of a 8PSK HSTCS versus the average transmit SNR, E_s/N_0, when the direct link experiences the FHS. The first, the second and the third satellite-relay links experience the ILS, the AS and the FHS respectively while their terrestrial links experience the Nakagami-m fading with m_{rd} equal to 3.5, 5.6 and 1.2 respectively.

2.5 Conclusion

In this chapter, we study the performance in terms of the outage probability and the SEP of an HSTCS. The SDF transmission scheme has been implemented. In the first phase, the satellite broadcasts its signal to all relay nodes and the destination node. In the second phase, only relays that can decode the satellite message correctly are allowed to forward the satellite message to the destination node. Then the destination combines the direct and the relay links signals using the MRC technique. The exact closed-form expressions for the outage probability and the average SEP of the general MPSK and MQAM HSTCS over independent but not necessarily identically distributed fading channels have been derived. The results have shown that a full diversity order of $L+1$ can be obtained when the total number of relays is equal to L. Moreover, it can be seen from the outage and the

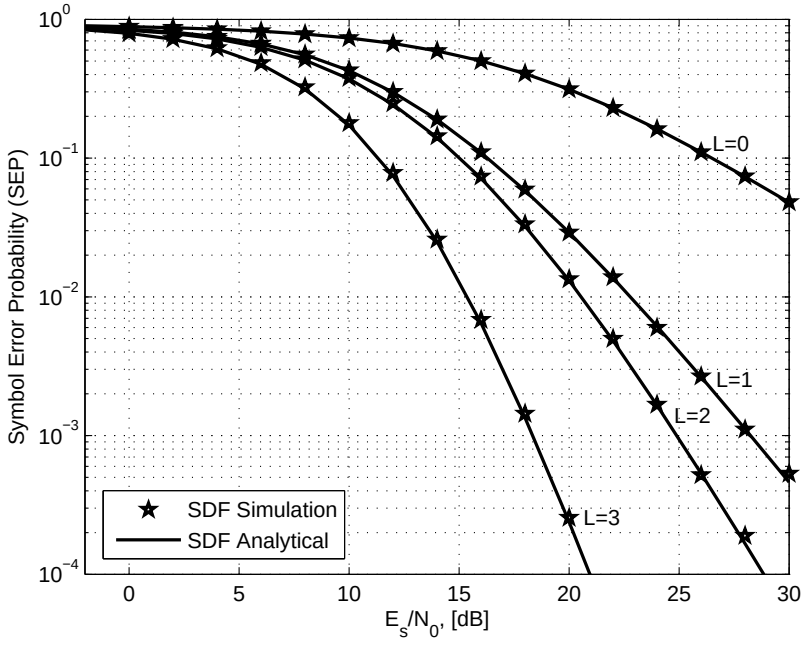

Figure 2.5: The average SEP of 16QAM HSTCS versus the average transmit SNR, E_s/N_0, when the direct link experiences the FHS. The first, the second and the third satellite-relay links experience the AS, the FHS and the ILS respectively while their terrestrial links experience the Nakagami-m fading with m_{rd} equal to 1, 0.5 and 2.8 respectively.

SEP curves that our analytical expressions show excellent agreement with the simulation results. The obtained outage and SEP expressions will provide valuable insight into the design of the HSTCS.

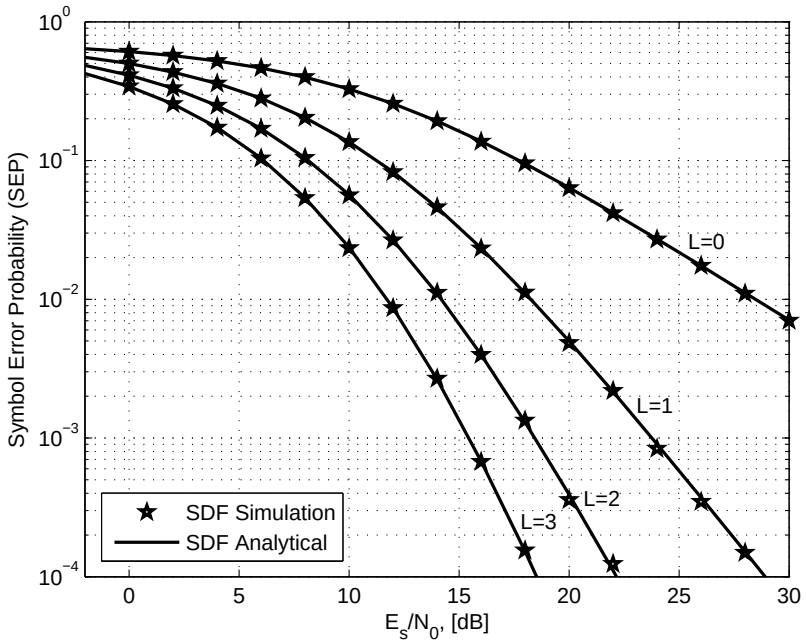

Figure 2.6: The average SEP of a QPSK HSTCS versus the average transmit SNR, E_s/N_0, when both direct and satellite-relay links experience the FHS and relay-destination links are Rayleigh fading ($m_{rd} = 1$) with the average channel power gain equal to unity.

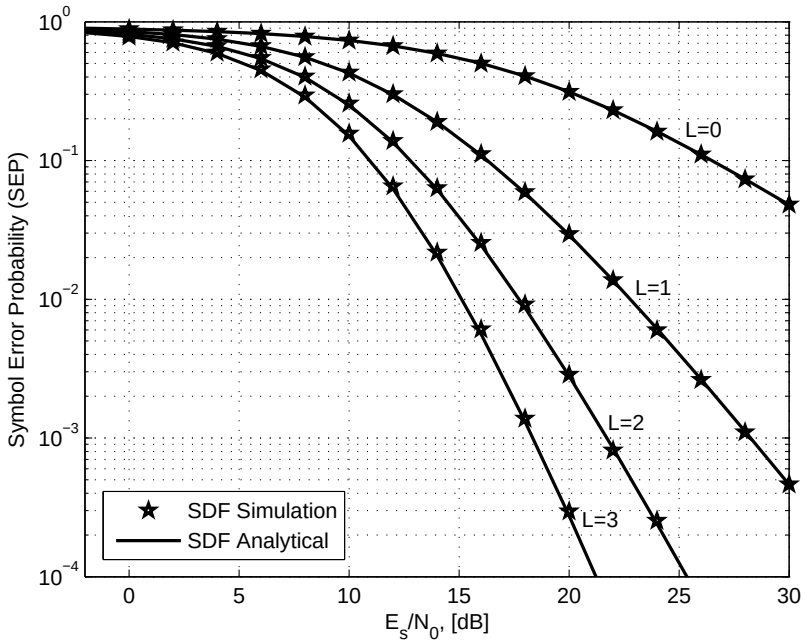

Figure 2.7: The average SEP of a 16QAM HSTCS versus the average transmit SNR, E_s/N_0, when the direct link experiences the FHS and the satellite-relay links experience the AS and relay-destination links are Rayleigh fading ($m_{rd} = 1$) with the average channel power gain equal to unity.

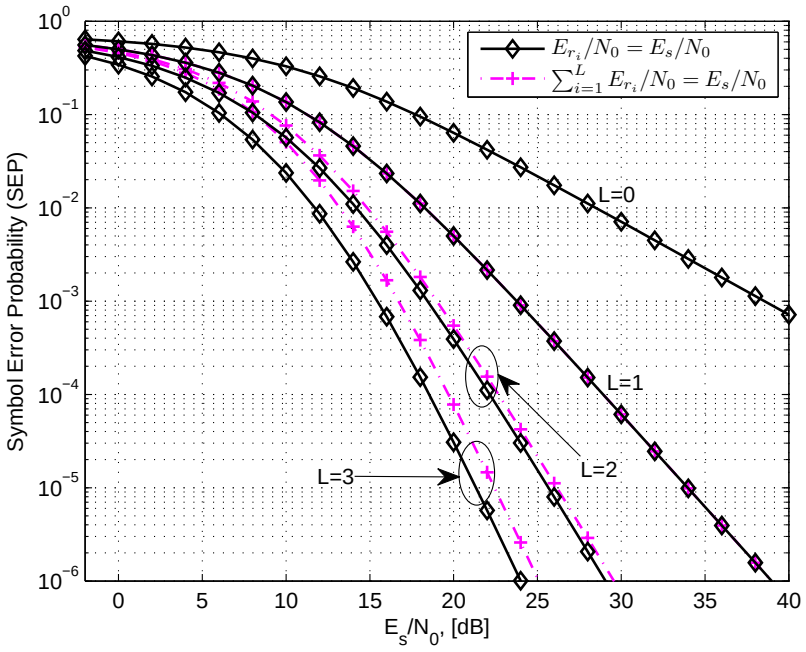

Figure 2.8: The analytical SEP of a QPSK HSTCS with different transmit SNR, E_{r_i}/N_0, scenarios, when both direct and satellite-relay links experience the FHS and relay-destination links are Rayleigh fading ($m_{rd} = 1$) with the average channel power gain equal to unity.

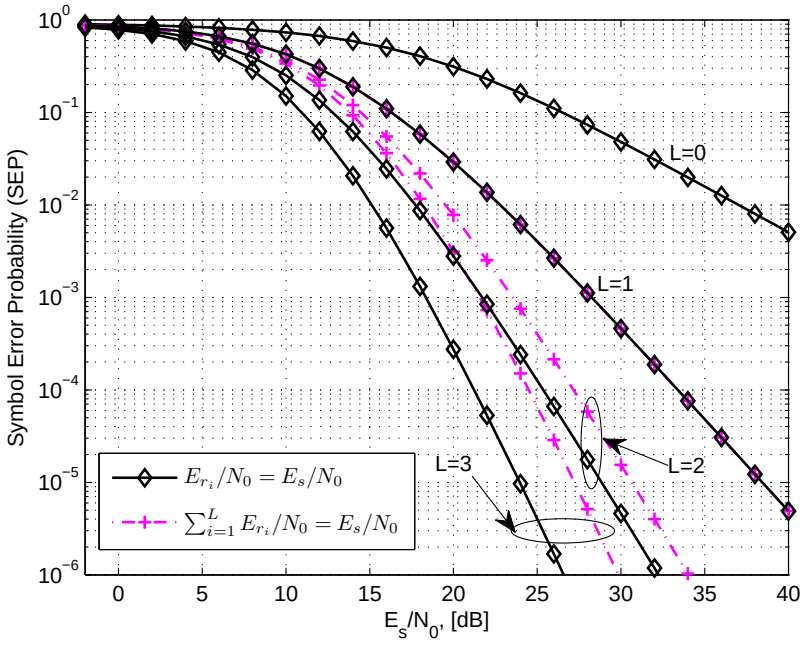

Figure 2.9: The analytical SEP curves of a 16QAM HSTCS with different transmit SNR, E_{r_i}/N_0, scenarios, when the direct link experiences the FHS and the satellite-relay links experience the AS and relay-destination links are Rayleigh fading ($m_{rd} = 1$) with the average channel power gain equal to unity.

Chapter 3

Performance analysis of HSTCSs with best relay selection

Contents

In this chapter, we study the performance in terms of outage probability and average SEP of an HSTCS with best relay selection. An SDF scheme is implemented between the satellite and a destination node, and a selection of the best relay terminal is performed. In this proposed system, a two time-slot scenario is considered. During the first time slot, the satellite is broadcasting the information to the terrestrial relays and the destination. In the second time slot, only the best relay is allowed to forward the satellite message to the destination node. The selected relay is the one that provides the best link quality between a relay and the destination. Then, both signals are combined using the MRC technique. The first part of this chapter focuses on the calculation of the exact closed-form SEP expressions of the arbitrary MPSK and MQAM signaling over independent but not necessarily identically distributed fading channels. These closed-form expressions are represented in

terms of a finite sum of Lauricella hypergeometric functions $\boldsymbol{F}_{\mathbf{D}}^{(\mathbf{n})}$, which can be numerically computed using their integral or converging series representation. In the second part of this chapter, the exact closed-form outage expressions are derived. These outage expressions are represented in terms of a sum of general hypergeometric functions ${}_pF_q(.)$ which is available in Matlab. The analytical expressions shows excellent agreement with the simulation results. Numerical results show that when the direct link experiences the frequent heavy shadowing and the satellite-relay links are under the average shadowed fading condition, the 1-relay system using QPSK can achieve the diversity gain of approximately 10 dB at the SEP of 10^{-1} with respect to the direct transmission. It increases to around 14.5 dB for the case of the 3-relay system.

3.1 System and channel models

The system model is represented in Fig. 3.1. The system consists of one satellite source denoted by s, L terrestrial relays denoted by r_1, r_2, ..., r_L, and a destination denoted by d. We assume that each terminal is equipped with a single antenna and is able to implement the cooperative functionality. The transmission is divided into two phases. In the first phase (broadcasting phase), the satellite broadcasts its signal to the set of L relay nodes and the destination node. The baseband received signal at the destination and the relay r_i can be modeled, respectively, as

$$\begin{aligned} y_{sd} &= \sqrt{E_s} h_{sd} x + n_{sd} \\ y_{sr_i} &= \sqrt{E_s} h_{sr_i} x + n_{sr_i} \end{aligned} \tag{3.1}$$

where E_s is the average transmitted energy per symbol of the satellite, h_{sd} is the channel coefficient between the satellite and the destination, h_{sr_i} is the channel coefficient between the satellite and the relay r_i, x is the transmitted symbol with unit power, n_{sd} and n_{sr_i} are the AWGN of the satellite-destination link and at the satellite-relay r_i link respectively.

We define the decoding set C, with cardinality $|C| \leq L$, as the set of relays that can decode the satellite message correctly, i.e., the relay node is said to belong to the decoding set provided that the channel between the source and the relay node is sufficiently good to allow for successful decoding. In the second phase, only one relay is selected from the decoding set C for forwarding the information.

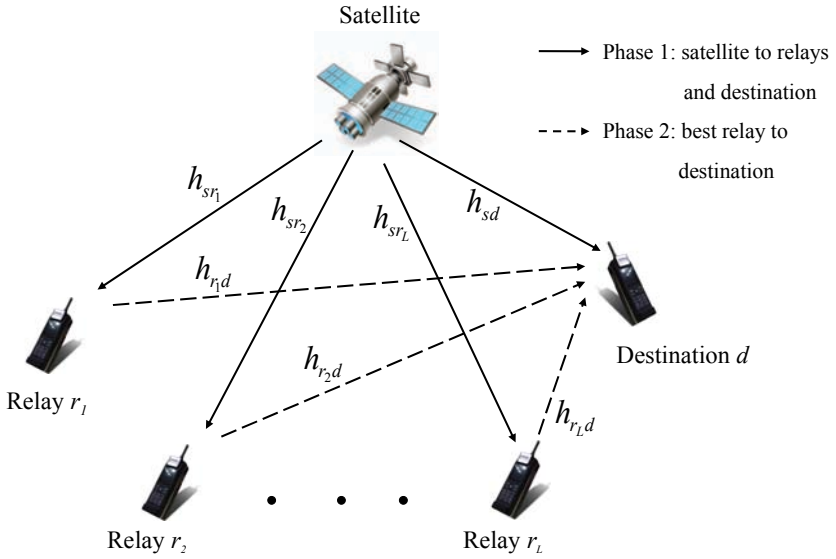

Figure 3.1: Hybrid satellite-terrestrial system with L relays and one destination.

Actually, the relay selection takes place between the two phases. The selection can be achieved using the same approach as in [BKRL06]. The selected relay is the one that provides the best link quality between a relay and the destination. The baseband received signal at the destination from the best relay r_{BR} can be modeled as

$$y_{r_{BR}d} = \sqrt{E_{r_{BR}}} h_{r_{BR}d} \widehat{x} + n_{r_{BR}d} \tag{3.2}$$

where

$$BR = \text{argmax}_{r_i \in C} \{|h_{r_i d}|^2\}, \tag{3.3}$$

$E_{r_{BR}}$ is the average transmitted energy per symbol of the best relay, $h_{r_{BR}d}$ is the channel coefficient between the best relay r_{BR} and the destination, $h_{r_i d}$ is channel coefficient between the relay r_i and the destination, $\widehat{x}$ is the decoded symbol at the relay r_i with unit power and $n_{r_{BR}d}$ is the AWGN of the best relay r_{BR}-destination link. Then, both signals from the two phases are combined using the

MRC technique.

We assume that the channels are frequency-flat, independent, but not necessarily identically distributed, fading channels. We also assume that the CSI is perfectly known at the receiver and not known at the transmitter. Furthermore, in our analysis, we assume that the AWGN terms of all links have zero mean and equal variance N_0. The statistics of the channel models are defined as follows.

- The satellite-destination and the satellite-relays link are modeled as LMS fading channels [ALAK03]. The probability density function (PDF), $f_{|h_{sx}|^2}(y)$ of the power channel gain, $|h_{sx}|^2$, is given in [ALAK03] as

$$f_{|h_{sx}|^2}(y) = \frac{1}{2b_{sx}} \left(\frac{2b_{sx}m_{sx}}{2b_{sx}m_{sx} + \Omega_{sx}} \right)^{m_{sx}} \exp\left(-\frac{y}{2b_{sx}} \right) \times {}_1F_1\left(m_{sx}; 1; \frac{\Omega_{sx} y}{2b_{sx}\left(2b_{sx}m_{sx} + \Omega_{sx}\right)} \right), \text{for } y > 0 \tag{3.4}$$

  where the second subscript $x \equiv d$ and $x \equiv r_i$ when we deal with the satellite to the destination and the satellite to the relay r_i channels respectively. The parameter Ω_{sx} is the average power of the LOS component, $2b_{sx}$ is the average power of the multipath component, and m_{sx} is the Nakagami parameter ranging from 0 to ∞. The function ${}_1F_1(a; b; z)$ is the confluent hypergeometric function defined in [GR07] by

$${}_1F_1(a; b; z) = \sum_{n=0}^{\infty} \frac{(a)_n}{(b)_n} \frac{z^n}{n!}$$

  where $(x)_n = x(x+1)...(x+n-1)$.

- The i^{th} relay-destination link is modeled as a Rayleigh fading channel. The PDF, $f_{|h_{r_id}|^2}(y)$ of the power channel gain, $|h_{r_id}|^2$, is defined in [SA05] as the exponential distribution

$$f_{|h_{r_id}|^2}(y) = \frac{1}{2b_{r_id}} \times \exp\left(-\frac{y}{2b_{r_id}} \right), \text{for } y > 0 \tag{3.5}$$

  where $2b_{r_id}$ is the average power of the multipath component of the i^{th} relay-destination link.

3.2 Average SEP of the HSTCS with best relay selection

3.2.1 The instantaneous received SNR

The instantaneous received SNR at the output of the MRC is given as

$$\gamma_{MRC}^{SDF-BR} = \gamma_{sd} + \max_{i \in C} (\gamma_{r_i d}) \,. \tag{3.6}$$

Actually, it will be difficult to find the PDF of γ_{MRC}^{SDF-BR} given in (3.6) because the decoding set C is unknown. To treat this problem we invoke the technique described in Subsection 2.2.2.

Let ξ_i be the instantaneous received SNR of the relayed link i at the destination which takes into account both the s to r_i and the r_i to d link. Therefore, the PDF of ξ_i can be obtained as

$$\begin{aligned} f_{\xi_i}(y) = f_{\xi_i | r_i \text{ Decodes Incorrectly}}(y) \Pr[r_i \text{ Decodes Incorrectly}] \\ + f_{\xi_i | r_i \text{ Decodes Correctly}}(y) \Pr[r_i \text{ Decodes Correctly}] \,. \end{aligned} \tag{3.7}$$

So, equation (3.6) is equivalent to (3.8)

$$\gamma_{MRC}^{SDF-BR} = \gamma_{sd} + \max_{i \in L} (\xi_i) \quad = \gamma_{sd} + \gamma_{BR} \tag{3.8}$$

where

$$\gamma_{BR} = \max_{i \in L} (\xi_i) \,. \tag{3.9}$$

The probability that the relay r_i decodes incorrectly is the average SEP, P_{sr_i}, of the satellite-relay r_i link. And the probability that the relay r_i decodes correctly is $(1 - P_{sr_i})$. The expressions of P_{sr_i} are given by equations (2.29) and (2.30) for MPSK and MQAM modulation schemes respectively.

The conditional PDF of $f_{\xi_i | r_i \text{ Decodes Incorrectly}}(y)$ is given by

$$f_{\xi_i | r_i \text{ Decodes Incorrectly}}(y) = \delta(y), \; y \geq 0 \tag{3.10}$$

where $\delta(y)$ is the Dirac Delta function. And the conditional PDF of $f_{\xi_i | r_i \text{ Decodes Correctly}}(y)$ is given by

$$f_{\xi_i | r_i \text{ Decodes Correctly}}(y) = \frac{1}{2 b_{r_i d} \overline{\gamma}_{r_i d}} \exp(-\frac{y}{2 b_{r_i d} \overline{\gamma}_{r_i d}}), \; y \geq 0 \tag{3.11}$$

where $\overline{\gamma}_{r_i d} = E_{r_i} / N_0$ is the average transmit SNR per symbol of the relay r_i.

Therefore, equation (3.31) can be written as

$$f_{\xi_i}(y) = P_{sr_i}\delta(y) + (1 - P_{sr_i})\frac{1}{2b_{r_i d}\overline{\gamma}_{r_i d}}\exp(-\frac{y}{2b_{r_i d}\overline{\gamma}_{r_i d}}),\ y \geq 0. \tag{3.12}$$

And the CDF of ξ_i can be written as

$$F_{\xi_i}(y) = 1 - (1 - P_{sr_i})\exp(-\frac{y}{2b_{r_i d}\overline{\gamma}_{r_i d}}),\ y \geq 0. \tag{3.13}$$

The CDF of γ_{BR} can be computed as follows

$$F_{\gamma_{BR}}(y) = \Pr\left[\max_{i\in L}(\xi_i) \leq y\right] = \prod_{i=1}^{L}\Pr\left(\xi_i \leq y\right) = \prod_{i=1}^{L}F_{\xi_i}(y). \tag{3.14}$$

The PDF of γ_{BR} can be found by taking the derivative of (3.14) with respect to y and after some mathematical computations, $f_{\gamma_{BR}}(y)$ can be written as

$$\begin{aligned} f_{\gamma_{BR}}(y) = &\left(\prod_{i=1}^{L}P_{sr_i}\right)\delta(y) + \sum_{k=1}^{L}(-1)^{(k+1)}\sum_{\lambda_1=1}^{L-k+1}\sum_{\lambda_2=\lambda_1+1}^{L-k+2}\cdots\sum_{\lambda_k=\lambda_{k-1}+1}^{L} \\ &\times\left[\prod_{n=1}^{k}\left(1 - P_{sr_{\lambda_n}}\right)\exp\left(-\frac{y}{2b_{r_{\lambda_n}d}\overline{\gamma}_{r_{\lambda_n}d}}\right)\right]\left(\sum_{n=1}^{k}\frac{1}{2b_{r_{\lambda_n}d}\overline{\gamma}_{r_{\lambda_n}d}}\right),\ y \geq 0. \end{aligned} \tag{3.15}$$

3.2.2 Moment generating function

The MGF of γ_{MRC}^{SDF-BR} can be obtained as

$$\phi_{\gamma_{MRC}^{SDF-BR}}(s) = \phi_{\gamma_{sd}}(s)\phi_{\gamma_{BR}}(s). \tag{3.16}$$

where $\phi_{\gamma_{BR}}(s)$ is the MGF of γ_{BR} and is given by

$$\begin{aligned} \phi_{\gamma_{BR}}(s) &= \mathbb{E}\left[e^{-sy}\right] = \int_0^\infty e^{-sy}f_{\gamma_{BR}}(y)dy \\ &= \left(\prod_{i=1}^{L}P_{sr_i}\right) + \sum_{k=1}^{L}(-1)^{(k+1)}\sum_{\lambda_1=1}^{L-k+1}\sum_{\lambda_2=\lambda_1+1}^{L-k+2}\cdots\sum_{\lambda_k=\lambda_{k-1}+1}^{L} \\ &\times\left[\prod_{n=1}^{k}\left(1 - P_{sr_{\lambda_n}}\right)\right]\left(\sum_{n=1}^{k}\frac{1}{2b_{r_{\lambda_n}d}\overline{\gamma}_{r_{\lambda_n}d}}\right)\left(s + \sum_{n=1}^{k}\frac{1}{2b_{r_{\lambda_n}d}\overline{\gamma}_{r_{\lambda_n}d}}\right)^{-1}. \end{aligned} \tag{3.17}$$

3.2.3 M-ary phase-shift keying (MPSK)

The average SEP of the HSTCS with best relay selection for coherent MPSK signals is given by [AT01]

$$P_{s,MPSK}^{SDF-BR}(E) = \frac{1}{\pi}\int_0^{\pi-\frac{\pi}{M}} \phi_{\gamma_{MRC}^{SDF-BR}}\left(\frac{g_{MPSK}}{\sin^2\theta}\right) d\theta \tag{3.18}$$

where $g_{MPSK} = \sin^2(\pi/M)$. By using the same approach as in (2.38), we can get $P_{s,MPSK}^{SDF-BR}(E)$ as shown below

$$\begin{aligned}
P_{s,MPSK}^{SDF-BR}(E) = {} & \frac{(2b_{sd}m_{sd})^{m_{sd}}G_{1,MPSK}^{m_{sd}-1}}{4G_{2,MPSK}^{m_{sd}}}\left(\prod_{i=1}^{L}P_{sr_i}\right)F_1\left(\frac{1}{2},1-m_{sd},m_{sd};2;\frac{1}{G_{1,MPSK}},\frac{2b_{sd}m_{sd}}{G_{2,MPSK}}\right) \\
& + \frac{3(2b_{sd}m_{sd})^{m_{sd}}G_{1,MPSK}^{m_{sd}-1}}{16G_{2,MPSK}^{m_{sd}}}\sum_{k=1}^{L}(-1)^{(k+1)}\sum_{\lambda_1=1}^{L-k+1}\sum_{\lambda_2=\lambda_1+1}^{L-k+2}\cdots\sum_{\lambda_k=\lambda_{k-1}+1}^{L} \\
& \prod_{n=1}^{k}\left(1-P_{sr_{\lambda_n}}\right)\left(\sum_{n=1}^{k}\frac{1}{2b_{r_{\lambda_n}d}\overline{\gamma}_{r_{\lambda_n}d}}\right)\frac{1}{U_{\lambda_n,MPSK}} \\
& \times F_D^{(3)}\left(\frac{1}{2},1-m_{sd},m_{sd},1;3;\frac{1}{G_{1,MPSK}},\frac{2b_{sd}m_{sd}}{G_{2,MPSK}},\frac{\sum_{n=1}^{k}\frac{1}{2b_{r_{\lambda_n}d}\overline{\gamma}_{r_{\lambda_n}d}}}{U_{\lambda_n,MPSK}}\right) \\
& + \frac{\sqrt{\omega}(2b_{sd}m_{sd})^{m_{sd}}G_{1,MPSK}^{m_{sd}-1}}{\pi G_{2,MPSK}^{m_{sd}}}\left(\prod_{i=1}^{L}P_{sr_i}\right) \\
& \times F_D^{(3)}\left(\frac{1}{2},-\frac{1}{2},1-m_{sd},m_{sd};\frac{3}{2};\omega,\frac{\omega}{G_{1,MPSK}},\frac{2b_{sd}m_{sd}\omega}{G_{2,MPSK}}\right) \\
& + \frac{\sqrt{\omega}(2b_{sd}m_{sd})^{m_{sd}}G_{1,MPSK}^{m_{sd}-1}}{\pi G_{2,MPSK}^{m_{sd}}}\sum_{k=1}^{L}(-1)^{(k+1)}\sum_{\lambda_1=1}^{L-k+1}\sum_{\lambda_2=\lambda_1+1}^{L-k+2}\cdots\sum_{\lambda_k=\lambda_{k-1}+1}^{L} \\
& \prod_{n=1}^{k}\left(1-P_{sr_{\lambda_n}}\right)\left(\sum_{n=1}^{k}\frac{1}{2b_{r_{\lambda_n}d}\overline{\gamma}_{r_{\lambda_n}d}}\right)\frac{1}{U_{\lambda_n,MPSK}} \\
& \times F_D^{(4)}\left(\frac{1}{2},-\frac{3}{2},1-m_{sd},m_{sd},1;\frac{3}{2};\omega,\frac{\omega}{G_{1,MPSK}},\frac{2b_{sd}m_{sd}\omega}{G_{2,MPSK}},\frac{\omega\sum_{n=1}^{k}\frac{1}{2b_{r_{\lambda_n}d}\overline{\gamma}_{r_{\lambda_n}d}}}{U_{\lambda_n,MPSK}}\right)
\end{aligned} \tag{3.19}$$

where

$$\begin{aligned} G_{1,MPSK} &= 1 + 2b_{sd}\overline{\gamma}_{sd}g_{MPSK}, \\ G_{2,MPSK} &= 2b_{sd}m_{sd} + 2b_{sd}\overline{\gamma}_{sd}g_{MPSK}(2b_{sd}m_{sd} + \Omega_{sd}), \\ U_{\lambda_n,MPSK} &= g_{MPSK} + \sum_{n=1}^{k} \frac{1}{2b_{r_{\lambda_n}d}\overline{\gamma}_{r_{\lambda_n}d}}. \end{aligned} \tag{3.20}$$

In the case of i.i.d fading channels, all relays are experiencing the same fading environment, i.e., $m_{sr_i} = m_{sr}$, $b_{sr_i} = b_{sr}$, $\Omega_{sr_i} = \Omega_{sr}$ and $b_{r_id} = b_{rd}$ for all $i \in L$. And we assume that $\overline{\gamma}_{r_id} = \overline{\gamma}_{rd} = \overline{\gamma}$ for all $i \in L$. So, $U_{\lambda_i,MPSK} = U_{k,MPSK}$ for all $i \in L$. Then the average SEP, $P_{s,MPSK}^{SDF-BR}(E)$, can be simplified as

$$\begin{aligned} P_{s,MPSK}^{SDF-BR}(E) = {} & \frac{(2b_{sd}m_{sd})^{m_{sd}}G_{1,MPSK}^{m_{sd}-1}}{4G_{2,MPSK}^{m_{sd}}} \left(P_{sr}^{L}\right) F_1\left(\frac{1}{2}, 1-m_{sd}, m_{sd}; 2; \frac{1}{G_{1,MPSK}}, \frac{2b_{sd}m_{sd}}{G_{2,MPSK}}\right) \\ & + \frac{3(2b_{sd}m_{sd})^{m_{sd}}G_{1,MPSK}^{m_{sd}-1}}{16G_{2,MPSK}^{m_{sd}}} \sum_{k=1}^{L}(-1)^{(k+1)}\binom{L}{k}(1-P_{sr})^k \left(\frac{k}{2b_{rd}\overline{\gamma}_{rd}}\right)\frac{1}{U_{k,MPSK}} \\ & \times F_D^{(3)}\left(\frac{1}{2}, 1-m_{sd}, m_{sd}, 1; 3; \frac{1}{G_{1,MPSK}}, \frac{2b_{sd}m_{sd}}{G_{2,MPSK}}, \frac{\frac{k}{2b_{rd}\overline{\gamma}_{rd}}}{U_{k,MPSK}}\right) \\ & + \frac{\sqrt{\omega}(2b_{sd}m_{sd})^{m_{sd}}G_{1,MPSK}^{m_{sd}-1}}{\pi G_{2,MPSK}^{m_{sd}}} \left(P_{sr}^{L}\right) F_D^{(3)}\left(\frac{1}{2}, -\frac{1}{2}, 1-m_{sd}, m_{sd}; \frac{3}{2}; \omega, \frac{\omega}{G_{1,MPSK}}, \frac{2b_{sd}m_{sd}\omega}{G_{2,MPSK}}\right) \\ & + \frac{\sqrt{\omega}(2b_{sd}m_{sd})^{m_{sd}}G_{1,MPSK}^{m_{sd}-1}}{\pi G_{2,MPSK}^{m_{sd}}} \sum_{k=1}^{L}(-1)^{(k+1)}\binom{L}{k}(1-P_{sr})^k \left(\frac{k}{2b_{rd}\overline{\gamma}_{rd}}\right)\frac{1}{U_{k,MPSK}} \\ & \times F_D^{(4)}\left(\frac{1}{2}, -\frac{3}{2}, 1-m_{sd}, m_{sd}, 1; \frac{3}{2}; \omega, \frac{\omega}{G_{1,MPSK}}, \frac{2b_{sd}m_{sd}\omega}{G_{2,MPSK}}, \frac{\omega\frac{k}{2b_{rd}\overline{\gamma}_{rd}}}{U_{k,MPSK}}\right) \end{aligned} \tag{3.21}$$

where

$$U_{k,MPSK} = g_{MPSK} + \frac{k}{2b_{rd}\overline{\gamma}_{rd}}. \tag{3.22}$$

3.2.4 M-ary quadrature amplitude modulation (MQAM)

The average SEP of the HSTCS with best relay selection for coherent MQAM signals is given by [AT01]

$$P_{s,MQAM}^{SDF-BR}(E) = \frac{4q}{\pi}\int_0^{\frac{\pi}{2}} \phi_{\gamma_{MRC}^{SDF-BR}}\left(\frac{g_{MQAM}}{\sin^2\theta}\right) d\theta - \frac{4q^2}{\pi}\int_0^{\frac{\pi}{4}} \phi_{\gamma_{MRC}^{SDF-BR}}\left(\frac{g_{MQAM}}{\sin^2\theta}\right) d\theta \tag{3.23}$$

where $g_{MQAM} = 3/2(M-1)$ and $q = \left(1 - 1/\sqrt{M}\right)$. $P_{s,MQAM}^{SDF-BR}$ can be calculated by using the same approach as in (2.46).

$$\begin{aligned}
P_{s,MQAM}^{SDF-BR}(E) = {} & \frac{q(2b_{sd}m_{sd})^{m_{sd}} G_{1,MQAM}^{m_{sd}-1}}{G_{2,MQAM}^{m_{sd}}} \left(\prod_{i=1}^{L} P_{sr_i}\right) F_1\left(\frac{1}{2}, 1-m_{sd}, m_{sd}; 2; \frac{1}{G_{1,MQAM}}, \frac{2b_{sd}m_{sd}}{G_{2,MQAM}}\right) \\
& + \frac{3q(2b_{sd}m_{sd})^{m_{sd}} G_{1,MQAM}^{m_{sd}-1}}{4G_{2,MQAM}^{m_{sd}}} \sum_{k=1}^{L}(-1)^{(k+1)} \sum_{\lambda_1=1}^{L-k+1} \sum_{\lambda_2=\lambda_1+1}^{L-k+2} \cdots \sum_{\lambda_k=\lambda_{k-1}+1}^{L} \\
& \prod_{n=1}^{k}\left(1 - P_{sr_{\lambda_n}}\right) \left(\sum_{n=1}^{k} \frac{1}{2b_{r_{\lambda_n}d}\overline{\gamma}_{r_{\lambda_n}d}}\right) \frac{1}{U_{\lambda_n,MQAM}} \\
& \times F_D^{(3)}\left(\frac{1}{2}, 1-m_{sd}, m_{sd}, 1; 3; \frac{1}{G_{1,MQAM}}, \frac{2b_{sd}m_{sd}}{G_{2,MQAM}}, \frac{\sum_{n=1}^{k} \frac{1}{2b_{r_{\lambda_n}d}\overline{\gamma}_{r_{\lambda_n}d}}}{U_{\lambda_n,MQAM}}\right) \\
& - \frac{2q^2(2b_{sd}m_{sd})^{m_{sd}} L_{1,MQAM}^{m_{sd}-1}}{3\pi L_{2,MQAM}^{m_{sd}}} \left(\prod_{i=1}^{L} P_{sr_i}\right) \\
& \times F_D^{(3)}\left(1, 1, 1-m_{sd}, m_{sd}; \frac{5}{2}; \frac{1}{2}, \frac{G_{1,MQAM}}{L_{1,MQAM}}, \frac{G_{2,MQAM}}{L_{2,MQAM}}\right) \\
& - \frac{2q^2(2b_{sd}m_{sd})^{m_{sd}} L_{1,MQAM}^{m_{sd}-1}}{5\pi L_{2,MQAM}^{m_{sd}}} \sum_{k=1}^{L}(-1)^{(k+1)} \sum_{\lambda_1=1}^{L-k+1} \sum_{\lambda_2=\lambda_1+1}^{L-k+2} \cdots \sum_{\lambda_k=\lambda_{k-1}+1}^{L} \\
& \prod_{n=1}^{k}\left(1 - P_{sr_{\lambda_n}}\right) \left(\sum_{n=1}^{k} \frac{1}{2b_{r_{\lambda_n}d}\overline{\gamma}_{r_{\lambda_n}d}}\right) \frac{1}{V_{\lambda_n,MQAM}} \\
& \times F_D^{(4)}\left(1, 1, 1-m_{sd}, m_{sd}, 1; \frac{7}{2}; \frac{1}{2}, \frac{G_{1,MQAM}}{L_{1,MQAM}}, \frac{G_{2,MQAM}}{L_{2,MQAM}}, \frac{U_{\lambda_n,MQAM}}{V_{\lambda_n,MQAM}}\right)
\end{aligned} \tag{3.24}$$

where

$$\begin{aligned}
G_{1,MQAM} &= 1 + 2b_{sd}\overline{\gamma}_{sd}g_{MQAM}, \\
G_{2,MQAM} &= 2b_{sd}m_{sd} + 2b_{sd}\overline{\gamma}_{sd}g_{MQAM}\left(2b_{sd}m_{sd} + \Omega_{sd}\right), \\
L_{1,MQAM} &= 1 + 4b_{sd}\overline{\gamma}_{sd}g_{MQAM}, \\
L_{2,MQAM} &= 2b_{sd}m_{sd} + 4b_{sd}\overline{\gamma}_{sd}g_{MQAM}(2b_{sd}m_{sd} + \Omega_{sd}), \\
U_{\lambda_n,MQAM} &= g_{MQAM} + \sum_{n=1}^{k} \frac{1}{2b_{r_{\lambda_n}d}\overline{\gamma}_{r_{\lambda_n}d}}, \\
V_{\lambda_n,MQAM} &= 2g_{MQAM} + \sum_{n=1}^{k} \frac{1}{2b_{r_{\lambda_n}d}\overline{\gamma}_{r_{\lambda_n}d}}.
\end{aligned} \tag{3.25}$$

In the case of i.i.d fading channels, all relays are experiencing the same fading environment, i.e., $m_{sr_i} = m_{sr}$, $b_{sr_i} = b_{sr}$, $\Omega_{sr_i} = \Omega_{sr}$ and $b_{r_id} = b_{rd}$ for all $i \in L$. And we assume that $\overline{\gamma}_{r_id} = \overline{\gamma}_{rd} = \overline{\gamma}$ for all $i \in L$. So, $U_{\lambda_i,MQAM} = U_{k,MQAM}$ and $V_{\lambda_i,MQAM} = V_{k,MQAM}$ for all $i \in L$. Then the average SEP, $P_{s,MPSK}^{SDF-BR}(E)$, can be simplified as follows

$$\begin{aligned}
P_{s,MQAM}^{SDF-BR}(E) = {} & \frac{q(2b_{sd}m_{sd})^{m_{sd}}G_{1,MQAM}^{m_{sd}-1}}{G_{2,MQAM}^{m_{sd}}}\left(P_{sr}^{L}\right)F_1\left(\frac{1}{2}, 1-m_{sd}, m_{sd}; 2; \frac{1}{G_{1,MQAM}}, \frac{2b_{sd}m_{sd}}{G_{2,MQAM}}\right) \\
& + \frac{3q(2b_{sd}m_{sd})^{m_{sd}}G_{1,MQAM}^{m_{sd}-1}}{4G_{2,MQAM}^{m_{sd}}}\sum_{k=1}^{L}(-1)^{(k+1)}\binom{L}{k}(1-P_{sr})^{k}\left(\frac{k}{2b_{rd}\overline{\gamma}_{rd}}\right)\frac{1}{U_{k,MQAM}} \\
& \times F_D^{(3)}\left(\frac{1}{2}, 1-m_{sd}, m_{sd}, 1; 3; \frac{1}{G_{1,MQAM}}, \frac{2b_{sd}m_{sd}}{G_{2,MQAM}}, \frac{\frac{k}{2b_{rd}\overline{\gamma}_{rd}}}{U_{k,MQAM}}\right) \\
& - \frac{2q^2(2b_{sd}m_{sd})^{m_{sd}}L_{1,MQAM}^{m_{sd}-1}}{3\pi L_{2,MQAM}^{m_{sd}}}\left(P_{sr}^{L}\right)F_D^{(3)}\left(1, 1, 1-m_{sd}, m_{sd}; \frac{5}{2}; \frac{1}{2}, \frac{G_{1,MQAM}}{L_{1,MQAM}}, \frac{G_{2,MQAM}}{L_{2,MQAM}}\right) \\
& - \frac{2q^2(2b_{sd}m_{sd})^{m_{sd}}L_{1,MQAM}^{m_{sd}-1}}{5\pi L_{2,MQAM}^{m_{sd}}}\sum_{k=1}^{L}(-1)^{(k+1)}\binom{L}{k}(1-P_{sr})^{k}\left(\frac{k}{2b_{rd}\overline{\gamma}_{rd}}\right)\frac{1}{V_{k,MQAM}} \\
& \times F_D^{(4)}\left(1, 1, 1-m_{sd}, m_{sd}, 1; \frac{7}{2}; \frac{1}{2}, \frac{G_{1,MQAM}}{L_{1,MQAM}}, \frac{G_{2,MQAM}}{L_{2,MQAM}}, \frac{U_{k,MQAM}}{V_{k,MQAM}}\right)
\end{aligned} \tag{3.26}$$

where

$$\begin{aligned} U_{k,MQAM} &= g_{MQAM} + \frac{k}{2b_{rd}\overline{\gamma}_{rd}}, \\ V_{k,MQAM} &= 2g_{MQAM} + \frac{k}{2b_{rd}\overline{\gamma}_{rd}}. \end{aligned} \tag{3.27}$$

3.3 Outage probability of the HSTCS with best relay selection

The instantaneous mutual information of the HSTCS with best relay selection is defined as

$$I_{SDF-BR} = \frac{1}{2}\log_2\left(1+\tilde{\gamma}_{MRC}^{SDF-BR}\right) \tag{3.28}$$

where $\tilde{\gamma}_{MRC}^{SDF-BR}$ is the instantaneous received SNR at the output of the MRC and is given by

$$\tilde{\gamma}_{MRC}^{SDF-BR} = \gamma_{sd} + \max_{i\in C}\left(\gamma_{r_i d}\right). \tag{3.29}$$

The fraction 1/2 comes from the fact that there are only two channels (two time slots) are used, one is allocated to the relay link and another one is allocated to the direct link.

Therefore, the outage of the HSTCS with best relay selection can be computed as follows

$$\begin{aligned} P_{SDF-BR}^{out} &= \Pr\left[I_{SDF-BR} < R\right] = \Pr\left[\gamma_{MRC}^{SDF-BR} < 2^{2R}-1\right] \\ &= \Pr\left[\gamma_{MRC}^{SDF-BR} < \gamma_{th}\right] = F_{\gamma_{MRC}^{SDF-BR}}(\gamma_{th}) \end{aligned} \tag{3.30}$$

where $\gamma_{th} = 2^{2R}-1$.

Actually, it will be difficult to find the PDF of $\tilde{\gamma}_{MRC}^{SDF-BR}$ given in (3.29) because the decoding set C is unknown. To treat this problem we invoke the technique described in Subsection 2.3.2.

Let $\tilde{\xi}_i$ be the instantaneous received SNR of the relayed link i at the destination which takes into account both the s to r_i and the r_i to d link. Therefore, the PDF of $\tilde{\xi}_i$ can be obtained as

$$\begin{aligned} f_{\tilde{\xi}_i}(y) = {} & f_{\tilde{\xi}_i|r_i \text{ Decodes Incorrectly}}(y)\Pr\left[r_i \text{ Decodes Incorrectly}\right] \\ & + f_{\tilde{\xi}_i|r_i \text{ Decodes Correctly}}(y)\Pr\left[r_i \text{ Decodes Correctly}\right]. \end{aligned} \tag{3.31}$$

So, equation (3.29) is equivalent to (3.32)

$$\tilde{\gamma}_{MRC}^{SDF-BR} = \gamma_{sd} + \max_{i\in L}\left(\tilde{\xi}_i\right) \quad = \gamma_{sd} + \tilde{\gamma}_{BR} \tag{3.32}$$

where

$$\tilde{\gamma}_{BR} = \max_{i \in L} \left(\tilde{\xi}_i \right). \tag{3.33}$$

The probability that the relay r_i decodes incorrectly is the outage probability, $P_{sr_i}^{out}$, of the satellite-relay r_i link and the probability that the relay r_i decodes correctly is $(1 - P_{sr_i}^{out})$. The expression of $P_{sr_i}^{out}$ is given in (2.66).

The conditional PDF of $f_{\tilde{\xi}_i | r_i \text{ Decodes Incorrectly}}(y)$ is given by

$$f_{\tilde{\xi}_i | r_i \text{ Decodes Incorrectly}}(y) = \delta(y), \ y \geq 0 \tag{3.34}$$

where $\delta(y)$ is the Dirac Delta function. And the conditional PDF of $f_{\tilde{\xi}_i | r_i \text{ Decodes Correctly}}(y)$ is given by

$$f_{\tilde{\xi}_i | r_i \text{ Decodes Correctly}}(y) = \frac{1}{2b_{r_i d}\overline{\gamma}_{r_i d}} \exp(-\frac{y}{2b_{r_i d}\overline{\gamma}_{r_i d}}), \ y \geq 0 \tag{3.35}$$

where $\overline{\gamma}_{r_i d} = E_{r_i}/N_0$ is the average transmit SNR per symbol of the relay r_i.

Therefore, equation (3.31) can be written as, for $y \geq 0$,

$$f_{\tilde{\xi}_i}(y) = P_{sr_i}^{out}\delta(y) + (1 - P_{sr_i}^{out})\frac{1}{2b_{r_i d}\overline{\gamma}_{r_i d}} \exp(-\frac{y}{2b_{r_i d}\overline{\gamma}_{r_i d}}). \tag{3.36}$$

And the CDF of $\tilde{\xi}_i$ can be written as

$$F_{\tilde{\xi}_i}(y) = 1 - (1 - P_{sr_i}^{out}) \exp(-\frac{y}{2b_{r_i d}\overline{\gamma}_{r_i d}}). \tag{3.37}$$

Hence, the CDF of $\tilde{\gamma}_{BR}$ can be computed as follows

$$F_{\tilde{\gamma}_{BR}}(y) = \Pr\left[\max_{i \in L}\left(\tilde{\xi}_i\right) \leq y\right] = \prod_{i=1}^{L} \Pr\left(\tilde{\xi}_i \leq y\right) = \prod_{i=1}^{L} F_{\tilde{\xi}_i}(y). \tag{3.38}$$

By using the following property,

$$\prod_{k=1}^{L}(1 + A_k) = 1 + \sum_{k=1}^{L}\sum_{\lambda_1=1}^{L-k+1}\sum_{\lambda_2=\lambda_1+1}^{L-k+2}\cdots\sum_{\lambda_k=\lambda_{k-1}+1}^{L}\prod_{n=1}^{k} A_{\lambda_n} \tag{3.39}$$

the CDF of $\tilde{\gamma}_{BR}$ can be rewritten as below

$$F_{\tilde{\gamma}_{BR}}(y) = 1 + \sum_{k=1}^{L}(-1)^k \sum_{\lambda_1=1}^{L-k+1}\sum_{\lambda_2=\lambda_1+1}^{L-k+2}\cdots\sum_{\lambda_k=\lambda_{k-1}+1}^{L}\left[\prod_{n=1}^{k}\left(1 - P_{sr_{\lambda_n}}^{out}\right)\right]\exp\left(-\sum_{n=1}^{k}\frac{y}{2b_{r_{\lambda_n} d}\overline{\gamma}_{r_{\lambda_n} d}}\right). \tag{3.40}$$

The PDF of the sum of two independent random variables is the convolution product of these two variables. Therefore, the PDF of $\tilde{\gamma}_{MRC}^{SDF-BR}$ is given as

$$f_{\tilde{\gamma}_{MRC}^{SDF-BR}}(y) = \int_{-\infty}^{+\infty} f_{\tilde{\gamma}_{BR}}(y-\tau) f_{\gamma_{sd}}(\tau) d\tau. \tag{3.41}$$

After some mathematical computations, the CDF of $\tilde{\gamma}_{MRC}^{SDF-BR}$ can be expressed as

$$F_{\tilde{\gamma}_{MRC}^{SDF-BR}}(y) = \int_{0}^{y} F_{\tilde{\gamma}_{BR}}(y-\tau) f_{\gamma_{sd}}(\tau) d\tau. \tag{3.42}$$

By using the same approach as in (2.78), the CDF of $\tilde{\gamma}_{MRC}^{SDF-BR}$, $F_{\tilde{\gamma}_{MRC}^{SDF-BR}}(y)$, can be obtained as below

$$\begin{aligned} F_{\tilde{\gamma}_{MRC}^{SDF-BR}}(y) = F_{\gamma_{sd}}(y) + A_{sd} \sum_{k=1}^{L} (-1)^k \sum_{\lambda_1=1}^{L-k+1} \sum_{\lambda_2=\lambda_1+1}^{L-k+2} \cdots \sum_{\lambda_k=\lambda_{k-1}+1}^{L} \left[\prod_{n=1}^{k} \left(1 - P_{sr_{\lambda_n}}^{out}\right) \right] \\ \times \exp\left(- \sum_{n=1}^{k} \frac{y}{2b_{r_{\lambda_n} d} \overline{\gamma}_{r_{\lambda_n} d}} \right) \left[y_1 F_1\left(m_{sd}; 2; B_{sd} y\right) + \sum_{j=1}^{+\infty} (-1)^j \left(\frac{1}{2b_{sd}\overline{\gamma}_{sd}} - \sum_{n=1}^{k} \frac{1}{2b_{r_{\lambda_n} d}\overline{\gamma}_{r_{\lambda_n} d}} \right)^j \right. \\ \left. \times \frac{y^{(j+1)}}{(j+1)!} {}_2F_2\left(j+1, m_{sd}; j+2, 1; B_{sd} y\right) \right]. \end{aligned} \tag{3.43}$$

So, the outage probability of the HSTCS with best relay selection is finally given by

$$\begin{aligned} P_{SDF-BR}^{out} = P_{sd}^{out} + A_{sd} \sum_{k=1}^{L} (-1)^k \sum_{\lambda_1=1}^{L-k+1} \sum_{\lambda_2=\lambda_1+1}^{L-k+2} \cdots \sum_{\lambda_k=\lambda_{k-1}+1}^{L} \left[\prod_{n=1}^{k} \left(1 - P_{sr_{\lambda_n}}^{out}\right) \right] \\ \times \exp\left(- \sum_{n=1}^{k} \frac{\gamma_{th}}{2b_{r_{\lambda_n} d} \overline{\gamma}_{r_{\lambda_n} d}} \right) \left[\gamma_{th} {}_1F_1\left(m_{sd}; 2; B_{sd}\gamma_{th}\right) + \sum_{j=1}^{+\infty} (-1)^j \left(\frac{1}{2b_{sd}\overline{\gamma}_{sd}} - \sum_{n=1}^{k} \frac{1}{2b_{r_{\lambda_n} d}\overline{\gamma}_{r_{\lambda_n} d}} \right)^j \right. \\ \left. \times \frac{\gamma_{th}^{(j+1)}}{(j+1)!} {}_2F_2\left(j+1, m_{sd}; j+2, 1; B_{sd}\gamma_{th}\right) \right]. \end{aligned} \tag{3.44}$$

In the case of i.i.d fading channels, all relays are experiencing the same fading environment, i.e., $m_{sr_i} = m_{sr}$, $b_{sr_i} = b_{sr}$, $\Omega_{sr_i} = \Omega_{sr}$, $b_{r_i d} = b_{rd}$ and $\overline{\gamma}_{r_i d} = \overline{\gamma}_{rd}$ for all $i \in L$. Then the outage probability, $P_{\tilde{\gamma}_{MRC}^{SDF-BR}}^{out}$, is reduced to (3.45).

$$P_{SDF-BR}^{out} = P_{sd}^{out} + A_{sd} \sum_{k=1}^{L} \binom{L}{k} (-1)^k \left(1 - P_{sr}^{out}\right)^k \exp\left(-\frac{k}{2b_{rd}\overline{\gamma}_{rd}}\gamma_{th}\right)$$
$$\times \left[\gamma_{th1} F_1\left(m_{sd}; 2; B_{sd}\gamma_{th}\right) + \sum_{j=1}^{+\infty} (-1)^j \left(\frac{1}{2b_{sd}\overline{\gamma}_{sd}} - \frac{k}{2b_{rd}\overline{\gamma}_{rd}}\right)^j \right. \tag{3.45}$$
$$\left. \times \frac{\gamma_{th}^{(j+1)}}{(j+1)!} {}_2F_2\left(j+1, m_{sd}; j+2, 1; B_{sd}\gamma_{th}\right)\right].$$

Although the outage probability in (3.44) and (3.45) is expressed as an infinite sum of general hypergeometric functions, it is convergent when the number of terms j in the sum of (3.44) and (3.45) is high enough, i.e., $j \gg 1$.

3.4 Simulation results

In this section, the outage probability and the average SEP of an HSTCS are obtained through simulation. The results are compared to the analytical results presented in the previous sections. The outage and SEP curves are plotted versus the average transmit SNR per symbol, E_s/N_0, for different number of participating relays $L = 0, 1, 2, 3$ ($L = 0$, corresponds to the direct transmission only). The numerical values for the LMS channel are shown in Table 2.1 and the relay-destination links are Rayleigh fading channels. The target spectral efficiency R is assumed to be 0.5 bits/s/Hz which corresponds to $\gamma_{th} = 0\ dB$. In order to show the diversity order, we assume that the average transmit SNR per symbol of the satellite-destination link is equal to the one of the relay-destination links ($E_s/N_0 = E_{r_i}/N_0$). The figures illustrate that our analytical results show excellent agreement with the simulation results for both i.n.i.d fading channels and i.i.d fading channels. This confirms the accuracy of our performance analysis.

The theoretical curves of the system without best relay selection SDF schemes are also plotted as the base line for the comparison. The results also show that the system without best relay selection provides some small diversity gain over the system with best relay selection in the high-SNR regime. However, the transmission scheme without best relay selection requires $L + 1$ orthogonal channels while only two orthogonal channels are needed for the best relay selection scheme.

3.4.1 Outage curves

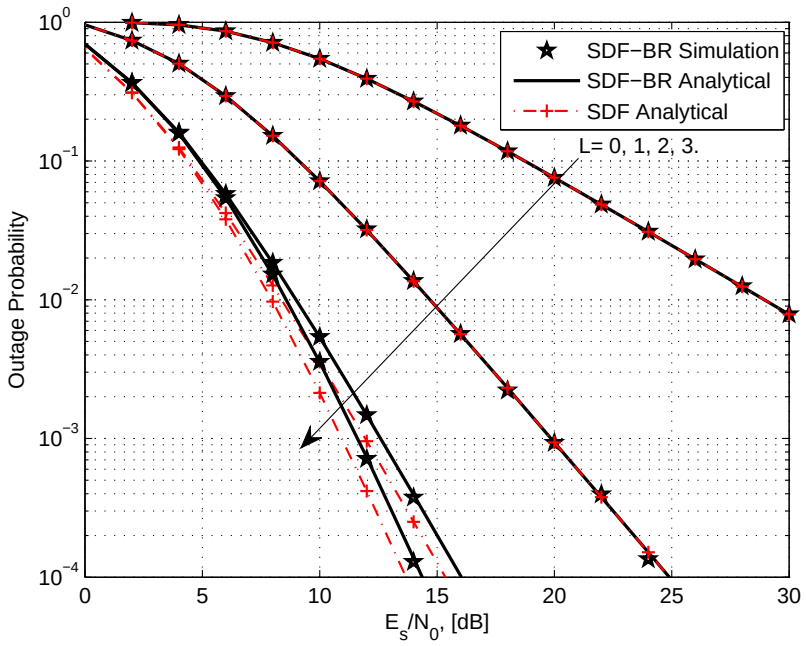

Figure 3.2: The outage probability of an HSTCS with best relay selection versus the average transmit SNR, E_s/N_0, when the direct link experiences the FHS. The first, the second and the third satellite-relays experience the AS, the ILS and the FHS respectively while their terrestrial links experience the Rayleigh fading with the average power channel gain equal to 0.5, 1 and 0.25 respectively.

Fig. 3.2 shows the outage probability of an HSTCS with best relay selection over i.n.i.d fading channels when the direct link experiences the FHS. The first, the second and the third satellite-relay links experience the AS, the ILS and the FHS respectively while their terrestrial links experience the Rayleigh fading with the average power channel gain equal to 0.5, 1 and 0.25 respectively. We can observe from the figure that the 3-relay system curve and the 2-relay system curve are superimposed in the low-SNR regime. This is because of the strong fading of the third relay link. We can observe in the figure that the 1-relay system provides a diversity gain of 10 dB at the outage rate of 10^{-1} over the direct link while the 2-relay system provides a diversity gain of 14 dB over the direct link at the same outage rate.

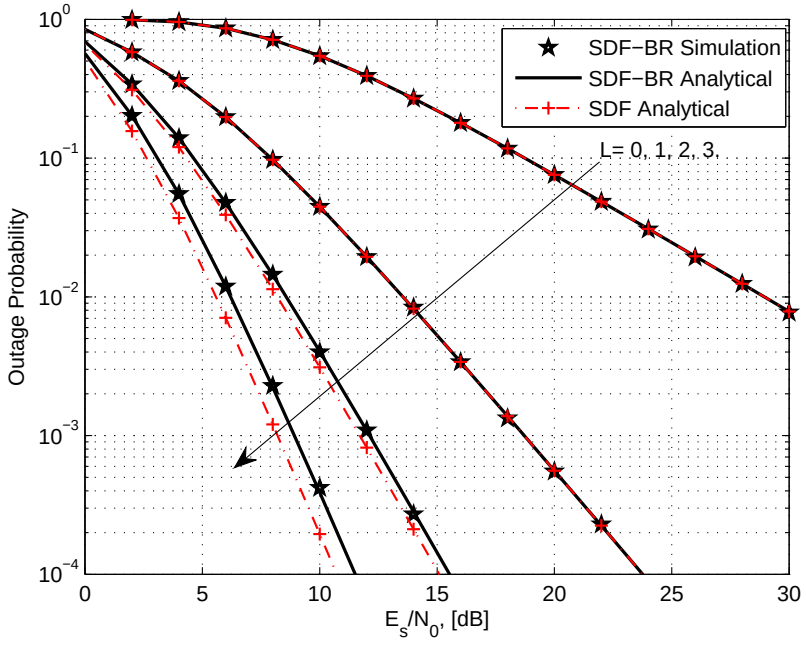

Figure 3.3: The outage probability of an HSTCS with best relay selection versus the average transmit SNR, E_s/N_0, when the direct link experiences the FHS and the relay links experience the AS while their terrestrial links experience the Rayleigh fading with the average power channel gain equal to unity.

Fig. 3.3 shows the outage probability of an HSTCS with best relay selection over i.i.d fading channels when the direct link experiences the FHS and the relay links experience the AS while all terrestrial links are Rayleigh with average channel power gain equal to unity. We can achieve approximately 5.5 dB of diversity gain at the outage probability of 10^{-1} when only one relay is participating. In addition, this diversity gain does increase to approximately 9 dB when $L = 3$.

3.4.2 SEP curves

Figs. 3.4, 3.5 and 3.6 plot the average SEP of QPSK, 8PSK and 16QAM HSTCS with best relay selection respectively over i.n.i.d fading channels. The channel parameters for each curve simulation are summarized in Table 3.1 and the diversity gains at the SEP of 10^{-1} are provided in Table 3.2.

Fig. 3.5 shows that the 2-relay system and the 3-relay system curves are superimposed in the low-SNR regime, i.e., E_s/N_0<12 dB. This is due to the fact that the third relay link experiences the strong fading (FHS).

Table 3.1: Parameters of SEP simulation curves over i.n.i.d fading channels

	Modulation scheme	$s-r_i$ links	r_i-d links
Fig. 3.4	QPSK	$s-r_1$: FHS $s-r_2$: AS $s-r_3$: ILS	r_1-d: $2b_{r_1d}=1$ r_2-d: $2b_{r_2d}=0.5$ r_3-d: $2b_{r_3d}=0.25$
Fig. 3.5	8PSK	$s-r_1$: ILS $s-r_2$: AS $s-r_3$: FHS	r_1-d: $2b_{r_1d}=1$ r_2-d: $2b_{r_2d}=0.5$ r_3-d: $2b_{r_3d}=0.25$
Fig. 3.6	16QAM	$s-r_1$: ILS $s-r_2$: AS $s-r_3$: ILS	r_1-d: $2b_{r_1d}=1$ r_2-d: $2b_{r_2d}=1$ r_3-d: $2b_{r_3d}=0.5$

Table 3.2: Diversity gain of the HSTCS with best relay selection at the SEP of 10^{-1} over i.n.i.d fading channels

	1-relay system	2-relay system	3-relay system
Fig. 3.4	7 dB	11 dB	11.5 dB
Fig. 3.5	10.5 dB	12.5 dB	12.5 dB
Fig. 3.6	10 dB	13 dB	13.5 dB

Furthermore, Figs. 3.7, 3.8 and 3.9 illustrate the average SEP of QPSK, 8PSK and 16QAM HSTCS with best relay selection respectively over i.i.d fading channels. The channel parameters for each curve simulation are summarized in Table 3.3 and the diversity gains at the SEP of 10^{-1} are provided in Table 3.4. Table 3.4 shows that the 1-relay system provides around 10 dB of diversity gain at the

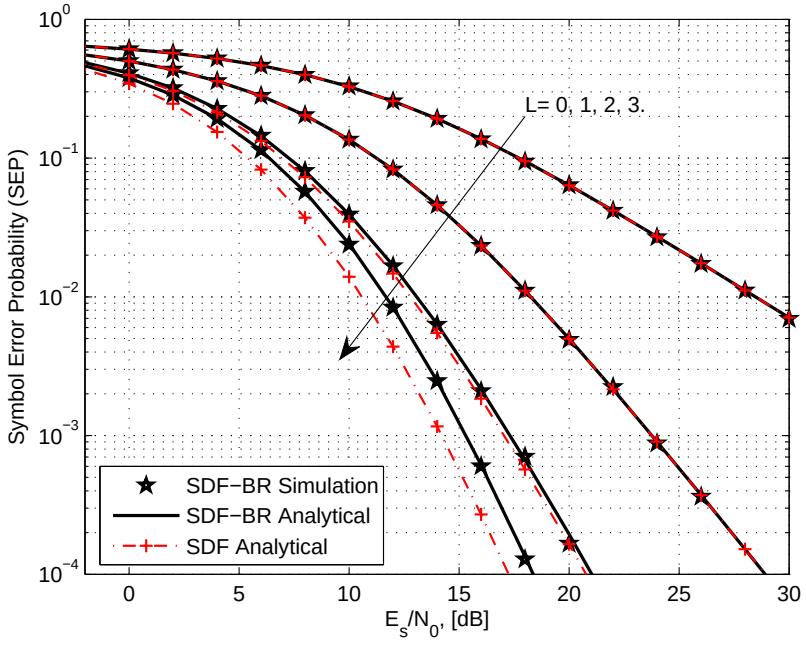

Figure 3.4: The average SEP of a QPSK HSTCS with best relay selection versus the average transmit SNR, E_s/N_0, when the direct link experiences the FHS. The first, the second and the third relay experience the FHS, the AS and the ILS respectively while their terrestrial links experience the Rayleigh fading with the average power channel gain equal to 1, 0.5 and 0.25 respectively.

SEP of 10^{-1} while the diversity gain of 14.5 dB can be obtained for case of 3-relay system.

Table 3.3: Parameters of SEP simulation curves over i.i.d fading channels

	Modulation scheme	$s-r$ links	$r-d$ links
Fig. 3.7	QPSK	$s-r$: AS	$r-d$: $2b_{rd}=1$
Fig. 3.8	8PSK	$s-r$: AS	$r-d$: $2b_{rd}=1$
Fig. 3.9	16QAM	$s-r$: ILS	$r-d$: $2b_{rd}=1$

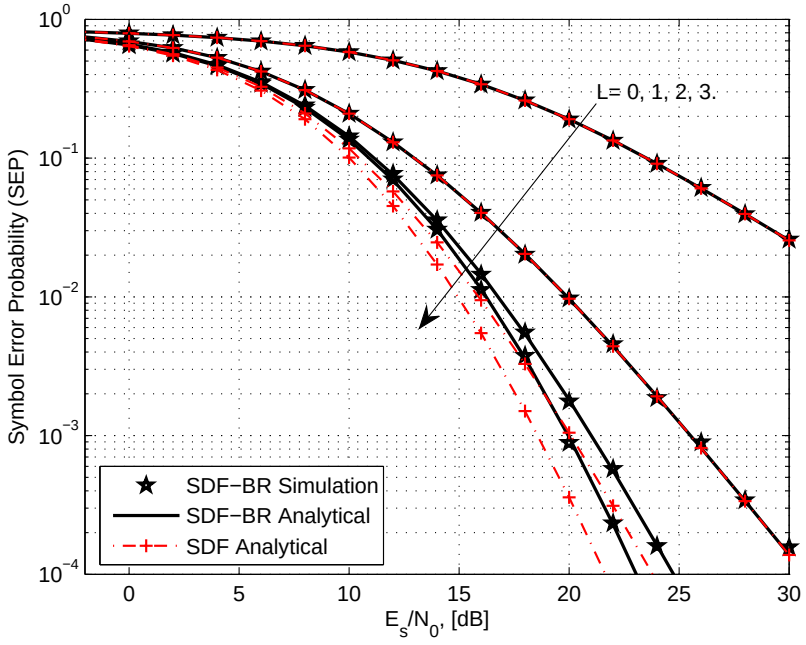

Figure 3.5: The average SEP of a 8PSK HSTCS with best relay selection versus the average transmit SNR, E_s/N_0, when the direct link experiences the FHS. The first, the second and the third relay experience the ILS, the AS and the FHS respectively while their terrestrial links experience the Rayleigh fading with the average power channel gain equal to 1, 0.5 and 0.25 respectively.

Table 3.4: Diversity gain of the HSTCS with best relay selection at the SEP of 10^{-1} over i.i.d fading channels

	1-relay system	2-relay system	3-relay system
Fig. 3.7	10 dB	13 dB	14.5 dB
Fig. 3.8	10 dB	13 dB	14.5 dB
Fig. 3.9	10 dB	13.5 dB	14.5 dB

3.5 Conclusion

In this chapter, we study the performance in terms of the outage probability and the SEP of an HSTCS with best relay selection. The SDF transmission scheme has been implemented. The two

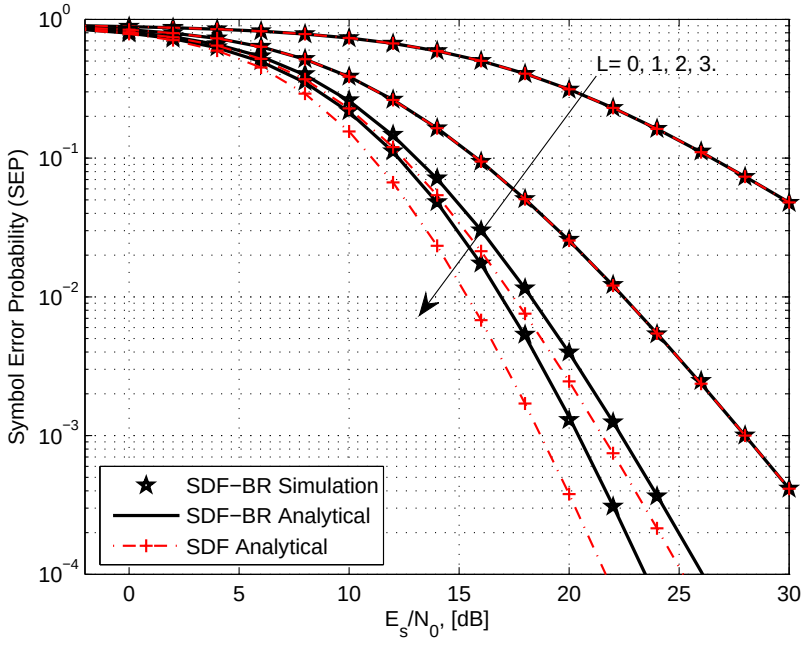

Figure 3.6: The average SEP of a 16QAM HSTCS with best relay selection versus the average transmit SNR, E_s/N_0, when the direct link experiences the FHS. The first, the second and the third relay experience the ILS, the AS and the ILS respectively while their terrestrial links experience the Rayleigh fading with the average power channel gain equal to 1, 1 and 0.5 respectively.

time-slot scenario is considered. During the first time slot, the satellite broadcasts the information to the terrestrial relays and the destination. In the second time slot, only the best relay is transmitting toward the destination node. The selected relay is the one that provides the best link quality between a relay and the destination. Then, both signals are combined using the MRC technique. The exact outage probability and the exact closed-form SEP expressions of the general MPSK and MQAM HSTCS with best relay selection over independent but not necessarily identically distributed fading channels have been derived. The results have shown that a full diversity order of $L+1$ can be obtained when the number of participating relays is equal to L. Moreover, it can be seen from the SEP curves that our analytical expressions show excellent agreement with the simulation results. The obtained outage and SEP expressions will provide valuable insight into the design of an HSTCS with best relay

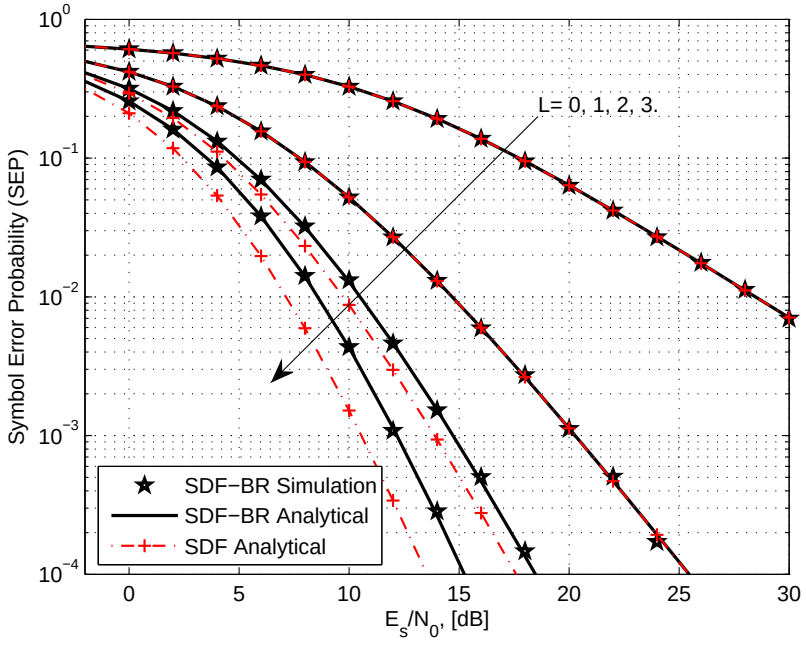

Figure 3.7: The average SEP of a QPSK HSTCS with best relay selection versus the average transmit SNR, E_s/N_0, when the direct link experiences the FHS and satellite-relay links experience the AS while their terrestrial links experience the Rayleigh fading with the average power channel gain equal to unity.

selection especially in the emergency communication systems.

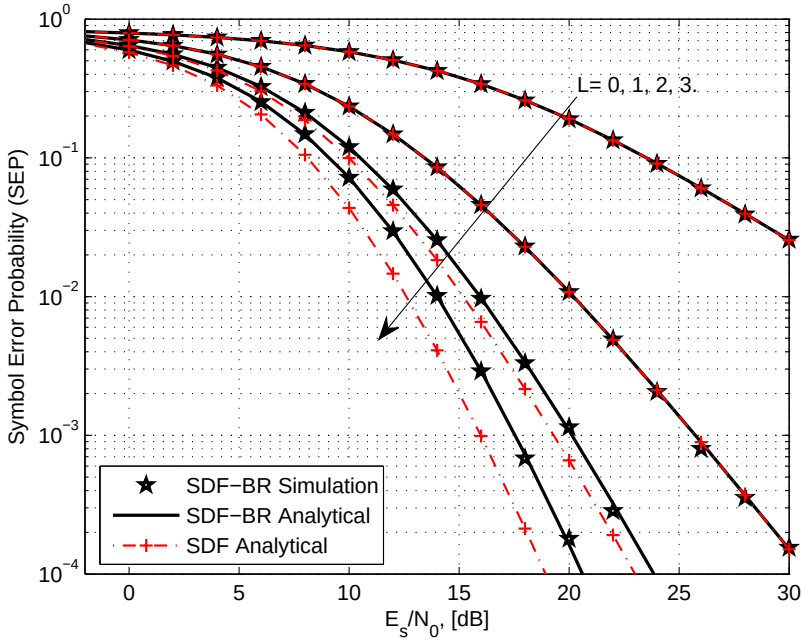

Figure 3.8: The average SEP of a 8PSK HSTCS with best relay selection versus the average transmit SNR, E_s/N_0, when the direct link experiences the FHS and satellite-relay links experience the AS while their terrestrial links experience the Rayleigh fading with the average power channel gain equal to unity.

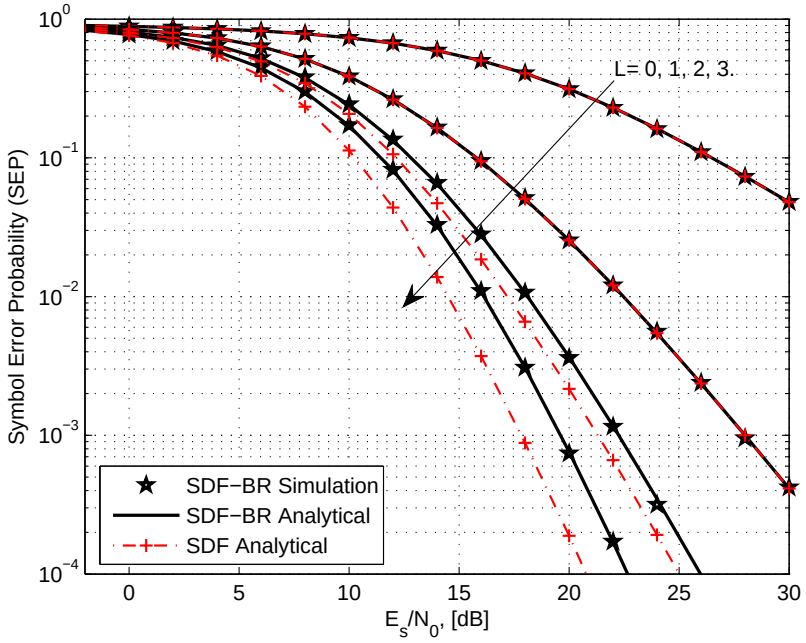

Figure 3.9: The average SEP of a 16QAM HSTCS with best relay selection versus the average transmit SNR, E_s/N_0, when the direct link experiences the FHS and the satellite-relay links experience the ILS while their terrestrial links experience the Rayleigh fading with the average power channel gain equal to unity.

Chapter 4

Performance analysis of OFDM-HSTCS

Contents

In this chapter, we investigate the performance in terms of SEP of Orthogonal Frequency Division Multiplexing HSTCS (OFDM-HSTCS) systems. We focuse on Doppler spread issues. Indeed, the mobility of the Ground Mobile Terminal[5] (GMT) induces a Doppler spread in the OFDM signal that destroys the orthogonality of subcarriers. The loss of orthogonality produces Inter-subCarrier Interference (ICI) and hence a degradation of the system performance in terms of SEP. Furthermore, we present the conditions in which this degradation can be compensated for by an increase in the average transmitted SNR (required margin) at the transmitter side. The results show that the required margin depends on both the modulation scheme and the speed of GMTs. Moreover, the SEP performance can be improved considerably when the number of participating relays increases.

4.1 OFDM system models

OFDM is one of the multicarrier modulation techniques which has gained more acceptance as the modulation technique for high-speed wireless networks and 4G mobile broadband standards. The

[5]The GMT in this section refers to the mobile destination.

OFDM transmission scheme has been already proposed for terrestrial communications and it has been recently implemented in digital satellite broadcasting standards such as the DVB-SH. However, the OFDM is sensitive to the synchronization issues (time/frequency shift and Doppler spread). A base-band OFDM system model with N subcarriers is represented in Fig. 4.1.

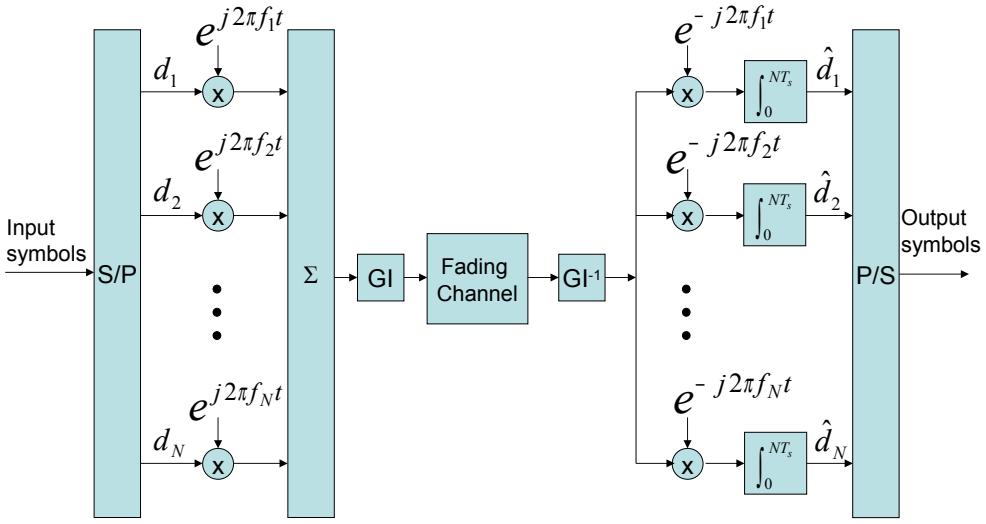

Figure 4.1: Base-band OFDM system model with N subcarriers.

In an OFDM system, the transmitted symbols are divided into groups of N symbols. Then each block of N sysmbols is transferred to the serial-to-parallel converter (S/P). If T_s is the duration of each symbol d_k, the duration of each OFDM symbol is increased to NT_s, which makes the system more robust against the channel delay spread. The parallel symbols modulate a group of orthogonal subcarriers which satisfy the condition below

$$\frac{1}{NT_s}\int_0^{NT_s} \exp(j2\pi f_k t)\exp(j2\pi f_m t)dt = \begin{cases} 1, & \text{if } k = m \\ 0, & \text{if } k \neq m \end{cases} \tag{4.1}$$

where

$$f_k = \frac{k-1}{NT_s}, \text{ for } k = 1, 2, \ldots, N. \tag{4.2}$$

4.2 Synchronization issues

In an HISTCS, the global synchronization between the satellite and the ground segment can be achieved by the implementation of an SH frame Information Packet (SHIP) [ETS08, Kel09]. This synchronization scheme is similar to the Megaframe Initialization Packet (MIP) of the Digital Video Broadcasting-Terrestrial (DVB-T). The pre-compensation of the time delay variation is performed at the gateway location. The principles of synchronization can be summarized as follows.

- SHIP inserter performs the insertion of a Global Positioning System (GPS)-based time stamp ($\pm 0.1 \mu s$ accuracy) in the SH-Frame indicating the transmission time of the beginning of the next SH Frame.
- Single Frequency Network (SFN)[6] adapters in the transmitters (repeaters) perform the buffering of incoming MPEG-TS packets and transmission of SH frame aligned with GPS relative time stamps.

On the other hand, the Doppler spread issues has not been addressed to the same extend. This issue needs to be investigated accurately because the Doppler spread has a great impact on the physical layer performance. Indeed, the Doppler spread destroys the orthogonality of subcarriers in the OFDM signal and generate power leakage among subcarriers, known as ICI. The loss of orthogonality has been characterized in [HZ97, RK99b, RK99a, WPMZ06]. The purpose of this chapter does not consist in proposing a receiving technique in order to reduce the Doppler spread. Instead, system parameters will be adjusted in order to cope with the constraints. More precisely, the effect of the Doppler spread can be reduced by limiting the mobile velocity. Another approach consists in adding an additional margin on the transmitted SNR per symbol. To avoid Doppler spread impairments, the speed of GMTs should not exceeds a maximum allowable value.

[6] The SFN-HISTCS refers to the hybrid/integrated satellite systems that use the same frequency band for the satellite and terrestrial links

4.2.1 Propagation time delay issues

When terrestrial relays are not fed by terrestrial segments (i.e., terrestrial relays receive the signal from the satellite only), the differential propagation time delay between the satellite-destination and the satellite-relay-destination links must be taken into account in the case of SFN-HSTCSs.

In an OFDM system, a Guard Interval (GI) is inserted between each transmitted symbol in order to cope with the Inter-Symbol Interference (ISI) caused by multipath propagation. The GI must be larger than the maximum differential time delay spread of the channel. So, the maximum differential time delay spread has to be taken into account to determine the maximum cell radius as a function of the GI.

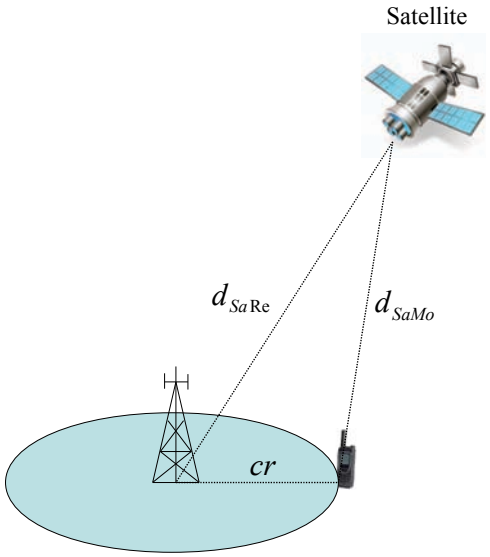

Figure 4.2: HSTCS with one repeater.

An HSTCS with one repeater is shown in Fig. 4.2. We assume that the receiver is at the cell

boundary (the worst condition). The maximum differential time delay $\Delta\tau$ is given by

$$\Delta\tau = \frac{d_{SaRe} + cr - d_{SaMo}}{c} \tag{4.3}$$

where d_{SaRe} and d_{SaMo} are the distance from the satellite to the repeater and from the satellite to the mobile receiver respectively, cr is the cell radius, and $c = 3.10^8 m/s$ is the speed of light.

The parameter $\Delta\tau$ is a function of the longitudinal difference between the repeater center and the satellite, the latitude of the repeater center and the radius of the repeater.

Hence, the GI can be chosen according to $\Delta\tau$ and R.

Table 4.1: Maximum cell radius versus GI for a 5 MHz DVB-SH 2k mode [ETS08].

Max. cell radius	Max. delay in μs	GI=1/4	GI=1/8	GI=1/16	GI=1/32
12 km	79.8	80.64			
6 km	39.9		40.32		
3 km	19.65			20.16	
1 km	6.55				10.08

The maximum cell radius is the maximum distance between the repeater and the receiver to allow the implementation of an SFN between the satellite and the terrestrial network at the edge of one repeater. The maximum cell radius of a 5 MHz DVB-SH operating in 2k mode are provided in Table. 4.1, when the longitudinal difference between the repeater center and the satellite is around 70°. We can observe from Table. 4.1 that the maximum cell radius of 12 km allows a guard interval of 1/4 while the maximum cell radius of 3 km can allow guard intervals of 1/16 or higher.

4.2.2 Doppler spread issues

Doppler spread induced on the satellite segment

The satellite motion and the ground terminal mobility induce a Doppler shift and a Doppler spread [FMV+01].

- The Doppler shift ν_0 is given by, $\nu_0 = V_{sr}/\lambda$, where V_{sr} represents the radial velocity of the satellite and λ is the signal wavelength.
- The Doppler spread σ_ν is defined such that σ_ν^2 is a sum of three terms.

$$\sigma_\nu^2 = \sigma_{\nu,g}^2 + \sigma_{\nu,s}^2 + \sigma_{\nu,ch}^2 \quad = \left(\frac{V_g}{\Lambda_c}\right)^2 + \left(\frac{\Omega_s}{\alpha_c}\right)^2 + \left(\frac{1}{T_{ch}}\right)^2 \tag{4.4}$$

The first term $\sigma_{\nu,g}^2 = (V_g/\Lambda_c)^2$ is due to the ground terminal motion, where V_g represents the ground terminal velocity and Λ_c is the coherence length, usually of the order of the signal wavelength.

The second term $\sigma_{\nu,s}^2 = (\Omega_s/\alpha_c)^2$ is the Doppler spread originated by the motion of satellite. Ω_s is the angular velocity of the satellite and α_c is the coherence angle. The angular velocity of Geostationary Earth Orbit (GEO) satellite should theoretically be zero. In practical cases, this parameter is non zero but it is some four orders less than the same parameter for a Low Earth Orbit (LEO) satellite.

The third term $\sigma_{\nu,ch}^2 = (1/T_{ch})^2$ is the channel self Doppler spread, where T_{ch} is the characteristic time constant which describes the effects of moving and changing objects in the vicinity of the ground station.

Doppler spread induced on the ground segment

On the CGC segment, the Doppler spread is mainly produced by the mobility of the GMTs for fixed relay stations. For mobile relay stations, the total Doppler spread is the sum of the Doppler spreads induced by both GMTs and relay stations [AH86]. The average Doppler shift is zero. Let V_g be the velocity of a GMT and V_r, the velocity of the relay station, then the total Doppler spread can be expressed as:

$$F_d = \frac{V_g}{c} \times f_c + \frac{V_r}{c} \times f_c \tag{4.5}$$

where f_c is the carrier frequency and $c = 3.10^8 m/s$ is the speed of light.

ICI and degradation

We assume that each subcarrier is transmitted in a frequency flat Rayleigh fading channel. The OFDM system uses N subcarriers. For typical modulation schemes such as MPSK and MQAM, the

Carrier to Interference ratio C/I on the subcarrier i is given in [WPMZ06] as

$$\frac{C}{I} = \frac{1}{\frac{(NT_sF_d)^2}{2}\sum_{\substack{k=1\\k\neq i}}^{N}\frac{1}{(k-i)^2}} \tag{4.6}$$

where F_d is the maximum Doppler spread.

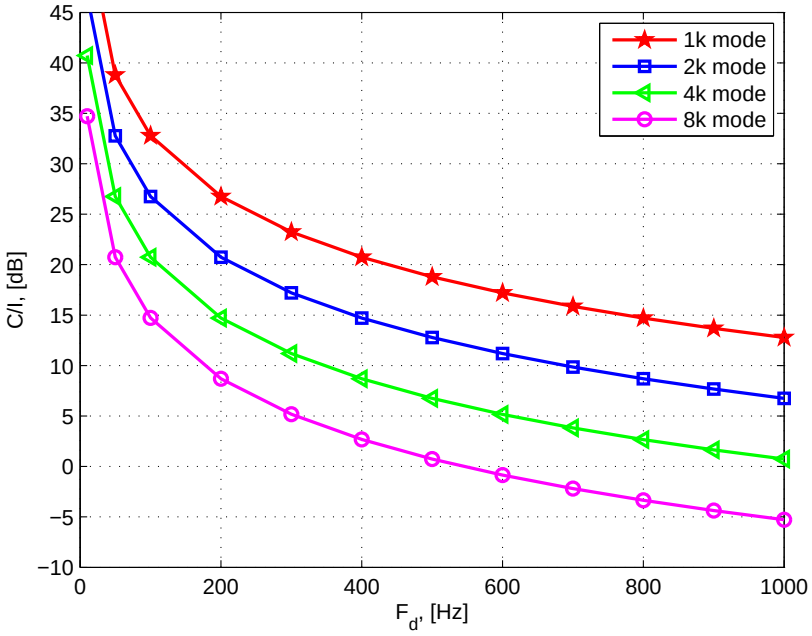

Figure 4.3: C/I curves as a function of the Doppler spread F_d.

The C/I curves of the middle subcarrier index $k = N/2$ are plotted versus the Doppler spread F_d in Figure 4.3 for several DVB-SH transmission modes at a carrier frequency of 2.175 GHz and a bandwidth of 5 MHz. The 8k mode is experiencing more interference than the other modes because its subcarrier spacing is smaller than the one of other modes.

For a given C/I of 15 dB, the 1k mode can support a Doppler spread of 800 Hz and Doppler spread of 400 Hz for the 2k mode. For the same value of C/I, the 4k mode allows a maximum Doppler spread of 200 Hz while the 8k mode can support only 100 Hz. According to these Doppler spread values, we can calculate the maximum allowable velocity for the GMT. The numerical values of the

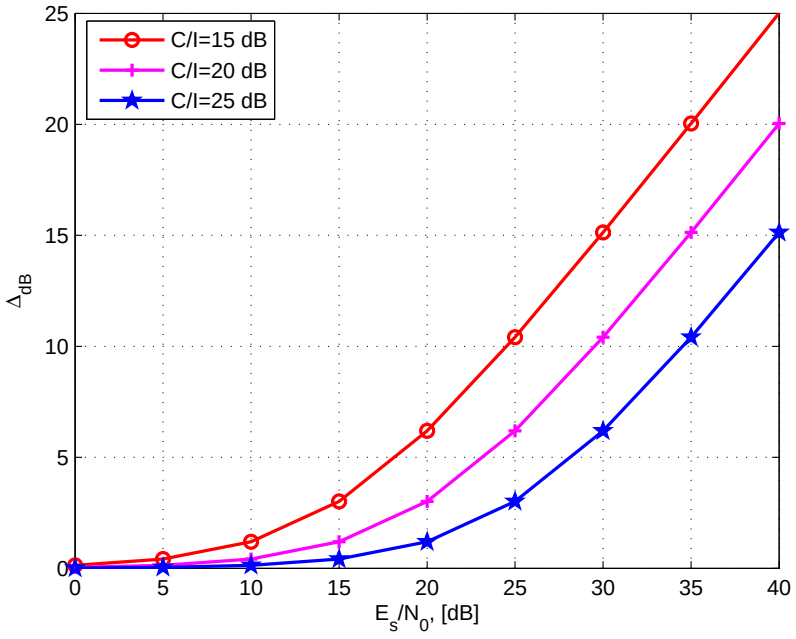

Figure 4.4: Degradation Δ_{dB} as a function of E_s/N_0.

maximum allowable velocity for the GMT for a 5 MHz DVB-SH bandwidth channel at 2.175 GHz and C/I of 15 dB are shown in Table 4.2.

Table 4.2: Maximum allowable velocity for the GMT for a 5 MHz DVB-SH bandwidth channel at 2.175 GHz and a C/I of 15 dB.

Mode	FFT size	Subcarrier spacing [kHz]	Doppler spread [Hz]	Maximum speed [km/h]
1k	1024	5.580	800	397.22
2k	2048	2.790	400	198.61
4k	4096	1.395	200	99.30
8k	8192	0.698	100	49.65

As in typical C/I computations, the ICI can be modeled as an additional near-Gaussian noise [RK99a, RK99b]. Without the interference and Doppler spread, the average transmitted signal to

noise ratio per symbol is E_s/N_0. And with the interference and Doppler spread, the average transmitted signal to interference plus noise ratio can be written as $E_s/(N_0+N_I)$. Then, using $E_s = C/R_s$ and $N_I = I/R_s$, we obtain

$$\frac{E_s}{N_0+N_I} = \frac{\frac{E_s}{N_0}}{1+\frac{E_s}{N_0}(\frac{C}{I})^{-1}} \tag{4.7}$$

where $R_s = 1/T_s$ is the input symbol rate.

So, the degradation due to Dopper spread can be expressed in decibel as below

$$\Delta_{dB} = \left[\frac{E_s}{N_0+N_I}\right]_{dB} - \left[\frac{E_s}{N_0}\right]_{dB} = -10\log\left[1+\frac{E_s}{N_0}\left(\frac{C}{I}\right)^{-1}\right] \tag{4.8}$$

Equation 4.7 shows that when $\frac{E_s}{N_0} \to +\infty$, the expression

$$\frac{E_s}{N_0+N_I} \simeq \frac{C}{I}. \tag{4.9}$$

Equation 4.9 shows that the ICI is the limiting factor in performance.

Figure 4.4 illustrates the degradation due to Doppler spread with respect to the E_s/N_0 ratio for several values of C/I. We observe that the degradation not only depends on the C/I ratio but also on the E_s/N_0 ratio. For small values of E_s/N_0, the degradation has less influence on the system. In particular, when E_s/N_0 is smaller than 10 dB, the degradation is less than 2 dB.

4.3 Performance analysis of the OFDM-HSTCS

In this section, we study the performance in terms of SEP of the OFDM-HSTCS. The worst case scenario where the non-LOS link between the satellite and the destination is considered and shown in Fig. 4.5. We assume that the relays are fixed or mobile with a low speed and the system is synchronized in time and frequency. Only the Doppler spread issues are taken into account for the SEP computation. In this case, the SEP performance of multicarrier OFDM systems is the same as the SEP perfomance of single carrier systems if there is no Doppler spread. This is consistent since each subcarrier channel can be modeled as a frequency flat fading channel. So, in the following analysis, we derive the SEP of single carrier systems and then we add the ICI to the AWGN noise (i.e., replacing E_{r_i}/N_0 by $E_{r_i}/(N_0+N_I)$ in the obtained SEP expression).

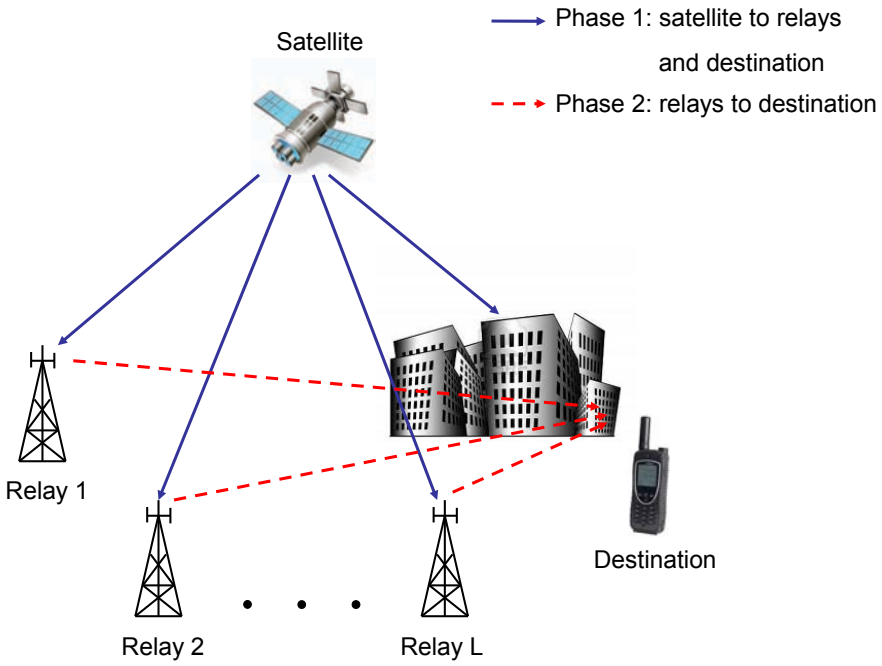

Figure 4.5: HSTCS with NLOS link.

4.3.1 SEP of the OFDM-HSTCS without direct link

System model

The system model is defined as in chapter 2. In the first phase, the satellite broadcasts the information to relays. In the second phase, only the relays that can decode the satellite message correctly are allowed to forward the satellite message to the destination. Furthermore, the satellite-relay links are modeled as the LMS channel as defined in chapter 2 while the relay-destination links are Rayleigh fading channels.

MGF of the instantaneous received SNR at the MRC output

By using the same approach as in subsection 2.2.2, the total instantaneous received SNR at the MRC output without the direct link, γ_{MRC}^{WD}, can be expressed as below[7]

$$\gamma_{MRC}^{WD} = \sum_{i=1}^{L} \chi_i. \tag{4.10}$$

Hence, the MGF of γ_{MRC}^{WD} is given by

$$\phi_{\gamma_{MRC}^{WD}}(s) = \prod_{i=1}^{L} \phi_{\chi_i}(s) \tag{4.11}$$

and

$$\phi_{\chi_i}(s) = P_{sr_i} + (1 - P_{sr_i}) \left(1 + 2b_{r_i d}\overline{\gamma}_{r_i d} s\right)^{-1} \tag{4.12}$$

where P_{sr_i} are given in chapter 2 by equations (2.29) and (2.30) for MPSK and MQAM modulation schemes respectively and

$$\overline{\gamma}_{r_i d} = \begin{cases} E_{r_i}/N_0, \text{ without ICI} \\ E_{r_i}/(N_0 + N_I), \text{ with ICI.} \end{cases} \tag{4.13}$$

M-ary phase-shift keying (M-PSK)

The average SEP of the HSTCS without direct link for coherent MPSK signals is given by [AT01]

$$P_{s,MPSK}^{WD}(E) = \frac{1}{\pi} \int_0^{\pi - \frac{\pi}{M}} \phi_{\gamma_{MRC}^{WD}} \left(\frac{g_{MPSK}}{\sin^2 \theta} \right) d\theta \tag{4.14}$$

where $g_{MPSK} = \sin^2(\pi/M)$. By using the same approach as in 2.38, $P_{s,MPSK}^{WD}(E)$ is finally given as follows

$$\begin{aligned} P_{s,MPSK}^{WD}(E) = \frac{1}{2} \prod_{i=1}^{L} \left(\frac{H_{i,MPSK}}{K_{i,MPSK}} \right) F_D^{(2L)} \Bigg(& \frac{1}{2}, -1, 1, \ldots, -1, 1; 1; \\ & \frac{1}{H_{1,MPSK}}, \frac{1}{K_{1,MPSK}}, \ldots, \frac{1}{H_{L,MPSK}}, \frac{1}{K_{L,MPSK}} \Bigg) \\ + \frac{\sqrt{\omega}}{\pi} \prod_{i=1}^{L} \left(\frac{H_{i,MPSK}}{K_{i,MPSK}} \right) F_D^{(2L+1)} \Bigg(& \frac{1}{2}, \frac{1}{2}, -1, 1, \ldots, -1, 1; \frac{3}{2}; \\ & \omega, \frac{\omega}{H_{1,MPSK}}, \frac{\omega}{K_{1,MPSK}}, \ldots, \frac{\omega}{H_{L,MPSK}}, \frac{\omega}{K_{L,MPSK}} \Bigg) \end{aligned} \tag{4.15}$$

[7] The index WD refers to Without Direct link

where

$$\begin{aligned} H_{i,MPSK} &= 1 + P_{sr_i,MPSK} 2b_{r_id}\overline{\gamma}_{r_id} g_{MPSK}, \\ K_{i,MPSK} &= 1 + 2b_{r_id}\overline{\gamma}_{r_id} g_{MPSK}. \end{aligned} \tag{4.16}$$

In the case of i.i.d fading channels, all relays experience the same fading environment, i.e., $m_{sr_i} = m_{sr}$, $b_{sr_i} = b_{sr}$, $\Omega_{sr_i} = \Omega_{sr}$ and $b_{r_id} = b_{rd}$ for all $i \in L$. Moreover, we assume that $\overline{\gamma}_{r_id} = \overline{\gamma}_{rd} = \overline{\gamma}$ for all $i \in L$. So, $H_{i,MPSK} = H_{MPSK}$ and $K_{i,MPSK} = K_{MPSK}$ for all $i \in L$. Hence, the average SEP, $P^{WD}_{s,MPSK}(E)$ can be simplified as below

$$\begin{aligned} P^{WD}_{s,MPSK}(E) = &\frac{1}{2}\left(\frac{H_{MPSK}}{K_{MPSK}}\right)^L F_1\left(\frac{1}{2}, -L, L; 1; \frac{1}{H_{MPSK}}, \frac{1}{K_{MPSK}}\right) \\ &+ \frac{\sqrt{\omega}}{\pi}\left(\frac{H_{MPSK}}{K_{MPSK}}\right)^L F_D^{(3)}\left(\frac{1}{2}, \frac{1}{2}, -L, L; \frac{3}{2}; \omega, \frac{\omega}{H_{MPSK}}, \frac{\omega}{K_{MPSK}}\right). \end{aligned} \tag{4.17}$$

where

$$\begin{aligned} H_{MPSK} &= 1 + P_{sr,MPSK} 2b_{rd}\overline{\gamma}_{rd} g_{MPSK}, \\ K_{MPSK} &= 1 + 2b_{rd}\overline{\gamma}_{rd} g_{MPSK}. \end{aligned} \tag{4.18}$$

In order to illustrate the diversity property we calculate the approximation of $P^{WD}_{s,MPSK}(E)$ in the high-SNR regime. We obtain as follows (see Appendix I.1)

$$\begin{aligned} \lim_{SNR\to\infty} P^{WD}_{s,MPSK}(E) = &\frac{1}{2}\frac{1}{\left(1 + 2b_{rd}\left(\frac{C}{I}\right) g_{MPSK}\right)^L} F_1\left(\frac{1}{2}, -L, L; 1; 1, \frac{1}{1 + 2b_{rd}\left(\frac{C}{I}\right) g_{MPSK}}\right) \\ &+ \frac{\sqrt{\omega}}{\pi}\frac{1}{\left(1 + 2b_{rd}\left(\frac{C}{I}\right) g_{MPSK}\right)^L} F_1\left(\frac{1}{2}, \frac{1}{2} - L, L; \frac{3}{2}; \omega, \frac{\omega}{1 + 2b_{rd}\left(\frac{C}{I}\right) g_{MPSK}}\right). \end{aligned} \tag{4.19}$$

We can see that the expression 4.19 does not depend on the SNR but depends on the C/I. Hence, for a given C/I value, $P^{WD}_{s,MPSK}(E)$ becomes a constant value when SNR is large. Hence, the asymptotic diversity order is equal to zero. On the other hand, it is not zero in the medium-SNR regime. Moreover, this expression 4.19 represents the minimum value of the $P^{WD}_{s,MPSK}(E)$ and can be served as the condition in which the degradation can be compensated for by a required margin. In this case, this minimum value of the $P^{WD}_{s,MPSK}(E)$ should be smaller than the target SEP. And, the minimum value of C/I can be obtained by solving the equation 4.19.

M-ary quadrature amplitude modulation (MQAM)

The average SEP of the HSTCS without direct link for coherent MQAM signals is given by [AT01]

$$P_{s,MQAM}^{WD}(E) = \frac{4q}{\pi}\int_0^{\frac{\pi}{2}} \phi_{\gamma_{MRC}^{WD}}\left(\frac{g_{MQAM}}{\sin^2\theta}\right)d\theta - \frac{4q^2}{\pi}\int_0^{\frac{\pi}{4}} \phi_{\gamma_{MRC}^{WD}}\left(\frac{g_{MQAM}}{\sin^2\theta}\right)d\theta \tag{4.20}$$

where $g_{MQAM} = 3/2(M-1)$ and $q = \left(1 - 1/\sqrt{M}\right)$. $P_{s,MQAM}^{WD}(E)$ can be obtained by using the same computation as in 2.46 and given as follows

$$\begin{aligned} P_{s,MQAM}^{WD}(E) = 2q\prod_{i=1}^{L}\left(\frac{H_{i,MQAM}}{K_{i,MQAM}}\right) F_D^{(2L)}\Bigg(&\frac{1}{2}, -1, 1, \ldots, -1, 1; 1; \\ &\frac{1}{H_{1,MQAM}}, \frac{1}{K_{1,MQAM}}, \ldots, \frac{1}{H_{L,MQAM}}, \frac{1}{K_{L,MQAM}}\Bigg) \\ -\frac{2q^2}{\pi}\prod_{i=1}^{L}\left(\frac{W_{i,MQAM}}{Z_{i,MQAM}}\right) F_D^{(2L+1)}\Bigg(&1, 1, -1, 1, \ldots, -1, 1; \frac{3}{2}; \\ &\frac{1}{2}, \frac{H_{1,MQAM}}{W_{1,MQAM}}, \frac{K_{1,MQAM}}{Z_{1,MQAM}}, \ldots, \frac{H_{L,MQAM}}{W_{L,MQAM}}, \frac{K_{L,MQAM}}{Z_{L,MQAM}}\Bigg) \end{aligned} \tag{4.21}$$

where

$$\begin{aligned} H_{i,MQAM} &= 1 + 2P_{sr_i,MQAM}b_{r_id}\overline{\gamma}_{r_id}g_{MQAM},\ K_{i,MQAM} = 1 + 2b_{r_id}\overline{\gamma}_{r_id}g_{MQAM}, \\ W_{i,MQAM} &= 1 + 4P_{sr_i,MQAM}b_{r_id}\overline{\gamma}_{r_id}g_{MQAM},\ Z_{i,MQAM} = 1 + 4b_{r_id}\overline{\gamma}_{r_id}g_{MQAM}. \end{aligned} \tag{4.22}$$

In the case of i.i.d fading channels, all relays experience the same fading environment, i.e., $m_{sr_i} = m_{sr}$, $b_{sr_i} = b_{sr}$, $\Omega_{sr_i} = \Omega_{sr}$ and $b_{r_id} = b_{rd}$ for all $i \in L$. Moreover, we assume that $\overline{\gamma}_{r_id} = \overline{\gamma}_{rd} = \overline{\gamma}$ for all $i \in L$. So, $H_{i,MQAM} = H_{MQAM}$, $K_{i,MQAM} = K_{MQAM}$, $W_{i,MQAM} = W_{MQAM}$ and $Z_{i,MQAM} = Z_{MQAM}$ for all $i \in L$. So, the average SEP, $P_{s,MQAM}^{WD}(E)$ can be given by

$$\begin{aligned} P_{s,MQAM}^{WD}(E) = 2q\left(\frac{H_{MQAM}}{K_{MQAM}}\right)^L F_1\left(\frac{1}{2}, -L, L; 1; \frac{1}{H_{MQAM}}, \frac{1}{K_{MQAM}}\right) \\ -\frac{2q^2}{\pi}\left(\frac{W_{MQAM}}{Z_{MQAM}}\right)^L F_D^{(3)}\left(1, 1, -L, L; \frac{3}{2}; \frac{1}{2}, \frac{H_{MQAM}}{W_{MQAM}}, \frac{K_{MQAM}}{Z_{MQAM}}\right). \end{aligned} \tag{4.23}$$

where

$$\begin{aligned} H_{MQAM} &= 1 + 2P_{sr,MQAM}b_{rd}\overline{\gamma}_{rd}g_{MQAM},\ K_{MQAM} = 1 + 2b_{rd}\overline{\gamma}_{rd}g_{MQAM}, \\ W_{MQAM} &= 1 + 4P_{sr,MQAM}b_{rd}\overline{\gamma}_{rd}g_{MQAM},\ Z_{MQAM} = 1 + 4b_{rd}\overline{\gamma}_{rd}g_{MQAM}. \end{aligned} \tag{4.24}$$

In order to illustrate the diversity property we calculate the approximation of $P^{WD}_{s,MQAM}(E)$ in the high-SNR regime. We obtain as below (see Appendix I.2)

$$\lim_{SNR\to\infty} P^{WD}_{s,MQAM}(E) = 2q\frac{1}{\left(1+2b_{rd}\left(\frac{C}{I}\right)g_{MQAM}\right)^{L}}F_1\left(\frac{1}{2},-L,L;1;1,\frac{1}{1+2b_{rd}\left(\frac{C}{I}\right)g_{MQAM}}\right) - \frac{2q^2}{\pi}\frac{1}{\left(1+4b_{rd}\left(\frac{C}{I}\right)g_{MQAM}\right)^{L}}F_D^{(3)}\left(1,1,-L,L;\frac{3}{2};\frac{1}{2},1,\frac{1+2b_{rd}\left(\frac{C}{I}\right)g_{MQAM}}{1+4b_{rd}\left(\frac{C}{I}\right)g_{MQAM}}\right). \tag{4.25}$$

Again, we can notice that the expression 4.25 does not depend on the SNR but depends on the C/I. Hence, for a given C/I value, $P^{WD}_{s,MQAM}(E)$ becomes a constant value when SNR is large. Hence, the asymptotic diversity order is equal to zero. On the other hand, it is not zero in the medium-SNR regime. Moreover, this expression 4.25 represents the minimum value of the $P^{WD}_{s,MQAM}(E)$ and can be served as the condition in which the degradation can be compensated for by a required margin. In this case, this minimum value of the $P^{WD}_{s,MQAM}(E)$ should be smaller than the target SEP. And, the minimum value of C/I can be obtained by solving the equation 4.25.

4.3.2 Numerical results

In this section, the average SEP cuves of the OFDM-HSTCS which take into account the Doppler spread issues are plotted versus the average transmitted SNR for several DVB-SH modes at a carrier frequency of 2.175 GHz and a bandwidth of 5 MHz. The satellite-relay links experience the ILS while the relay-destination links are Rayleigh fading with the average channel power gain equal to unity. The curves are plotted for different number of participating relays $L = 1, 2, 3$. The SEP curve with no ICI is also provided as the baseline for the comparison. The required margin can be computed by calculating the difference in SNR between the SEP curve affected by the ICI and the one without the ICI with respect to the same target SEP value. First, we plot the SEP curves by assuming that the average transmitted SNR per symbol of the satellite-destination link is equal to the one of the relay-destination links ($E_s/N_0 = E_{r_i}/N_0$). Second, we plot the SEP curves versus the average transmitted SNR per symbol of the relay links, E_{r_i}/N_0, and we set E_s/N_0 as a constant value (i.e., or equivalently P_{sr_i} is constant). We can observe from all figures that the ICI is the limiting factor in performance

at any mobile speed when the SNR is large. Furthermore, we can also notice that the degradation due to Doppler spread can be improved when the number of participating relays increases.

First case: $E_s/N_0 = E_{r_i}/N_0$

Figs. 4.6(a) and 4.7(a) show the average SEP of QPSK OFDM-HSTCS and 16QAM OFDM-HSTCS respectively under the Doppler spread, F_d corresponding to the mobile speed of 50 km/h. In this case, when the target SEP is in the order of 10^{-2}, the required margin of the 1-relay QPSK OFDM-HSTCS system are 0 dB for 1k mode, 1 dB for 2k mode and around 6 dB for 4k mode while the required margin can not be computed (NC) for 8k mode. However, this 8k mode can be compensated for by a margin of 2 dB in the case of 2-relay system and only 1 dB is needed in the case of 3-relay system. The required margin for other modes of QPSK and 16QAM are summarized in Table 4.3.

The other performance curves of QPSK OFDM-HSTCS and 16QAM OFDM-HSTCS are plotted in Figs. 4.6(b) and 4.7(b) respectively under the Doppler spread, F_d corresponding to the mobile speed of 100 km/h. We see that the SEP of 1-relay 16QAM OFDM-HSTCS system is larger than 10^{-2} for all modes. So, for the target SEP of 10^{-2} we can not compensate for by a margin because their minimum SEP are higher then the target value. On the other hand, this 16QAM OFDM-HSTCS system can be compensated for by a margin operating in 1k and 2k modes in the case of 2-relay system. The required margin corresponding to the QPSK OFDM-HSTCS and 16QAM OFDM-HSTCS are provided in Table 4.4.

Second case: E_s/N_0 **or** P_{sr_i} **is constant**

In order to show in more detail the effect of the Doppler spread on the terrestrial links, we assume that the average transmitted SNR of the satellite E_s/N_0 is constant (i.e., or equivalently P_{sr_i} is constant). Furthermore, we plot the SEP curves versus the average transmitted SNR of the relay-destination links, E_r/N_0.

Figs. 4.8(a) and 4.9(a) illustrate the average SEP of 8PSK OFDM-HSTCS and 16QAM OFDM-HSTCS versus the average transmitted SNR of the relay, E_r/N_0 respectively, when $P_{sr_i} = 10^{-4}$, and under the Doppler spread, F_d corresponding to the mobile speed of 50 km/h. Moreover, the

Table 4.3: The required margin for a 5 MHz DVB-SH bandwidth channel at 2.175 GHz and mobile speed of 50 km/h with the target SEP of 10^{-2}.

	Mode	1k	2k	4k	8k
1-relay system	QPSK	0 dB	1 dB	6 dB	NC
	16QAM	2 dB	NC	NC	NC
2-relay system	QPSK	0 dB	0 dB	0.5 dB	2 dB
	16QAM	0 dB	0.7 dB	3.5 dB	NC
3-relay system	QPSK	0 dB	0 dB	0.2 dB	1 dB
	16QAM	0 dB	0 dB	1 dB	11 dB

Table 4.4: The required margin for a 5 MHz DVB-SH bandwidth channel at 2.175 GHz and mobile speed of 100 km/h with the target SEP of 10^{-2}.

	Mode	1k	2k	4k	8k
1-relay system	QPSK	1 dB	6 dB	NC	NC
	16QAM	NC	NC	NC	NC
2-relay system	QPSK	0 dB	0.2 dB	2 dB	NC
	16QAM	0.5 dB	3.5 dB	NC	NC
3-relay system	QPSK	0 dB	0 dB	0.5 dB	3.5 dB
	16QAM	0.2 dB	1 dB	11 dB	NC

SEP curves correspond to the mobile speed of 100 km/h are shown in Figs. 4.8(b) and 4.9(b) for 8PSK OFDM-HSTCS and 16QAM OFDM-HSTCS respectively. The correspond required margin are summarized in Table 4.5 and 4.6 for the mobile speed of 50 km/h and 100 km/h respectively. The results show that with cooperative relaying the required margin can be reduced considerably.

Table 4.5: The required margin for a 5 MHz DVB-SH bandwidth channel at 2.175 GHz and mobile speed of 50 km/h when $P_{sr_i} = 10^{-4}$ and with the target SEP of 10^{-2}.

	Mode	1k	2k	4k	8k
1-relay system	8PSK	1 dB	6 dB	NC	NC
	16QAM	2 dB	NC	NC	NC
2-relay system	8PSK	0 dB	0.1 dB	1.5 dB	NC
	16QAM	0 dB	0.5 dB	4 dB	NC
3-relay system	8PSK	0 dB	0 dB	0.5 dB	3.5 dB
	16QAM	0 dB	0 dB	1 dB	11 dB

Table 4.6: The required margin for a 5 MHz DVB-SH bandwidth channel at 2.175 GHz and mobile speed of 100 km/h when $P_{sr_i} = 10^{-4}$ and with the target SEP of 10^{-2}.

	Mode	1k	2k	4k	8k
1-relay system	8PSK	5 dB	NC	NC	NC
	16QAM	NC	NC	NC	NC
2-relay system	8PSK	0.5 dB	1.5 dB	NC	NC
	16QAM	1 dB	4 dB	NC	NC
3-relay system	8PSK	0 dB	0.5 dB	3.5 dB	NC
	16QAM	0 dB	1.5 dB	12 dB	NC

4.4 Conclusion

In this chapter, the SEP performance of the OFDM-HSTCS was investigated. The lower bound of SEP were examined. The maximum mobile speed of GMTs with respect to the required minimum C/I value was determined. Furthermore, the required margins were also evaluated with respect to the target SEP. The degradation due to Doppler spread could be compensated for by the margin before decoding. It was also shown that the required margin does not only depend on the mobile velocity

but also depend on the modulation scheme. For high Doppler spread, for example when the velocity of the GMT is 100 km/h, the 1-relay system using 16QAM OFDM modulation is totally degraded and the compensation is not possible. So, one way to solve this problem is to limit the velocity of the GMT to an appropriate level. The results also shown that the required margin is reduced when the number of participating relays increases.

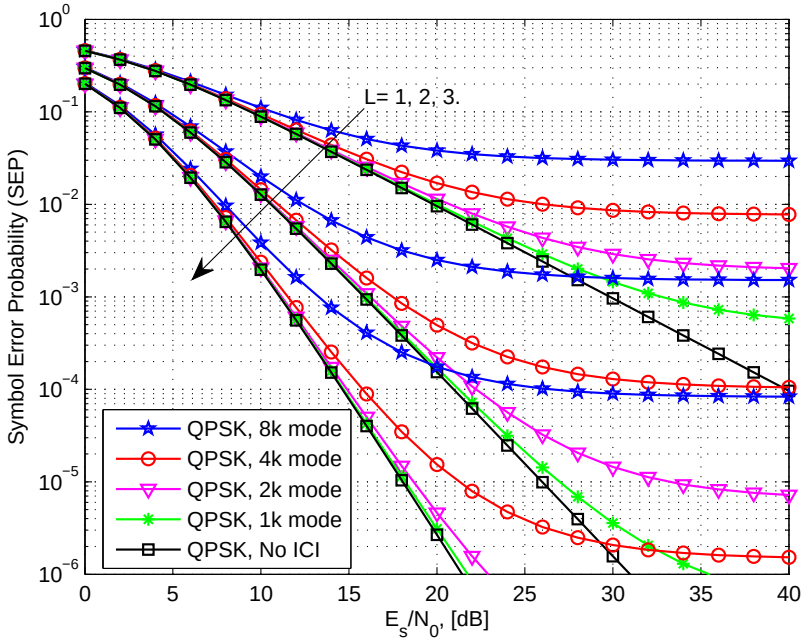

(a)

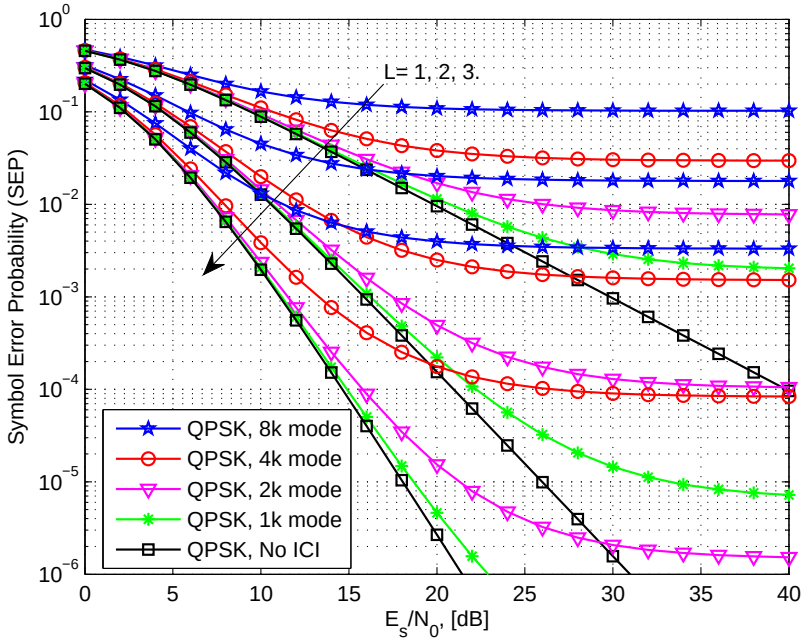

(b)

Figure 4.6: The average SEP of a QPSK OFDM-HSTCS versus the average transmitted SNR, E_s/N_0, (a) mobile speed of 50 km/h, (b) mobile speed of 100 km/h.

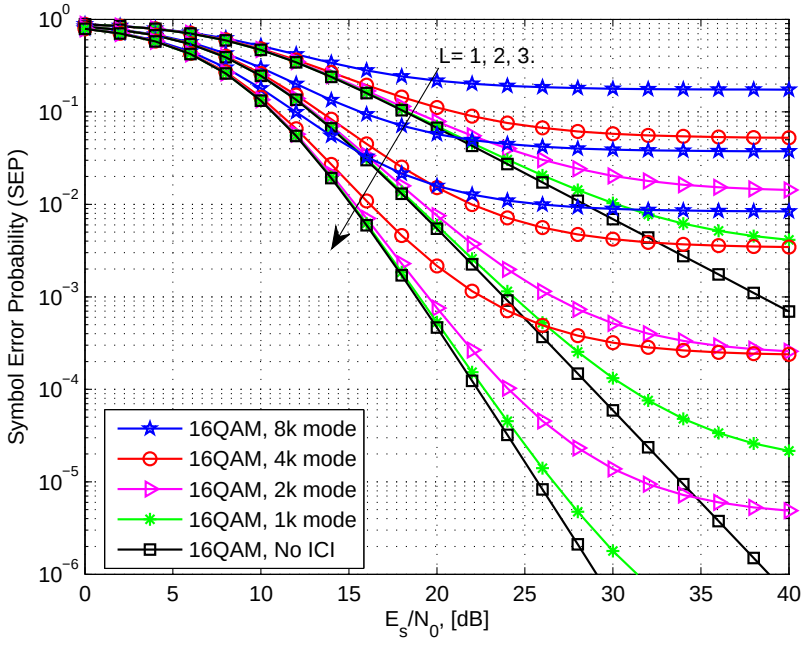

(a)

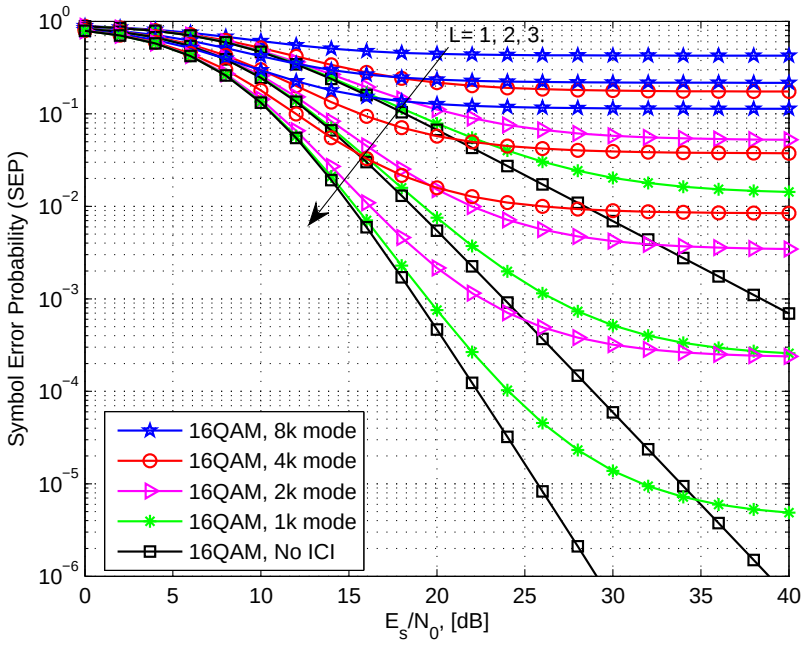

(b)

Figure 4.7: The average SEP of a 16QAM OFDM-HSTCS versus the average transmitted SNR, E_s/N_0, (a) mobile speed of 50 km/h, (b) mobile speed of 100 km/h.

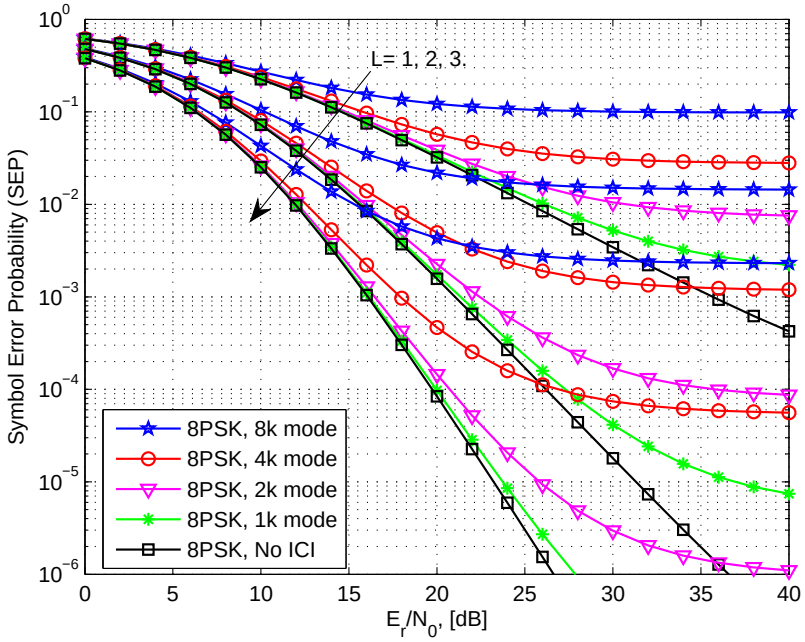

(a)

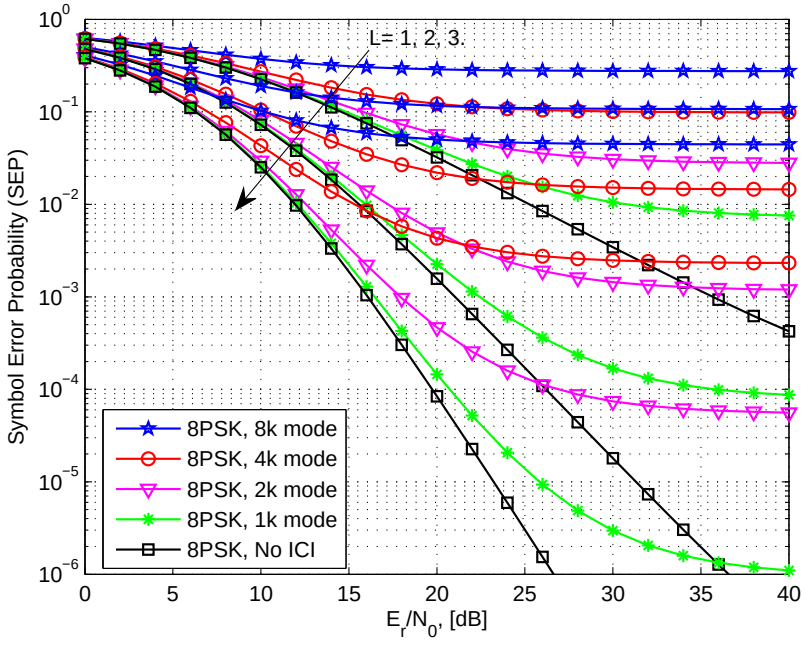

(b)

Figure 4.8: The average SEP of a 8PSK OFDM-HSTCS versus the average transmitted SNR, E_r/N_0, when $P_{sr_i} = 10^{-4}$, (a) mobile speed of 50 km/h, (b) mobile speed of 100 km/h.

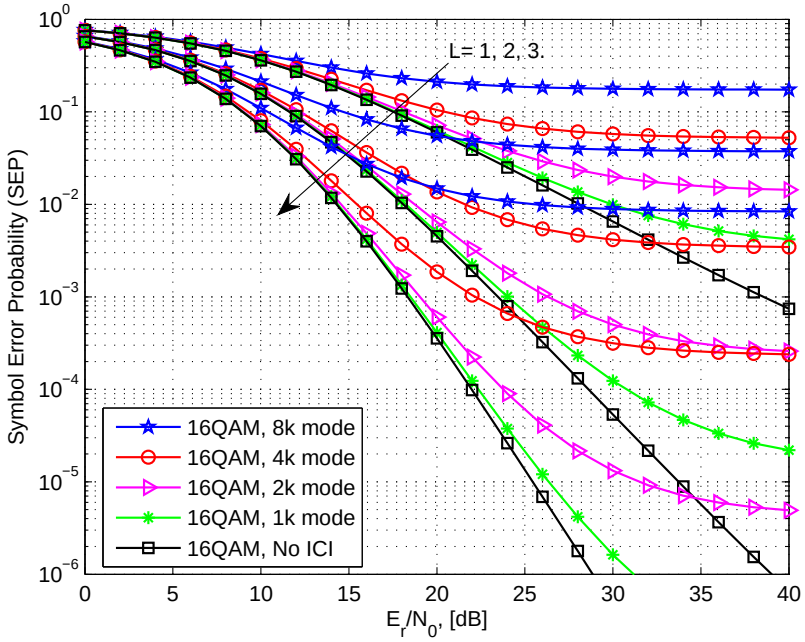

(a)

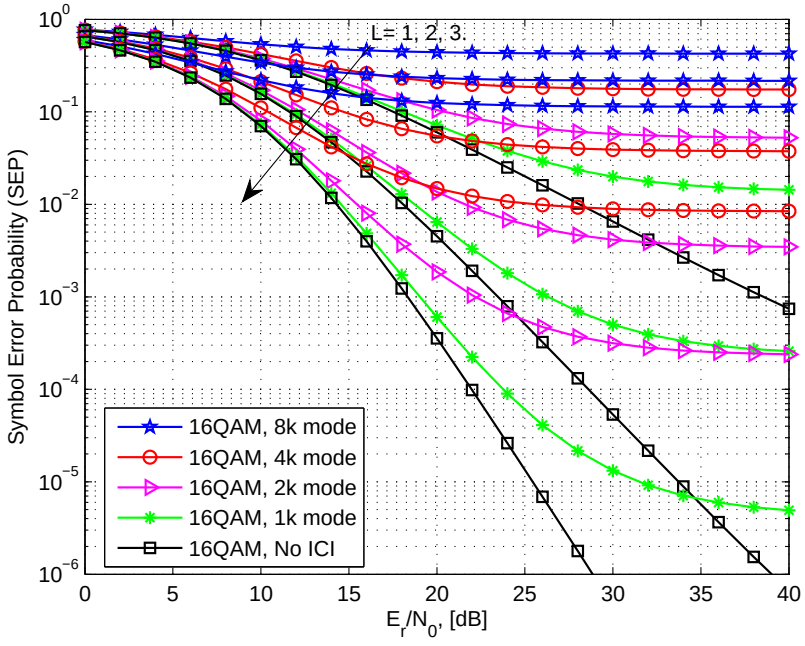

(b)

Figure 4.9: The average SEP of a 16QAM OFDM-HSTCS versus the average transmitted SNR, E_r/N_0, when $P_{sr_i} = 10^{-4}$, (a) mobile speed of 50 km/h, (b) mobile speed of 100 km/h.

Chapter 5

Conclusions and future works

This dissertation aims at providing the analytical computation of both outage probability and average SEP of HSTCSs. Both analytical performance expressions are very important for evaluating the system performance over fading channels since it provide valuable insight into the design of the systems. HSTCSs have been proposed in order to extend the coverage area of satellite systems where services provided by the satellite only are interrupted due to masking effect. In an HSTCS, the terrestrial relays are used to forward the satellite signal to the destination. So, the destination can exploit the spatial diversity by combining the received signals from the satellite and relay stations. Several cooperative scenarios have been proposed and studied for different application purposes (e.g., broadcasting, emergency communications, disaster relief). However, most of those previous studies have provided only the SEP performance based on simulations. The exact closed-form outage probability and SEP expressions have not been derived yet.

5.1 Contributions

In this dissertation, the performance of HSTCSs has been studied. The exact closed-form outage probability and exact SEP have been derived for general MPSK and MQAM modulation schemes over i.i.d and i.n.i.d fading channels. The obtained analytical outage probability and SEP expressions are valid for both fixed and mobile relaying techniques. The cooperative scenarios with and without best relay selection have been examined. Furthermore, the performance of OFDM-HSTCSs has been also investigated.

In chapter 2, the performance of SDF HSTCSs has been evaluated. In the first phase, the satellite broadcasts its signal to all relay nodes and the destination node. In the second phase, only relays

that can decode the satellite message correctly are allowed to forward the satellite message to the destination node. Then the destination combines the direct and the relay link signals using the MRC technique. The exact closed-form expressions for the outage probability and the average SEP of the general MPSK and MQAM HSTCSs over independent but not necessarily identically distributed fading channels have been derived. The results have shown that a full diversity order of $L+1$ can be obtained when the total number of relays is equal to L.

The performance of SDF HSTCSs with best relay selection has been addressed in chapter 3. The two time-slot scenario is considered. During the first time slot, the satellite broadcasts the information to the terrestrial relays and the destination. In the second time slot, only the best relay is transmitting toward the destination node. The selected relay is the one that provides the best link quality between a relay and the destination. Then, both signals are combined using the MRC technique. The exact outage probability and the exact closed-form SEP expressions of the general MPSK and MQAM HSTCSs with best relay selection over independent but not necessarily identically distributed fading channels have been derived. The results have shown that a full diversity order of $L+1$ can be obtained when the number of participating relays is equal to L.

Chapter 2 and 3 deal with the frequency-flat fading channels. It is well known that the implementation of the OFDM transmission techniques can convert a frequency-selective fading channel to several frequency-flat fading channels. In chapter 4, the SEP performance of OFDM-HSTCSs was investigated. The lower bound of SEP has been also examined. The maximum mobile speed of GMTs with respect to the required minimum C/I value was determined. Furthermore, the required margins were also evaluated with respect to the target SEP. The degradation due to Doppler spread could be compensated for by the margin before decoding. It was also shown that the required margin does not only depend on the mobile velocity but also depend on the modulation scheme. For high Doppler spread, for example when the velocity of the GMT is 100 km/h, the 1-relay system using 16QAM OFDM modulation is totally degraded and the compensation is not possible. So, one way to solve this problem is to limit the velocity of the GMT to an appropriate level. The results also shown that the required margin is reduced when the number of participating relays increases.

5.2 Future works

In this dissertation, the analytical outage probability and SEP have been derived using the single-state LMS channel model (shadowed Rice model). For the multi-state LMS channel model such as Fontan's model, the average outage probability and the average SEP can be obtained by computed for each state of the channel model and then calculate the average value over the three states using Markov chain properties. The analytical performance of HSTCSs with channel coding is also an interesting future work.

5.3 List of publications

5.3.1 International journal

1. Sokchenda Sreng, Benoît Escrig, Marie-Laure Boucheret. "Exact Symbol Error Probability of Hybrid/Integrated Satellite-Terrestrial Cooperative Network". Accepted in IEEE Transactions on Wireless Communications, 2013 (to appear).

5.3.2 International conferences

1. Sokchenda Sreng, Benoît Escrig, Marie-Laure Boucheret. "Exact Outage Probability of a Hybrid Satellite Terrestrial Cooperative System with Best Relay Selection". Submitted to 2013 IEEE International Conference on Communications (2013 IEEE ICC).

2. Sokchenda Sreng, Benoît Escrig, Marie-Laure Boucheret. "Outage Analysis of Hybrid Satellite-Terrestrial Cooperative Network with Best Relay Selection (regular paper)". In Proc. IEEE Wireless Telecommunications Symposium, London, 18/04/2012-20/04/2012, IEEE Communications Society, avril 2012.

3. Sokchenda Sreng, Benoît Escrig, Marie-Laure Boucheret. "Adapting DVB-SH system parameters to mobile environments (regular paper)". In Proc. International Conference on Advances in Satellite and Space Communications, Budapest, Hungary, 17/04/2011-22/04/2011, IARIA, avril 2011.

Annexes

Appendix A

SEP of the direct link

A.1 SEP of MPSK

The average SEP of the direct link for coherent MPSK signals is defined in 2.9 by

$$\begin{aligned} P_{sd,MPSK}(E) &= \frac{1}{\pi}\int_0^{\pi-\frac{\pi}{M}} \phi_{\gamma_{sd}}\left(\frac{g_{MPSK}}{\sin^2\theta}\right) d\theta \\ &= \underbrace{\frac{1}{\pi}\int_0^{\frac{\pi}{2}} \phi_{\gamma_{sd}}\left(\frac{g_{MPSK}}{\sin^2\theta}\right) d\theta}_{I^{sd}_{1,MPSK}} + \underbrace{\frac{1}{\pi}\int_{\frac{\pi}{2}}^{\pi-\frac{\pi}{M}} \phi_{\gamma_{sd}}\left(\frac{g_{MPSK}}{\sin^2\theta}\right) d\theta}_{I^{sd}_{2,MPSK}} \end{aligned} \tag{A.1}$$

where

$$g_{MPSK} = \sin^2(\pi/M). \tag{A.2}$$

and $\phi_{\gamma_{sd}}(s)$ is defined in 2.8 as

$$\phi_{\gamma_{sd}}(s) = \frac{(2b_{sd}m_{sd})^{m_{sd}}(1+2b_{sd}\overline{\gamma}_{sd}s)^{m_{sd}-1}}{\left[(2b_{sd}m_{sd}+\Omega_{sd})(1+2b_{sd}\overline{\gamma}_{sd}s)-\Omega_{sd}\right]^{m_{sd}}}. \tag{A.3}$$

Therefore,

$$\phi_{\gamma_{sd}}\left(\frac{g_{MPSK}}{\sin^2\theta}\right) = (2b_{sd}m_{sd})^{m_{sd}}\sin^2\theta\frac{\left(\sin^2\theta+2b_{sd}\overline{\gamma}_{sd}g_{MPSK}\right)^{m_{sd}-1}}{\left[2b_{sd}m_{sd}\sin^2\theta+2b_{sd}\overline{\gamma}_{sd}g_{MPSK}(\Omega_{sd}+2b_{sd}m_{sd})\right]^{m_{sd}}}. \tag{A.4}$$

The first integral

$$I^{sd}_{1,MPSK} = \frac{1}{\pi}\int_0^{\frac{\pi}{2}} \phi_{\gamma_{sd}}\left(\frac{g_{MPSK}}{\sin^2\theta}\right) d\theta \tag{A.5}$$

can be calculated by changing the variable $t = \cos^2(\theta)$.

Hence, when $\theta = 0 \Rightarrow t = 1$, when $\theta = \pi/2 \Rightarrow t = 0$, and $dt = -2\sqrt{t}\sqrt{1-t}d\theta$.

The equation A.4 can be rewritten as

$$\phi_{\gamma_{sd}}\left(\frac{g_{MPSK}}{\sin^2\theta}\right) = (2b_{sd}m_{sd})^{m_{sd}}(1-t)\frac{G^{m_{sd}-1}_{1,MPSK}\left(1-t\frac{1}{G_{1,MPSK}}\right)^{m_{sd}-1}}{G^{m_{sd}}_{2,MPSK}\left(1-t\frac{2b_{sd}m_{sd}}{G_{2,MPSK}}\right)^{m_{sd}}}. \tag{A.6}$$

where

$$\begin{aligned} G_{1,MPSK} &= 1 + 2b_{sd}\overline{\gamma}_{sd}g_{MPSK}, \\ G_{2,MPSK} &= 2b_{sd}m_{sd} + 2b_{sd}\overline{\gamma}_{sd}g_{MPSK}(2b_{sd}m_{sd} + \Omega_{sd}). \end{aligned} \tag{A.7}$$

So, $I^{sd}_{1,MPSK}$ can be rewritten as

$$I^{sd}_{1,MPSK} = \frac{(2b_{sd}m_{sd})^{m_{sd}}\, G^{m_{sd}-1}_{1,MPSK}}{2\pi G^{m_{sd}}_{2,MPSK}} \int_0^1 t^{-\frac{1}{2}}(1-t)^{\frac{1}{2}} \left(1 - t\frac{1}{G_{1,MPSK}}\right)^{m_{sd}-1} \left(1 - t\frac{2b_{sd}m_{sd}}{G_{2,MPSK}}\right)^{-m_{sd}} dt \tag{A.8}$$

By using the Appell function,

$$\begin{aligned} F_1(a, b_1, b_2; c; x_1, x_2) &= \frac{1}{B(a, c-a)} \int_0^1 t^{a-1}(1-t)^{c-a-1}(1-x_1 t)^{-b_1}(1-x_2 t)^{-b_2} dt, \\ &\mathrm{Re}(c) > \mathrm{Re}(a) > 0 \end{aligned} \tag{A.9}$$

$I^{sd}_{1,MPSK}$ can be obtained as

$$I^{sd}_{1,MPSK} = \frac{(2b_{sd}m_{sd})^{m_{sd}}\, G^{m_{sd}-1}_{1,MPSK}}{4G^{m_{sd}}_{2,MPSK}} F_1\left(\frac{1}{2}, 1-m_{sd}, m_{sd}; 2; \frac{1}{G_{1,MPSK}}, \frac{2b_{sd}m_{sd}}{G_{2,MPSK}}\right) \tag{A.10}$$

The second integral $I^{sd}_{2,MPSK}$ can be rewritten as

$$I^{sd}_{2,MPSK} = \frac{1}{\pi} \int_{\frac{\pi}{M}}^{\frac{\pi}{2}} \phi_{\gamma_{sd}}\left(\frac{g_{MPSK}}{\sin^2\theta}\right) d\theta. \tag{A.11}$$

Let change the variable

$$z = \frac{\cos^2\theta}{\cos^2(\pi/M)} = \frac{\cos^2\theta}{1 - g_{MPSK}} = \frac{\cos^2\theta}{\omega}. \tag{A.12}$$

Hence, when $\theta = \pi/M \Rightarrow z = 1$, when $\theta = \pi/2 \Rightarrow z = 0$, and $dz = -(2/\omega)\sqrt{\omega z}\sqrt{1-\omega z}d\theta$.

And equation A.4 can be written as follows

$$\phi_{\gamma_{sd}}(z) = (2b_{sd}m_{sd})^{m_{sd}}(1-z\omega)\frac{G^{m_{sd}-1}_{1,MPSK}\left(1 - z\frac{\omega}{G_{1,MPSK}}\right)^{m_{sd}-1}}{G^{m_{sd}}_{2,MPSK}\left(1 - z\frac{2b_{sd}m_{sd}\omega}{G_{2,MPSK}}\right)^{m_{sd}}}. \tag{A.13}$$

Therefore, $I^{sd}_{2,MPSK}$ can be rewritten as below

$$\begin{aligned} I^{sd}_{2,MPSK} = \frac{\sqrt{\omega}\,(2b_{sd}m_{sd})^{m_{sd}}\, G^{m_{sd}-1}_{1,MPSK}}{2\pi G^{m_{sd}}_{2,MPSK}} \int_0^1 z^{-\frac{1}{2}}(1-z\omega)^{\frac{1}{2}} \\ \times \left(1 - z\frac{\omega}{G_{1,MPSK}}\right)^{m_{sd}-1} \left(1 - z\frac{2b_{sd}m_{sd}\omega}{G_{2,MPSK}}\right)^{-m_{sd}} dz \end{aligned} \tag{A.14}$$

By using the Lauricella function,

$$F_D^{(n)}(a,b_1,\ldots,b_n;c;x_1,\ldots,x_n)=\frac{1}{B(a,c-a)}\int_0^1 t^{a-1}(1-t)^{c-a-1}\prod_{i=1}^{n}(1-x_it)^{-b_i}dt, \\ \mathrm{Re}(c)>\mathrm{Re}(a)>0, \tag{A.15}$$

$I_{2,MPSK}^{sd}$ is given as

$$I_{2,MPSK}^{sd}=\frac{\sqrt{\omega}\left(2b_{sd}m_{sd}\right)^{m_{sd}}G_{1,MPSK}^{m_{sd}-1}}{\pi G_{2,MPSK}^{m_{sd}}}F_D^{(3)}\left(\frac{1}{2},-\frac{1}{2},1-m_{sd},m_{sd};\frac{3}{2};\omega,\frac{\omega}{G_{1,MPSK}},\frac{2b_{sd}m_{sd}\omega}{G_{2,MPSK}}\right) \tag{A.16}$$

Hence, $P_{sd,MPSK}\left(E\right)$ is finally obtained as below

$$\begin{aligned}P_{sd,MPSK}(E)=&\frac{\left(2b_{sd}m_{sd}\right)^{m_{sd}}G_{1,MPSK}^{m_{sd}-1}}{4G_{2,MPSK}^{m_{sd}}}F_1\left(\frac{1}{2},1-m_{sd},m_{sd};2;\frac{1}{G_{1,MPSK}},\frac{2b_{sd}m_{sd}}{G_{2,MPSK}}\right)\\&+\frac{\sqrt{\omega}\left(2b_{sd}m_{sd}\right)^{m_{sd}}G_{1,MPSK}^{m_{sd}-1}}{\pi G_{2,MPSK}^{m_{sd}}}F_D^{(3)}\left(\frac{1}{2},-\frac{1}{2},1-m_{sd},m_{sd};\frac{3}{2};\omega,\frac{\omega}{G_{1,MPSK}},\frac{2b_{sd}m_{sd}\omega}{G_{2,MPSK}}\right).\end{aligned} \tag{A.17}$$

A.2 SEP of MQAM

The average SEP of the direct link for coherent MQAM signals is defined in 2.17 by

$$P_{sd,MQAM}(E)=\underbrace{\frac{4q}{\pi}\int_0^{\frac{\pi}{2}}\phi_{\gamma_{sd}}\left(\frac{g_{MQAM}}{\sin^2\theta}\right)d\theta}_{I_{1,MQAM}^{sd}}-\underbrace{\frac{4q^2}{\pi}\int_0^{\frac{\pi}{4}}\phi_{\gamma_{sd}}\left(\frac{g_{MQAM}}{\sin^2\theta}\right)d\theta}_{I_{2,MQAM}^{sd}} \tag{A.18}$$

where $g_{MQAM}=3/2(M-1)$ and $q=\left(1-1/\sqrt{M}\right)$ and

$$\phi_{\gamma_{sd}}\left(\frac{g_{MQAM}}{\sin^2\theta}\right)=\left(2b_{sd}m_{sd}\right)^{m_{sd}}\sin^2\theta\frac{\left(\sin^2\theta+2b_{sd}\overline{\gamma}_{sd}g_{MQAM}\right)^{m_{sd}-1}}{\left[2b_{sd}m_{sd}\sin^2\theta+2b_{sd}\overline{\gamma}_{sd}g_{MQAM}\left(\Omega_{sd}+2b_{sd}m_{sd}\right)\right]^{m_{sd}}}. \tag{A.19}$$

The first integral $I_{1,MQAM}^{sd}$ can be computed by using the same approach as in $I_{1,MPSK}^{sd}$. We only change g_{MPSK} to g_{MQAM} and multiply the factor $4q$ into $I_{1,MPSK}^{sd}$.

Hence, we obtain

$$I_{1,MQAM}^{sd}=\frac{q\left(2b_{sd}m_{sd}\right)^{m_{sd}}G_{1,MQAM}^{m_{sd}-1}}{G_{2,MQAM}^{m_{sd}}}F_1\left(\frac{1}{2},1-m_{sd},m_{sd};2;\frac{1}{G_{1,MQAM}},\frac{2b_{sd}m_{sd}}{G_{2,MQAM}}\right) \tag{A.20}$$

where

$$\begin{aligned} G_{1,MQAM} &= 1 + 2b_{sd}\overline{\gamma}_{sd}g_{MQAM}, \\ G_{2,MQAM} &= 2b_{sd}m_{sd} + 2b_{sd}\overline{\gamma}_{sd}g_{MQAM}\left(2b_{sd}m_{sd} + \Omega_{sd}\right). \end{aligned} \tag{A.21}$$

In order to derive $I^{sd}_{2,MQAM}$, we change the variable, $t = 1 - \tan^2\theta$.

Hence, when $\theta = 0 \Rightarrow t = 1$, when $\theta = \pi/4 \Rightarrow t = 0$, and $dt = -2\sqrt{1-t}(2-t)d\theta$.

So, the equation A.19 can be rewritten as below

$$\phi_{\gamma_{sd}}\left(\frac{g_{MQAM}}{\sin^2\theta}\right) = \left(2b_{sd}m_{sd}\right)^{m_{sd}}(1-t)\frac{L^{m_{sd}-1}_{1,MQAM}\left(1 - t\frac{G_{1,MQAM}}{L_{1,MQAM}}\right)^{m_{sd}-1}}{L^{m_{sd}}_{2,MQAM}\left(1 - t\frac{G_{2,MQAM}}{L_{2,MQAM}}\right)^{m_{sd}}} \tag{A.22}$$

where

$$\begin{aligned} L_{1,MQAM} &= 1 + 4b_{sd}\overline{\gamma}_{sd}g_{MQAM}, \\ L_{2,MQAM} &= 2b_{sd}m_{sd} + 4b_{sd}\overline{\gamma}_{sd}g_{MQAM}(2b_{sd}m_{sd} + \Omega_{sd}). \end{aligned} \tag{A.23}$$

Therefore, $I^{sd}_{2,MQAM}$ can be written as below

$$\begin{aligned} I^{sd}_{2,MQAM} = \frac{q^2\left(2b_{sd}m_{sd}\right)^{m_{sd}}L^{m_{sd}-1}_{1,MQAM}}{\pi L^{m_{sd}}_{2,MQAM}}\int_0^1 (1-t)^{\frac{1}{2}}\left(1-\frac{t}{2}\right)^{-1} \\ \times\left(1 - t\frac{G_{1,MQAM}}{L_{1,MQAM}}\right)^{m_{sd}-1}\left(1 - t\frac{G_{2,MQAM}}{L_{2,MQAM}}\right)^{-m_{sd}}dt \end{aligned} \tag{A.24}$$

By using the Lauricella function, $I^{sd}_{2,MQAM}$ is given as

$$I^{sd}_{2,MQAM} = \frac{2q^2\left(2b_{sd}m_{sd}\right)^{m_{sd}}L^{m_{sd}-1}_{1,MQAM}}{3\pi L^{m_{sd}}_{2,MQAM}}F_D^{(3)}\left(1,1,1-m_{sd},m_{sd};\frac{5}{2};\frac{1}{2},\frac{G_{1,MQAM}}{L_{1,MQAM}},\frac{G_{2,MQAM}}{L_{2,MQAM}}\right) \tag{A.25}$$

So, the average SEP of the direct link, $P_{sd,MQAM}(E)$, is finally given by

$$\begin{aligned} P_{sd,MQAM}(E) = \frac{q\left(2b_{sd}m_{sd}\right)^{m_{sd}}G^{m_{sd}-1}_{1,MQAM}}{G^{m_{sd}}_{2,MQAM}}F_1\left(\frac{1}{2},1-m_{sd},m_{sd};2;\frac{1}{G_{1,MQAM}},\frac{2b_{sd}m_{sd}}{G_{2,MQAM}}\right) \\ - \frac{2q^2\left(2b_{sd}m_{sd}\right)^{m_{sd}}L^{m_{sd}-1}_{1,MQAM}}{3\pi L^{m_{sd}}_{2,MQAM}}F_D^{(3)}\left(1,1,1-m_{sd},m_{sd};\frac{5}{2};\frac{1}{2},\frac{G_{1,MQAM}}{L_{1,MQAM}},\frac{G_{2,MQAM}}{L_{2,MQAM}}\right). \end{aligned} \tag{A.26}$$

Appendix B

SEP of the HSTCS

B.1 SEP of MPSK

The average SEP of the HSTCS for coherent MPSK signals is defined in 2.38 by

$$\begin{aligned} P_{s,MPSK}^{SDF}(E) &= \frac{1}{\pi}\int_0^{\pi-\frac{\pi}{M}} \phi_{\gamma_{MRC}^{SDF}}\left(\frac{g_{MPSK}}{\sin^2\theta}\right) d\theta \\ &= \underbrace{\frac{1}{\pi}\int_0^{\frac{\pi}{2}} \phi_{\gamma_{MRC}^{SDF}}\left(\frac{g_{MPSK}}{\sin^2\theta}\right) d\theta}_{I_{1,MPSK}^{SDF}} + \underbrace{\frac{1}{\pi}\int_{\frac{\pi}{2}}^{\pi-\frac{\pi}{M}} \phi_{\gamma_{MRC}^{SDF}}\left(\frac{g_{MPSK}}{\sin^2\theta}\right) d\theta}_{I_{2,MPSK}^{SDF}} \end{aligned} \tag{B.1}$$

where $g_{MPSK} = \sin^2(\pi/M)$ and $\phi_{\gamma_{MRC}^{SDF}}(s)$ is defined in 2.37 by

$$\begin{aligned} \phi_{\gamma_{MRC}^{SDF}}(s) &= \phi_{\gamma_{sd}}(s)\left(\prod_{i=1}^{L} P_{sr_i}\right) + \phi_{\gamma_{sd}}(s)\left(\prod_{i=1}^{L} P_{sr_i}\right) \\ &\times \sum_{k=1}^{L}\sum_{\lambda_1=1}^{L-k+1}\sum_{\lambda_2=\lambda_1+1}^{L-k+2}\cdots\sum_{\lambda_k=\lambda_{k-1}+1}^{L}\prod_{n=1}^{k}\left(\frac{1-P_{sr_{\lambda_n}}}{P_{sr_{\lambda_n}}}\right)\left(1+s\frac{\overline{\gamma}_{r_{\lambda_n}d}\Omega_{r_{\lambda_n}d}}{m_{r_{\lambda_n}d}}\right)^{-m_{r_{\lambda_n}d}}. \end{aligned} \tag{B.2}$$

So,

$$\begin{aligned} \phi_{\gamma_{MRC}^{SDF}}\left(\frac{g_{MPSK}}{\sin^2\theta}\right) &= \phi_{\gamma_{sd}}\left(\frac{g_{MPSK}}{\sin^2\theta}\right)\left(\prod_{i=1}^{L} P_{sr_i}\right) + \phi_{\gamma_{sd}}\left(\frac{g_{MPSK}}{\sin^2\theta}\right)\left(\prod_{i=1}^{L} P_{sr_i}\right) \\ &\times \sum_{k=1}^{L}\sum_{\lambda_1=1}^{L-k+1}\sum_{\lambda_2=\lambda_1+1}^{L-k+2}\cdots\sum_{\lambda_k=\lambda_{k-1}+1}^{L}\prod_{n=1}^{k}\left(\frac{1-P_{sr_{\lambda_n}}}{P_{sr_{\lambda_n}}}\right) \\ &\left(\frac{m_{r_{\lambda_n}d}\sin^2\theta + g_{MPSK}\overline{\gamma}_{r_{\lambda_n}d}\Omega_{r_{\lambda_n}d}}{m_{r_{\lambda_n}d}\sin^2\theta}\right)^{-m_{r_{\lambda_n}d}}. \end{aligned} \tag{B.3}$$

where $\phi_{\gamma_{sd}}\left(\frac{g_{MPSK}}{\sin^2\theta}\right)$ is given in A.4.

The first integral $I_{1,MPSK}^{SDF}$ can be derived by changing the variable $t = \cos^2(\theta)$.

So, $\phi_{\gamma_{MRC}^{SDF}}\left(\frac{g_{MPSK}}{\sin^2\theta}\right)$ can be rewritten as below

$$\begin{aligned}\phi_{\gamma_{MRC}^{SDF}}\left(\frac{g_{MPSK}}{\sin^2\theta}\right) &= (2b_{sd}m_{sd})^{m_{sd}}(1-t)\frac{G_{1,MPSK}^{m_{sd}-1}\left(1-t\frac{1}{G_{1,MPSK}}\right)^{m_{sd}-1}}{G_{2,MPSK}^{m_{sd}}\left(1-t\frac{2b_{sd}m_{sd}}{G_{2,MPSK}}\right)^{m_{sd}}}\left(\prod_{i=1}^{L}P_{sr_i}\right)\\ &+ (2b_{sd}m_{sd})^{m_{sd}}(1-t)\frac{G_{1,MPSK}^{m_{sd}-1}\left(1-t\frac{1}{G_{1,MPSK}}\right)^{m_{sd}-1}}{G_{2,MPSK}^{m_{sd}}\left(1-t\frac{2b_{sd}m_{sd}}{G_{2,MPSK}}\right)^{m_{sd}}}\left(\prod_{i=1}^{L}P_{sr_i}\right)\\ &\times\sum_{k=1}^{L}\sum_{\lambda_1=1}^{L-k+1}\sum_{\lambda_2=\lambda_1+1}^{L-k+2}\cdots\sum_{\lambda_k=\lambda_{k-1}+1}^{L}\prod_{n=1}^{k}\left[\left(\frac{1-P_{sr_{\lambda_n}}}{P_{sr_{\lambda_n}}}\right)\left(\frac{m_{r_{\lambda_n}d}}{H_{\lambda_n,MPSK}}\right)^{m_{r_{\lambda_n}d}}\right]\\ &\times\prod_{n=1}^{k}\left[(1-t)^{m_{r_{\lambda_n}d}}\left(1-t\frac{m_{r_{\lambda_n}d}}{H_{\lambda_n,MPSK}}\right)^{-m_{r_{\lambda_n}d}}\right]\end{aligned} \tag{B.4}$$

where

$$H_{\lambda_n,MPSK} = m_{r_{\lambda_n}d} + g_{MPSK}\Omega_{r_{\lambda_n}d}\overline{\gamma}_{r_{\lambda_n}d}. \tag{B.5}$$

Therefore, $I_{1,MPSK}^{SDF}$ can be written as

$$\begin{aligned}I_{1,MPSK}^{SDF} &= \frac{(2b_{sd}m_{sd})^{m_{sd}}G_{1,MPSK}^{m_{sd}-1}}{2\pi G_{2,MPSK}^{m_{sd}}}\left(\prod_{i=1}^{L}P_{sr_i}\right)\\ &\times\int_0^1 t^{-\frac{1}{2}}(1-t)^{\frac{1}{2}}\left(1-t\frac{1}{G_{1,MPSK}}\right)^{m_{sd}-1}\left(1-t\frac{2b_{sd}m_{sd}}{G_{2,MPSK}}\right)^{-m_{sd}}dt\\ &+\frac{(2b_{sd}m_{sd})^{m_{sd}}G_{1,MPSK}^{m_{sd}-1}}{2\pi G_{2,MPSK}^{m_{sd}}}\left(\prod_{i=1}^{L}P_{sr_i}\right)\sum_{k=1}^{L}\sum_{\lambda_1=1}^{L-k+1}\sum_{\lambda_2=\lambda_1+1}^{L-k+2}\cdots\sum_{\lambda_k=\lambda_{k-1}+1}^{L}\\ &\prod_{n=1}^{k}\left[\left(\frac{1-P_{sr_{\lambda_n}}}{P_{sr_{\lambda_n}}}\right)\left(\frac{m_{r_{\lambda_n}d}}{H_{\lambda_n,MPSK}}\right)^{m_{r_{\lambda_n}d}}\right]\int_0^1 t^{-\frac{1}{2}}(1-t)^{\frac{1}{2}}\prod_{n=1}^{k}(1-t)^{m_{r_{\lambda_n}d}}\\ &\times\prod_{n=1}^{k}\left(1-t\frac{m_{r_{\lambda_n}d}}{H_{\lambda_n,MPSK}}\right)^{-m_{r_{\lambda_n}d}}\left(1-t\frac{1}{G_{1,MPSK}}\right)^{m_{sd}-1}\left(1-t\frac{2b_{sd}m_{sd}}{G_{2,MPSK}}\right)^{-m_{sd}}dt\end{aligned} \tag{B.6}$$

By using the Lauricellla function, $I_{1,MPSK}^{SDF}$ can be obtained as below

$$\begin{aligned}
I_{1,MPSK}^{SDF} = & \frac{(2b_{sd}m_{sd})^{m_{sd}} G_{1,MPSK}^{m_{sd}-1}}{4G_{2,MPSK}^{m_{sd}}} \left(\prod_{i=1}^{L} P_{sr_i}\right) F_1\left(\frac{1}{2}, 1-m_{sd}, m_{sd}; 2; \frac{1}{G_{1,MPSK}}, \frac{2b_{sd}m_{sd}}{G_{2,MPSK}}\right) \\
& + \frac{(2b_{sd}m_{sd})^{m_{sd}} G_{1,MPSK}^{m_{sd}-1}}{2\pi G_{2,MPSK}^{m_{sd}}} \left(\prod_{i=1}^{L} P_{sr_i}\right) \sum_{k=1}^{L} \sum_{\lambda_1=1}^{L-k+1} \sum_{\lambda_2=\lambda_1+1}^{L-k+2} \cdots \sum_{\lambda_k=\lambda_{k-1}+1}^{L} \\
& \prod_{n=1}^{k} \left(\frac{1-P_{sr_{\lambda_n}}}{P_{sr_{\lambda_n}}}\right) \left(\frac{m_{r_{\lambda_n}d}}{H_{\lambda_n,MPSK}}\right)^{m_{r_{\lambda_n}d}} \frac{\Gamma\left(\frac{1}{2}\right)\Gamma\left(\frac{3}{2}+\sum_{n=1}^{k} m_{r_{\lambda_n}d}\right)}{\Gamma\left(2+\sum_{n=1}^{k} m_{r_{\lambda_n}d}\right)} F_D^{(k+2)}\left(\frac{1}{2}, 1-m_{sd},\right. \\
& \left. m_{sd}, m_{r_{\lambda_1}d}, \ldots, m_{r_{\lambda_k}d}; 2+\sum_{n=1}^{k} m_{r_{\lambda_n}d}; \frac{1}{G_{1,MPSK}}, \frac{2b_{sd}m_{sd}}{G_{2,MPSK}}, \frac{m_{r_{\lambda_1}d}}{H_{\lambda_1,MPSK}}, \ldots, \frac{m_{r_{\lambda_k}d}}{H_{\lambda_k,MPSK}}\right)
\end{aligned} \tag{B.7}$$

The second integral $I_{2,MPSK}^{SDF}$ can be derived by changing the variable

$$z = \frac{\cos^2\theta}{\cos^2(\pi/M)} = \frac{\cos^2\theta}{1-g_{MPSK}} = \frac{\cos^2\theta}{\omega}. \tag{B.8}$$

In this case, $\phi_{\gamma_{MRC}^{SDF}}\left(\frac{g_{MPSK}}{\sin^2\theta}\right)$ can be rewritten as below

$$\begin{aligned}
\phi_{\gamma_{MRC}^{SDF}}\left(\frac{g_{MPSK}}{\sin^2\theta}\right) = & (2b_{sd}m_{sd})^{m_{sd}} (1-z\omega) \frac{G_{1,MPSK}^{m_{sd}-1}\left(1-z\frac{\omega}{G_{1,MPSK}}\right)^{m_{sd}-1}}{G_{2,MPSK}^{m_{sd}}\left(1-z\frac{2b_{sd}m_{sd}\omega}{G_{2,MPSK}}\right)^{m_{sd}}} \left(\prod_{i=1}^{L} P_{sr_i}\right) \\
& + (2b_{sd}m_{sd})^{m_{sd}} (1-z\omega) \frac{G_{1,MPSK}^{m_{sd}-1}\left(1-z\frac{\omega}{G_{1,MPSK}}\right)^{m_{sd}-1}}{G_{2,MPSK}^{m_{sd}}\left(1-z\frac{2b_{sd}m_{sd}\omega}{G_{2,MPSK}}\right)^{m_{sd}}} \left(\prod_{i=1}^{L} P_{sr_i}\right) \\
& \times \sum_{k=1}^{L} \sum_{\lambda_1=1}^{L-k+1} \sum_{\lambda_2=\lambda_1+1}^{L-k+2} \cdots \sum_{\lambda_k=\lambda_{k-1}+1}^{L} \prod_{n=1}^{k} \left[\left(\frac{1-P_{sr_{\lambda_n}}}{P_{sr_{\lambda_n}}}\right)\left(\frac{m_{r_{\lambda_n}d}}{H_{\lambda_n,MPSK}}\right)^{m_{r_{\lambda_n}d}}\right] \\
& \times \prod_{n=1}^{k} \left[(1-z\omega)^{m_{r_{\lambda_n}d}} \left(1-z\omega\frac{m_{r_{\lambda_n}d}}{H_{\lambda_n,MPSK}}\right)^{-m_{r_{\lambda_n}d}}\right]
\end{aligned} \tag{B.9}$$

Therefore, $I_{2,MPSK}^{SDF}$ can be written as

$$
\begin{aligned}
I_{2,MPSK}^{SDF} = & \frac{\sqrt{\omega}\left(2b_{sd}m_{sd}\right)^{m_{sd}} G_{1,MPSK}^{m_{sd}-1}}{2\pi G_{2,MPSK}^{m_{sd}}} \left(\prod_{i=1}^{L} P_{sr_i}\right) \\
& \times \int_0^1 z^{-\frac{1}{2}}(1-z\omega)^{\frac{1}{2}} \left(1 - z\frac{\omega}{G_{1,MPSK}}\right)^{m_{sd}-1} \left(1 - z\frac{2b_{sd}m_{sd}\omega}{G_{2,MPSK}}\right)^{-m_{sd}} dz \\
& + \frac{\sqrt{\omega}\left(2b_{sd}m_{sd}\right)^{m_{sd}} G_{1,MPSK}^{m_{sd}-1}}{2\pi G_{2,MPSK}^{m_{sd}}} \left(\prod_{i=1}^{L} P_{sr_i}\right) \sum_{k=1}^{L} \sum_{\lambda_1=1}^{L-k+1} \sum_{\lambda_2=\lambda_1+1}^{L-k+2} \cdots \sum_{\lambda_k=\lambda_{k-1}+1}^{L} \\
& \prod_{n=1}^{k} \left[\left(\frac{1-P_{sr_{\lambda_n}}}{P_{sr_{\lambda_n}}}\right) \left(\frac{m_{r_{\lambda_n}d}}{H_{\lambda_n,MPSK}}\right)^{m_{r_{\lambda_n}d}}\right] \int_0^1 z^{-\frac{1}{2}}(1-z\omega)^{\frac{1}{2}} \prod_{n=1}^{k}(1-z\omega)^{m_{r_{\lambda_n}d}} \\
& \times \prod_{n=1}^{k} \left(1 - z\frac{\omega m_{r_{\lambda_n}d}}{H_{\lambda_n,MPSK}}\right)^{-m_{r_{\lambda_n}d}} \left(1 - z\frac{\omega}{G_{1,MPSK}}\right)^{m_{sd}-1} \left(1 - z\frac{2b_{sd}m_{sd}\omega}{G_{2,MPSK}}\right)^{-m_{sd}} dz
\end{aligned}
\tag{B.10}
$$

By using the Lauricella function, $I_{2,MPSK}^{SDF}$ can be obtained as follows

$$
\begin{aligned}
I_{2,MPSK}^{SDF} = & \frac{\sqrt{\omega}\left(2b_{sd}m_{sd}\right)^{m_{sd}} G_{1,MPSK}^{m_{sd}-1}}{\pi G_{2,MPSK}^{m_{sd}}} \left(\prod_{i=1}^{L} P_{sr_i}\right) \\
& \times F_D^{(3)}\left(\frac{1}{2}, -\frac{1}{2}, 1-m_{sd}, m_{sd}; \frac{3}{2}; \omega, \frac{\omega}{G_{1,MPSK}}, \frac{2b_{sd}m_{sd}\omega}{G_{2,MPSK}}\right) \\
& + \frac{\sqrt{\omega}\left(2b_{sd}m_{sd}\right)^{m_{sd}} G_{1,MPSK}^{m_{sd}-1}}{\pi G_{2,MPSK}^{m_{sd}}} \left(\prod_{i=1}^{L} P_{sr_i}\right) \sum_{k=1}^{L} \sum_{\lambda_1=1}^{L-k+1} \sum_{\lambda_2=\lambda_1+1}^{L-k+2} \cdots \sum_{\lambda_k=\lambda_{k-1}+1}^{L} \\
& \prod_{n=1}^{k} \left(\frac{1-P_{sr_{\lambda_n}}}{P_{sr_{\lambda_n}}}\right) \left(\frac{m_{r_{\lambda_n}d}}{H_{\lambda_n,MPSK}}\right)^{m_{r_{\lambda_n}d}} F_D^{(k+3)}\left(\frac{1}{2}, -\frac{1}{2} - \sum_{n=1}^{k} m_{r_{\lambda_n}d}, 1-m_{sd}, m_{sd}, \right. \\
& \left. m_{r_{\lambda_1}d}, \ldots, m_{r_{\lambda_k}d}; \frac{3}{2}; \omega, \frac{\omega}{G_{1,MPSK}}, \frac{2b_{sd}m_{sd}\omega}{G_{2,MPSK}}, \frac{m_{r_{\lambda_1}d}\omega}{H_{\lambda_1,MPSK}}, \ldots, \frac{m_{r_{\lambda_k}d}\omega}{H_{\lambda_k,MPSK}}\right)
\end{aligned}
\tag{B.11}
$$

Therefore, $P_{s,MPSK}^{SDF}(E)$ is given as below

$$
\begin{aligned}
P_{s,MPSK}^{SDF}(E) = {} & \frac{(2b_{sd}m_{sd})^{m_{sd}}\, G_{1,MPSK}^{m_{sd}-1}}{4G_{2,MPSK}^{m_{sd}}} \left(\prod_{i=1}^{L} P_{sr_i}\right) F_1\left(\frac{1}{2}, 1-m_{sd}, m_{sd}; 2; \frac{1}{G_{1,MPSK}}, \frac{2b_{sd}m_{sd}}{G_{2,MPSK}}\right) \\
& + \frac{\sqrt{\omega}\,(2b_{sd}m_{sd})^{m_{sd}}\, G_{1,MPSK}^{m_{sd}-1}}{\pi G_{2,MPSK}^{m_{sd}}} \left(\prod_{i=1}^{L} P_{sr_i}\right) \\
& \times F_D^{(3)}\left(\frac{1}{2}, -\frac{1}{2}, 1-m_{sd}, m_{sd}; \frac{3}{2}; \omega, \frac{\omega}{G_{1,MPSK}}, \frac{2b_{sd}m_{sd}\omega}{G_{2,MPSK}}\right) \\
& + \frac{(2b_{sd}m_{sd})^{m_{sd}}\, G_{1,MPSK}^{m_{sd}-1}}{2\pi G_{2,MPSK}^{m_{sd}}} \left(\prod_{i=1}^{L} P_{sr_i}\right) \sum_{k=1}^{L} \sum_{\lambda_1=1}^{L-k+1} \sum_{\lambda_2=\lambda_1+1}^{L-k+2} \cdots \sum_{\lambda_k=\lambda_{k-1}+1}^{L} \\
& \prod_{n=1}^{k} \left(\frac{1-P_{sr_{\lambda_n}}}{P_{sr_{\lambda_n}}}\right) \left(\frac{m_{r_{\lambda_n}d}}{H_{\lambda_n,MPSK}}\right)^{m_{r_{\lambda_n}d}} \frac{\Gamma\left(\frac{1}{2}\right)\Gamma\left(\frac{3}{2}+\sum_{n=1}^{k} m_{r_{\lambda_n}d}\right)}{\Gamma\left(2+\sum_{n=1}^{k} m_{r_{\lambda_n}d}\right)} F_D^{(k+2)}\left(\frac{1}{2}, 1-m_{sd},\right. \\
& \left. m_{sd}, m_{r_{\lambda_1}d}, \ldots, m_{r_{\lambda_k}d}; 2+\sum_{n=1}^{k} m_{r_{\lambda_n}d}; \frac{1}{G_{1,MPSK}}, \frac{2b_{sd}m_{sd}}{G_{2,MPSK}}, \frac{m_{r_{\lambda_1}d}}{H_{\lambda_1,MPSK}}, \ldots, \frac{m_{r_{\lambda_k}d}}{H_{\lambda_k,MPSK}}\right) \\
& + \frac{\sqrt{\omega}\,(2b_{sd}m_{sd})^{m_{sd}}\, G_{1,MPSK}^{m_{sd}-1}}{\pi G_{2,MPSK}^{m_{sd}}} \left(\prod_{i=1}^{L} P_{sr_i}\right) \sum_{k=1}^{L} \sum_{\lambda_1=1}^{L-k+1} \sum_{\lambda_2=\lambda_1+1}^{L-k+2} \cdots \sum_{\lambda_k=\lambda_{k-1}+1}^{L} \\
& \prod_{n=1}^{k} \left(\frac{1-P_{sr_{\lambda_n}}}{P_{sr_{\lambda_n}}}\right) \left(\frac{m_{r_{\lambda_n}d}}{H_{\lambda_n,MPSK}}\right)^{m_{r_{\lambda_n}d}} F_D^{(k+3)}\left(\frac{1}{2}, -\frac{1}{2}-\sum_{n=1}^{k} m_{r_{\lambda_n}d}, 1-m_{sd}, m_{sd},\right. \\
& \left. m_{r_{\lambda_1}d}, \ldots, m_{r_{\lambda_k}d}; \frac{3}{2}; \omega, \frac{\omega}{G_{1,MPSK}}, \frac{2b_{sd}m_{sd}\omega}{G_{2,MPSK}}, \frac{m_{r_{\lambda_1}d}\omega}{H_{\lambda_1,MPSK}}, \ldots, \frac{m_{r_{\lambda_k}d}\omega}{H_{\lambda_k,MPSK}}\right)
\end{aligned}
\tag{B.12}
$$

B.2 SEP of MQAM

The average SEP of the HSTCS for coherent MQAM signals is defined in 2.46 by

$$
P_{s,MQAM}^{SDF}(E) = \underbrace{\frac{4q}{\pi}\int_0^{\frac{\pi}{2}} \phi_{\gamma_{MRC}^{SDF}}\left(\frac{g_{MQAM}}{\sin^2\theta}\right) d\theta}_{I_{1,MQAM}^{SDF}} - \underbrace{\frac{4q^2}{\pi}\int_0^{\frac{\pi}{4}} \phi_{\gamma_{MRC}^{SDF}}\left(\frac{g_{MQAM}}{\sin^2\theta}\right) d\theta}_{I_{2,MQAM}^{SDF}}
\tag{B.13}
$$

where $g_{MQAM} = 3/2(M-1)$, $q = \left(1 - 1/\sqrt{M}\right)$ and

$$\phi_{\gamma_{MRC}^{SDF}}\left(\frac{g_{MQAM}}{\sin^2\theta}\right) = \phi_{\gamma_{sd}}\left(\frac{g_{MQAM}}{\sin^2\theta}\right)\left(\prod_{i=1}^{L} P_{sr_i}\right) + \phi_{\gamma_{sd}}\left(\frac{g_{MQAM}}{\sin^2\theta}\right)\left(\prod_{i=1}^{L} P_{sr_i}\right) \times \sum_{k=1}^{L}\sum_{\lambda_1=1}^{L-k+1}\sum_{\lambda_2=\lambda_1+1}^{L-k+2}\cdots\sum_{\lambda_k=\lambda_{k-1}+1}^{L}\prod_{n=1}^{k}\left(\frac{1-P_{sr_{\lambda_n}}}{P_{sr_{\lambda_n}}}\right) \left(\frac{m_{r_{\lambda_n}d}\sin^2\theta + g_{MQAM}\overline{\gamma}_{r_{\lambda_n}d}\Omega_{r_{\lambda_n}d}}{m_{r_{\lambda_n}d}\sin^2\theta}\right)^{-m_{r_{\lambda_n}d}}. \tag{B.14}$$

where $\phi_{\gamma_{sd}}\left(\frac{g_{MQAM}}{\sin^2\theta}\right)$ is given in A.19.

The first integral $I_{1,MQAM}^{SDF}$ can be computed by using the same approach as in $I_{1,MPSK}^{SDF}$. We only change g_{MPSK} to g_{MQAM} and multiply the factor $4q$ into $I_{1,MPSK}^{SDF}$.

Hence, we obtain

$$I_{1,MQAM}^{SDF} = \frac{q\left(2b_{sd}m_{sd}\right)^{m_{sd}}G_{1,MQAM}^{m_{sd}-1}}{G_{2,MQAM}^{m_{sd}}}\left(\prod_{i=1}^{L}P_{sr_i}\right)F_1\left(\frac{1}{2}, 1-m_{sd}, m_{sd}; 2; \frac{1}{G_{1,MQAM}}, \frac{2b_{sd}m_{sd}}{G_{2,MQAM}}\right) + \frac{2q\left(2b_{sd}m_{sd}\right)^{m_{sd}}G_{1,MQAM}^{m_{sd}-1}}{\pi G_{2,MQAM}^{m_{sd}}}\left(\prod_{i=1}^{L}P_{sr_i}\right)\sum_{k=1}^{L}\sum_{\lambda_1=1}^{L-k+1}\sum_{\lambda_2=\lambda_1+1}^{L-k+2}\cdots\sum_{\lambda_k=\lambda_{k-1}+1}^{L} \prod_{n=1}^{k}\left(\frac{1-P_{sr_{\lambda_n}}}{P_{sr_{\lambda_n}}}\right)\left(\frac{m_{r_{\lambda_n}d}}{H_{\lambda_n,MPSK}}\right)^{m_{r_{\lambda_n}d}}\frac{\Gamma\left(\frac{1}{2}\right)\Gamma\left(\frac{3}{2}+\sum_{n=1}^{k}m_{r_{\lambda_n}d}\right)}{\Gamma\left(2+\sum_{n=1}^{k}m_{r_{\lambda_n}d}\right)}F_D^{(k+2)}\left(\frac{1}{2}, 1-m_{sd}, m_{sd}, m_{r_{\lambda_1}d}, \ldots, m_{r_{\lambda_k}d}; 2+\sum_{n=1}^{k}m_{r_{\lambda_n}d}; \frac{1}{G_{1,MQAM}}, \frac{2b_{sd}m_{sd}}{G_{2,MQAM}}, \frac{m_{r_{\lambda_1}d}}{H_{\lambda_1,MQAM}}, \ldots, \frac{m_{r_{\lambda_k}d}}{H_{\lambda_k,MQAM}}\right) \tag{B.15}$$

where

$$H_{\lambda_n,MQAM} = m_{r_{\lambda_n}d} + g_{MQAM}\Omega_{r_{\lambda_n}d}\overline{\gamma}_{r_{\lambda_n}d}. \tag{B.16}$$

In order to derive $I_{2,MQAM}^{SDF}$, we change the variable, $t = 1 - \tan^2\theta$

So, $\phi_{\gamma_{MRC}^{SDF}}\left(\frac{g_{MQAM}}{\sin^2\theta}\right)$ can be rewritten as below

$$\begin{aligned}\phi_{\gamma_{MRC}^{SDF}}\left(\frac{g_{MQAM}}{\sin^2\theta}\right) &= (2b_{sd}m_{sd})^{m_{sd}}(1-t)\frac{L_{1,MQAM}^{m_{sd}-1}\left(1-t\frac{G_{1,MQAM}}{L_{1,MQAM}}\right)^{m_{sd}-1}}{L_{2,MQAM}^{m_{sd}}\left(1-t\frac{G_{2,MQAM}}{L_{2,MQAM}}\right)^{m_{sd}}}\left(\prod_{i=1}^{L}P_{sr_i}\right)\\ &+(2b_{sd}m_{sd})^{m_{sd}}(1-t)\frac{L_{1,MQAM}^{m_{sd}-1}\left(1-t\frac{G_{1,MQAM}}{L_{1,MQAM}}\right)^{m_{sd}-1}}{L_{2,MQAM}^{m_{sd}}\left(1-t\frac{G_{2,MQAM}}{L_{2,MQAM}}\right)^{m_{sd}}}\\ &\times\sum_{k=1}^{L}\sum_{\lambda_1=1}^{L-k+1}\sum_{\lambda_2=\lambda_1+1}^{L-k+2}\cdots\sum_{\lambda_k=\lambda_{k-1}+1}^{L}\prod_{n=1}^{k}\left[\left(\frac{1-P_{sr_{\lambda_n}}}{P_{sr_{\lambda_n}}}\right)\left(\frac{m_{r_{\lambda_n}d}}{Q_{\lambda_n,MQAM}}\right)^{m_{r_{\lambda_n}d}}\right]\\ &\times\prod_{n=1}^{k}\left[(1-t)^{m_{r_{\lambda_n}d}}\left(1-t\frac{H_{\lambda_n,MQAM}}{Q_{\lambda_n,MQAM}}\right)^{-m_{r_{\lambda_n}d}}\right]\end{aligned} \tag{B.17}$$

where

$$Q_{\lambda_n,MQAM} = m_{r_{\lambda_n}d} + 2g_{MQAM}\Omega_{r_{\lambda_n}d}\overline{\gamma}_{r_{\lambda_n}d}. \tag{B.18}$$

Therefore, $I_{2,MPSK}^{SDF}$ can be written as

$$\begin{aligned}I_{2,MQAM}^{SDF} &= \frac{q^2(2b_{sd}m_{sd})^{m_{sd}}L_{1,MQAM}^{m_{sd}-1}}{\pi L_{2,MQAM}^{m_{sd}}}\left(\prod_{i=1}^{L}P_{sr_i}\right)\\ &\times\int_0^1(1-t)^{\frac{1}{2}}\left(1-\frac{t}{2}\right)^{-1}\left(1-t\frac{G_{1,MQAM}}{L_{1,MQAM}}\right)^{m_{sd}-1}\left(1-t\frac{G_{2,MQAM}}{L_{2,MQAM}}\right)^{-m_{sd}}dt\\ &+\frac{q^2(2b_{sd}m_{sd})^{m_{sd}}L_{1,MQAM}^{m_{sd}-1}}{\pi L_{2,MQAM}^{m_{sd}}}\left(\prod_{i=1}^{L}P_{sr_i}\right)\sum_{k=1}^{L}\sum_{\lambda_1=1}^{L-k+1}\sum_{\lambda_2=\lambda_1+1}^{L-k+2}\cdots\sum_{\lambda_k=\lambda_{k-1}+1}^{L}\\ &\prod_{n=1}^{k}\left[\left(\frac{1-P_{sr_{\lambda_n}}}{P_{sr_{\lambda_n}}}\right)\left(\frac{m_{r_{\lambda_n}d}}{Q_{\lambda_n,MQAM}}\right)^{m_{r_{\lambda_n}d}}\right]\\ &\times\int_0^1(1-t)^{\frac{1}{2}}\left(1-\frac{t}{2}\right)^{-1}\left(1-t\frac{G_{1,MQAM}}{L_{1,MQAM}}\right)^{m_{sd}-1}\left(1-t\frac{G_{2,MQAM}}{L_{2,MQAM}}\right)^{-m_{sd}}\\ &\times\prod_{n=1}^{k}\left[(1-t)^{m_{r_{\lambda_n}d}}\left(1-t\frac{H_{\lambda_n,MQAM}}{Q_{\lambda_n,MQAM}}\right)^{-m_{r_{\lambda_n}d}}\right]dt\end{aligned} \tag{B.19}$$

By using the Lauricella function, $I_{2,MQAM}^{SDF}$ can be obtained as below

$$I_{2,MQAM}^{SDF} = \frac{2q^2\left(2b_{sd}m_{sd}\right)^{m_{sd}} L_{1,MQAM}^{m_{sd}-1}}{3\pi L_{2,MQAM}^{m_{sd}}}\left(\prod_{i=1}^{L} P_{sr_i}\right) F_D^{(3)}\left(1,1,1-m_{sd},m_{sd};\frac{5}{2};\frac{1}{2},\frac{G_{1,MQAM}}{L_{1,MQAM}},\frac{G_{2,MQAM}}{L_{2,MQAM}}\right)$$
$$-\frac{q^2\left(2b_{sd}m_{sd}\right)^{m_{sd}} L_{1,MQAM}^{m_{sd}-1}}{\pi L_{2,MQAM}^{m_{sd}}}\left(\prod_{i=1}^{L} P_{sr_i}\right)\sum_{k=1}^{L}\sum_{\lambda_1=1}^{L-k+1}\sum_{\lambda_2=\lambda_1+1}^{L-k+2}\cdots\sum_{\lambda_k=\lambda_{k-1}+1}^{L}$$
$$\prod_{n=1}^{k}\left(\frac{1-P_{sr_{\lambda_n}}}{P_{sr_{\lambda_n}}}\right)\left(\frac{m_{r_{\lambda_n}d}}{Q_{\lambda_n MQAM}}\right)^{m_{r_{\lambda_n}d}}\frac{1}{\left(\frac{3}{2}+\sum_{n=1}^{k} m_{r_{\lambda_n}d}\right)} F_D^{(k+3)}\left(1,1,1-m_{sd},m_{sd},\right.$$
$$\left.m_{r_{\lambda_1}d},\ldots,m_{r_{\lambda_k}d};\frac{5}{2}+\sum_{n=1}^{k} m_{r_{\lambda_n}d};\frac{1}{2},\frac{G_{1,MQAM}}{L_{1,MQAM}},\frac{G_{2,MQAM}}{L_{2,MQAM}},\frac{H_{\lambda_1,MQAM}}{Q_{\lambda_1,MQAM}},\ldots,\frac{H_{\lambda_k,MQAM}}{Q_{\lambda_k,MQAM}}\right) \tag{B.20}$$

So, $P_{s,MQAM}^{SDF}(E)$ is finally given as follows

$$
\begin{aligned}
P_{s,MQAM}^{SDF}(E) = & \frac{q\left(2b_{sd}m_{sd}\right)^{m_{sd}} G_{1,MQAM}^{m_{sd}-1}}{G_{2,MQAM}^{m_{sd}}} \left(\prod_{i=1}^{L} P_{sr_i}\right) F_1\left(\frac{1}{2}, 1-m_{sd}, m_{sd}; 2; \frac{1}{G_{1,MQAM}}, \frac{2b_{sd}m_{sd}}{G_{2,MQAM}}\right) \\
& - \frac{2q^2\left(2b_{sd}m_{sd}\right)^{m_{sd}} L_{1,MQAM}^{m_{sd}-1}}{3\pi L_{2,MQAM}^{m_{sd}}} \left(\prod_{i=1}^{L} P_{sr_i}\right) \\
& \times F_D^{(3)}\left(1, 1, 1-m_{sd}, m_{sd}; \frac{5}{2}; \frac{1}{2}, \frac{G_{1,MQAM}}{L_{1,MQAM}}, \frac{G_{2,MQAM}}{L_{2,MQAM}}\right) \\
& + \frac{2q\left(2b_{sd}m_{sd}\right)^{m_{sd}} G_{1,MQAM}^{m_{sd}-1}}{\pi G_{2,MQAM}^{m_{sd}}} \left(\prod_{i=1}^{L} P_{sr_i}\right) \sum_{k=1}^{L} \sum_{\lambda_1=1}^{L-k+1} \sum_{\lambda_2=\lambda_1+1}^{L-k+2} \cdots \sum_{\lambda_k=\lambda_{k-1}+1}^{L} \\
& \prod_{n=1}^{k} \left(\frac{1-P_{sr_{\lambda_n}}}{P_{sr_{\lambda_n}}}\right) \left(\frac{m_{r_{\lambda_n}d}}{H_{\lambda_n,MQAM}}\right)^{m_{r_{\lambda_n}d}} \frac{\Gamma\left(\frac{1}{2}\right)\Gamma\left(\frac{3}{2}+\sum_{n=1}^{k} m_{r_{\lambda_n}d}\right)}{\Gamma\left(2+\sum_{n=1}^{k} m_{r_{\lambda_n}d}\right)} F_D^{(k+2)}\left(\frac{1}{2}, 1-m_{sd}, m_{sd},\right. \\
& \left. m_{r_{\lambda_1}d}, \ldots, m_{r_{\lambda_k}d}; 2+\sum_{n=1}^{k} m_{r_{\lambda_n}d}; \frac{1}{G_{1,MQAM}}, \frac{2b_{sd}m_{sd}}{G_{2,MQAM}}, \frac{m_{r_{\lambda_1}d}}{H_{\lambda_1,MQAM}}, \ldots, \frac{m_{r_{\lambda_k}d}}{H_{\lambda_k,MQAM}}\right) \\
& - \frac{q^2\left(2b_{sd}m_{sd}\right)^{m_{sd}} L_{1,MQAM}^{m_{sd}-1}}{\pi L_{2,MQAM}^{m_{sd}}} \left(\prod_{i=1}^{L} P_{sr_i}\right) \sum_{k=1}^{L} \sum_{\lambda_1=1}^{L-k+1} \sum_{\lambda_2=\lambda_1+1}^{L-k+2} \cdots \sum_{\lambda_k=\lambda_{k-1}+1}^{L} \\
& \prod_{n=1}^{k} \left(\frac{1-P_{sr_{\lambda_n}}}{P_{sr_{\lambda_n}}}\right) \left(\frac{m_{r_{\lambda_n}d}}{Q_{\lambda_n MQAM}}\right)^{m_{r_{\lambda_n}d}} \frac{1}{\left(\frac{3}{2}+\sum_{n=1}^{k} m_{r_{\lambda_n}d}\right)} F_D^{(k+3)}\left(1, 1, 1-m_{sd}, m_{sd},\right. \\
& \left. m_{r_{\lambda_1}d}, \ldots, m_{r_{\lambda_k}d}; \frac{5}{2}+\sum_{n=1}^{k} m_{r_{\lambda_n}d}; \frac{1}{2}, \frac{G_{1,MQAM}}{L_{1,MQAM}}, \frac{G_{2,MQAM}}{L_{2,MQAM}}, \frac{H_{\lambda_1,MQAM}}{Q_{\lambda_1,MQAM}}, \ldots, \frac{H_{\lambda_k,MQAM}}{Q_{\lambda_k,MQAM}}\right)
\end{aligned}
\tag{B.21}
$$

Appendix C

Asymtotic Diversity Order of $P^{SDF}_{s,MPSK}$

In order to show the diversity order, we assume that $\overline{\gamma}_{sd} = \overline{\gamma}_{sr_i} = \overline{\gamma}_{r_id} = \overline{\gamma}$.

The asymptotic diversity order $D_{g,MPSK}$ of $P^{SDF}_{s,MPSK}(E)$ is given in [ZT03] as

$$D_{g,MPSK} = -\lim_{\overline{\gamma}\to+\infty} \frac{\log P^{SDF}_{s,MPSK}(\overline{\gamma})}{\log(\overline{\gamma})} \tag{C.1}$$

where $P^{SDF}_{s,MPSK}(\overline{\gamma})$ is given in 2.45. So, the asymptotic diversity order $D_{g,MPSK}$ can be rewritten as

$$\begin{aligned} D_{g,MPSK} &= -\lim_{\overline{\gamma}\to+\infty} \frac{1}{\log(\overline{\gamma})} \times \log\left(A_1 \times A_2 \times A_3 \times A_4\right) \\ &= -\lim_{\overline{\gamma}\to+\infty} \frac{1}{\log(\overline{\gamma})} \times \left[\log\left(A_1\right) + \log\left(A_2\right) + \log\left(A_3\right) + \log\left(A_4\right)\right] \end{aligned} \tag{C.2}$$

where

$$A_1 = (2b_{sd}m_{sd})^{m_{sd}}\,,\ A_2 = \frac{G^{m_{sd}-1}_{1,MPSK}}{G^{m_{sd}}_{2,MPSK}},\ A_3 = \left(\frac{H_{MPSK}}{K_{MPSK}}\right)^L,$$

$$\begin{aligned} A_4 = {} & \frac{1}{4}F^{(4)}_D\left(\frac{1}{2}, 1-m_{sd}, m_{sd}, -L, L; 2; \frac{1}{G_{1,MPSK}}, \frac{2b_{sd}m_{sd}}{G_{2,MPSK}}, \frac{1}{H_{MPSK}}, \frac{1}{K_{MPSK}}\right) \\ & + \frac{\sqrt{\omega}}{\pi}F^{(5)}_D\left(\frac{1}{2}, -\frac{1}{2}, 1-m_{sd}, m_{sd}, -L, L; \frac{3}{2}; \omega, \frac{\omega}{G_{1,MPSK}}, \frac{2b_{sd}m_{sd}\omega}{G_{2,MPSK}}, \frac{\omega}{H_{MPSK}}, \frac{\omega}{K_{MPSK}}\right) \end{aligned}$$

At the high SNR regime, we obtain

$$A_2 \approx \frac{1}{\overline{\gamma}}\,,$$

$$P_{sr,MPSK} \approx c_1 \times \frac{1}{\overline{\gamma}} \Rightarrow A_3 \approx \left(\frac{c_2}{\overline{\gamma}}\right)^L,$$

$$\begin{aligned} A_4 \approx {} & \frac{1}{4}F^{(4)}_D\left(\frac{1}{2}, 1-m_{sd}, m_{sd}, -L, L; 2; 0, 0, c_3, 0\right) \\ & + \frac{\sqrt{\omega}}{\pi}F^{(5)}_D\left(\frac{1}{2}, -\frac{1}{2}, 1-m_{sd}, m_{sd}, -L, L; \frac{3}{2}; \omega, 0, 0, c_4, 0\right) \end{aligned}$$

where the symbol $\approx$ denotes the approximation for the high SNR regime and c_i $(i = 1, 2, 3, 4)$ is a constant value. We observe that in the high SNR regime, A_4 converges to a constant value.

So, the asymptotic diversity $D_{g,MPSK}$ is finally given as

$$D_{g,MPSK} = -\lim_{\overline{\gamma}\to+\infty} \frac{1}{\log(\overline{\gamma})} \times \left[\log\left(A_1\right) + \log\left(\frac{1}{\overline{\gamma}}\right) + \log\left(\frac{c_2}{\overline{\gamma}}\right)^L + \log\left(A_4\right)\right] = L + 1. \qquad \text{(C.3)}$$

Appendix D

Asymtotic Diversity Order of $P^{SDF}_{s,MQAM}$

In order to show the diversity order, we assume that $\overline{\gamma}_{sd} = \overline{\gamma}_{sr_i} = \overline{\gamma}_{r_id} = \overline{\gamma}$.

The asymptotic diversity order $D_{g,MQAM}$ of $P^{SDF}_{s,MQAM}(E)$ is given in [ZT03] as

$$D_{g,MQAM} = -\lim_{\overline{\gamma}\to+\infty} \frac{\log P^{SDF}_{s,MQAM}(\overline{\gamma})}{\log(\overline{\gamma})}. \tag{D.1}$$

where $P^{SDF}_{s,MQAM}(\overline{\gamma})$ is given in 2.52. So, the asymptotic diversity order $D_{g,MQAM}$ can be rewritten as

$$D_{g,MQAM} = -\lim_{\overline{\gamma}\to+\infty} \frac{1}{\log(\overline{\gamma})} \times \log\left(B_1 \times B_2 \times B_3 \times B_4 - C_1 \times C_2 \times C_3 \times C_4\right) \tag{D.2}$$

where

$$B_1 = q\left(2b_{sd}m_{sd}\right)^{m_{sd}},\ B_2 = \frac{G^{m_{sd}-1}_{1,MQAM}}{G^{m_{sd}}_{2,MQAM}},\ B_3 = \left(\frac{H_{MQAM}}{K_{MQAM}}\right)^L,$$
$$B_4 = F^{(4)}_D\left(\frac{1}{2}, 1-m_{sd}, m_{sd}, -L, L; 2; \frac{1}{G_{1,MQAM}}, \frac{2b_{sd}m_{sd}}{G_{2,MQAM}}, \frac{1}{H_{MQAM}}, \frac{1}{K_{MQAM}}\right),$$
$$C_1 = \frac{2q^2\left(2b_{sd}m_{sd}\right)^{m_{sd}}}{3\pi},\ C_2 = \frac{L^{m_{sd}-1}_{1,MQAM}}{L^{m_{sd}}_{2,MQAM}},\ C_3 = \left(\frac{W_{MQAM}}{Z_{MQAM}}\right)^L,$$
$$C_4 = F^{(5)}_D\left(1, 1, 1-m_{sd}, m_{sd}, -L, L; \frac{5}{2}; \frac{1}{2}, \frac{G_{1,MQAM}}{L_{1,MQAM}}, \frac{G_{2,MQAM}}{L_{2,MQAM}}, \frac{H_{MQAM}}{W_{MQAM}}, \frac{K_{MQAM}}{Z_{MQAM}}\right)$$

At the high SNR regime, we have that

$$\begin{aligned}
B_2 &\approx \frac{1}{\overline{\gamma}}\ , \\
P_{sr,MQAM} \approx e_1 \times \frac{1}{\overline{\gamma}} &\Rightarrow B_3 \approx \left(\frac{e_2}{\overline{\gamma}}\right)^L , \\
B_4 &\approx F_D^{(4)}\left(\frac{1}{2}, 1-m_{sd}, m_{sd}, -L, L; 2; 0, 0, e_3, 0\right), \\
C_2 &\approx \frac{1}{\overline{\gamma}},\ C_3 \approx \left(\frac{e_4}{\overline{\gamma}}\right)^L , \\
C_4 &\approx F_D^{(5)}\left(1, 1, 1-m_{sd}, m_{sd}, -L, L; \frac{5}{2}; \frac{1}{2}, \frac{1}{2}, \frac{1}{2}, e_5, \frac{1}{2}\right)
\end{aligned}$$

where e_i $(i = 1, 2, 3, 4, 5)$ is a constant value. We observe that in the high SNR regime, B_4 and C_4 converge to constant values.

So, the asymptotic diversity $D_{g,MQAM}$ is finally given as

$$\begin{aligned}
D_{g,MQAM} &= -\lim_{\overline{\gamma}\to+\infty} \frac{1}{\log(\overline{\gamma})} \times \log\left[B_1 \times \left(\frac{1}{\overline{\gamma}}\right) \times \left(\frac{e_2}{\overline{\gamma}}\right)^L \times B_4 - C_1 \times \left(\frac{1}{\overline{\gamma}}\right) \times \left(\frac{e_4}{\overline{\gamma}}\right)^L \times C_4\right] \\
&= -\lim_{\overline{\gamma}\to+\infty} \frac{1}{\log(\overline{\gamma})} \times \left[\log\left(\frac{1}{\overline{\gamma}}\right)^{(L+1)} + \log\left(B_1 \times e_2^L \times B_4 - C_1 \times e_4^L \times C_4\right)\right] \\
&= L + 1.
\end{aligned} \tag{D.3}$$

Appendix E

Outage probability of the direct link

In order to derive the outage probability of the direct link we first derive the CDF of γ_{sd}. The CDF of γ_{sd} is given as

$$F_{\gamma_{sd}}(y) = \int_0^y f_{\gamma_{sd}}(\tau) d\tau. \tag{E.1}$$

where

$$f_{\gamma_{sd}}(\tau) = A_{sd} \exp\left(-\frac{\tau}{2b_{sd}\overline{\gamma}_{sd}}\right) {}_1F_1\left(m_{sd}; 1; B_{sd}\tau\right), \text{for } \tau > 0. \tag{E.2}$$

and

$$\begin{aligned} A_{sd} &= \frac{1}{2b_{sd}\overline{\gamma}_{sd}} \left(\frac{2b_{sd}m_{sd}}{2b_{sd}m_{sd} + \Omega_{sd}}\right)^{m_{sd}}, \\ B_{sd} &= \frac{\Omega_{sd}}{2b_{sd}\overline{\gamma}_{sd}(2b_{sd}m_{sd} + \Omega_{sd})}, \end{aligned} \tag{E.3}$$

Let change the variable $\tau = yu$. When $\tau = 0 \Rightarrow u = 0$, when $\tau = y \Rightarrow u = 1$ and $d\tau = ydu$.

So, equation E.1 can be rewritten as

$$F_{\gamma_{sd}}(y) = A_{sd} y \int_0^1 \exp\left(-\frac{yu}{2b_{sd}\overline{\gamma}_{sd}}\right) {}_1F_1\left(m_{sd}; 1; B_{sd}yu\right) du \tag{E.4}$$

By using the Maclaurin series expansions of $\exp\left(-\frac{yu}{2b_{sd}\overline{\gamma}_{sd}}\right)$,

$$\exp\left(-\frac{yu}{2b_{sd}\overline{\gamma}_{sd}}\right) = 1 + \sum_{j=1}^{+\infty} (-1)^j \frac{y^j}{j!\left(2b_{sd}\overline{\gamma}_{sd}\right)^j} u^j \tag{E.5}$$

equation E.4 can be rewritten as

$$F_{\gamma_{sd}}(y) = A_{sd} y \left[\int_0^1 {}_1F_1\left(m_{sd}; 1; B_{sd}yu\right) du + \sum_{j=1}^{+\infty} (-1)^j \frac{y^j}{j!\left(2b_{sd}\overline{\gamma}_{sd}\right)^j} \int_0^1 u^j {}_1F_1\left(m_{sd}; 1; B_{sd}yu\right) du\right]. \tag{E.6}$$

By using the table of integrals in [GR07],

$$\begin{aligned}\int_0^1 (1-x)^{\mu-1}x^{\nu-1}{}_pF_q\left(a_1,\ldots,a_p;\nu,b_2,\ldots,b_q;ax\right)dx \\ = \frac{\Gamma(\mu)\Gamma(\nu)}{\Gamma(\mu+\nu)}{}_pF_q\left(a_1,\ldots,a_p;\mu+\nu,b_2,\ldots,b_q;a\right)\end{aligned} \tag{E.7}$$

and

$$\begin{aligned}\int_0^1 (1-x)^{\mu-1}x^{\nu-1}{}_pF_q\left(a_1,\ldots,a_p;b_1,\ldots,b_q;ax\right)dx \\ = \frac{\Gamma(\mu)\Gamma(\nu)}{\Gamma(\mu+\nu)}{}_{p+1}F_{q+1}\left(\nu,a_1,\ldots,a_p;\mu+\nu,b_1,\ldots,b_q;a\right)\end{aligned} \tag{E.8}$$

where $\mathrm{Re}(\mu),\ \mathrm{Re}(\nu)>0,\ p\leq q+1,$ if $p=q+1$ then $|a|<1$.

So, $F_{\gamma_{sd}}(y)$ is finally given as follows

$$F_{\gamma_{sd}}(y) = A_{sd}y\,{}_1F_1\left(m_{sd};2;B_{sd}y\right)+\sum_{j=1}^{+\infty}(-1)^j\frac{A_{sd}y^{(j+1)}}{(j+1)!(2b_{sd}\overline{\gamma}_{sd})^j}\,{}_2F_2\left(j+1,m_{sd};j+2,1;B_{sd}y\right) \tag{E.9}$$

and the outage of the direct link is obtained as below

$$P_{sd}^{out} = A_{sd}\gamma_{th}\,{}_1F_1\left(m_{sd};2;B_{sd}\gamma_{th}\right)+\sum_{j=1}^{+\infty}(-1)^j\frac{A_{sd}(\gamma_{th})^{(j+1)}}{(j+1)!(2b_{sd}\overline{\gamma}_{sd})^j}\,{}_2F_2\left(j+1,m_{sd};j+2,1;B_{sd}\gamma_{th}\right). \tag{E.10}$$

Appendix F

Outage probability of the HSTCS

The PDF of $\tilde{\gamma}_{MRC}^{SDF}$ is defined in 2.77 as

$$\begin{aligned} f_{\tilde{\gamma}_{MRC}^{SDF}}(y) &= \int_{-\infty}^{+\infty} f_{\tilde{\gamma}_{DF}}(y-\tau) f_{\gamma_{sd}}(\tau) d\tau \\ &= \int_{0}^{+\infty} f_{\tilde{\gamma}_{DF}}(y-\tau) f_{\gamma_{sd}}(\tau) d\tau, \text{ for } \tau > 0. \end{aligned} \tag{F.1}$$

So, the CDF of $\tilde{\gamma}_{MRC}^{SDF}$ is defined by

$$\begin{aligned} F_{\tilde{\gamma}_{MRC}^{SDF}}(y) &= \int_{-\infty}^{y} f_{\tilde{\gamma}_{MRC}^{SDF}}(x) dx \\ &= \int_{-\infty}^{y} \int_{0}^{+\infty} f_{\tilde{\gamma}_{DF}}(x-\tau) f_{\gamma_{sd}}(\tau) d\tau dx \\ &= \int_{0}^{+\infty} \int_{-\infty}^{y} f_{\tilde{\gamma}_{DF}}(x-\tau) dx f_{\gamma_{sd}}(\tau) d\tau \end{aligned} \tag{F.2}$$

Let change the variable $t = x - \tau$, then, equation F.2 can be rewritten as

$$\begin{aligned} F_{\tilde{\gamma}_{MRC}^{SDF}}(y) &= \int_{0}^{+\infty} \int_{-\infty}^{y-\tau} f_{\tilde{\gamma}_{DF}}(t) dt f_{\gamma_{sd}}(\tau) d\tau \\ &= \int_{0}^{+\infty} F_{\tilde{\gamma}_{DF}}(y-\tau) f_{\gamma_{sd}}(\tau) d\tau. \end{aligned} \tag{F.3}$$

The CDF of $\tilde{\gamma}_{MRC}^{SDF}$, $F_{\tilde{\gamma}_{DF}}(y-\tau)$, is equal to zero when $y - \tau < 0$. So, the CDF of $\tilde{\gamma}_{MRC}^{SDF}$ can be expressed as below

$$F_{\tilde{\gamma}_{MRC}^{SDF}}(y) = \int_{0}^{y} F_{\tilde{\gamma}_{DF}}(y-\tau) f_{\gamma_{sd}}(\tau) d\tau. \tag{F.4}$$

F.1 Outage probability of HSTCS over i.n.i.d fading channels

the CDF of $\tilde{\gamma}_{DF}$ is defined in 2.76 by

$$F_{\tilde{\gamma}_{DF}}(y) = \left(\prod_{i=1}^{L} P_{sr_i}^{out}\right)\left[1 + \sum_{k=1}^{L}\sum_{\lambda_1=1}^{L-k+1}\sum_{\lambda_2=\lambda_1+1}^{L-k+2}\cdots\sum_{\lambda_k=\lambda_{k-1}+1}^{L} \prod_{n=1}^{k}\left(\frac{1-P_{sr_{\lambda_n}}^{out}}{P_{sr_{\lambda_n}}^{out}}\right)\sum_{n=1}^{k}\frac{\beta_{\lambda_1}\ldots\beta_{\lambda_k}}{\beta_{\lambda_n}\prod_{m=1,m\neq n}^{k}\left(\beta_{\lambda_m}-\beta_{\lambda_n}\right)}\left(1-\exp\left(-\beta_{\lambda_n}y\right)\right)\right]. \tag{F.5}$$

and

$$f_{\gamma_{sd}}(\tau) = A_{sd}\exp\left(-\frac{\tau}{2b_{sd}\overline{\gamma}_{sd}}\right){}_1F_1\left(m_{sd};1;B_{sd}\tau\right), \text{for } \tau > 0. \tag{F.6}$$

By using equation F.4, the CDF of $\tilde{\gamma}_{MRC}^{SDF}$ can be rewritten as below

$$\begin{aligned} F_{\tilde{\gamma}_{MRC}^{SDF}}(y) &= \left(\prod_{i=1}^{L} P_{sr_i}^{out}\right)\left[\int_0^y f_{\gamma_{sd}}(\tau)d\tau + \sum_{k=1}^{L}\sum_{\lambda_1=1}^{L-k+1}\sum_{\lambda_2=\lambda_1+1}^{L-k+2}\cdots\sum_{\lambda_k=\lambda_{k-1}+1}^{L} \prod_{n=1}^{k}\left(\frac{1-P_{sr_{\lambda_n}}^{out}}{P_{sr_{\lambda_n}}^{out}}\right)\sum_{n=1}^{k}\frac{\beta_{\lambda_1}\ldots\beta_{\lambda_k}}{\beta_{\lambda_n}\prod_{m=1,m\neq n}^{k}\left(\beta_{\lambda_m}-\beta_{\lambda_n}\right)}\right. \\ &\left.\times\int_0^y f_{\gamma_{sd}}(\tau)\left(1-\exp\left(-\beta_{\lambda_n}(y-\tau)\right)\right)d\tau\right] \\ &= \left(\prod_{i=1}^{L} P_{sr_i}^{out}\right)\left[F_{\gamma_{sd}}(y) + \sum_{k=1}^{L}\sum_{\lambda_1=1}^{L-k+1}\sum_{\lambda_2=\lambda_1+1}^{L-k+2}\cdots\sum_{\lambda_k=\lambda_{k-1}+1}^{L} \prod_{n=1}^{k}\left(\frac{1-P_{sr_{\lambda_n}}^{out}}{P_{sr_{\lambda_n}}^{out}}\right)\sum_{n=1}^{k}\frac{\beta_{\lambda_1}\ldots\beta_{\lambda_k}}{\beta_{\lambda_n}\prod_{m=1,m\neq n}^{k}\left(\beta_{\lambda_m}-\beta_{\lambda_n}\right)}I(y)\right] \end{aligned} \tag{F.7}$$

where

$$\begin{aligned} I(y) &= \int_0^y f_{\gamma_{sd}}(\tau)\left(1-\exp\left(-\beta_{\lambda_n}(y-\tau)\right)\right)d\tau \\ &= F_{\gamma_{sd}}(y) - A_{sd}\exp\left(-\beta_{\lambda_n}y\right)\int_0^y \exp\left[-\left(\frac{1}{2b_{sd}\overline{\gamma}_{sd}}-\beta_{\lambda_n}\right)\tau\right]{}_1F_1\left(m_{sd};1;B_{sd}\tau\right)d\tau. \end{aligned} \tag{F.8}$$

By using the same approach as in equation E.4 of appendix E, $I(y)$ can be obtained as

$$I(y) = F_{\gamma_{sd}}(y) - A_{sd}\exp\left(-\beta_{\lambda_n}y\right)\left[y{}_1F_1\left(m_{sd};2;B_{sd}y\right) + \sum_{j=1}^{+\infty}(-1)^j\frac{y^{(j+1)}}{(j+1)!} \times\left(\frac{1}{2b_{sd}\overline{\gamma}_{sd}}-\beta_{\lambda_n}\right)^j{}_2F_2\left(j+1,m_{sd};j+2,1;B_{sd}y\right)\right]. \tag{F.9}$$

Then, by replacing $\beta_{\lambda_n} = \frac{1}{2b_{r_{\lambda_n}d}\overline{\gamma}_{r_{\lambda_n}d}}$ and the obtained $I(y)$ into equation F.7, the CDF of $\tilde{\gamma}_{MRC}^{SDF}$, $F_{\tilde{\gamma}_{MRC}^{SDF}}(y)$ is finally obtained as

$$F_{\tilde{\gamma}_{MRC}^{SDF}}(y) = \left(\prod_{i=1}^{L} P_{sr_i}^{out}\right)\left[F_{\gamma_{sd}}(y) + \sum_{k=1}^{L}\sum_{\lambda_1=1}^{L-k+1}\sum_{\lambda_2=\lambda_1+1}^{L-k+2}\cdots\sum_{\lambda_k=\lambda_{k-1}+1}^{L}\prod_{n=1}^{k}\left(\frac{1-P_{sr_{\lambda_n}}^{out}}{P_{sr_{\lambda_n}}^{out}}\right)\right.$$
$$\times\sum_{n=1}^{k}\frac{\beta_{\lambda_1}\ldots\beta_{\lambda_k}}{\beta_{\lambda_n}\prod_{m=1,m\neq n}^{k}(\beta_{\lambda_m}-\beta_{\lambda_n})}\left(F_{\gamma_{sd}}(y) - A_{sd}\exp(-\beta_{\lambda_n}y)\left[y_1F_1(m_{sd};2;B_{sd}y)\right.\right.$$
$$\left.\left.+\sum_{j=1}^{+\infty}(-1)^j\left(\frac{1}{2b_{sd}\overline{\gamma}_{sd}}-\frac{1}{2b_{r_{\lambda_n}d}\overline{\gamma}_{r_{\lambda_n}d}}\right)^j\frac{y^{j+1}}{(j+1)!}{}_2F_2\left(j+1,m_{sd};j+2,1;B_{sd}y\right)\right]\right)\Bigg]. \tag{F.10}$$

Hence, the outage probability of HSTCS over i.n.i.d fading channels is finally given as

$$P_{SDF}^{out} = \left(\prod_{i=1}^{L} P_{sr_i}^{out}\right)\left[P_{sd}^{out} + \sum_{k=1}^{L}\sum_{\lambda_1=1}^{L-k+1}\sum_{\lambda_2=\lambda_1+1}^{L-k+2}\cdots\sum_{\lambda_k=\lambda_{k-1}+1}^{L}\prod_{n=1}^{k}\left(\frac{1-P_{sr_{\lambda_n}}^{out}}{P_{sr_{\lambda_n}}^{out}}\right)\right.$$
$$\times\sum_{n=1}^{k}\frac{\beta_{\lambda_1}\ldots\beta_{\lambda_k}}{\beta_{\lambda_n}\prod_{m=1,m\neq n}^{k}(\beta_{\lambda_m}-\beta_{\lambda_n})}\left(P_{sd}^{out} - A_{sd}\exp(-\beta_{\lambda_n}\gamma_{th})\left[\gamma_{th1}F_1(m_{sd};2;B_{sd}\gamma_{th})\right.\right. \tag{F.11}$$
$$\left.\left.+\sum_{j=1}^{+\infty}(-1)^j\left(\frac{1}{2b_{sd}\overline{\gamma}_{sd}}-\frac{1}{2b_{r_{\lambda_n}d}\overline{\gamma}_{r_{\lambda_n}d}}\right)^j\frac{\gamma_{th}^{j+1}}{(j+1)!}{}_2F_2\left(j+1,m_{sd};j+2,1;B_{sd}\gamma_{th}\right)\right]\right)\Bigg].$$

F.2 Outage probability of HSTCS over i.i.d fading channels

The CDF of $\tilde{\gamma}_{DF}$ is given by equation 2.83 as

$$F_{\tilde{\gamma}_{DF}}(y) = \int_0^y f_{\tilde{\gamma}_{DF}}(\tau)d\tau = (P_{sr}^{out})^L\left[1+\sum_{k=1}^{L}\binom{L}{k}\left(\frac{1-P_{sr}^{out}}{P_{sr}^{out}}\right)^k\left(1-\exp\left(-\beta y\right)\sum_{m=0}^{k-1}\frac{\beta^m y^m}{m!}\right)\right]. \tag{F.12}$$

And the CDF of $\tilde{\gamma}_{MRC}$ can be written as below

$$\begin{aligned} F_{\tilde{\gamma}_{MRC}^{SDF}}(y) &= \int_0^y F_{\tilde{\gamma}_{DF}}(y-\tau)f_{\gamma_{sd}}(\tau)d\tau \\ &= (P_{sr}^{out})^L\left[F_{\gamma_{sd}}(y)+\sum_{k=1}^{L}\binom{L}{k}\left(\frac{1-P_{sr}^{out}}{P_{sr}^{out}}\right)^k J(y)\right] \end{aligned} \tag{F.13}$$

where

$$J(y) = \int_0^y \left(1 - \exp\left(-\beta(y-\tau)\right) \sum_{m=0}^{k-1} \frac{\beta^m (y-\tau)^m}{m!}\right) f_{\gamma_{sd}}(\tau) d\tau$$
$$= F_{\gamma_{sd}}(y) - A_{sd} \exp(-\beta y) \sum_{m=0}^{k-1} \frac{\beta^m}{m!} \int_0^y (y-\tau)^m \exp\left[-\left(\frac{1}{2b_{sd}\overline{\gamma}_{sd}} - \beta\right)\tau\right] {}_1F_1\left(m_{sd}; 1; B_{sd}\tau\right) d\tau. \tag{F.14}$$

Let change the variable $\tau = yu$. So, $J(y)$ can be rewritten as

$$J(y) = F_{\gamma_{sd}}(y) - A_{sd} \exp(-\beta y) \sum_{m=0}^{k-1} \frac{\beta^m}{m!} y^{m+1}$$
$$\times \int_0^1 (1-u)^m \exp\left[-\left(\frac{1}{2b_{sd}\overline{\gamma}_{sd}} - \beta\right) yu\right] {}_1F_1\left(m_{sd}; 1; B_{sd} yu\right) du. \tag{F.15}$$

The integral

$$J_1(y) = \int_0^1 (1-u)^m \exp\left[-\left(\frac{1}{2b_{sd}\overline{\gamma}_{sd}} - \beta\right) yu\right] {}_1F_1\left(m_{sd}; 1; B_{sd} yu\right) du \tag{F.16}$$

can be obtained by using the same approach as in equation E.4 of appendix E and is given as follows

$$J_1(y) = \Big[\frac{1}{m+1} {}_1F_1\left(m_{sd}; m+2; B_{sd} y\right) + \sum_{j=1}^{+\infty} (-1)^j \frac{m! y^j}{(j+m+1)!}$$
$$\times \left(\frac{1}{2b_{sd}\overline{\gamma}_{sd}} - \beta\right)^j {}_2F_2\left(j+1, m_{sd}; j+m+2, 1; B_{sd} y\right)\Big]. \tag{F.17}$$

Therefore, $J(y)$ is obtained as

$$J(y) = F_{\gamma_{sd}}(y) - A_{sd} \exp(-\beta y) \sum_{m=0}^{k-1} \beta^m$$
$$\times \Big[\frac{y^{m+1}}{(m+1)!} {}_1F_1\left(m_{sd}; m+2; B_{sd} y\right) + \sum_{j=1}^{+\infty} (-1)^j \frac{y^{m+j+1}}{(m+j+1)!}$$
$$\times \left(\frac{1}{2b_{sd}\overline{\gamma}_{sd}} - \beta\right)^j {}_2F_2\left(j+1, m_{sd}; m+j+2, 1; B_{sd} y\right)\Big]. \tag{F.18}$$

So, the CDF of $\tilde{\gamma}_{MRC}$ is finally given as follows

$$F_{\tilde{\gamma}_{MRC}^{SDF}}(y) = (P_{sr}^{out})^L \Bigg[F_{\gamma_{sd}}(y) + \sum_{k=1}^{L} \binom{L}{k} \left(\frac{1-P_{sr}^{out}}{P_{sr}^{out}} \right)^k \Bigg(F_{\gamma_{sd}}(y) - A_{sd} \exp(-\frac{y}{2b_{rd}\overline{\gamma}_{rd}}) \sum_{m=0}^{k-1} \left(\frac{1}{2b_{rd}\overline{\gamma}_{rd}} \right)^m \times \Bigg[\frac{y^{m+1}}{(m+1)!} {}_1F_1(m_{sd}; m+2; B_{sd}y) + \sum_{j=1}^{+\infty} (-1)^j \left(\frac{1}{2b_{sd}\overline{\gamma}_{sd}} - \frac{1}{2b_{rd}\overline{\gamma}_{rd}} \right)^j \times \frac{y^{m+j+1}}{(m+j+1)!} {}_2F_2(j+1, m_{sd}; m+j+2, 1; B_{sd}y) \Bigg] \Bigg) \Bigg]. \tag{F.19}$$

where $\beta = \frac{1}{2b_{rd}\overline{\gamma}_{rd}}$.

Hence, the outage probability of HSTCS over i.i.d fading channels is finally given as

$$P_{SDF}^{out} = (P_{sr}^{out})^L \Bigg[P_{sd}^{out} + \sum_{k=1}^{L} \binom{L}{k} \left(\frac{1-P_{sr}^{out}}{P_{sr}^{out}} \right)^k \Bigg(P_{sd}^{out} - A_{sd} \exp(-\frac{\gamma_{th}}{2b_{rd}\overline{\gamma}_{rd}}) \sum_{m=0}^{k-1} \left(\frac{1}{2b_{rd}\overline{\gamma}_{rd}} \right)^m \times \Bigg[\frac{\gamma_{th}^{m+1}}{(m+1)!} {}_1F_1(m_{sd}; m+2; B_{sd}\gamma_{th}) + \sum_{j=1}^{+\infty} (-1)^j \left(\frac{1}{2b_{sd}\overline{\gamma}_{sd}} - \frac{1}{2b_{rd}\overline{\gamma}_{rd}} \right)^j \times \frac{\gamma_{th}^{m+j+1}}{(m+j+1)!} {}_2F_2(j+1, m_{sd}; m+j+2, 1; B_{sd}\gamma_{th}) \Bigg] \Bigg) \Bigg]. \tag{F.20}$$

Appendix G

SEP of the HSTCS with best relay selection

G.1 SEP of MPSK

The average SEP of the HSTCS with best relay selection for coherent MPSK signals is defined in 3.18 by

$$\begin{aligned} P_{s,MPSK}^{SDF-BR}(E) &= \frac{1}{\pi}\int_0^{\pi-\frac{\pi}{M}} \phi_{\gamma_{MRC}^{SDF-BR}}\left(\frac{g_{MPSK}}{\sin^2\theta}\right)d\theta \\ &= \underbrace{\frac{1}{\pi}\int_0^{\frac{\pi}{2}} \phi_{\gamma_{MRC}^{SDF-BR}}\left(\frac{g_{MPSK}}{\sin^2\theta}\right)d\theta}_{I_{1,MPSK}^{SDF-BR}} + \underbrace{\frac{1}{\pi}\int_{\frac{\pi}{2}}^{\pi-\frac{\pi}{M}} \phi_{\gamma_{MRC}^{SDF-BR}}\left(\frac{g_{MPSK}}{\sin^2\theta}\right)d\theta}_{I_{2,MPSK}^{SDF-BR}} \end{aligned} \tag{G.1}$$

where $g_{MPSK} = \sin^2(\pi/M)$ and

$$\phi_{\gamma_{MRC}^{SDF-BR}}(s) = \phi_{\gamma_{sd}}(s)\phi_{\gamma_{BR}}(s) \tag{G.2}$$

where $\phi_{\gamma_{sd}}(s)$ is given in A.4 of appendix A and $\phi_{\gamma_{BR}}(s)$ is given in 3.17 as

$$\begin{aligned} \phi_{\gamma_{BR}}(s) &= \mathbb{E}\left[e^{-sy}\right] = \int_0^{\infty} e^{-sy} f_{\gamma_{BR}}(y)dy \\ &= \left(\prod_{i=1}^{L} P_{sr_i}\right) + \sum_{k=1}^{L}(-1)^{(k+1)} \sum_{\lambda_1=1}^{L-k+1} \sum_{\lambda_2=\lambda_1+1}^{L-k+2} \cdots \sum_{\lambda_k=\lambda_{k-1}+1}^{L} \\ &\times \left[\prod_{n=1}^{k}\left(1-P_{sr_{\lambda_n}}\right)\right]\left(\sum_{n=1}^{k}\frac{1}{2b_{r_{\lambda_n}d}\overline{\gamma}_{r_{\lambda_n}d}}\right)\left(s+\sum_{n=1}^{k}\frac{1}{2b_{r_{\lambda_n}d}\overline{\gamma}_{r_{\lambda_n}d}}\right)^{-1}. \end{aligned} \tag{G.3}$$

So,

$$\phi_{\gamma_{MRC}^{SDF}}\left(\frac{g_{MPSK}}{\sin^2\theta}\right)=\phi_{\gamma_{sd}}\left(\frac{g_{MPSK}}{\sin^2\theta}\right)\left(\prod_{i=1}^{L}P_{sr_i}\right)+\phi_{\gamma_{sd}}\left(\frac{g_{MPSK}}{\sin^2\theta}\right)\sum_{k=1}^{L}(-1)^{(k+1)}\sum_{\lambda_1=1}^{L-k+1}\sum_{\lambda_2=\lambda_1+1}^{L-k+2}\cdots \sum_{\lambda_k=\lambda_{k-1}+1}^{L}\left[\prod_{n=1}^{k}\left(1-P_{sr_{\lambda_n}}\right)\right]\left(\sum_{n=1}^{k}\frac{1}{2b_{r_{\lambda_n}d}\overline{\gamma}_{r_{\lambda_n}d}}\right)\left(\frac{g_{MPSK}}{\sin^2\theta}+\sum_{n=1}^{k}\frac{1}{2b_{r_{\lambda_n}d}\overline{\gamma}_{r_{\lambda_n}d}}\right)^{-1}. \tag{G.4}$$

The first integral $I_{1,MPSK}^{SDF-BR}$ can be derived by changing the variable $t=\cos^2(\theta)$.

Therefore, $\phi_{\gamma_{MRC}^{SDF-BR}}\left(\frac{g_{MPSK}}{\sin^2\theta}\right)$ can be rewritten as below

$$\begin{aligned}\phi_{\gamma_{MRC}^{SDF-BR}}\left(\frac{g_{MPSK}}{\sin^2\theta}\right)&=(2b_{sd}m_{sd})^{m_{sd}}(1-t)\frac{G_{1,MPSK}^{m_{sd}-1}\left(1-t\frac{1}{G_{1,MPSK}}\right)^{m_{sd}-1}}{G_{2,MPSK}^{m_{sd}}\left(1-t\frac{2b_{sd}m_{sd}}{G_{2,MPSK}}\right)^{m_{sd}}}\left(\prod_{i=1}^{L}P_{sr_i}\right)\\&+(2b_{sd}m_{sd})^{m_{sd}}(1-t)\frac{G_{1,MPSK}^{m_{sd}-1}\left(1-t\frac{1}{G_{1,MPSK}}\right)^{m_{sd}-1}}{G_{2,MPSK}^{m_{sd}}\left(1-t\frac{2b_{sd}m_{sd}}{G_{2,MPSK}}\right)^{m_{sd}}}\sum_{k=1}^{L}(-1)^{(k+1)}\\&\sum_{\lambda_1=1}^{L-k+1}\sum_{\lambda_2=\lambda_1+1}^{L-k+2}\cdots\sum_{\lambda_k=\lambda_{k-1}+1}^{L}\left[\prod_{n=1}^{k}\left(1-P_{sr_{\lambda_n}}\right)\right]\frac{1}{U_{\lambda_n,MPSK}}\left(\sum_{n=1}^{k}\frac{1}{2b_{r_{\lambda_n}d}\overline{\gamma}_{r_{\lambda_n}d}}\right)\\&\times(1-t)\left(1-t\frac{\sum_{n=1}^{k}\frac{1}{2b_{r_{\lambda_n}d}\overline{\gamma}_{r_{\lambda_n}d}}}{U_{\lambda_n,MPSK}}\right)^{-1}\end{aligned} \tag{G.5}$$

where

$$U_{\lambda_n,MPSK}=g_{MPSK}+\sum_{n=1}^{k}\frac{1}{2b_{r_{\lambda_n}d}\overline{\gamma}_{r_{\lambda_n}d}}. \tag{G.6}$$

So, $I_{1,MPSK}^{SDF-BR}$ can be written as

$$
\begin{aligned}
I_{1,MPSK}^{SDF-BR} &= \frac{(2b_{sd}m_{sd})^{m_{sd}}\, G_{1,MPSK}^{m_{sd}-1}}{2\pi G_{2,MPSK}^{m_{sd}}} \left(\prod_{i=1}^{L} P_{sr_i}\right) \\
&\times \int_0^1 t^{-\frac{1}{2}}(1-t)^{\frac{1}{2}} \left(1 - t\frac{1}{G_{1,MPSK}}\right)^{m_{sd}-1} \left(1 - t\frac{2b_{sd}m_{sd}}{G_{2,MPSK}}\right)^{-m_{sd}} dt \\
&+ \frac{(2b_{sd}m_{sd})^{m_{sd}}\, G_{1,MPSK}^{m_{sd}-1}}{2\pi G_{2,MPSK}^{m_{sd}}} \sum_{k=1}^{L} (-1)^{(k+1)} \\
&\sum_{\lambda_1=1}^{L-k+1} \sum_{\lambda_2=\lambda_1+1}^{L-k+2} \cdots \sum_{\lambda_k=\lambda_{k-1}+1}^{L} \left[\prod_{n=1}^{k} \left(1 - P_{sr_{\lambda_n}}\right)\right] \frac{1}{U_{\lambda_n,MPSK}} \left(\sum_{n=1}^{k} \frac{1}{2b_{r_{\lambda_n}d}\overline{\gamma}_{r_{\lambda_n}d}}\right) \\
&\times \int_0^1 t^{-\frac{1}{2}}(1-t)^{\frac{3}{2}} \left(1 - t\frac{1}{G_{1,MPSK}}\right)^{m_{sd}-1} \left(1 - t\frac{2b_{sd}m_{sd}}{G_{2,MPSK}}\right)^{-m_{sd}} \left(1 - t\frac{\sum_{n=1}^{k} \frac{1}{2b_{r_{\lambda_n}d}\overline{\gamma}_{r_{\lambda_n}d}}}{U_{\lambda_n,MPSK}}\right)^{-1} dt
\end{aligned}
\tag{G.7}
$$

By using the Lauricellla function, $I_{1,MPSK}^{SDF-BR}$ can be obtained as below

$$
\begin{aligned}
I_{1,MPSK}^{SDF-BR} &= \frac{(2b_{sd}m_{sd})^{m_{sd}} G_{1,MPSK}^{m_{sd}-1}}{4G_{2,MPSK}^{m_{sd}}} \left(\prod_{i=1}^{L} P_{sr_i}\right) F_1\left(\frac{1}{2}, 1-m_{sd}, m_{sd}; 2; \frac{1}{G_{1,MPSK}}, \frac{2b_{sd}m_{sd}}{G_{2,MPSK}}\right) \\
&+ \frac{3(2b_{sd}m_{sd})^{m_{sd}} G_{1,MPSK}^{m_{sd}-1}}{16G_{2,MPSK}^{m_{sd}}} \sum_{k=1}^{L} (-1)^{(k+1)} \sum_{\lambda_1=1}^{L-k+1} \sum_{\lambda_2=\lambda_1+1}^{L-k+2} \cdots \sum_{\lambda_k=\lambda_{k-1}+1}^{L} \\
&\prod_{n=1}^{k} \left(1 - P_{sr_{\lambda_n}}\right) \left(\sum_{n=1}^{k} \frac{1}{2b_{r_{\lambda_n}d}\overline{\gamma}_{r_{\lambda_n}d}}\right) \frac{1}{U_{\lambda_n,MPSK}} \\
&\times F_D^{(3)}\left(\frac{1}{2}, 1-m_{sd}, m_{sd}, 1; 3; \frac{1}{G_{1,MPSK}}, \frac{2b_{sd}m_{sd}}{G_{2,MPSK}}, \frac{\sum_{n=1}^{k} \frac{1}{2b_{r_{\lambda_n}d}\overline{\gamma}_{r_{\lambda_n}d}}}{U_{\lambda_n,MPSK}}\right)
\end{aligned}
\tag{G.8}
$$

The second integral $I_{2,MPSK}^{SDF-BR}$ can be derived by changing the variable

$$
z = \frac{\cos^2\theta}{\cos^2(\pi/M)} = \frac{\cos^2\theta}{1 - g_{MPSK}} = \frac{\cos^2\theta}{\omega}. \tag{G.9}
$$

In this case, $\phi_{\gamma_{MRC}^{SDF-BR}}\left(\frac{g_{MPSK}}{\sin^2\theta}\right)$ can be rewritten as below

$$\begin{aligned}\phi_{\gamma_{MRC}^{SDF-BR}}\left(\frac{g_{MPSK}}{\sin^2\theta}\right) &= (2b_{sd}m_{sd})^{m_{sd}}(1-z\omega)\frac{G_{1,MPSK}^{m_{sd}-1}\left(1-z\frac{\omega}{G_{1,MPSK}}\right)^{m_{sd}-1}}{G_{2,MPSK}^{m_{sd}}\left(1-z\frac{2b_{sd}m_{sd}\omega}{G_{2,MPSK}}\right)^{m_{sd}}}\left(\prod_{i=1}^{L}P_{sr_i}\right)\\ &+(2b_{sd}m_{sd})^{m_{sd}}(1-z\omega)\frac{G_{1,MPSK}^{m_{sd}-1}\left(1-z\frac{\omega}{G_{1,MPSK}}\right)^{m_{sd}-1}}{G_{2,MPSK}^{m_{sd}}\left(1-z\frac{2b_{sd}m_{sd}\omega}{G_{2,MPSK}}\right)^{m_{sd}}}\sum_{k=1}^{L}(-1)^{(k+1)}\\ &\sum_{\lambda_1=1}^{L-k+1}\sum_{\lambda_2=\lambda_1+1}^{L-k+2}\cdots\sum_{\lambda_k=\lambda_{k-1}+1}^{L}\left[\prod_{n=1}^{k}\left(1-P_{sr_{\lambda_n}}\right)\right]\frac{1}{U_{\lambda_n,MPSK}}\left(\sum_{n=1}^{k}\frac{1}{2b_{r_{\lambda_n}}d\overline{\gamma}_{r_{\lambda_n}}d}\right)\\ &\times(1-z\omega)\left(1-z\frac{\omega\sum_{n=1}^{k}\frac{1}{2b_{r_{\lambda_n}}d\overline{\gamma}_{r_{\lambda_n}}d}}{U_{\lambda_n,MPSK}}\right)^{-1}\end{aligned} \tag{G.10}$$

Therefore, $I_{2,MPSK}^{SDF-BR}$ can be written as below

$$\begin{aligned}I_{2,MPSK}^{SDF-BR} &= \frac{\sqrt{\omega}\,(2b_{sd}m_{sd})^{m_{sd}}\,G_{1,MPSK}^{m_{sd}-1}}{2\pi G_{2,MPSK}^{m_{sd}}}\left(\prod_{i=1}^{L}P_{sr_i}\right)\\ &\times\int_0^1 z^{-\frac{1}{2}}(1-z\omega)^{\frac{1}{2}}\left(1-z\frac{\omega}{G_{1,MPSK}}\right)^{m_{sd}-1}\left(1-z\frac{2b_{sd}m_{sd}\omega}{G_{2,MPSK}}\right)^{-m_{sd}}dz\\ &+\frac{\sqrt{\omega}\,(2b_{sd}m_{sd})^{m_{sd}}\,G_{1,MPSK}^{m_{sd}-1}}{2\pi G_{2,MPSK}^{m_{sd}}}\sum_{k=1}^{L}(-1)^{(k+1)}\sum_{\lambda_1=1}^{L-k+1}\sum_{\lambda_2=\lambda_1+1}^{L-k+2}\cdots\sum_{\lambda_k=\lambda_{k-1}+1}^{L}\\ &\left[\prod_{n=1}^{k}\left(1-P_{sr_{\lambda_n}}\right)\right]\frac{1}{U_{\lambda_n,MPSK}}\left(\sum_{n=1}^{k}\frac{1}{2b_{r_{\lambda_n}}d\overline{\gamma}_{r_{\lambda_n}}d}\right)\int_0^1 z^{-\frac{1}{2}}(1-z\omega)^{\frac{3}{2}}\\ &\times\left(1-z\frac{\omega}{G_{1,MPSK}}\right)^{m_{sd}-1}\left(1-z\frac{2b_{sd}m_{sd}\omega}{G_{2,MPSK}}\right)^{-m_{sd}}\left(1-z\frac{\omega\sum_{n=1}^{k}\frac{1}{2b_{r_{\lambda_n}}d\overline{\gamma}_{r_{\lambda_n}}d}}{U_{\lambda_n,MPSK}}\right)^{-1}dz\end{aligned} \tag{G.11}$$

By using the Lauricella function, $I_{2,MPSK}^{SDF-BR}$ can be obtained as follows

$$
\begin{aligned}
I_{2,MPSK}^{SDF-BR} = & \frac{\sqrt{\omega}(2b_{sd}m_{sd})^{m_{sd}}G_{1,MPSK}^{m_{sd}-1}}{\pi G_{2,MPSK}^{m_{sd}}}\left(\prod_{i=1}^{L}P_{sr_i}\right)F_D^{(3)}\left(\frac{1}{2},-\frac{1}{2},1-m_{sd},m_{sd};\frac{3}{2};\omega,\frac{\omega}{G_{1,MPSK}},\frac{2b_{sd}m_{sd}\omega}{G_{2,MPSK}}\right) \\
& + \frac{\sqrt{\omega}(2b_{sd}m_{sd})^{m_{sd}}G_{1,MPSK}^{m_{sd}-1}}{\pi G_{2,MPSK}^{m_{sd}}}\sum_{k=1}^{L}(-1)^{(k+1)}\sum_{\lambda_1=1}^{L-k+1}\sum_{\lambda_2=\lambda_1+1}^{L-k+2}\cdots\sum_{\lambda_k=\lambda_{k-1}+1}^{L} \\
& \prod_{n=1}^{k}\left(1-P_{sr_{\lambda_n}}\right)\left(\sum_{n=1}^{k}\frac{1}{2b_{r_{\lambda_n}d}\overline{\gamma}_{r_{\lambda_n}d}}\right)\frac{1}{U_{\lambda_n,MPSK}} \\
& \times F_D^{(4)}\left(\frac{1}{2},-\frac{3}{2},1-m_{sd},m_{sd},1;\frac{3}{2};\omega,\frac{\omega}{G_{1,MPSK}},\frac{2b_{sd}m_{sd}\omega}{G_{2,MPSK}},\frac{\omega\sum_{n=1}^{k}\frac{1}{2b_{r_{\lambda_n}d}\overline{\gamma}_{r_{\lambda_n}d}}}{U_{\lambda_n,MPSK}}\right)
\end{aligned}
\tag{G.12}
$$

Therefore, $P_{s,MPSK}^{SDF-BR}(E)$ is given as below

$$
\begin{aligned}
P_{s,MPSK}^{SDF-BR}(E) = & \frac{(2b_{sd}m_{sd})^{m_{sd}}G_{1,MPSK}^{m_{sd}-1}}{4G_{2,MPSK}^{m_{sd}}}\left(\prod_{i=1}^{L}P_{sr_i}\right)F_1\left(\frac{1}{2},1-m_{sd},m_{sd};2;\frac{1}{G_{1,MPSK}},\frac{2b_{sd}m_{sd}}{G_{2,MPSK}}\right) \\
& + \frac{3(2b_{sd}m_{sd})^{m_{sd}}G_{1,MPSK}^{m_{sd}-1}}{16G_{2,MPSK}^{m_{sd}}}\sum_{k=1}^{L}(-1)^{(k+1)}\sum_{\lambda_1=1}^{L-k+1}\sum_{\lambda_2=\lambda_1+1}^{L-k+2}\cdots\sum_{\lambda_k=\lambda_{k-1}+1}^{L} \\
& \prod_{n=1}^{k}\left(1-P_{sr_{\lambda_n}}\right)\left(\sum_{n=1}^{k}\frac{1}{2b_{r_{\lambda_n}d}\overline{\gamma}_{r_{\lambda_n}d}}\right)\frac{1}{U_{\lambda_n,MPSK}} \\
& \times F_D^{(3)}\left(\frac{1}{2},1-m_{sd},m_{sd},1;3;\frac{1}{G_{1,MPSK}},\frac{2b_{sd}m_{sd}}{G_{2,MPSK}},\frac{\sum_{n=1}^{k}\frac{1}{2b_{r_{\lambda_n}d}\overline{\gamma}_{r_{\lambda_n}d}}}{U_{\lambda_n,MPSK}}\right) \\
& + \frac{\sqrt{\omega}(2b_{sd}m_{sd})^{m_{sd}}G_{1,MPSK}^{m_{sd}-1}}{\pi G_{2,MPSK}^{m_{sd}}}\left(\prod_{i=1}^{L}P_{sr_i}\right) \\
& \times F_D^{(3)}\left(\frac{1}{2},-\frac{1}{2},1-m_{sd},m_{sd};\frac{3}{2};\omega,\frac{\omega}{G_{1,MPSK}},\frac{2b_{sd}m_{sd}\omega}{G_{2,MPSK}}\right) \\
& + \frac{\sqrt{\omega}(2b_{sd}m_{sd})^{m_{sd}}G_{1,MPSK}^{m_{sd}-1}}{\pi G_{2,MPSK}^{m_{sd}}}\sum_{k=1}^{L}(-1)^{(k+1)}\sum_{\lambda_1=1}^{L-k+1}\sum_{\lambda_2=\lambda_1+1}^{L-k+2}\cdots\sum_{\lambda_k=\lambda_{k-1}+1}^{L} \\
& \prod_{n=1}^{k}\left(1-P_{sr_{\lambda_n}}\right)\left(\sum_{n=1}^{k}\frac{1}{2b_{r_{\lambda_n}d}\overline{\gamma}_{r_{\lambda_n}d}}\right)\frac{1}{U_{\lambda_n,MPSK}} \\
& \times F_D^{(4)}\left(\frac{1}{2},-\frac{3}{2},1-m_{sd},m_{sd},1;\frac{3}{2};\omega,\frac{\omega}{G_{1,MPSK}},\frac{2b_{sd}m_{sd}\omega}{G_{2,MPSK}},\frac{\omega\sum_{n=1}^{k}\frac{1}{2b_{r_{\lambda_n}d}\overline{\gamma}_{r_{\lambda_n}d}}}{U_{\lambda_n,MPSK}}\right)
\end{aligned}
\tag{G.13}
$$

G.2 SEP of MQAM

The average SEP of the HSTCS with best relay selection for coherent MQAM signals is defined in 3.23 as

$$
P_{s,MQAM}^{SDF-BR}(E) = \underbrace{\frac{4q}{\pi}\int_0^{\frac{\pi}{2}}\phi_{\gamma_{MRC}^{SDF-BR}}\left(\frac{g_{MQAM}}{\sin^2\theta}\right)d\theta}_{I_{1,MQAM}^{SDF_BR}} - \underbrace{\frac{4q^2}{\pi}\int_0^{\frac{\pi}{4}}\phi_{\gamma_{MRC}^{SDF-BR}}\left(\frac{g_{MQAM}}{\sin^2\theta}\right)d\theta}_{I_{2,MQAM}^{SDF-BR}} \tag{G.14}
$$

where $g_{MQAM} = 3/2(M-1)$, $q = \left(1 - 1/\sqrt{M}\right)$ and

$$\phi_{\gamma_{MRC}^{SDF}}\left(\frac{g_{MQAM}}{\sin^2\theta}\right) = \phi_{\gamma_{sd}}\left(\frac{g_{MQAM}}{\sin^2\theta}\right)\left(\prod_{i=1}^{L} P_{sr_i}\right) + \phi_{\gamma_{sd}}\left(\frac{g_{MQAM}}{\sin^2\theta}\right)\sum_{k=1}^{L}(-1)^{(k+1)}\sum_{\lambda_1=1}^{L-k+1}\sum_{\lambda_2=\lambda_1+1}^{L-k+2}\cdots \sum_{\lambda_k=\lambda_{k-1}+1}^{L}\left[\prod_{n=1}^{k}\left(1-P_{sr_{\lambda_n}}\right)\right]\left(\sum_{n=1}^{k}\frac{1}{2b_{r_{\lambda_n}d}\overline{\gamma}_{r_{\lambda_n}d}}\right)\left(\frac{g_{MQAM}}{\sin^2\theta} + \sum_{n=1}^{k}\frac{1}{2b_{r_{\lambda_n}d}\overline{\gamma}_{r_{\lambda_n}d}}\right)^{-1}. \tag{G.15}$$

where $\phi_{\gamma_{sd}}\left(\frac{g_{MQAM}}{\sin^2\theta}\right)$ is given in A.19.

The first integral $I_{1,MQAM}^{SDF-BR}$ can be computed by using the same approach as in $I_{1,MPSK}^{SDF-BR}$. We only change g_{MPSK} to g_{MQAM} and multiply the factor $4q$ into $I_{1,MPSK}^{SDF-BR}$.

Hence, we obtain

$$\begin{aligned} I_{1,MQAM}^{SDF-BR} &= \frac{q(2b_{sd}m_{sd})^{m_{sd}}G_{1,MQAM}^{m_{sd}-1}}{G_{2,MQAM}^{m_{sd}}}\left(\prod_{i=1}^{L}P_{sr_i}\right)F_1\left(\frac{1}{2}, 1-m_{sd}, m_{sd}; 2; \frac{1}{G_{1,MQAM}}, \frac{2b_{sd}m_{sd}}{G_{2,MQAM}}\right) \\ &+ \frac{3q(2b_{sd}m_{sd})^{m_{sd}}G_{1,MQAM}^{m_{sd}-1}}{4G_{2,MQAM}^{m_{sd}}}\sum_{k=1}^{L}(-1)^{(k+1)}\sum_{\lambda_1=1}^{L-k+1}\sum_{\lambda_2=\lambda_1+1}^{L-k+2}\cdots\sum_{\lambda_k=\lambda_{k-1}+1}^{L} \\ &\prod_{n=1}^{k}\left(1-P_{sr_{\lambda_n}}\right)\left(\sum_{n=1}^{k}\frac{1}{2b_{r_{\lambda_n}d}\overline{\gamma}_{r_{\lambda_n}d}}\right)\frac{1}{U_{\lambda_n,MQAM}} \\ &\times F_D^{(3)}\left(\frac{1}{2}, 1-m_{sd}, m_{sd}, 1; 3; \frac{1}{G_{1,MQAM}}, \frac{2b_{sd}m_{sd}}{G_{2,MQAM}}, \frac{\sum_{n=1}^{k}\frac{1}{2b_{r_{\lambda_n}d}\overline{\gamma}_{r_{\lambda_n}d}}}{U_{\lambda_n,MQAM}}\right) \end{aligned} \tag{G.16}$$

where

$$U_{\lambda_n,MQAM} = g_{MQAM} + \sum_{n=1}^{k}\frac{1}{2b_{r_{\lambda_n}d}\overline{\gamma}_{r_{\lambda_n}d}}. \tag{G.17}$$

In order to derive $I_{2,MQAM}^{SDF-BR}$, we change the variable, $t = 1 - \tan^2\theta$. In this case, $I_{2,MPSK}^{SDF}$ can be

written as below

$$
\begin{aligned}
I_{2,MQAM}^{SDF-BR} = & \frac{q^2\left(2b_{sd}m_{sd}\right)^{m_{sd}} L_{1,MQAM}^{m_{sd}-1}}{\pi L_{2,MQAM}^{m_{sd}}} \left(\prod_{i=1}^{L} P_{sr_i}\right) \\
& \times \int_0^1 (1-t)^{\frac{1}{2}} \left(1-\frac{t}{2}\right)^{-1} \left(1-t\frac{G_{1,MQAM}}{L_{1,MQAM}}\right)^{m_{sd}-1} \left(1-t\frac{G_{2,MQAM}}{L_{2,MQAM}}\right)^{-m_{sd}} dt \\
& + \frac{q^2\left(2b_{sd}m_{sd}\right)^{m_{sd}} L_{1,MQAM}^{m_{sd}-1}}{\pi L_{2,MQAM}^{m_{sd}}} \sum_{k=1}^{L} (-1)^{(k+1)} \sum_{\lambda_1=1}^{L-k+1} \sum_{\lambda_2=\lambda_1+1}^{L-k+2} \cdots \sum_{\lambda_k=\lambda_{k-1}+1}^{L} \\
& \left[\prod_{n=1}^{k} \left(1-P_{sr_{\lambda_n}}\right)\right] \frac{1}{V_{\lambda_n,MQAM}} \left(\sum_{n=1}^{k} \frac{1}{2b_{r_{\lambda_n}d}\overline{\gamma}_{r_{\lambda_n}d}}\right) \int_0^1 (1-t)^{\frac{3}{2}} \left(1-\frac{t}{2}\right)^{-1} \\
& \times \left(1-t\frac{G_{1,MQAM}}{L_{1,MQAM}}\right)^{m_{sd}-1} \left(1-t\frac{G_{2,MQAM}}{L_{2,MQAM}}\right)^{-m_{sd}} \left(1-t\frac{U_{\lambda_n,MQAM}}{V_{\lambda_n,MQAM}}\right)^{-1} dt
\end{aligned}
\tag{G.18}
$$

where

$$
V_{\lambda_n,MQAM} = 2g_{MQAM} + \sum_{n=1}^{k} \frac{1}{2b_{r_{\lambda_n}d}\overline{\gamma}_{r_{\lambda_n}d}}. \tag{G.19}
$$

By using the Lauricella function, $I_{2,MPSK}^{SDF-BR}$ can be obtained as below

$$
\begin{aligned}
I_{2,MPSK}^{SDF-BR} = & \frac{2q^2(2b_{sd}m_{sd})^{m_{sd}} L_{1,MQAM}^{m_{sd}-1}}{3\pi L_{2,MQAM}^{m_{sd}}} \left(\prod_{i=1}^{L} P_{sr_i}\right) F_D^{(3)}\left(1,1,1-m_{sd},m_{sd};\frac{5}{2};\frac{1}{2},\frac{G_{1,MQAM}}{L_{1,MQAM}},\frac{G_{2,MQAM}}{L_{2,MQAM}}\right) \\
& + \frac{2q^2(2b_{sd}m_{sd})^{m_{sd}} L_{1,MQAM}^{m_{sd}-1}}{5\pi L_{2,MQAM}^{m_{sd}}} \sum_{k=1}^{L} (-1)^{(k+1)} \sum_{\lambda_1=1}^{L-k+1} \sum_{\lambda_2=\lambda_1+1}^{L-k+2} \cdots \sum_{\lambda_k=\lambda_{k-1}+1}^{L} \\
& \prod_{n=1}^{k} \left(1-P_{sr_{\lambda_n}}\right) \left(\sum_{n=1}^{k} \frac{1}{2b_{r_{\lambda_n}d}\overline{\gamma}_{r_{\lambda_n}d}}\right) \frac{1}{V_{\lambda_n,MQAM}} \\
& \times F_D^{(4)}\left(1,1,1-m_{sd},m_{sd},1;\frac{7}{2};\frac{1}{2},\frac{G_{1,MQAM}}{L_{1,MQAM}},\frac{G_{2,MQAM}}{L_{2,MQAM}},\frac{U_{\lambda_n,MQAM}}{V_{\lambda_n,MQAM}}\right)
\end{aligned}
\tag{G.20}
$$

So, $P_{s,MQAM}^{SDF-BR}(E)$ is finally given as follows

$$
\begin{aligned}
P_{s,MQAM}^{SDF-BR}(E) = & \frac{q(2b_{sd}m_{sd})^{m_{sd}}G_{1,MQAM}^{m_{sd}-1}}{G_{2,MQAM}^{m_{sd}}}\left(\prod_{i=1}^{L}P_{sr_i}\right)F_1\left(\frac{1}{2},1-m_{sd},m_{sd};2;\frac{1}{G_{1,MQAM}},\frac{2b_{sd}m_{sd}}{G_{2,MQAM}}\right) \\
& + \frac{3q(2b_{sd}m_{sd})^{m_{sd}}G_{1,MQAM}^{m_{sd}-1}}{4G_{2,MQAM}^{m_{sd}}}\sum_{k=1}^{L}(-1)^{(k+1)}\sum_{\lambda_1=1}^{L-k+1}\sum_{\lambda_2=\lambda_1+1}^{L-k+2}\cdots\sum_{\lambda_k=\lambda_{k-1}+1}^{L} \\
& \prod_{n=1}^{k}\left(1-P_{sr_{\lambda_n}}\right)\left(\sum_{n=1}^{k}\frac{1}{2b_{r_{\lambda_n}d}\overline{\gamma}_{r_{\lambda_n}d}}\right)\frac{1}{U_{\lambda_n,MQAM}} \\
& \times F_D^{(3)}\left(\frac{1}{2},1-m_{sd},m_{sd},1;3;\frac{1}{G_{1,MQAM}},\frac{2b_{sd}m_{sd}}{G_{2,MQAM}},\frac{\sum_{n=1}^{k}\frac{1}{2b_{r_{\lambda_n}d}\overline{\gamma}_{r_{\lambda_n}d}}}{U_{\lambda_n,MQAM}}\right) \\
& - \frac{2q^2(2b_{sd}m_{sd})^{m_{sd}}L_{1,MQAM}^{m_{sd}-1}}{3\pi L_{2,MQAM}^{m_{sd}}}\left(\prod_{i=1}^{L}P_{sr_i}\right) \\
& \times F_D^{(3)}\left(1,1,1-m_{sd},m_{sd};\frac{5}{2};\frac{1}{2},\frac{G_{1,MQAM}}{L_{1,MQAM}},\frac{G_{2,MQAM}}{L_{2,MQAM}}\right) \\
& - \frac{2q^2(2b_{sd}m_{sd})^{m_{sd}}L_{1,MQAM}^{m_{sd}-1}}{5\pi L_{2,MQAM}^{m_{sd}}}\sum_{k=1}^{L}(-1)^{(k+1)}\sum_{\lambda_1=1}^{L-k+1}\sum_{\lambda_2=\lambda_1+1}^{L-k+2}\cdots\sum_{\lambda_k=\lambda_{k-1}+1}^{L} \\
& \prod_{n=1}^{k}\left(1-P_{sr_{\lambda_n}}\right)\left(\sum_{n=1}^{k}\frac{1}{2b_{r_{\lambda_n}d}\overline{\gamma}_{r_{\lambda_n}d}}\right)\frac{1}{V_{\lambda_n,MQAM}} \\
& \times F_D^{(4)}\left(1,1,1-m_{sd},m_{sd},1;\frac{7}{2};\frac{1}{2},\frac{G_{1,MQAM}}{L_{1,MQAM}},\frac{G_{2,MQAM}}{L_{2,MQAM}},\frac{U_{\lambda_n,MQAM}}{V_{\lambda_n,MQAM}}\right)
\end{aligned}
\tag{G.21}
$$

Appendix H

Outage probability of the HSTCS with best relay selection

The CDF of $\tilde{\gamma}_{MRC}^{SDF-BR}$ is defined in 3.42 as

$$F_{\tilde{\gamma}_{MRC}^{SDF-BR}}(y) = \int_0^y F_{\tilde{\gamma}_{BR}}(y-\tau) f_{\gamma_{sd}}(\tau) d\tau. \tag{H.1}$$

where $F_{\tilde{\gamma}_{BR}}(y)$ is given in 3.40 as

$$F_{\tilde{\gamma}_{BR}}(y) = 1 + \sum_{k=1}^{L} (-1)^k \sum_{\lambda_1=1}^{L-k+1} \sum_{\lambda_2=\lambda_1+1}^{L-k+2} \cdots \sum_{\lambda_k=\lambda_{k-1}+1}^{L} \left[\prod_{n=1}^{k} \left(1 - P_{sr_{\lambda_n}}^{out}\right) \right] \exp\left(- \sum_{n=1}^{k} \frac{y}{2b_{r_{\lambda_n} d} \overline{\gamma}_{r_{\lambda_n} d}} \right). \tag{H.2}$$

So, the CDF of $\tilde{\gamma}_{MRC}^{SDF-BR}$ can be rewritten as follows

$$\begin{aligned} F_{\tilde{\gamma}_{MRC}^{SDF-BR}}(y) &= \int_0^y f_{\gamma_{sd}}(\tau) d\tau + \sum_{k=1}^{L} (-1)^k \sum_{\lambda_1=1}^{L-k+1} \sum_{\lambda_2=\lambda_1+1}^{L-k+2} \cdots \sum_{\lambda_k=\lambda_{k-1}+1}^{L} \left[\prod_{n=1}^{k} \left(1 - P_{sr_{\lambda_n}}^{out}\right) \right] \\ &\times \int_0^y \exp\left(- \sum_{n=1}^{k} \frac{y-\tau}{2b_{r_{\lambda_n} d} \overline{\gamma}_{r_{\lambda_n} d}} \right) f_{\gamma_{sd}}(\tau) d\tau \\ &= F_{\gamma_{sd}}(y) + \sum_{k=1}^{L} (-1)^k \sum_{\lambda_1=1}^{L-k+1} \sum_{\lambda_2=\lambda_1+1}^{L-k+2} \cdots \sum_{\lambda_k=\lambda_{k-1}+1}^{L} \\ &\left[\prod_{n=1}^{k} \left(1 - P_{sr_{\lambda_n}}^{out}\right) \right] A_{sd} \exp\left(- \sum_{n=1}^{k} \frac{y}{2b_{r_{\lambda_n} d} \overline{\gamma}_{r_{\lambda_n} d}} \right) \\ &\times \underbrace{\int_0^y \exp\left[- \left(\frac{1}{2b_{sd} \overline{\gamma}_{sd}} - \sum_{n=1}^{k} \frac{1}{2b_{r_{\lambda_n} d} \overline{\gamma}_{r_{\lambda_n} d}} \right) \tau \right] {}_1F_1\left(m_{sd}; 1; B_{sd}\tau\right) d\tau}_{I_1(y)}. \end{aligned} \tag{H.3}$$

The integral $I_1(y)$ can be calculated by using the same approach as in equation E.4 of appendix E

and is given as follows

$$I_1(y) = y_1 F_1\left(m_{sd}; 2; B_{sd} y\right) + \sum_{j=1}^{+\infty} (-1)^j \left(\frac{1}{2b_{sd}\overline{\gamma}_{sd}} - \sum_{n=1}^{k} \frac{1}{2b_{r_{\lambda_n} d}\overline{\gamma}_{r_{\lambda_n} d}} \right)^j \times \frac{y^{(j+1)}}{(j+1)!} {}_2F_2\left(j+1, m_{sd}; j+2, 1; B_{sd} y\right). \tag{H.4}$$

Hence, the CDF of $\tilde{\gamma}_{MRC}^{SDF-BR}$ is given as below

$$F_{\tilde{\gamma}_{MRC}^{SDF-BR}}(y) = F_{\gamma_{sd}}(y) + A_{sd} \sum_{k=1}^{L} (-1)^k \sum_{\lambda_1=1}^{L-k+1} \sum_{\lambda_2=\lambda_1+1}^{L-k+2} \cdots \sum_{\lambda_k=\lambda_{k-1}+1}^{L} \left[\prod_{n=1}^{k} \left(1 - P_{sr_{\lambda_n}}^{out}\right) \right] \times \exp\left(- \sum_{n=1}^{k} \frac{y}{2b_{r_{\lambda_n} d}\overline{\gamma}_{r_{\lambda_n} d}} \right) \left[y_1 F_1\left(m_{sd}; 2; B_{sd} y\right) + \sum_{j=1}^{+\infty} (-1)^j \left(\frac{1}{2b_{sd}\overline{\gamma}_{sd}} - \sum_{n=1}^{k} \frac{1}{2b_{r_{\lambda_n} d}\overline{\gamma}_{r_{\lambda_n} d}} \right)^j \times \frac{y^{(j+1)}}{(j+1)!} {}_2F_2\left(j+1, m_{sd}; j+2, 1; B_{sd} y\right) \right]. \tag{H.5}$$

Therefore, the outage probability of the HSTCS with best relay selection is finally given by

$$P_{SDF-BR}^{out} = P_{sd}^{out} + A_{sd} \sum_{k=1}^{L} (-1)^k \sum_{\lambda_1=1}^{L-k+1} \sum_{\lambda_2=\lambda_1+1}^{L-k+2} \cdots \sum_{\lambda_k=\lambda_{k-1}+1}^{L} \left[\prod_{n=1}^{k} \left(1 - P_{sr_{\lambda_n}}^{out}\right) \right] \times \exp\left(- \sum_{n=1}^{k} \frac{\gamma_{th}}{2b_{r_{\lambda_n} d}\overline{\gamma}_{r_{\lambda_n} d}} \right) \left[\gamma_{th} {}_1F_1\left(m_{sd}; 2; B_{sd}\gamma_{th}\right) + \sum_{j=1}^{+\infty} (-1)^j \left(\frac{1}{2b_{sd}\overline{\gamma}_{sd}} - \sum_{n=1}^{k} \frac{1}{2b_{r_{\lambda_n} d}\overline{\gamma}_{r_{\lambda_n} d}} \right)^j \times \frac{\gamma_{th}^{(j+1)}}{(j+1)!} {}_2F_2\left(j+1, m_{sd}; j+2, 1; B_{sd}\gamma_{th}\right) \right]. \tag{H.6}$$

Appendix I

Asymtotic SEP of the OFDM-HSTCS

I.1 Asymtotic of $P^{WD}_{s,MPSK}(E)$

The average SEP of the OFDM-HSTCS for coherent MPSK signals over i.i.d fading channel is given in 4.17 as

$$\begin{aligned} P^{WD}_{s,MPSK}(E) = & \frac{1}{2}\left(\frac{H_{MPSK}}{K_{MPSK}}\right)^{L} F_1\left(\frac{1}{2}, -L, L; 1; \frac{1}{H_{MPSK}}, \frac{1}{K_{MPSK}}\right) \\ & + \frac{\sqrt{\omega}}{\pi}\left(\frac{H_{MPSK}}{K_{MPSK}}\right)^{L} F_D^{(3)}\left(\frac{1}{2}, \frac{1}{2}, -L, L; \frac{3}{2}; \omega, \frac{\omega}{H_{MPSK}}, \frac{\omega}{K_{MPSK}}\right) \end{aligned} \tag{I.1}$$

where

$$\begin{aligned} H_{MPSK} &= 1 + P_{sr,MPSK} 2 b_{rd} \overline{\gamma}_{rd} g_{MPSK}, \\ K_{MPSK} &= 1 + 2 b_{rd} \overline{\gamma}_{rd} g_{MPSK}. \end{aligned} \tag{I.2}$$

When $\overline{\gamma}_{sr} \to +\infty \Rightarrow P_{sr,MPSK} \to 0$. When $E_r/N_0 \to +\infty \Rightarrow \overline{\gamma}_{rd} = \frac{E_r}{N_0 + N_I} \to \frac{C}{I}$.

So, $H_{MPSK} \to 1$ and $K_{MPSK} \to 1 + 2 b_{rd} \left(\frac{C}{I}\right) g_{MPSK}$.

Hence,

$$\begin{aligned} \lim_{SNR \to +\infty} P^{WD}_{s,MPSK}(E) = & \frac{1}{\left[1 + 2 b_{rd}\left(\frac{C}{I}\right) g_{MPSK}\right]^{L}} \left[\frac{1}{2} F_1\left(\frac{1}{2}, -L, L; 1; 1, \frac{1}{1 + 2 b_{rd}\left(\frac{C}{I}\right) g_{MPSK}}\right)\right. \\ & \left. + \frac{\sqrt{\omega}}{\pi} F_D^{(3)}\left(\frac{1}{2}, \frac{1}{2}, -L, L; \frac{3}{2}; \omega, \omega, \frac{\omega}{1 + 2 b_{rd}\left(\frac{C}{I}\right) g_{MPSK}}\right)\right] \\ = & \frac{1}{\left[1 + 2 b_{rd}\left(\frac{C}{I}\right) g_{MPSK}\right]^{L}} \left[\frac{1}{2} F_1\left(\frac{1}{2}, -L, L; 1; 1, \frac{1}{1 + 2 b_{rd}\left(\frac{C}{I}\right) g_{MPSK}}\right)\right. \\ & \left. + \frac{\sqrt{\omega}}{\pi} F_1\left(\frac{1}{2}, \frac{1}{2} - L, L; \frac{3}{2}; \omega, \frac{\omega}{1 + 2 b_{rd}\left(\frac{C}{I}\right) g_{MPSK}}\right)\right]. \end{aligned} \tag{I.3}$$

I.2 Asymtotic of $P_{s,MQAM}^{WD}(E)$

The average SEP of the OFDM-HSTCS for coherent MQAM signals over i.i.d fading channel is given in 4.23 as

$$\begin{aligned} P_{s,MQAM}^{WD}(E) = 2q \left(\frac{H_{MQAM}}{K_{MQAM}}\right)^{L} F_1\left(\frac{1}{2}, -L, L; 1; \frac{1}{H_{MQAM}}, \frac{1}{K_{MQAM}}\right) \\ - \frac{2q^2}{\pi}\left(\frac{W_{MQAM}}{Z_{MQAM}}\right)^{L} F_D^{(3)}\left(1, 1, -L, L; \frac{3}{2}; \frac{1}{2}, \frac{H_{MQAM}}{W_{MQAM}}, \frac{K_{MQAM}}{Z_{MQAM}}\right) \end{aligned} \tag{I.4}$$

where

$$\begin{aligned} H_{MQAM} &= 1 + 2P_{sr,MQAM} b_{rd} \overline{\gamma}_{rd} g_{MQAM}, \;\; K_{MQAM} = 1 + 2b_{rd}\overline{\gamma}_{rd} g_{MQAM}, \\ W_{MQAM} &= 1 + 4P_{sr,MQAM} b_{rd} \overline{\gamma}_{rd} g_{MQAM}, \;\; Z_{MQAM} = 1 + 4b_{rd}\overline{\gamma}_{rd} g_{MQAM}. \end{aligned} \tag{I.5}$$

When $\overline{\gamma}_{sr} \to +\infty \Rightarrow P_{sr,MQAM} \to 0$. When $E_r/N_0 \to +\infty \Rightarrow \overline{\gamma}_{rd} = \frac{E_r}{N_0 + N_I} \to \frac{C}{I}$.
So, $H_{MQAM} \to 1$, $K_{MQAM} \to 1 + 2b_{rd}\left(\frac{C}{I}\right) g_{MQAM}$, $W_{MQAM} \to 1$ and $Z_{MQAM} \to 1 + 4b_{rd}\left(\frac{C}{I}\right) g_{MQAM}$.
Hence,

$$\begin{aligned} \lim_{SNR \to +\infty} P_{s,MQAM}^{WD}(E) = 2q \frac{1}{\left[1 + 2b_{rd}\left(\frac{C}{I}\right) g_{MQAM}\right]^{L}} F_1\left(\frac{1}{2}, -L, L; 1; 1, \frac{1}{1 + 2b_{rd}\left(\frac{C}{I}\right) g_{MQAM}}\right) \\ - \frac{2q^2}{\pi} \frac{1}{\left[1 + 4b_{rd}\left(\frac{C}{I}\right) g_{MQAM}\right]^{L}} F_D^{(3)}\left(1, 1, -L, L; \frac{3}{2}; \frac{1}{2}, 1, \frac{1 + 2b_{rd}\left(\frac{C}{I}\right) g_{MQAM}}{1 + 4b_{rd}\left(\frac{C}{I}\right) g_{MQAM}}\right). \end{aligned} \tag{I.6}$$

Bibliography

[AH86] A.S. Akki and F. Haber. A statistical model of mobile-to-mobile land communication channel. *IEEE Trans. Veh. Technol.*, 35(1):2–7, Feb. 1986.

[Akk08] M. Akkouchi. On the convolution of exponential distributions. *Journal of the chungcheong mathematical society*, 21(4):501–510, Dec. 2008.

[AKKP10] Do-Seob Ahn, Sooyoung Kim, Hee Wook Kim, and Dong-Chul Park. A cooperative transmit diversity scheme for mobile satellite broadcasting systems. *Int. J. Sat. Commun.*, 28:352–368, 2010.

[ALAK03] A. Abdi, W.C. Lau, M.-S. Alouini, and M. Kaveh. A new simple model for land mobile satellite channels: first-and second-order statistics. *IEEE Trans. Wireless Commun.*, 2(3):519–528, May 2003.

[AT01] A. Annamalai and C. Tellambura. Error rates for Nakagami-m fading multichannel reception of binary and M-ary signals. *IEEE Trans. Commun.*, 49(1):58–68, Jan. 2001.

[AV97] R. Akturan and W.J. Vogel. Path diversity for leo satellite-pcs in the urban environment. *IEEE Trans. Antennas Propagat.*, 45(7):1107–1116, Jul. 1997.

[BH06] Norman C. Beaulieu and Jeremiah Hu. A closed-form expression for the outage probability of decode-and-forward relaying in dissimilar rayleigh fading channels. *IEEE Commun. Lett.*, 10(12):813–815, Dec. 2006.

[BKRL06] A. Bletsas, A. Khisti, D. P. Reed, and A. Lippman. A simple cooperative diversity method based on network path selection. 24(3):659–672, 2006.

[BS92] R.M. Barts and W.L. Stutzman. Modeling and simulation of mobile satellite propagation. *IEEE Trans. Antennas Propagat.*, 40(4):375–382, Apr. 1992.

[CCL+08] N. Chuberre, O. Courseille, P. Laine, L. Roullet, T. Quignon, and M. Tatard. Hybrid satellite and terrestrial infrastructure for mobile broadcast services delivery: An outlook to the Unlimited mobile TV system performance. *Int. J. Sat. Commun.*, 26:405–426, 2008.

[CFV+99] M.A.V. Castro, F.P. Fontan, A.A. Villamarin, S. Buonomo, P. Baptista, and B. Arbesser. L-band land mobile satellite (LMS) amplitude and multipath phase modeling in urban areas. *IEEE Commun. Lett.*, 3(1):12 –14, Jan. 1999.

[CGK09] P. Chini, G. Giambene, and S. Kota. A survey on mobile satellite systems. *Int. J. Sat. Commun.*, 28:29–57, 2009.

[CIdRH10] G. Cocco, C. Ibars, and O. del Rio Herrero. Cooperative satellite to land mobile gap-filler-less interactive system architecture. In *5th Advanced satellite multimedia systems conference and the 11th signal processing for space communications workshop*, pages 309–314, 2010.

[CwSZL10] Xu Chen, Ting wai Siu, Q.F. Zhou, and F.C.M. Lau. High-SNR analysis of opportunistic relaying based on the maximum harmonic mean selection criterion. *IEEE Signal Process. Lett.*, 17(8):719–722, Aug. 2010.

[DRMJS09] E. Del Re, S. Morosi, S. Jayousi, and C. Sacchi. Salice - satellite-assisted localization and communication systems for emergency services. In *1st International Conference on Wireless Communication, Vehicular Technology, Information Theory and Aerospace Electronic Systems Technology*, pages 544–548, 2009.

[Esc10] B. Escrig. On-demand cooperation MAC protocols with optimal diversity-multiplexing tradeoff. In *IEEE Wireless Commun. and Netw. Conf.*, pages 1–6, 2010.

[ETS08] ETSI. *Digital Video Broadcasting (DVB); DVB-SH Implementation Guidelines.* 2008.

[EWL+05] B. Evans, M. Werner, E. Lutz, M. Bousquet, G.E. Corazza, G. Maral, and R. Rumeau. Integration of satellite and terrestrial systems in future multimedia communications. *IEEE Wireless Commun.*, 12(5):72–80, Oct. 2005.

[Ext76] H. Exton. *Multiple Hypergeometric Functions and Applications.* Wiley, New York, 1976.

[FLCA07] F.P. Fontan, I.S. Lago, R.P. Cerdeira, and A.B. Alamanac. Consolidation of a multi-state narrowband land mobile satellite channel model. In *European Conf. Antennas Propagat.*, pages 1–6, Nov. 2007.

[FMV+01] I. Frigyes, B. G. Molnár, R. Vallet, Z. Herczku, and Z. Bodnár. Doppler spread characteristics of satellite personal communication channels. *Int. J. Sat. Commun.*, 19:251Ű262, 2001.

[FR08] Mayo-A. Marote D. Prieto-Cerdeira R. Mariño P. Machado F. Fontan, F. P. and N. Riera. Review of generative models for the narrowband land mobile satellite propagation channel. *Int. J. Sat. Commun.*, 26:291Ű316, 2008.

[FVCC+01] F.P. Fontan, M. Vazquez-Castro, C.E. Cabado, J.P. Garcia, and E. Kubista. Statistical modeling of the LMS channel. *IEEE Trans. Veh. Technol.*, 50(6):1549–1567, Nov. 2001.

[GR07] I. S. Gradshteyn and I. M. Ryzhik. *Table of Integrals, Series, and Products*. Academic Press, New York, 2007.

[HZ97] D.T. Harvatin and R.E. Ziemer. Orthogonal frequency division multiplexing performance in delay and Doppler spread channels. In *IEEE Vehicular Technology Conf.*, volume 3, pages 1644 –1647, May 1997.

[IBdRH+08] G. Iapichino, C. Bonnet, O. del Rio Herrero, C. Baudoin, and I. Buret. Advanced hybrid satellite and terrestrial system architecture for emergency mobile communications. In *AIAA International Communications Satellite Systems Conference*, pages 1–8, Jun. 2008.

[Kel09] P. Kelley. Overview of the DVB-SH specifications. *Int. J. Sat. Commun.*, 20:198–214, May 2009.

[KK10] Giambene G. Kota, S. and S. Kim. Satellite component of NGN: Integrated and hybrid networks. *Int. J. Sat. Commun.*, 29:191–208, 2010.

[KKM97] Y. Karasawa, K. Kimura, and K. Minamisono. Analysis of availability improvement in lmss by means of satellite diversity based on three-state propagation channel model. *IEEE Trans. Veh. Technol.*, 46(4):1047–1056, Nov. 1997.

[LB98] C. Loo and J.S. Butterworth. Land mobile satellite channel measurements and modeling. *Proc. IEEE*, 86(7):1442–1463, Jul. 1998.

[LCD+91] E. Lutz, D. Cygan, M. Dippold, F. Dolainsky, and W. Papke. The land mobile satellite communication channel-recording, statistics, and channel model. *IEEE Trans. Veh. Technol.*, 40(2):375–386, May 1991.

[Loo85] Chun Loo. A statistical model for a land mobile satellite link. *IEEE Trans. Veh. Technol.*, 34(3):122–127, Aug. 1985.

[Loo90] C. Loo. Digital transmission through a land mobile satellite channel. *IEEE Trans. Commun.*, 38(5):693–697, May 1990.

[Loo91] C. Loo. Further results on the statistics of propagation data at L-band (1542 MHz) for mobile satellite communications. In *IEEE Vehicular Technology Conf.*, pages 51–56, May 1991.

[LTW04] J.N. Laneman, D.N.C. Tse, and G.W. Wornell. Cooperative diversity in wireless networks: Efficient protocols and outage behavior. *IEEE Trans. Inf. Theory*, 50(12):3062–3080, Dec. 2004.

[LW03] J.N. Laneman and G.W. Wornell. Distributed space-time-coded protocols for exploiting cooperative diversity in wireless networks. *IEEE Trans. Inf. Theory*, 49(10):2415–2425, Oct. 2003.

[MJDR10] S. Morosi, S. Jayousi, and E. Del Re. Cooperative delay diversity in hybrid satellite/terrestrial DVB-SH system. In *IEEE International Conference on Communications*, pages 1–5, May 2010.

[MOS66] W. Magnus, F. Oberhettinger, and R. P. Soni. *Formulas and Theorems for the Special Functions of Mathematical Physics.* Springer, New York, 1966.

[Nak60] M. Nakagami. The m-distribution- a general formula of intensity distribution of rapid fading. *Statistical Methods in Radio Wave Propagation*, pages 3–36, 1960.

[PCPFB+10] R. Prieto-Cerdeira, F. Perez-Fontan, P. Burzigotti, A. Bolea-Alamañac, and I. Sanchez-Lago. Versatile two-state land mobile satellite channel model with first application to DVB-SH analysis. *Int. J. Sat. Commun.*, 28:291Ű315, 2010.

[PED+11] B. Paillassa, B. Escrig, R. Dhaou, M.-L. Boucheret, and C. Bes. Improving satellite services with cooperative communications. *Int. J. Sat. Commun.*, 29:479–500, 2011.

[PFHS+08] F. Perez-Fontan, V. Hovinen, M. Schonhuber, R. Prieto-Cerdeira, J. Rivera-Castro, P. Valtr, J. Kyrolainen, and F. Teschl. Characterisation of the satellite-to-indoor propagation channel. In *4th Advanced Satellite Mobile Systems*, pages 105–110, Aug. 2008.

[PFVCB+98] F. Perez-Fontan, M.A. Vazquez-Castro, S. Buonomo, J.P. Poiares-Baptista, and B. Arbesser-Rastburg. S-band LMS propagation channel behaviour for different environments, degrees of shadowing and elevation angles. *IEEE Trans. Broadcasting*, 44(1):40–76, Mar. 1998.

[QB04] Xiangping Qin and R. Berry. Opportunistic splitting algorithms for wireless networks. In *IEEE INFOCOM Conference*, volume 3, pages 1662–1672, Mar. 2004.

[RK99a] P. Robertson and S. Kaiser. Analysis of the loss of orthogonality through doppler spread in OFDM systems. In *IEEE Global Telecommunications Conference*, volume 1, pages 701 –706, 1999.

[RK99b] P. Robertson and S. Kaiser. The effects of doppler spreads in OFDM(A) mobile radio systems. In *IEEE Vehicular Technology Conf.*, volume 1, pages 329–333, 1999.

[RLSSK09] K.J. Ray Liu, Ahmed K. Sadek, Weifeng Su, and Andres Kwasinski. *Cooperative Communications and Networking.* Cambridge, 2009.

[SA05] Marvin K Simon and Mohamed-Slim Alouini. *Digital Communication over Fading Channels.* Wiley, 2005.

[SMY10a] V. Shah, N. Mehta, and R. Yim. Optimal timer based selection schemes. *IEEE Trans. Commun.*, 58(6):1814–1823, Jun. 2010.

[SMY10b] V. Shah, N.B. Mehta, and R. Yim. Splitting algorithms for fast relay selection: Generalizations, analysis, and a unified view. *IEEE Trans. Wireless Commun.*, 9(4):1525–1535, Apr. 2010.

[VCS02] Perez-Fontan F. Vazquez-Castro, M. and S. R. (2002) Saunders. Shadowing correlation assessment and modeling for satellite diversity in urban environments. *Int. J. Sat. Commun.*, 20:151–166, 2002.

[Vog97] W.J. Vogel. Satellite diversity for personal satellite communications-modeling and measurements. In *Int. Conf. Antennas Propagat.*, volume 1, pages 269–272, 1997.

[WPMZ06] Tiejun Wang, J.G. Proakis, E. Masry, and J.R. Zeidler. Performance degradation of OFDM systems due to doppler spreading. *IEEE Trans Wireless Commun.*, 5(6):1422–1432, Jun. 2006.

[ZT03] Lizhong Zheng and D.N.C. Tse. Diversity and multiplexing: a fundamental tradeoff in multiple-antenna channels. *IEEE Trans. Inf. Theory*, 49(5):1073–1096, May 2003.